

# Cell-Free expression of GPCRs: the endothelin system

## **Dissertation**

zur Erlangung des Doktorgrades  
der Naturwissenschaften

vorgelegt beim Fachbereich  
Biochemie, Chemie und Pharmazie (FB 14)  
der Goethe-Universität  
in Frankfurt am Main

von

**Davide Proverbio**  
aus Milano (Italien)

Frankfurt am Main 2013  
(D30)

Vom Fachbereich Biochemie, Chemie und Pharmazie (FB 14)  
der Goethe-Universität als Dissertation angenommen.

Dekan: Prof. Dr. Thomas Prisner

Gutachter: Prof. Dr. Volker Dötsch  
PD Dr. Rupert Abele

Datum der Disputation: 28. Mai 2014

## Table of contents

<b>Table of contents</b> .....	<b>1</b>
<b>Abbreviations</b> .....	<b>4</b>
<b>Summary</b> .....	<b>7</b>
<b>Zusammenfassung</b> .....	<b>10</b>
<b>1. Introduction</b> .....	<b>17</b>
1.1 Membrane proteins .....	17
1.2 G-protein coupled receptors -GPCRs .....	17
1.3 GPCRs activation .....	19
1.4 GPCRs trafficking .....	22
1.5 GPCRs dimerization and oligomerization .....	23
1.6 The endothelin system .....	24
1.7 The endothelin receptors .....	25
1.8 Endothelin receptors dimerization .....	28
1.9 Post-translational modifications of the endothelin receptors .....	28
1.10 Current insight into ligand-receptor interaction .....	30
1.11 Endothelin receptors antagonism .....	32
1.12 Cell-based systems for the heterologous expression of GPCRs .....	32
1.13 Cell-Free expression system .....	34
1.14 Cell-Free extract sources .....	36
1.15 Template design and reaction compounds .....	38
1.16 Configurations of the Cell-Free reaction .....	39
1.17 Cell-Free expression of the endothelin receptors .....	43
1.18 Aim of this project .....	44
<b>2. Materials</b> .....	<b>45</b>
2.1 General equipment .....	45
2.2 DNA template preparation and analysis .....	45
2.3 Protein expression and analysis .....	45
2.4 Protein processing, quality and functional analysis .....	46
2.5 Antibodies .....	46
2.6 Detergents .....	47
2.7 Lipids .....	47
2.8 General reagents and chemicals .....	47
2.9 Labelled chemicals and ligands .....	49
2.10 Microbial strains .....	49
2.11 General buffers and media .....	49
2.12 Reagents and buffers for cell-free expression .....	50
2.13 Buffers for DNA-Agarose gels, SDS-PAGE and Western Blotting .....	51
2.14 Buffers for protein purification and protein analysis .....	51
2.15 Softwares .....	53
<b>3. Methods</b> .....	<b>54</b>
3.1 DNA techniques .....	54

---

3.2 Plasmid DNA transformation into competent <i>E. coli</i> cells .....	55
3.3 Preparation of <i>E. coli</i> S30 extract .....	55
3.4 CECF Configurations .....	56
3.5 Nanodiscs preparation .....	59
3.6 SDS-PAGE and Western-blot .....	60
3.7 Determination of protein concentration .....	61
3.8 IMAC: Ni-NTA chromatography .....	61
3.9 Low temperature-SDS-PAGE (LT-SDS-PAGE) .....	62
3.10 Streptavidin affinity chromatography .....	62
3.11 Size exclusion chromatography (SEC).....	62
3.12 Reconstitution of proteoliposomes .....	63
3.13 Ligand affinity chromatography .....	63
3.14 Radioactive ligand binding assays .....	64
3.15 Ligand binding assay using Cy-3-ET-1 .....	65
3.16 Ligand binding assay by fluorescence anisotropy .....	65
3.17 Ligand binding analysis by ELISA assay .....	66
3.18 Confocal microscopy .....	66
3.19 Surface Plasmon Resonance Assay (SPR) .....	67
3.20 Microscale Thermophoresis Assay (MST) .....	68
3.21 OCTET Assay .....	68
3.22 Analysis of the activity of the $G\alpha_s$ subunit: fluorescent assay .....	68
3.23 Analysis of the activity of the $G\alpha_s$ subunit: radioactive assay.....	69
<b>4. Results.....</b>	<b>70</b>
4.1 Cell-Free expression of ETB: P-CF mode .....	70
4.2 Evaluation of detergents for the post-translational solubilization .....	71
4.3 Post-translational reconstitution into liposomes and functional assays .....	72
4.4 Cell-Free expression of ETB: D-CF mode .....	75
4.5 Post-translational reconstitution into liposomes and functional assays .....	77
4.6 Cell-Free expression of ETB: L-CF mode.....	78
4.7 L-CF expression mode in presence of liposomes, functional assays.....	79
4.8 Effect of the temperature in L-CF mode .....	81
4.9 Effect of cholesterol in L-CF mode .....	82
4.10 A mixed approach: L-CF in presence of detergent.....	83
4.11 L-CF expression mode in presence of nanodiscs .....	84
4.12 Binding of Cy3-ET-1 to ETB-sGFP/ND complexes .....	87
4.13 Ligand binding analysis by ELISA.....	89
4.14 Radioligand binding assay .....	91
4.15 Surface Plasmon Resonance (SPR) Assay .....	92
4.16 Microscale Thermophoresis (MST) .....	100
4.17 OCTET SYTEM .....	101
4.18 N-terminal processing of the CF synthesized ETB.....	104
4.19 SDS resistant complex formation of CF synthesized ETB with the ligand ET-1 .....	106
4.20 CF expression of Galpha subunits .....	107
4.21 Functional analysis of the P-CF produced $G\alpha_s$ .....	108

---

4.22 Ligand induced activation of $G\alpha_s$ .....	111
<b>5. Discussion .....</b>	<b>113</b>
5.1 Cell-Free expression of GPCRs .....	113
5.2 Optimization of the expression, general considerations .....	113
5.3 P-CF and D-CF mode: solubilization of the receptor in detergents .....	115
5.4 Following the classical track: post-translational reconstitution of ETB into liposomes	118
5.5 L-CF expression mode: Co-translational association of ETB to liposomes.....	120
5.6 L-CF expression mode: Co-translational association of ETB to nanodiscs .....	122
5.7 Functional characterization of the ET receptors in NDs .....	124
5.8 CF expression of $G\alpha$ subunits.....	128
5.9 Conclusions and perspectives .....	132
<b>6. References.....</b>	<b>134</b>
<b>Acknowledgements .....</b>	<b>150</b>
<b>Curriculum vitae .....</b>	<b>151</b>
<b>Eidesstattliche Versicherung .....</b>	<b>156</b>

## Abbreviations

°	degree
μ	micro
4-Ala-ET-1	4-alanine 1,3,11,15 ET-1
A	Ampere
aa	amino acid(s)
AC	adenylyl cyclase
AcP	acetyl phosphate
APS	ammoniumperoxodisulfate
Aso-PC	L-α-phosphatidylcholine from soybean, type IV-S
ATP	adenosine triphosphate
b-ET-1	biotynilated ET-1
β-OG	n-β-octyl-D-glucopyranoside
bp	base pairs
Brij35	polyoxyethylene-(23)-lauryl-ether
Brij58	polyoxyethylene-(20)-cetyl-ether
Brij78	polyoxyethylene-(20)-stearylether
Brij98	polyoxyethylene-(20)-oleyl-ether
BSA	bovine serum albumine
BTE	total lipid extract from bovine brain
C	Celsius
cAMP	cyclic adenosine monophosphate
CCP	clathrin-coated pit
CECF	contiuous-exchange cell-free
CF	cell-free
CHAPS	3-[(3-Cholamidopropyl)dimethylammonio]propanesulfonic acid
CHS	cholesteryl hemisuccinate
CMC	critical micellar concentration
CTP	cytidine triphosphate
CV	column volumes
Da	Dalton
DAG	diacylglycerol
D-CF	cell-free expression in presence of detergents
DDM	n-dodecyl-β-D-maltoside
DMPC	1,2-dimyristoyl-sn-phosphatidylcholine
DMSO	dimethyl sulfoxide
DNA	desoxyribonucleic acid
dNTP	desoxyribonucleitriphosphate
DPC	n-dodecylphosphocholine
DTT	dithiothreitol
<i>E. coli</i>	<i>Escherichia coli</i>
e.g.	for example
ECE	<i>E. coli</i> extract
ECL	extracellular loop / enhanced cehemioluminescence

---

EDTA	ethylenediaminetetraacetic acid
EPL	polar lipid extract from <i>E. coli</i>
ER	endoplasmatic reticulum
ERA	endothelin receptor antagonist
et al.	and others
ET	endothelin
ETA	endothelin A receptor
ETB	endothelin B receptor
EtBr	ethidium bromide
FM	feeding mixture
Fos-12	n-dodecylphosphocholine
Fos-16	n-hexadecylphosphocholine
FRET	fluorescence energy transfer
g	gram
GAP	GTPase-activating protein
GDI	guanine nucleotide dissociation inhibitor
GDP	guanosine diphosphate
GEF	guanine nucleotide exchange factor
GFP	green fluorescent protein
GPCR	G-protein coupled receptor
GRK	GPCR kinase
GTP	guanosine triphosphate
h	hour(s)
HEPES	4-(2-hydroxyethyl)-1-piperazineethanesulfonic acid
HRP	horse radish peroxidase
HTE	total lipid extract from bovine heart
IC <sub>50</sub>	half maximal inhibitory concentration
IL	intracellular loops
IMAC	immobilized metal affinity chromatography
IP3	inositol 1,4,5-triphosphate
K <sub>a</sub>	association constant
K <sub>d</sub>	dissociation constant
K <sub>D</sub>	Equilibrium dissociation constant
L	liter(s)
LB	Luria-Bertani
L-CF	cell-free protein synthesis in presence of lipids
LMPC	1-myristoyl-2-hydroxy-sn-glycero-3-phosphocholine
LMPG	1-myristoyl-2-hydroxy-sn-glycero-3-[phospho-rac-(1-glycerol)]
LPPG	1-palmitoyl-2-hydroxy-sn-glycero-3-[phospho-rac-(1-glycerol)]
m	milli
M	molar (mol/L)
mg	milligram(s)
min	minute(s)
ml	milliliter(s)
MP	membrane protein
mRNA	messenger mRNA
MSP	membrane scaffold protein
MST	microscale thermophoresis

---

MW	molecular weight
MWCO	molecular weight cut-off
n	nano
ND	nanodiscs
Ni-NTA	nickel-nitrilotriacetic acid
nm	nanometer
NMR	nuclear magnetic resonance
NTP	nucleotide triphosphate
o.n.	over night
p	pico
P-20	polyoxyethylene-sorbitane-monolaurate 20
PAGE	polyacrylamide gel electrophoresis
PBS	phosphate buffer saline
PC	phosphatidylcholine
P-CF	precipitating generating cell-free synthesis
PCR	polymerase chain reaction
PE	phosphatidylethanolamine
PEG	polyethyglycol
PEI	polyethyeneimine
PEP	phosphoenol pyruvate
PI	phosphatidylinositol
PIP2	phosphatidyl 4,5-diphosphate
PLC- $\beta$	phospholipase C- $\beta$
PMSF	phenylmethylsufonyl fluoride
POPC	1-palmitoyl-2-oleoyl-sn-glycero-3-phosphocholine
PR	proteorhodopsin
PTM	post-translational modification
RM	reaction mixture
RNA	ribonucleic acid
rpm	revolution per minute
RT	room temperature
RU	resonance unit
s	second(s)
S30	<i>E. coli</i> extract centrifuged at 30,000 x g
SDS	sodium dodecylsulfate
SEC	size exclusion chromatography
SPR	surface plasmon resonance
T7RNAP	T7 RNA polymerase
TM	transmembrane
Tris	tris(hydroxymethyl)methylamine
Triton X-100	polyethylene-glycol P-1,1,3,3-tetra-methyl-butylphenyl-ether
tRNA	transfer tRNA
Tween20	polyoxyethylene-sorbitane-monolaurate 20
UTP	uridine triphosphate
WG	wheat germ extract



## Summary

The Cell-Free (CF) expression system is a relatively new technology for the production of membrane proteins (MPs). The characteristic *in vitro* synthesis overcomes some major limitations that are commonly encountered using a classical *in vivo* approach for the overexpression of proteins. Furthermore, the open nature and the high versatility of the CF system allows modulation of the sample quality by modifying the reaction conditions.

Focusing on this alternative expression strategy, the main topic of this thesis was to develop protocols for the expression and the functional characterization of the endothelin receptor B (ETB).

ETB, together with the endothelin receptor A (ETA), belongs to the G-protein coupled receptors family (GPCRs). These two receptors are widely distributed in the human body and their activity is regulated by the three endothelin peptides ET-1, ET-2 and ET-3.

ETA and ETB are key players in cardiovascular regulation and dysfunction of their activity can result in pathologic conditions like systemic and pulmonary hypertension or arteriosclerosis.

Using the CF expression system, GPCRs can be synthesized as initial precipitate (P-CF) and subsequently resolubilized in detergent. Alternatively, proteomicelles can be co-translationally produced by supplementing appropriate detergents directly into the CF reaction (D-CF). The solubilized GPCRs obtained from these two expression modes can then be reconstituted into lipid membranes by classical *in vitro* techniques. A third option is the co-translational reconstitution of the MPs directly into a lipid bilayer (L-CF). In this case the lipids, in the form of pre-formed liposomes or nanodiscs (NDs), are directly added to the reaction.

Starting from the three standard CF expression modes, the ETB receptor, and to some extent the ETA receptor, have been co- or post- translationally reconstituted into lipid bilayers and their activity has been evaluated using a set of different complementary techniques.

After P-CF expression mode and resolubilization of the pellet in the detergent, 1-1.5 mg/ml of purified ETB was obtained. Analysis of the sample by SDS-PAGE revealed the presence of a single band corresponding to a molecular weight of approximately 40 kDa. After reconstitution of the receptor into liposomes, upon detergent removal using Biobeads, a relatively low affinity for the ligand ET-1 was determined using radioactive as well as fluorescent anisotropy assays.

In the D-CF expression mode, the detergent Brij78, used for the co-translational solubilization of the receptor, was exchanged into a secondary detergent upon metal chelate chromatography, before proteoliposome reconstitution. In contrast to the P-CF expressed protein, two bands corresponding to approximately 40 kDa and 35 kDa were detected by SDS-PAGE gel analysis. A specific cleavage of the first 64 amino acids by a putative metalloprotease has been previously

reported for the ETB receptor expressed *in vivo*.

Different experiments proved the presence of the same cleavage in the D-CF produced sample. The ligand binding competence of the truncated receptor in detergent micelles, similar to the one observed for the full length receptor, was confirmed.

After purification of the D-CF sample and proteoliposomes reconstitution, a slight reduction of the sample activity was observed in radioligand binding assay in comparison to the sample produced in the P-CF mode.

In the L-CF expression mode, liposomes or NDs were directly supplemented into the reaction mixture in order to allow the co-translational association of the newly synthesized receptor.

In this expression mode an ETB-sGFP fusion construct was used for the fast optimization of conditions.

After expression in the presence of liposomes, a fluorescent pellet was recovered. The resuspended pellet, analyzed by confocal microscopy, revealed the presence of a heterogeneous population of liposomes, ranging in size between 5 and 20  $\mu\text{m}$ . For the formation of liposomes, different lipids were tested and the expression yields and activity of the obtained proteoliposomes was evaluated for each condition. Radioligand binding assay revealed, also in this case, a low specific activity.

L-CF expression was also performed in presence of NDs, discoidal membrane structures composed of a lipid core surrounded by two membrane scaffold proteins (MSPs).

NDs of different lipid composition and of two different sizes, formed by either MSP1 or MSP1E3D1 were tested. The highest reconstitution and activity was detected using MSP1E3D1 and DMPC lipids for both the ETA and ETB receptor. In contrast to the other tested methods, in this specific expression environment, radioligand binding analysis revealed an affinity of the receptors to ET-1 similar to the one observed *in vivo*.

Due to the soluble nature of the GPCRs/NDs complex, SPR experiments were performed in order to better characterize the ligand binding properties of the two receptors. Direct binding assays, to ligand or receptor immobilized on a biochip, as well as competition assays have been developed. The measured dissociation equilibrium constant and  $\text{IC}_{50}$  values of a panel of agonist and antagonist were in the same range as previously published, confirming the production of ligand binding competent receptors.

Furthermore, preliminary experiments using Microscale Thermophoresis and OCTET system suggested the possibility to also use these two alternative techniques in combination with the NDs technology.

Once obtained a ligand binding competent receptor, a further task of this thesis project was to verify the ability of ETB to activate specific signaling pathways.

ETA and ETB, as members of the GPCRs family, are able to induce heterotrimeric G proteins activation upon stimulation with an agonist. Conformational changes induced by the ligand interaction cause the re-arrangement of the cytoplasmic domains of the receptor, leading to a dissociation of the heterotrimeric complex and to the exchange of GDP to GTP in the  $G\alpha$  subunit. As the over expression of G proteins is still a challenging task *in vivo*, the CF expression system was chosen for the production of  $G\alpha_s$  and  $G\alpha_q$ .

Soluble expression of the two proteins was achieved upon P-CF and D-CF mode and the production of an active  $G\alpha_s$  subunit was confirmed by fluorescent as well as radioactive based assays. Nevertheless, different incorporation rate of the fluorescent analogue BODIPY-GTP- $\gamma$ -S, compared to the radioactive GTP- $\gamma$ -S<sup>[35]</sup> was observed.

Similarly, in the preliminary G protein activation assays, performed upon co-incubation of ETB in NDs and ligands, different responses were obtained using the two analogues. Due to these results, further experiments will therefore be necessary in order to clarify the activation mechanism.

In conclusion, our results document a new process for the production of the two endothelin receptors, ETA and ETB, in a ligand binding competent form. The combination of CF and NDs technology will allow to analyze the ligand binding properties of a reconstituted GPCR as well as to characterize the signaling pathway. Furthermore, the developed SPR based assay, which can be performed with crude material obtained directly from the CF reaction, will open new possibilities for the fast screening of GPCRs ligands.

## Zusammenfassung

Das zellfreie Expressionssystem („Cell-Free expression system“, CF), basierend auf einem unbehandelten Lysat prokaryotischer und eukaryotischer Zellen, ist eine effiziente Technik für die Produktion von Membranproteinen, indem es die *in vitro*-Expression von Membranproteinen erlaubt und dabei die Komplexität lebender Zellen ausklammert.

Im Gegensatz zu den konventionellen *in vivo*-Ansätzen bei der Proteinproduktion, weist das CF-System die folgenden Vorteile auf. Analytische Expressionen können in  $\mu$ l-Volumenreaktionen, die leicht bis zu ml-Volumen zu präparativen Zwecken erweitert werden können, durchgeführt werden und ergeben in der Regel eine hohe Ausbeute. Die flexible Modifizierbarkeit des Systems ermöglicht die leichte Anpassung der Expressionsbedingungen für die Produktion funktionaler Membranproteine.

Das CF-System wurde im Rahmen des Dissertationsprojektes für die Entwicklung von Expressionsprotokollen von in Lipiddoppelschichten integrierten Endothelin B Rezeptoren (ETB) angewandt.

ETB als Teil der Familie G-Protein-gekoppelter Rezeptoren (GPCR) ist zusammen mit dem Endothelin A Rezeptor (ETA) ein Schlüsselfaktor für die Regulierung vieler physiologischer Prozesse im menschlichen Körper. Aufgrund der ubiquitären Expression dieser beiden Rezeptoren führt ihre Deregulation zu vielen pathologischen Effekten: u.a. systemischer und pulmonaler Bluthochdruck, Diabetes, Atherosklerose und sogar Krebs.

Physiologische Liganden von ETA und ETB sind die drei Endothelinpeptide ET-1, ET-2 und ET-3. Obwohl ETA und ETB eine sehr hohe Sequenzidentität aufweisen, zeigen sie eine unterschiedliche Affinität zu den genannten Endothelinpeptiden. ETB weist eine gleichmäßige nanomolare Affinität zu jedem ET auf, während ETA nur zu ET-1 und ET-2 eine solche erkennen lässt und eine mikromolare zu ET-3.

Für die Gewinnung funktionaler in Lipiddoppelschichten integrierten Rezeptoren wurden drei bekannte CF-Expressionsmodi getestet: der „precipitate“ Modus (P-CF), der „detergent“ Modus (D-CF) und der „lipid“ Modus (L-CF). Nach der Expression im P-CF bzw. D-CF Modus wurden in Detergens solubilisierte Rezeptoren posttranslational nach Entfernung des Detergens in Liposomen rekonstituiert. Im L-CF Modus wurden die Rezeptoren während der Reaktion kotranslational in Liposomen oder Nanodiscs inseriert.

Im P-CF Modus wurden 1-1,5 mg/ml ETB Rezeptoren produziert. Die Resolubilisierung in LMPG war quantitativ und die SDS-PAGE zeigte eine einzelne Bande mit dem Molekulargewicht von etwa 40 kDa nach der Reinigung der Probe durch eine Metallionenchelate-Chromatographie. Das gereinigte Protein wurde in Liposomen bei unterschiedlichem Protein-Lipid-Verhältnis nach der Entfernung des Detergens durch Biobeads rekonstituiert. Die höchste Bindungs- und Aktivitätsrate konnte bei einem Rekonstitutionsverhältnis von 1:1000 (Protein/Lipid) festgestellt werden. Durch die Anwendung eines Konkurrenzexperimentes mit Radioliganden wurde eine Inhibitionskonstante ( $K_i$ ) von 2,1  $\mu$ M für ET-1 ermittelt, während eine Dissoziationskonstante ( $K_D$ ) von 700 nM für den fluoreszent markierten ETB-Agonisten 4-Ala-ET-1 durch Fluoreszenzanisotropie errechnet wurde.

Nach der Expression des Rezeptors im D-CF Modus bei Vorhandensein des Detergens Brij78 ergaben sich zwei separate Banden, die in etwa 40 kDa und 35 kDa entsprachen. Analysen anhand von Western Blot wiesen Verkürzung am N-Terminus des 35 kDa ETB Derivats auf. *In vivo* ist eine spezifische Abtrennung der ersten 64 Aminosäuren von ETB durch eine Metalloprotease bereits dokumentiert worden. In der CF Reaktion konnte durch erhöhte EDTA-Konzentrationen die Menge des 35 kDa Produkts reduziert werden und die Edmann-Sequenzierung unterstützte die Hypothese, dass CF produziertes ETB durch Proteasen spezifisch an Position 64 geschnitten wird. Folglich unterstützt die Beobachtung, dass die Abtrennung von der sekundärstruktur des Rezeptors und nicht von der Aminosäuresequenz abhängt, die Annahme, dass ETB bei der Expression im D-CF Modus eine der nativen Konformation entsprechende Struktur annimmt.

Die trunkierte Variante  $\Delta$ ETB mit der Deletion der ersten 64 Aminosäuren resultierte in einer einzigen Bande nach D-CF Expression in Brij78 und ko-migrierte in der SDS-PAGE mit der unteren 35 kDa Bande des Volllängen-ETB Proteins.

Bindung zum ETB voller Länge bei einer Niedrigtemperatur-SDS-PAGE Analyse wurde ebenso festgestellt wie zur trunkierten Variante  $\Delta$ ETB. Außerdem belegte die Liganden-Affinitätschromatographie eine nahezu übereinstimmende Bindungsfähigkeit der zwei Formen des Rezeptors ETB.

Das Detergens Brij78, das für die direkte Solubilisierung des Rezeptors voller Länge im D-CF Modus gebraucht wurde, wurde durch die Metallionenchelate-Chromatographie vor der Rekonstitution des Rezeptors in Liposomen gegen ein anderes Detergens ausgetauscht. Dieser Vorgang wurde für verschiedene Detergentien wiederholt. Die Analyse der

Proteoliposomenaktivität durch Radioligand Bindungsexperimente ergab hohe unspezifische Bindung des radioaktiv markierten ET-1. Die besten Ergebnisse wurden mit ETB-Proben in 0.1% DPC als Zweitdetergens erzielt, wenn auch generell eine relativ geringe Aktivität vorlag.

Der L-CF Modus erlaubt die kotranslationale Insertion von ETB in vorgeformte Lipiddoppelschicht, ohne das Protein einem Detergens auszusetzen, das die funktionelle Faltung hemmen könnte.

Um die Optimierung der Reaktionsbedingungen zu beschleunigen, wurde ein ETB-sGFP Fusionsprotein erzeugt. Gefaltete fluoreszente ETB-sGFP konnte nur in Anwesenheit von Liposomen detektiert werden, während die Fusionsproteine nach der P-CF Expression vollständig zu einem nicht-fluoreszierenden Rückstand präzipitierten. Folglich ist der Nachweis von fluoreszierendem ETB-sGFP ein Hinweis auf eine Stabilisierung der synthetisierten Proteine durch die hinzugefügten Liposomen. Nach dem Hinzufügen vorgeformter, aus verschiedenen Lipiden zusammengesetzter Liposomen in die CF Reaktion wurde die sGFP Fluoreszenz nach der Expression gemessen. Bei Liposomen aus Aso-PC Lipiden wurde die maximale Fluoreszenzintensität gemessen, die annähernd 40 µg pro ml von ETB-sGFP entspricht. Während der Expression präzipitierten die hinzugefügten Liposomen zu einem fluoreszierenden Rückstand und die Untersuchung der Proben durch Konfokalmikroskopie ergab, dass sich eine heterogene Population von Liposomen mit einer Größe von 5-20 µm gebildet hatte. Gemäß der Radioligandenbindungsanalyse lag eine spezifische Bindung in der Größenordnung von 31-36% vor mit einem Bmax Wert von 3,5 pmol/mg. Die Zugabe von 2,5% Cholesterin zu den Liposomen ergab eine leichte Verbesserung der spezifischen Bindung und Aktivität von ETB-sGFP. Durch Modifikationen des L-CF Standardprotokolls (wie z.B. Veränderung der Temperatur der Reaktion und der Zugabe durch Detergentien destabilisierter Liposomen) konnten keine Effekte in Bezug auf die Modulation der Rezeptoraktivität nachgewiesen werden.

Zusätzlich wurde die Möglichkeit des Gebrauchs von Nanodiscs für den L-CF Expressionmodus getestet. Nanodiscs (NDs) sind diskoidale Membranstrukturen von 10-20 nm Durchmesser, die aus einem zweilagigen Lipidkern bestehen und von einem Gerüstprotein (*membrane scaffold protein* - MSP) umgeben sind.

Erstes Screening wurde mittels zweier verschiedener Typen von DMPC-NDs unterschiedlicher Größe (mit MSP1 bzw. mit MSP1E3D1) durchgeführt. Die NDs wurden der Reaktion in unterschiedlicher Konzentration hinzugefügt. Im Anschluss wurde die Fluoreszenz im Überstand bzw. Präzipitat quantifiziert. Die Menge an fluoreszierendem, löslichen ETB-sGFPs stieg mit

steigender Konzentration von MSP1E3D1-NDs im Reaktionsgemisch und erreichte ein Plateau bei einer Konzentration zwischen 60 und 180  $\mu\text{M}$ . Bei 40  $\mu\text{M}$  befanden sich alle fluoreszierenden ETB-sGFPs im Überstand. Die kleineren NDs, die mit MSP1 gebildet wurden, erzielten eine geringere Gesamtausbeute mit einem darüberhinaus geringeren Anteil in der löslichen Fraktion. Gemäß der sGFP-Fluoreszenz wurden annähernd 150  $\mu\text{g/ml}$  ETB-sGFP in MSP1E3D1-NDs synthetisiert und die Analyse durch Konfokalmikroskopie belegte die Bildung langer ND-Cluster im Präzipitat und eine bessere Homogenität im Überstand.

In einem weiteren Schritt wurde MSP1E3D1, das sich als effizienter als MSP1 erwies, beibehalten und mit NDs unterschiedlicher Lipide kombiniert. Im Falle von NDs mit POPC, BTE (brain total lipid extracts) und Aso-PC lag eine Reduktion der Ausbeute fluoreszierender ETB-sGFPs im Vergleich zu DMPC-NDs vor. Im Gegensatz dazu war die Ausbeute fluoreszierender ETB-sGFPs bei NDs, die aus anionischem Lipid-DMPG gebildet waren, zweimal höher als bei DMPC-NDs.

Dasselbe Screening wurde für die Expressionsoptimierung von ETA-sGFPs durchgeführt und ergab unter allen Bedingungen einen geringeren Ertrag als bei ETB-sGFPs. Zudem befand sich der Anteil fluoreszenter Proteine überwiegend im Präzipitat. Wie bei ETB-sGFP erwiesen sich jedoch auch bei ETA-sGFP die DMPG-NDs als besonders effizient.

Für die Bestimmung spezifischer Ligandenbindung an den Rezeptor konnten aufgrund des löslichen Verhaltens der NDs mehrere Techniken angewandt werden. Hierfür wurden jedes Mal DMPC-NDs mit MSP1E3D1 verwendet, weil die Bestimmung der spezifischen Ligandenbindung des Rezeptors an die DMPG-ND durch die hohe Interaktion des Liganden ET-1 mit DMPG verhindert wird.

Mithilfe des fluoreszenten Derivats Cy3-ET-1 wurde spezifische Bindung von ETB an MSP1E3D1-NDs (DMPC) festgestellt und an die 25% ligandenkompetenter Rezeptoren in der durch eine Metallionenchelate-Chromatographie gereinigten Probe ermittelt. Bei einer wiederholten Reinigung durch Größenausschlusschromatographie (SEC) wurde eine Konzentrationssteigerung aktiver Rezeptoren um bis zu 50% ermöglicht.

Der ELISA basierte Ligandenbindungstest erwies sich als geeignete ergänzende Methode zum Nachweis spezifischer Bindung an ET-1 und an die anderen beiden ETB-Agonisten ET-3 und 4-Ala-ET-1.

Um die Affinität der Bindung genauer charakterisieren zu können, wurde ein Radioligandenbindungsexperiment durchgeführt. In einem Sättigungsexperiment ergab sich ein  $K_D$  von 0,45 nM und ein  $B_{\text{max}}$  von 58.6 pmol/mg. Das homologe Konkurrenzexperiment ergab eine  $K_i$  von 6,1 nM.

Aufgrund der guten Löslichkeit des Rezeptor-Nanodisc-Komplexes konnten SPR Experimente als weiterer Untersuchungsansatz in Bezug auf die charakteristischen Eigenschaften der Ligandenbindung der Probe durchgeführt werden.

Für die Bestimmung der Bindungseigenschaften von ETA, ETB und ihren jeweiligen mit MSP1E3D1-NDs kotranslational verbundenen sGFP Fusionskonstrukten wurden 50 Resonanzeinheiten (RU) von ETA/ETB spezifischen Liganden b-ET-1 bzw. von ETB spezifischen Liganden b-ET-3 auf SA Biosensorenchips immobilisiert. Um die unspezifische Bindung der NDs mit der Dextranmatrix des Chips zu reduzieren, war eine extensive Pufferoptimierung erforderlich.

Sowohl für die IMAC gereinigten, als auch für die ungereinigten Proben der ETB-sGFP Rezeptoren wurden Werte von 0,4 beziehungsweise 0,5 nM als apparenter  $K_D$  für die Bindung an b-ET-1 ermittelt. Ähnliche Werte wurden für die nicht-fusionierten ETB Rezeptoren ( $K_D$  von 0,5 nM) und die trunkierte Variante  $\Delta$ ETB ( $K_D$  von 0,6 nM) bestimmt. Für ETA-sGFP IMAC gereinigte Proben ergaben sich für die Interaktion mit b-ET-1  $K_D$ -Werte von ungefähr 1,7 nM. Die beiden Rezeptoren unterschieden sich deutlich in ihrer Affinität zu immobilisiertem b-ET-3. Während ETB-sGFP weiterhin eine hohe Affinität mit einem  $K_D$  von 0,2 nM aufwies, betrug der  $K_D$  für ETA-sGFP 3,4  $\mu$ M. Die ermittelten Ergebnisse bestätigen frühere Beobachtungen, die andere Expressionssysteme für die in dieser Studie untersuchten GPCRs angewendet haben.

Da dieser Ansatz auf die Verwendung biotinylierter Liganden eingeschränkt ist, wurde ein Verdrängungsexperiment mit SPR entwickelt. Denn existierende Liganden sind entweder Derivate natürlichen ET-1, oder künstliche, nicht-peptidische Agonisten oder Antagonisten, die ein unterschiedliches Bindungsverhalten aufweisen und nicht in biotinylierter Form verfügbar sind. Für die Verdrängungsexperimente wurden die peptidischen, ETB spezifischen Agonisten 4-Ala-ET-1 und IRL-1620, sowie der ETA selektive Antagonist BQ-123 ausgewählt.

Für die Interaktion dieser Liganden mit in MSP1E3D1-NDs exprimierten ETA-sGFP und ETB-sGFP wurden in Konkurrenz zu den immobilisierten b-ET-1  $IC_{50}$  Werte im erwarteten Rahmen ermittelt.

In einem komplementären SPR Experiment wurde ein in MSP1E3D1-NDs kotranslational insertierter ETB-Strep markierter Rezeptor auf der Oberfläche eines mit anti-Strep Antikörpern gekoppelten CM5 Chips immobilisiert. Im Gegensatz zum Bindungsverhalten von BQ-123 konnte eine hohe Affinität von ET-1 und IRL-1620 an ETB beobachtet werden.

In ersten Experimenten unter der Verwendung zweier weiterer Methoden für die Echtzeit-



Messung der Bindung, die Thermophorese (microscale thermophoresis - MST) und das Octet-System, wurde abermals hohe Affinität im nM-Bereich beobachtet.

Eine weitere Aufgabe des Dissertationsprojektes war die Verifizierung der Fähigkeit des in NDs rekonstituierten ETB Rezeptors, die  $G\alpha$  Untereinheit nach der Inkubation mit einem Agonisten zu aktivieren. Als Teile der GPCR-Familie können ETA und ETB die Aktivierung heterotrimerer G-Proteine nach Stimulierung durch einen Agonisten induzieren. Durch die Ligandeninteraktion ausgelöste Konformationsänderungen bewirken Konformationsänderungen der zytoplasmatischen Domäne der Rezeptoren, was zur Dissoziation des heterotrimeren Komplexes und zum Austausch von GDP durch GTP in der  $G\alpha$  Untereinheit führt.

Überexpression der  $G\alpha$  Untereinheit *in vivo* stellt immer noch eine Herausforderung dar, weswegen das CF-Expressionssystem für die Expression von  $G\alpha_s$  und  $G\alpha_q$  angewandt wurden. Nach der Expression im P-CF Modus verblieb nur ein geringer Teil der beiden löslichen Proteine im Überstand, während der Großteil der Proteine präzipitierte. Durch den D-CF Expressionsmodus konnte eine höhere Löslichkeit der Proteine erreicht werden. Beim Screening verschiedener Detergentien wurde die höchste Produktionsrate mit Brij78 für  $G\alpha_s$  und Brij35 für  $G\alpha_q$  erzielt. Da Detergentien einen negativen Effekt auf nachfolgende Experimente mit NDs haben können, wurden nur die durch den P-CF Expressionsmodus gewonnenen löslichen Fraktionen verwendet. Aufgrund der höheren Produktionsrate wurden alle weiteren Experimente mit  $G\alpha_s$  durchgeführt.

Radioaktive Experimente mit GTP- $\gamma$ -S<sup>[35]</sup> und Fluoreszenzexperimente mit BODIPY-GTP- $\gamma$ -S wurden parallel durchgeführt, um zunächst die basale Aktivität von  $G\alpha_s$  zu verifizieren und anschließend den Aktivierungseffekt eines Agonisten oder Antagonisten zusammen mit dem in MSP1E3D1-NDs kotranslational insertierten ETB Rezeptor zu analysieren. Die ersten Experimente bestätigten für beide Methoden die Funktionalität des in CF produzierten  $G\alpha_s$ . In Abwesenheit von GDP wurde die zunehmende Inkorporation von GTP festgestellt. Im Gegensatz zum fluoreszenzmarkierten GTP wurde eine schnellere Inkorporation beim radioaktiv markierten Analog beobachtet.

Nach der Inkubation von ETB/NDs und ET-1 wurde in den Fluoreszenzexperimenten eine zunehmende Aktivität von  $G\alpha_s$  festgestellt. Im Negativkontrollexperiment wurde nach der Inkubation einer trunkierten Version von ETB, der ein Großteil der zytoplasmatischen Domänen fehlt, keine Steigerung beobachtet. Im komplementären radioaktiven Experiment konnte nach der Inkubation von ET-1 oder des Agonisten IRL-1620 keine zunehmende Aktivität von  $G\alpha_s$  verzeichnet werden. Bei derselben Methode wurde eine abnehmende Aktivität des G-Proteins bei Vorhandensein des Antagonisten IRL-2500 beobachtet und ein ähnlicher Effekt wurde in

einer Positivkontrollmembran, die exprimierte ETB Rezeptoren aufwies und mit G-Proteinen verbunden war, gemessen. Die durch unterschiedliche Experimente ermittelten Ergebnisse erfordern weitere Untersuchungen, um die Aktivierung von G-Proteinen durch Ligandenbindung genauer bestimmen zu können.

Die Analysen der gewonnenen Ergebnisse dokumentieren eine neue Methode, die beiden Endothelinrezeptoren ETA und ETB in einer bindungskompetenten Form zu produzieren. Die Insertion der Rezeptoren in Lipiddoppelschichten ermöglicht nicht nur die Untersuchung der Ligandenbindungseigenschaften von ETA und ETB, sondern auch die Bestimmung ihrer spezifischen Signalwege.

Darüber hinaus erlauben die Kombination der Zellfrei-Technologie mit SPR und die Durchführung von Experimenten mit Rezeptor/NDs-Komplexen ohne vorherige Reinigungsschritte das Hochdurchsatz screening von Liganden für GPCRs.

# 1. Introduction

## 1.1 Membrane proteins

Every biological membrane is characterized by a phospholipid bilayer structure, which consist of a hydrophobic core, formed by the fatty acyl tails of phospholipid molecules and a hydrophilic surface, formed by their polar head groups. Associated with the membranes are the membrane proteins (MPs). MPs can be divided in two groups: integral MPs that span the bilayer completely and peripheral MPs that are associated only to one side of the membrane. MPs are encoded by approximately 20-30% of open reading frame of an averaged genome and they have different functions like transporters, channels, receptors or enzymes (Wallin and Von Heijne 1998).

Two class of membrane spanning domains are present in integral MPs:  $\alpha$  helices and  $\beta$  barrels. The latter class is commonly found in transporters, MPs that allow the transport of ion and small molecules that cannot freely diffuse across the cellular membrane. These MPs are commonly present in the outer membrane of gram-negative bacteria (like *E. coli*) as well as in chloroplast and mitochondria.  $\beta$  barrels are mainly composed by beta-sheet organized in an anti-parallel way ( Schulz 2000).

In  $\alpha$  helix domains the amino acids are arranged in a right-handed helical structure that is stabilized by the formation of hydrogen bonds. Typical amino acids present in  $\alpha$  helix structures are methionine, alanine, leucine, as well as glutamate and lysine. Some amino acids are not suitable for the formation of  $\alpha$  helix like proline and glycine. The first disrupts or kink the helix, as it cannot form any hydrogen bond, the latter alters the structure due to is high conformational flexibility (Ulmschneider et al. 2006).

The presence of seven hydrophobic  $\alpha$  helices is a characteristic feature of a large group of integral MPs, the so called G-protein coupled receptors (GPCRs).

## 1.2 G-protein coupled receptors -GPCRs

GPCRs represent a vast and diverse family of cell-surface receptors, encoded by nearly 800 human genes, approximately 2% of the entire human genome (Fredriksson et al. 2003). These MPs play an important role in the transduction of extracellular signals into intracellular responses. GPCRs can respond to various molecules and stimuli, such as hormones, neurotransmitter, odorants, amino acids, nucleotides and light. Their diversity of action is also dictated by the possibility to activate various intracellular signaling pathways, via differential

coupling with specific heterotrimeric G-proteins.

GPCRs can be divided into 5 families based on sequence homology and function similarities: rhodopsin, secretin, adhesion, glutamate and frizzled-taste2 (Fig.1). The rhodopsin family is the largest one and is the most studied (Fredriksson et al. 2003). This family contains receptors for odorants, small molecules, light and peptides. The proteins that belong to this family are very heterogeneous concerning the primary structure, especially within the transmembranes (TMs) regions. Some conserved motifs in this family are the sequence DRY in TM3, CWxP in TM6 and NPxxY in the TM7 (Fritze et al. 2003, Rovati et al. 2007). A disulfide bridge is also commonly present in between the first and the third extracellular loops (ECLs) (Ji et al. 1998). This family can be further divided in 4 groups based on phylogenetic analysis (Fredriksson et al. 2003). The  $\alpha$ -group contains important drug targets like the receptor for histamine, serotonin and dopamine as well as the prostanoid receptor and muscarinic receptor. These receptors are able to bind biogenic monoamines in a binding pocket between the TM3, 5 and 6 (Strader et al. 1989). The  $\beta$ -group includes mainly receptors that are able to bind small peptides. Members of this group are the endothelin receptors, the oxytocin receptors and the gonadotropin releasing hormone receptors. TM regions, ECLs and N-terminal domain of the receptors are usually involved in the binding of the ligand (Lättig et al. 2009). The  $\gamma$ -group includes receptors for lipid-like compounds and peptides; opioid receptors, somatostatin receptors and the angiotensin receptors belong to this group. The  $\delta$ -group contains mostly olfactory receptors.

The secretin family is characterized by receptors with an extracellular hormone binding domain. The long N-terminal domain, that is approximately 60-80 amino acids in length, is crucial for ligand binding and it is stabilized by a network of disulfide bridges with cysteines present in the ECL1 and 2 (Grace et al. 2004).

The receptors that belong to the adhesion family are characterized by a long glycosylated N-terminal domain that contains adhesion like motifs, like cadherin, lectin and laminin, which may mediate cell-cell adhesion (Bjarnadóttir et al. 2004).

The GPCRs that belong to the Glutamate receptor family interact with their ligands in the long N-terminal domain. This region, which consists of two domains stabilized by disulfide bridges, binds the ligand through a mechanism that is often referred as "Venus flytrap" (Kunishima et al. 2000).

The frizzled family is characterized by long extracellular cysteine-rich domain, from 200 to 300 amino acids in length, which is important for ligand binding. Member of this family have a role in binding the glycoprotein Wnt (Dann et al. 2001). The Taste-2 receptors have a shorter N-terminal domain and they are involved in the sensation of sweet and bitter taste (Chandrashekar et al. 2000).

Specific ligands for GPCRs represent the largest family of pharmaceutical agents, accounting approximately for 30% of the current pharmaceutical market (Klabunde and Hessler 2002).

For a large fraction of GPCRs the physiological ligand is still unknown and in the last decade a lot of effort has been directed towards the “deorphanization” of these receptors. Starting from peptide ligands, and subsequently moving to lipid-like compounds, many GPCRs have been identified. Nevertheless, still 150 receptors that could be drug targets have yet to be characterized (Howard et al. 2001).

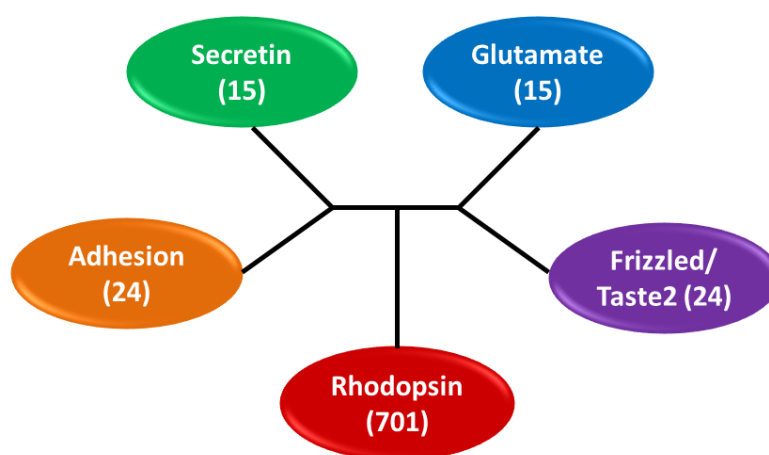


**Fig. 1: Phylogenetic tree representation of the human GPCR superfamily.** The GPCRs can be divided into five major families: Rhodopsin, Secretin, Adhesion, Glutamate and Frizzled/Taste2. The numbers in parenthesis indicate the members of each family.

### 1.3 GPCRs activation

Regardless the specific mode of ligand binding, the common result of an interaction of an agonist with a GPCR is a re-arrangement of the cytoplasmic domains of the receptor that induces heterotrimeric G proteins activation.

Heterotrimeric G proteins are composed by an  $\alpha$  subunit that is tightly associated with a  $\beta$  and a  $\gamma$  subunit (Fig.2). In humans there are 16  $G\alpha$  subunits that are divided in four main families based on primary sequence similarity:  $G\alpha_s$ ,  $G\alpha_q$ ,  $G\alpha_i$  and  $G\alpha_{12/13}$ , furthermore there are 5  $G\beta$  subunits and 11  $G\gamma$  (Hurowitz et al. 2000).

All the  $G\alpha$  subunits have two conserved domains: a GTPase domain and a helical domain. The

first is responsible for the hydrolysis of GTP and for the binding of the G $\beta\gamma$  dimer and effector proteins. The second domain consists of a six  $\alpha$ -helix bundle that covers the nucleotide binding pocket (Oldham and Hamm 2008). All the G $\alpha$  subunits are post-translationally modified with addition of the fatty acid palmitate at the N-terminal, whereas G $\alpha_i$  is also myristoylated (Chen and Manning 2001, Linder et al. 1993).

The G $\beta$  subunit is mainly composed by a  $\beta$ -propeller structure, with the exception of the N-terminal domain which adopts an  $\alpha$ -helical conformation, necessary for the interaction with G $\gamma$  (Wall et al. 1995).

The interaction of the G $\beta$  and G $\gamma$  subunit is very strong and can be dissociated only in denaturing conditions (Schmidt et al. 1992). Most of the different G $\alpha$ , G $\beta$  and G $\gamma$  subunits can interact with each other, suggesting that the expression levels of the different subunits and their cellular localization are important for regulate the specific signaling cascade (Graf et al. 1992).

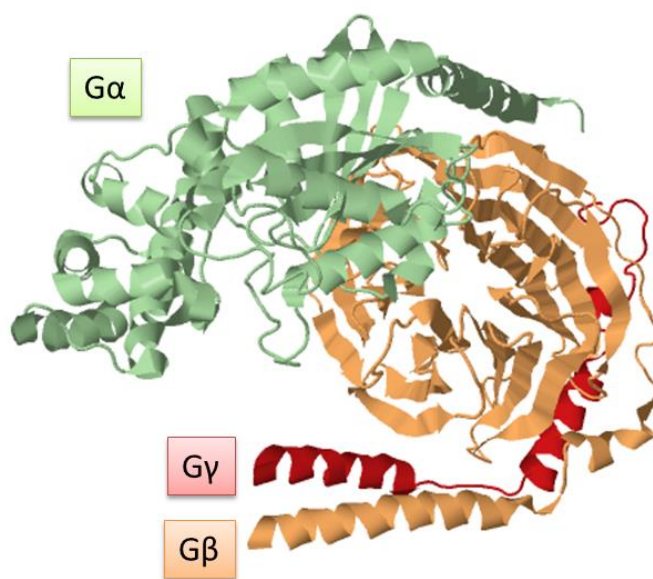


**Fig. 2: Crystal structure of the heterotrimeric G protein.** G $\alpha$  (green), G $\beta$  (orange), G $\gamma$  (red). Image created using Protein Data Bank data (PDB ID: 1GG2; Wall et al. 1995).

Two different models have been proposed in order to explain the interaction of the heterotrimeric G proteins with the receptor. In the “collision coupling model” (Tolkowsky et al. 1978) the heterotrimeric G proteins interact with the receptor only when it is in an active form, whereas in the “pre-coupled model” the G proteins can interact with the receptor before the binding of an agonist. Studies based on the overexpression of fluorescently labeled G proteins and receptors *in vivo* support the idea of a pre-coupling (Galés et al. 2006). Even though this model is attractive, it fails to explain the rapid signal amplification that occurs after ligand binding.

Upon binding of an agonist, conformational changes in the cytoplasmic domains of the GPCR induce the exchange of GDP to GTP in the  $G\alpha$  subunit and the dissociation of the  $G\beta\gamma$  complex (Fig. 3). Studies on G protein activation suggest that some  $G\alpha$  subunits may remain closely associated with the receptor, whereas others may dissociate (Digby et al. 2006, Gallés et al. 2005).

Different  $G\alpha$  subunits can activate different pathways (Marinissen and Gutkind 2001).  $G\alpha_i$  inhibits the adenylyl cyclase (AC) activity, decreasing the intracellular levels of cAMP. Most of the different isoforms can also activate  $K^+$  channels or inhibit  $Ca^{2+}$  channels.  $G\alpha_q$  activates the phospholipase C- $\beta$  (PLC- $\beta$ ). This event induces the hydrolysis of phosphatidyl 4,5-diphosphate (PIP<sub>2</sub>) into two second messengers, inositol 1,4,5-triphosphate (IP<sub>3</sub>) and diacylglycerol (DAG), causing an increase in intracellular  $Ca^{2+}$  concentration.  $G\alpha_s$  proteins activate AC, leading to the production of cAMP. Members of the  $G\alpha_{12/13}$  family can activate different effectors, like the Rho family GTPase proteins that are involved in cell migration (Fig. 3).

$G\beta\gamma$  complex can also activate some downstream effectors, like  $K^+$  channel, AC or PLC- $\beta$  (Fig. 3). The termination of the signal is caused by the subsequent hydrolysis of GTP to GDP, this event induces the reassociation of the heterotrimeric complex and the end of the cycle.

Many accessory proteins can regulate the exchange of GDP into GTP and the hydrolysis of GTP itself, allowing a finer tuning of the G proteins signaling (Siderovski and Willard 2005). GEFs (guanine nucleotide exchange factors) and GDIs (guanine nucleotide dissociation inhibitors) act in opposite ways, GEFs induce the exchange of GDP to GTP, GDIs stabilize the  $G\alpha$  proteins in an inactive GDP bounded state. GAPs (GTPase-activating proteins) antagonize the GEFs, accelerating the hydrolysis of GTP and promoting the re-association of the heterotrimeric complex.

Activation of GPCRs can also lead to heterotrimeric G proteins independent signaling pathways. These events can be mediated by the PDZ scaffolding proteins or the  $\beta$ arrestin transducer (Tilley 2011).

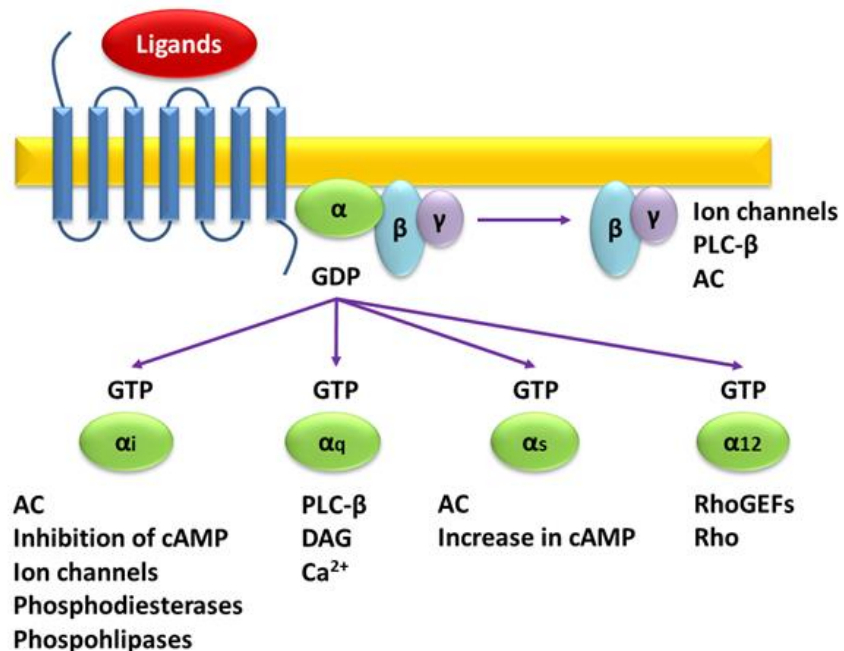


**Fig. 3: Signaling pathways activated by heterotrimeric G proteins.** Upon activation of a GPCR by an agonist, GDP is exchanged into GTP in the G $\alpha$  subunit and different down stream effectors are modulated. AC: adenylyl cyclase; PLC- $\beta$ : phospholipase C- $\beta$ ; DAG: diacylglycerol. Adapted from (Marinissen and Gutkind 2001).

#### 1.4 GPCRs trafficking

Like many other MPs, GPCRs are synthesized by ribosomes associated to the cytosolic face of the endoplasmic reticulum (ER). The insertion of the TM domains in the lipid bilayer is accomplished by the translocation complex (translocon), and is mediated by the presence of an N-terminal signal sequence in the nascent protein. As soon as this element is translated in the ribosome, it is recognized by the signal recognition particle (SRP) that binds the sequence in a hydrophobic pocket (Janda et al. 2010). This event, which occurs exactly at the exit tunnel of the ribosome, prevents the exposure of the hydrophobic sequence to the cytosol and transiently slows down the translation (Wild et al. 2004). The SRP-ribosome complex is recognized at the ER membrane by the SRP receptor and transferred to the Sec61 translocation channel. This channel recognizes the TM domains of the protein and transfers them in the lipid bilayer through a lateral access (Grudnik et al. 2009, Keenan et al. 2001).

Correctly folded proteins are collected in vesicles coated with the coat protein (COP)II. The proteins can then move from the ER to the Golgi complex where they are sorted to the plasma



membrane or targeted for degradation to the lysosomes (Barlowe 2003).

On the cell surface, upon ligand binding, the termination of the GPCRs signaling occurs via an internalization of the receptors. The GPCRs are phosphorylated at the C-terminal domain by members of the GPCR kinases (GRKs). This event allows the recruiting of  $\beta$ -arrestin that prevents any further interactions with heterotrimeric G proteins and induces the clustering of the receptors into clathrin-coated pits (CCPs). The CCPs form vesicles that are separated from the plasma membrane by the GTPase dynamin and internalized towards the endosomal compartment. From this compartment they can be directly degraded into the lysosomes, recycled back to the cell surface or retained, slowing down the process of degradation or recycling (DeWire et al. 2007, Moore et al. 2007)

### **1.5 GPCRs dimerization and oligomerization**

Oligomerization and dimerization of GPCRs are important events that can regulate receptor function, ligand binding properties and trafficking. Biochemical techniques, like receptors crosslinking, in combination with biophysical methods, like bioluminescence resonance energy transfer (BRET) and fluorescence resonance energy transfer (FRET), demonstrate that many GPCRs form homodimers. Computational studies suggested that TM domains are important for the dimerization process, in particular contact interfaces include TM5 and TM6, and possibly TM2 and TM3 (Gouldson et al. 2000). For some receptors, the dimerization process takes place during the biosynthesis in the ER. Some examples are the oxytocin receptor and the vasopressin receptors V1a and V2 (Terrillon et al. 2002). Occasionally, the presence of an agonist is required for the formation of dimers on the cell surface. For instance, the recorded BRET signal for the  $\beta$ 2-adrenergic receptor is increased of two times when an agonist is present (Angers et al. 2000). Heterodimerization between two closely related receptor subtypes is also possible. This event can result in a new receptor with enhanced ligand binding capabilities, as in the case of the  $\delta$ - $\kappa$  opioid receptor (Jordan and Devi 1999).

This process can also occur between two unrelated GPCRs that are responsive to different ligands. In this case the heterodimerization does not alter the ligand binding properties of the two receptors or the specific G protein activation but affect the receptors trafficking (Jordan et al. 2001).

Even though dimerization and oligomerization are important for the function of many receptors, it is still unclear if they are essential events for all the GPCRs.

## 1.6 The endothelin system

The endothelin ligand ET-1 was isolated for the first time from cultured porcine aortic endothelial cells (Yanagisawa et al. 1988). This 21 amino acids peptide is characterized by two disulfide bridges, one between the cysteines in position 1 and 15, another between the cysteines in position 3 and 11 (Fig. 4).

Within one year from its discovery, two related peptides were found in human, endothelin-2 (ET-2) and endothelin-3 (ET-3) (Inoue et al. 1989). These two peptides differ from ET-1 by two and six amino acids, respectively (Fig. 4).

The endothelins are particularly important for the regulation of blood pressure and they are implicated in vascular disease of several organ system.

The main sources of ET-1 are the endothelial cells, where the production is regulated at the level of peptide synthesis. Many factors can alter the expression of the ET-1 gene. Growth factors, adrenalin, vasopressin, and cytokines increase the expression of ET-1; in contrast, a reduction can be induced by prostacyclin, natriuretic peptide and heparin (Stow et al. 2011). In the vascular system the most important factor that regulates the release of ET-1 is the pressure and blood flow in the vessels. Vasodilatation induces the activation of the shear stress receptors of the endothelial cells and the subsequent release of nitric oxide induces a decrease in the production and in the secretion of ET-1 (Griffith et al. 1988).

All endothelins are synthesized from precursors called pre-pro-endothelins. The first cleavage by edopeptidase leads to the pro-endothelin that undergoes a second modification by mean of metalloendopeptidases, known as endothelin-converting enzymes (ECEs), finally leading to the production of the functional peptides. These enzymes are present on the cell surface of the smooth muscular cells in blood vessels as well as in the cytoplasm of the endothelial cells (Davenport and Maguire 2006).

ET-1 is not a circulating hormone, in fact its concentration in plasma is around 1 pM (Battistini et al. 1993) and once released it acts directly on the underlying surface of the smooth muscular cells. This peptide has also a very short life in blood due to the presence of endothelin degrading enzymes that metabolize it in an inactive form (Davenport and Maguire 2006).



**Fig. 4: Sequence alignment of the three physiological endothelin peptides and the structure of ET-1 (right).** Changes in the amino acids sequence compared to ET-1 are enlightened in green. Disulfide bridges are indicated. The crystal structure of ET-1 was obtained in PDB, ID: 1EDN (Janes et al. 1994).

### 1.7 The endothelin receptors

In 1990 two endothelin receptors were identified, ETA (Arai et al. 1990) and ETB (Sakurai et al. 1990). These two receptors present the characteristic GPCR features: seven transmembrane domains in length of 20-27 hydrophobic amino acids residues, a signal sequence on the extracellular N-terminal domain, a cytoplasmatic C-terminal domain and the ability to activate heterotrimeric G proteins upon ligand binding.

Despite 59% of amino acids identity, these two receptors show different affinity for the three endothelin peptides; ETB has equal nanomolar to picomolar affinities for both ET-1 ET-2 and ET-3, whereas ETA exhibits an affinity for ET-3 that is two orders of magnitude lower than for ET-1 or ET-2 (Nakajima et al. 1989).

These receptors can couple with many members of the G proteins family ( $G\alpha_s$ ,  $G\alpha_q$ ,  $G\alpha_i$  and  $G\alpha_{12/13}$ ) and the specific activation pathway depend by the cell type in which ETA and ETB are expressed. (Boualleque et al. 2007).

Almost every cell in the body expresses at least one of the endothelin receptors and for this reason they are widely distributed in many organs (Table 1).

TISSUE	ET-1	ETA	ETB
Endothelial Cells	+		+
Smooth muscle cells		+	+
Cardiomyocytes	+	+	+
Hepatocytes	+	+	+
Renal collecting-duct cells	+		+
Neurons	+	+	+
Osteoblast		+	+
Keratinocytes	+	+	+
Adipocytes		+	+

**Table 1: Tissue specific expression of ET-1 and of the two receptors ETA and ETB.** (+) indicates the presence of the ligand or of the receptors (Adapted from Kedzierski and Yanagisawa 2001).

In the vascular system, ETA and ETB receptors that are located on the surface of vascular smooth muscle cells are responsible for maintaining the physiological vascular tone (Fig. 5). In this system ET-1 induces also the proliferation of vascular endothelial cells, vascular smooth muscle cells and fibroblast (Golfman et al. 1993). In the heart ETA is predominantly expressed in myocytes, whereas ETB is expressed more heterogeneously. The activation of the receptors has a positive inotropic and chronotropic effects (Russell and Molenaar 2000). In the lungs ETA is expressed in the muscular media of pulmonary arteries, ETB in the media and intima, as well as in the endothelial cells (Soma et al. 1999). Activation of both receptors results in vasoconstriction, whereas activation of ETB alone leads to bronchoconstriction (Nagase et al. 1997). In the kidneys the two receptors are particularly expressed in the renal medulla at the ratio about 1:2, where they have an important role in controlling blood pressure and in regulating sodium and water excretion (Kohan 2009). ETA and ETB have also an important role during inflammatory processes. ET-1 has proinflammatory properties, it is required for T-Cell homing to the lungs, and it is necessary for endotoxin induced inflammation (Sampaio et al. 2004). ET-1 can also induce the transcription of the factor NF- $\kappa$ B via the ETB receptor in monocytes, inducing the production of proinflammatory molecules (Nett et al. 2006).

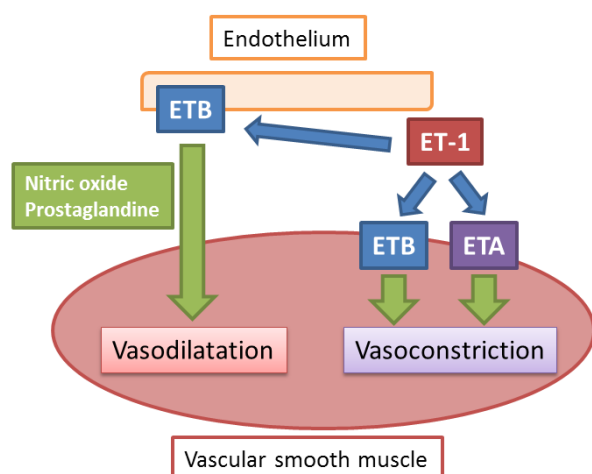


**Fig. 5: Role of ETA and ETB receptor in the vasculature.** ETA and ETB receptor localized on the surface of the vascular smooth muscle cells mediate the potent vasoconstrictor effect upon binding to ET-1. ETB receptor poses a dual role, as the activation of the receptor located in the endothelium induce the production of nitric oxide and prostaglandines, promoting vasodilatation on the underlying smooth muscle (Adapted from Schneider et al. 2007).

Due to the virtually ubiquitous expression of the endothelin ligands and receptors in the human body, many pathological conditions derive from a deregulation of this system. Pathologies like systemic and pulmonary hypertension have been correlated with increased production of ET-1 and the plasma concentrations of the ligand have been clearly correlated with the severity of the pulmonary pathology (Yoshiyashi et al. 1991). Different studies also proposed the involvement of ET-1 in renal diseases. In particular, the endothelin system is involved in the development and in the progression of the acute, as well as chronic, renal failure (Abassi et al. 1993). Furthermore, it has a role in mediating the nephrotoxic effects of cyclosporin, a potent immunosuppressive agent mostly used to prevent allograft rejection (Papachristou et al. 2010). Many vascular diseases are also associated with the proliferative response induced by ET-1 and the plasma level of the ligand correlates with the gravity of the pathology in the atherosclerotic disease (Lerman et al 1991). In chronic heart failure, the systemic neurohumoral reflex that is activated in order to maintain the cardiac output, organ perfusion and circulatory homeostasis, induces also an increase of ET-1 production, which has an overall long-term negative effect on the heart due to an increase in the peripheral vascular tone (Miyachi and Goto 1999). Strong evidences also suggest the involvement of the endothelin system in the growth and progression of many tumors. Different human tumor cell lines are able to over express ET-1, as well as the ETA and ETB receptors, and elevated plasma level of the ligand have been detected in patient with different kinds of solid tumor (Grant et al. 2003). Up regulation of ligand and receptors induce tumorigenesis and malignant progression through activation of pathways that lead to cell proliferation, inhibition of apoptosis, matrix remodelling, new vassels formation, invasion and metastatic dissemination (Nelson et al. 2003).

### 1.8 Endothelin receptors dimerization

The first hypothesis of an interaction between the ETA and the ETB receptor was postulated in 1997 (Ozaki et al. 1997). Ozaki and coworkers observed that cells expressing both receptors had different responses upon incubation with selective ETA or ETB ligands in comparison with cells expressing only one of the two receptors (Ozaki et al. 1997). Further studies in astrocytes, where the two receptors have an important role in the clearance of ET-1, confirmed a dimerization process, as the addition of selective antagonists for both receptors was necessary for blocking ET-1 uptake (Jensen et al. 1998). The possibility that ET-1 acts as a bivalent ligand was also proposed, in this case the peptide would form a bridge between the two receptors, with its N-terminal part binding ETA and its C-terminal part interacting with ETB, explaining the dimerization as a ligand-dependent process (Harada et al. 2002). Subsequent studies, based on FRET analysis and co-immunoprecipitation experiments, proposed also an alternative theory suggesting that the dimerization process is a constitutive event that occurs on the plasma membrane even in absence of ligand (Evans and Walker 2008).

### 1.9 Post-translational modifications of the endothelin receptors

Addition of post-translational modifications is a necessary step during the *in vivo* biosynthesis of proteins. These modifications are necessary for the protein to reach a mature state and they can have an effect on functionality, cell localization and modulation of interactions with other partner proteins. For both ETA and ETB receptors, different post-translational modifications have been identified (Fig. 6).

Palmitoylation consists in a covalent attachment of a palmitic acid to one or more cysteine residues, located on the cytoplasmatic tail of the GPCR, via a thioester bond. For ETB, at least two of the three cysteines 402-403-405 located in the cytoplasmatic tail, are subjected to palmitoylation *in vivo* (Okamoto et al. 1997); for the ETA receptor, the cysteines 383-385-386-387-388 are subject to palmitoylation (Horstmeyer et al. 1996). Site direct mutagenesis experiments showed that this post-translational modification was not required for a correct cell surface localization of the receptors, ligand binding abilities or internalization but was critically involved for the correct coupling with G proteins (Horstmeyer et al. 1996, Okamoto et al. 1997,). In COS cells transfected with the receptors, the unpalmitoylated mutant of ETB completely lost any G proteins coupling ability, whereas the ETA mutant was still able to bind  $G\alpha_s$ . For the palmitoyl deficient ETA receptor extracted from Sf9 cells and reconstituted in phospholipidic vesicles, a reduction in the activation  $G\alpha_i$  and  $G\alpha_q$  was observed, whereas no differences,

compared to the wild-type receptor, were shown in the ability to activate  $G\alpha_o$  (Doi et al. 1999). Phosphorylation of serine and threonine residues appears to be important for the desensitization process. Two different kinases are involved in the process. The GRKs mediate agonist dependent homologous desensitization, whereas second messengers dependent kinases like the cAMP-dependent-protein kinase or the protein kinase C are responsible for the heterologous desensitization (Kohout 2003). For both ETA and ETB receptors many phosphorylation sites have been predicted (Roos et al. 1998), but a detailed analysis is still missing. The serine in position 304 in the ETB receptor could be particularly important as missense mutation in this amino acid is involved in the onset of Hirschsprung 's disease (Auricchio et al. 1996).

GPCRs usually have one or more glycosylation sites in their N-terminal extracellular domain. Glycosylation is usually important for receptor localization and ligand binding (Wheatley and Hawtin 1999). Although ETB contains a glycosylation site in position asparagine 59 (Roos et al. 1998), there is no evidence for an actual glycosylation. For instance, mutation of this residue didn't change the receptor behavior in Sf9 cells (Doi et al. 1997). For the ETA receptors two glycosylation sites have been identified (asparagine 29 and 62) (Hashido et al. 1992). De-glycosylation of the ETA receptor in rat cerebellar and atrial membranes did not alter the affinity for the ligand ET-1 (Shraga-Levine and Sokolovsky 1998).

Disulfide bridges formation plays an important role in the folding and the stability of GPCRs (Dohlman et al. 1990). A disulfide bond is also found in ETA (Cys158-Cys239) and ETB (Cys174-Cys255) (Haendler et al. 1993) but the effective role of this post-translational modification in these receptors is still unclear. In cell membrane preparations from *E. coli* transfected with ETA and ETB mutants, where the cysteines were mutated into alanines, no specific ET-1 binding was detected, leading to the possibility that the receptors were not active or were not correctly localized on the cell surface (Haendler et al. 1993). Expression of ETA and ETB in cell-free system in reducing condition, in absence of disulfide bridges, led to the production of functionally active receptors (Junge et al. 2010, Klammt et al. 2007)

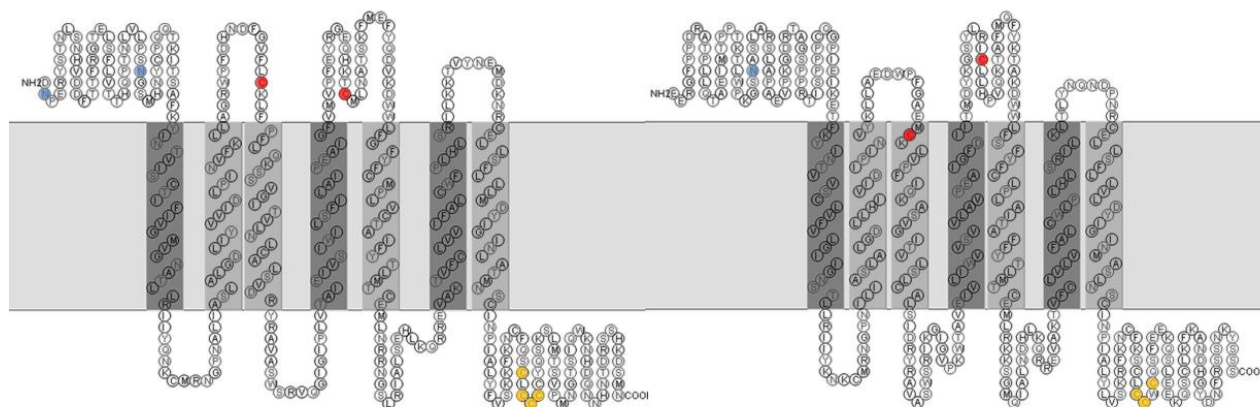


**Fig. 6: Topological model of human ETA (left) and ETB (right) receptors.** The two receptors contain seven transmembrane helices, as well as three extra- and three intra-cellular loops. The extracellular loops and the long N-terminal domain are important for the binding of the ligand; the intracellular loops are involved in the heterotrimeric G protein activation. Important residues have been enlightened. Red: cysteines involved in the formation of potential disulfide bonds. Yellow: palmitoylation sites. Blue: potential glycosylation sites. Secondary model obtained using SOSUI (“classification and secondary structure prediction of membrane proteins” <http://bp.nuap.nagoya-u.ac.jp/sosui/>). Primary sequence obtained from Swissprot (<http://www.uniprot.org/>). ID: P25101 (ETA); P24530 (ETB).

### 1.10 Current insight into ligand-receptor interaction

The molecular basis of the recognition of the endothelin peptides to their receptors is still not completely understood. Nevertheless, valuable information has been obtained using mutated or truncated versions of the ligands. Differences in affinity for the three endothelin isoforms can be explained by single amino acid mutation. The presence of the amino acid serine in position 2 of ET-1 and ET-2 is necessary for the high affinity binding with ETA (Galatino et al. 1995). Furthermore, the presence of the residues 9-21 is sufficient for the interaction with the ETB receptor, as ET analogues truncated in the N-terminal domain, from amino acid residues 1 to 8, still retain high affinity (Saeki et al. 1991). Disulfide bonds formation in the endothelin peptides is essential for the specific binding to ETA but not ETB, in fact, the ET-1 analogue [1,3,11,15-Ala]-ET-1 is still able to bind the ETB receptor with very high affinity (Saeki et al. 1991).

In order to define which parts of the receptors are crucial for the ligand affinity and selectivity, many chimeric ETA-ETB receptors have been generated, as well as different truncated versions of the two receptors. Using computational and experimental methods, Lättig and coworkers in 2009 were able to identify four different epitopes on the ligands (1L-2L-3L-4L) and four complementary domains on the receptors (Ar-Br-Cr-Dr) that could explain specific ligand



binding (Fig. 7). The four epitopes on the ligands are two selectivity providing regions (1L and 2L), from the residue 1 to residue 10, one high affinity binding region (3L), composed of the hydrophobic residues from position 11 to position 15 and the minimal ligand region (4L), from residue 16 to 21. In the same way, four distinct interaction sites have been identified on the receptors: a purely hydrophilic domain (Ar), that comprise the tunnel shaped entrance in ETA and the funnel like entrance in ETB, a charged edge like domain within the ECL2 (Br), a hydrophobic domain (Cr), that is located at the junctions of ECL1 with TM2 and TM3, and a transmembrane binding cleft domain (Dr), that is located in between TMs 2, 3, 5, 6 and 7. The interaction 1L-Ar is the main selectivity filter, 2L-Br provides additional feature for selectivity and separates agonist from antagonists, 3L-Cr is important for the high affinity binding and 4L-Dr modulates receptor activation and inhibition (Lättig et al. 2009).

Although these studies provided important information on receptor selectivity and affinity, detailed structural analysis are still required for defined which specific amino acids are involved in binding process.

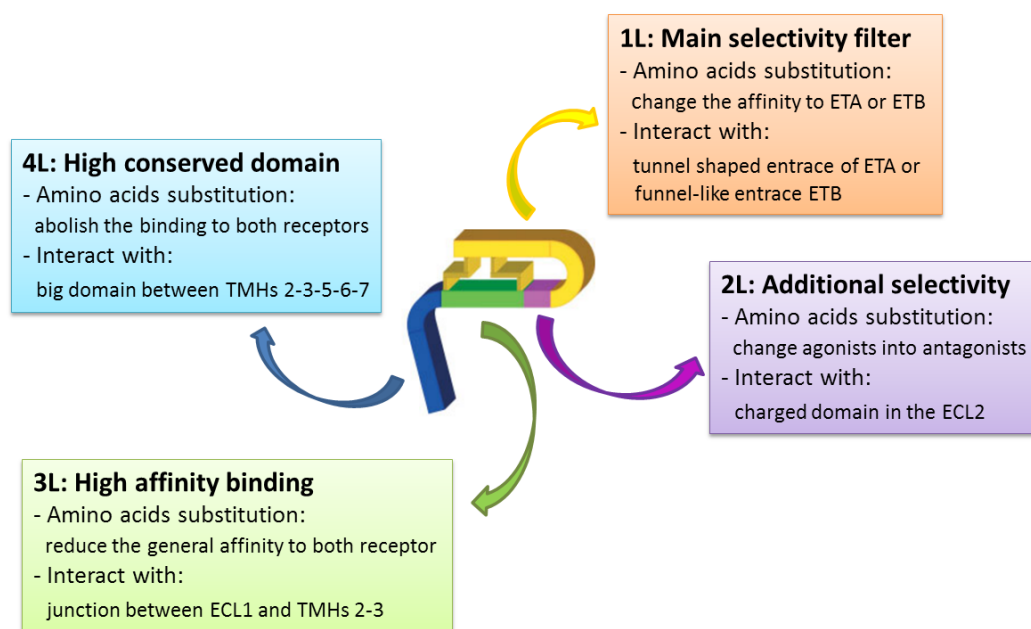


**Fig. 7: Overview on the ligand binding domains of ET-1.** Four different domains can be identified on ET-1. Yellow: 1L (amino acids 1-7); Purple: 2L (amino acids 8-10); Green: 3L (amino acids 11-15); Blue: 4L (amino acids 16-21). TMH: transmembrane helix. Each domain has a specific role in the binding and it is able to interact with different regions on the ETA or ETB receptor (Figured adapted from Lättig et al. 2009).

### 1.11 Endothelin receptors antagonism

Currently, experimental and clinical evidences support the importance of developing drugs that can block the production or the action of the endothelins. The benefits in using a selective antagonist or a non-selective one are still under evaluation for many human diseases.

ETA selective blocking proved to be, in many cases, the most effective treatment, as it induces a dilatation of the vessels and a removal of the excess of ETs from the circulation (Kusserow and Unger 2004). A well studied antagonist for the ETA receptor is Ambrisentan. This clinically available antagonist that shows 100 fold selectivity for ETA, is a orally active molecule that has been effective for the treatment of pulmonary arterial hypertension (D'Alto 2012). Sitaxsentan, an even more selective ETA antagonist, have been approved in Europe, Canada and Australia but not in the USA, due to cases of fatal hepatic failure (Lee et al. 2011).

For the ETB receptor, few antagonists have been developed, reflecting the limited clinical need for these compounds. Selective blocking of ETB usually leads to hypertension and reduced clearance of pulmonary ET-1 (Kirkby et al. 2008). Nevertheless, recent studies are now exploring the possibility to use ETB selective antagonists, like the peptidic BQ-788 and the non-peptidic A-192621, in cancer therapy. (Paolillo et al. 2010).

Administration of non-selective antagonists has proved to inhibit the vasoconstriction induced by ET-1 more effectively than by an ETA antagonist alone (Sato et al. 1995), but causing at the same time a reduced clearance of the circulating ET-1 due to ETB blockage.

One well characterized non selective ET-receptor antagonist is Bosentan. This molecule, that shows 20 to 50 fold selectivity for ETA, was the first ERA (endothelin receptor antagonist) approved in human clinical trials. Clinical studies have demonstrated that administration of this drug to patients with severe chronic heart failure improve their cardiac performance via an increase of pulmonary and peripheral vasodilatation (Davenport and Maguire 2002).

### 1.12 Cell-based systems for the heterologous expression of GPCRs

High level production of recombinant GPCRs is still a challenging task. Various aspects of protein folding and stability are not fully understood and a rational approach to heterologous expression is still missing.

Different hosts can be used for the over production of GPCRs, eukaryotic system as well as prokaryotic system, each one with its own advantages and drawbacks.

One of the most common overexpression system is based on *E. coli*. The major advantages are the low cost, the ease of use and the general fast growing rates that enable a rapid expression

optimization. However, this system has also some major drawbacks. For examples there are no specific G proteins or interacting proteins that can aid the correct GPCR folding, and the machinery for post-translational modification like glycosylation are entirely missing, reducing the number of possible expressed GPCRs. In *E. coli* the expression could be directed to inclusion bodies or to the cell surface. In the first case there are some added advantages like a reduction in the toxicity of the expressed heterologous proteins and the theoretical possibility to produce higher amounts. However, in order to achieve correctly folded receptors, refolding methods are then required. This refolding of a GPCR from inclusion bodies is a very challenging task. Information regarding the different factors that affect folding and refolding are still lacking and, as a matter of fact, in the past 15 years only 5 GPCRs have been correctly refolded from inclusion bodies (Banères et al. 2011).

Expression on the cell surface is in general achieved by fusion of the GPCRs with tags that target the protein to the periplasmic membrane. Some examples are the maltose binding protein, the outer membrane protein LamB and the alkaline phosphatase. An integral membrane protein from *Bacillus subtilis*, Mistic, has also been reported as a useful partner for cell-surface expression of various GPCRs (Roosild T. et al. 2005).

Nevertheless, the yields of cell surface expression are usually very little and large coulters are therefore necessary to obtain enough proteins for biophysical studies. Low cell surface expression of the ETB receptor has been previously reported (Haendler et al. 1993).

Another system for the overexpression of GPCRs is based on yeast. This system combines fast growth rates and folding capabilities. Post-translational modifications are possible in this system as well as disulfide bridges formation. Different yeast strains have been successfully used like *Saccharomyces cerevisiae*, *Pichia pastoris* and *Schizosaccharomyces pombe*. As expression of GPCRs has usually a toxic effect on the host cells, the production is controlled using inducible promoter like GAL (Mollaaghababa et al. 1996) or alcohol oxidase I (AOX1) (André N. et al. 2006). Altering the culture conditions, for example reducing the temperature, could increase the total yields. Furthermore, addition of antagonist or co-expression of different accessory proteins was in some case beneficial for increase the amount of functionally folded receptor (Fraser et al. 2006). The Limitations of this system are the non uniform glycosylation of the receptor that can lead to problem during crystallization trials. Furthermore, the lipid composition of the yeast membrane differs from the mammalian one with the presence of ergosterol instead of cholesterol. Regarding the endothelin receptors, this system has been effectively used for the production of the ETB. Expression in *Pichia pastoris* under the control of AOX1 promoter lead to the production of 60 pmol of receptor per mg of crude membrane and high specific binding of ET-1 was detected (Schiller et al. 2010).

In the insect cells system the first step for the overexpression process is the production of viruses that contain the MP coding sequence in a non-essential region of the genome via homologous recombination. The obtained recombinant viruses are then used for the infection of the insect cells and the production of the target protein is achieved (Fraser et al. 1992).

Using insect cells for the production of heterologous MPs has some major advantages, like the possibility to obtain post-translational modification that are similar to the mammalian cells (except for glycosylation), as well as generally correct disulfide bonds formation. The most commonly used insect cells line, Sf9, constitutionally express some G proteins, like  $G\alpha_s$  and  $G\alpha_q$ , and this can have a positive effect on ligand binding or correct GPCRs folding (Kleymann et al 1993). Different from mammalian cells, insect cells plasma membrane is composed mainly of unsaturated lipids and contains very low amount of cholesterol (Marheineke et al. 1998). Some drawbacks of this system are the very time consuming procedure that is needed for the production of high-tier viral stock for the infection of the cultures as well as variable post-translational modification that give rise to a heterogeneous population of MPs. The two endothelin receptors were successfully expressed in Sf9 cells, at about 100 pmol per mg of crude membrane. High specific binding of ET-1 was detected and unlysed cells showed an increase of intracellular  $Ca^{2+}$  concentration upon incubation with the ligand (Doi et al. 1997).

Using a mammalian cell system GPCRs can be expressed in native condition, with all the necessary chaperones and post-translational modifications. Expression can be transient or stable under selective conditions. Even though some cell lines, like HEK293, can be grown in suspension and scaled up for fermentation, high levels of GPCRs expression are usually toxic for the cells. Inducible system (Chelikani et al. 2006) or the use of the Semliki forest virus vector (Hassaine et al. 2006) can provide for some GPCRs enough quantities for structural determinations. In general mammalian cells systems are costly and time consuming and mostly used for functional and small scale biophysical studies.

### **1.13 Cell-Free expression system**

Cell-Free (CF) expression system has emerged as a powerful technique for the general production of MPs. This system is based on crude lysates obtained from prokaryotic as well as eukaryotic cells and contains all the necessary elements for transcription, translation, protein folding and energy metabolism. The synthesis of the target protein starts upon incubation of the cell extract with essential substrates, like DNA or mRNA template, amino acids, nucleotides, energy substrates and cofactors and continues until one of the substrates is depleted or toxic

byproducts reach inhibitory concentrations.

Compared to conventional *in vivo* approaches, the CF system has some key advantages. The expression of the target proteins can be accomplished in small  $\mu\text{l}$  volumes of reaction for analytical purpose and can be easily scaled up to ml volumes for preparative expressions. The production efficiencies are generally very high, up to mg of expressed protein for ml of reaction, and the possibility to add chemicals chaperones or other stabilizing compounds directly in the reaction allows modulating the quality of the expressed proteins. Many general problems that arise from the expression of MPs in *in vivo* systems, like possible toxicity of the expressed protein or inefficient targeting and translocation to the cell membrane are avoided. Different template can be used for the expression like plasmid DNA, PCR products as well as mRNA. CF expression systems from prokaryotic and eukaryotic sources have been developed and protocols for their preparation have been published (Table 2).

Two different CF configurations have been established. In the batch configuration the reaction is carried out in a single compartment and is particularly useful for analytical purpose, where the expression can be done in multiwall plates and the whole process can be automated using pipetting robots. The expression yields are usually low and the reaction time is limited for few hours, as soon as toxic byproducts reach inhibitory concentrations. Reaction time can be extended and yields of expression increased using a continuous exchange (CECF) configuration (Spirin et al. 1988). In this case the reaction is separated into two compartments by a semi-permeable membrane with a molecular weight cut-off between 10 and 50 kDa. In one compartment the reaction itself takes place, the reaction mixture (RM) contains the cell extract and all the other high molecular weight compounds, like the template and the necessary enzymes. The feeding mixture (FM), in the second compartment, provides the low-molecular weight precursor as well as energy sources. Vigorous shaking or stirring allow an efficient exchange of substances between the two compartments, providing a continue supply over time of necessary compounds for the reaction as well as diluting toxic byproducts. A volume ratio RM:FM between 1:10 and 1:50 allows the expression for several hours, resulting in high yields of expressed protein.

CF extract source	PTM	cT7	Yield [mg/ml]	MP	Kit	Protocol
<b>Eukaryotes</b>						
Human HeLa S3 cells	+	+	0.05 - 0.2	n.a.	+	Mikami et al. 2006
CHO			≤ 0.01			Mikami et al. 2008 Witherell et al. 2001
Rabbit reticulocytes	+	+	≤ 0.01	+	+	Arduengo et al. 2007 Craig et al. 1992
Wheat Germ	+	+	≤ 2 CECF 0.1- 0.4 B	+	+	Endo et al. 2005 Madin et al. 2000, Sawakasi et al. 2007 Takai et al. 2010
Spodoptera frugiperda 9, 21	+	+	≤ 0.1	+	+	Ezure et al. 2007 Ezure et al. 2010 Katzen et al. 2006 Stech et al. 2012
Saccharomyces cerevisiae	-	-	0.05 - 0.07	n.a.	-	Wang et al. 2006 Wang et al. 2008
Leishmania tarantolae	-	+	≤ 0.2	n.a.	+	Kovtun et al. 2011
<b>Prokaryotes</b>						
E. coli	-	+	≤ 5 - CECF 0.5-1 B	+	+	Katzen et al. 2005 Schwarz et al. 2008
Pseudomonas fluorescens	-	-	≤ 0.1	n.a.	-	Nakashima et al. 2004
E. coli - PURE (purified translation machinery)	-	+	≤ 0.5	+	+	Shimizu et al. 2001
Thermus thermophilus	-	-	≤ 0.06	n.a.	-	Uzawa et al. 2002 Zhou et al. 2012
Thermococcus kodakaraensis	-	-	≤ 0.007	n.a.	-	Endoh et al. 2008

**Table 2: CF extracts sources.** Different sources, eukaryotic as well as prokaryotic can be used for the CF production of proteins. PTM, post-translational modifications. cT7, coupled transcription/translation protocol reported. Yield, approximate range of expression, B: batch configuration, CECF: continuous exchange configuration. MP: expression of membrane proteins reported. Kit: commercial kits available. Protocol: protocols for extract preparation.

### 1.14 Cell-Free extract sources

The most used system for the CF production of MPs is based on *E. coli* extract (ECE). *E. coli* can be fermented in large volumes with inexpensive media and the cells can be easily disrupted. The S30 extract is obtained by the centrifugation of the lysed cells at 30.000 x g, in order to include important enzymes that are necessary for protein synthesis (Kigawa et al. 2004, Zubay 1973). Endogenous mRNA and other low molecular weight compounds are eliminated from the extract during the preparation procedure. Various *E. coli* strains have been used for extract preparation and detailed protocols have been published (Katzen et al. 2005, Schwarz et al. 2008); commercial kits from different companies are also available. Further advantages of the ECE system are the high efficiency for the production of even large eukaryotic MPs, achieving mg amounts of MPs per ml of RM, as well as the possibility to modulate disulfide bonds formation using an appropriate redox or shuffling systems (Goerke and Swartz 2008). On the other hand, typical eukaryotic post-translational modifications, as well as specific folding systems, are not present.

One alternative to overcome these problems is to use a eukaryotic based CF system like for

example the wheat germ (WG) system. Preparing the extract from this source can be laborious and time consuming, as the embryo, that contains all the necessary enzymes for the reaction, has to be carefully separated from the surrounding endosperm that contains many nucleic acid degrading enzymes as well as translation inhibitors (Endo and Sawasaki 2005). Another problem that can arise from using the WG extract is the very high batch quality variation. Despite these problems, the WG extract is very stable over time and protein expression can proceed for weeks if substrates and mRNA are continuously supplied, leading to expression up to 10 mg/ml in optimal condition (Sawakasi et al. 2007). Some post-translational modifications are possible using the WG extract. For example N-glycosylation had been detected when WG is supplemented with canine microsomal membranes (Zhang and Ling 1995). Other post-translational modifications, like phosphorylation (Janaki et al. 1995) and myristoylation (Martin et al. 1997) as well as some specific proteolytic processing are also possible (Mumford et al. 1981).

Alternative common cell-free expression systems are based on rabbit reticulocyte (RRL) and insect cells (IC) extracts. Both systems give the possibility to express eukaryotic MPs with a full set of post-translational modifications, in presence of the specific modifying enzymes or corresponding microsomes fractions (Schwarz et al. 2008). Preparation of these extracts is more complex compared to WG and ECE. Major limitations of these systems are the general low yields of MPs expression, allowing their use only for analytical purposes.

During recent years many new extracts, from eukaryotic and prokaryotic sources, have also been developed and protocols for their preparation have been published. Examples of less common extract sources are *Leishmania tarantolae* (Kovtun et al 2011), *Saccharomyces cerevisiae* (Wang et al. 2008), human Hela S3 cells (Mikami et al. 2008), *Pseudomonas fluorescens* (Nakashima et al. 2004), *Thermus thermophilus* (Zhou et al. 2012) and *Thermococcus kodrakaensis* (Endoh et al. 2008) (Table 2).

As an alternative to a complex cell extract, the PURE (protein system using recombinant element) system have been developed. In this case the complete *E. coli* translational mechanism is composed of purified recombinant components (Shimizu et al. 2001). This better defined environment could be useful for special purpose, like studying the folding pathway or the translation kinetics of MPs. The yields of expressed proteins are generally low and it is only used for analytical scale productions.

### 1.15 Template design and reaction compounds

In the coupled transcription/translation ECE system, the MP template DNA has to be provided under the control of a strong promoter. In general, the T7 promoter recognized by the T7 RNA polymerase is used. Suitable vectors for the expression are the pEt or the pIVEX. The productivity in the ECE system seems highly dependent on the rate of translation. Presence of rare codons or unfavorable initiation of the translation seems to be the major limiting steps in the protein synthesis (Kudla et al. 2009). The formation of complex secondary structure in the 5-prime end of the mRNA that involves the region of the ribosomal binding site, could slow down the expression and in the worst cases inhibit the translation process (Laursen et al. 2005). Presence of rare codons could cause a pause in the translation or mis-incorporation of amino acids, leading to premature termination events. In order to solve these problems, synthetic genes with optimized codons can be used and the addition of N-terminal tags, as T7-tag, His-tag (Schwarz et al. 2007) or even smaller non-functional tags (Haberstock et al. 2012), can considerably enhance the expression of eukaryotic MPs. In case of WG extract, mRNA with poly(A) capping is required for efficient expression and can be alternatively substituted with stable viral leader sequences. Popular sequences are the OMEGA leader sequence derived from the tobacco mosaic virus and its derivatives (Gallie 2002).

The CF extract already contains important factors for the translation, such as ribosomes, aminoacyl-tRNA synthetase as well as acetate kinase for energy regeneration; on the other hand, some essential precursors for the transcription and translation have to be added to the system. The four nucleoside triphosphates ATP, CTP, GTP and UTP has to be provided as they are essential energy sources and they are rapidly consumed during the CF reaction. As ECE has a high level of endogenous phosphatases and ATPase activities, components for energy regeneration have to be added to the system. In conventional protocols phosphoenol pyruvate, acetyl phosphate and creatine phosphate are supplied together with their respective enzymes (Klammt et al. 2006, Ryabova et al 1995, Zubay 1973). Amino acids are supplied in a concentration between 0.3 and 2 mM and unstable amino acids (arginine, cysteine, tryptophan, methionine, aspartic acid, glutamic acid) are usually provided at higher concentrations in order to increase the expression yield. Labeled amino acids can also be provided in the reaction. Selenomethionine or isotopes labelled amino acids are of particular value for structural investigations involving NMR or x-ray crystallography.

Other compounds, that are generally added in the reactions are the PEGs, that are used to induce molecular crowding effect, as well as DTT, that allows the reaction to be performed in reducing conditions, maintaining the T7 polymerase in an active form. On the other hand, oxidative conditions can also be chosen in order to support the formation of disulfide bridges in



the synthesized MP.

Furthermore, the CF system requires some essential compounds in a well defined concentration. The free concentration of divalent  $Mg^{2+}$  ions must be optimized for each new batch of extract, as suboptimal concentration can have a severe impact on the protein production (Schwarz et al. 2007). For the ECE system the concentration of  $Mg^{2+}$  typically ranges from 8 to 20 mM. Also potassium acetate has to be provided, usually at high concentration, at around 250 mM.

### 1.16 Configurations of the Cell-Free reaction

CF expression can be performed in 3 standard modes: in the precipitate forming mode (P-CF), in the detergent based mode (D-CF) or in the lipid based mode (L-CF) (Fig. 8).

In the P-CF mode, in absence of any supplied hydrophobic environment, the synthesized MPs precipitate immediately after the translation. In a standard preparation of CF extract, most of the membranes originated from the disruption of the cells are removed during the centrifugation steps. While residual lipids, in a concentration between 50-100  $\mu\text{g/ml}$ , are still present, no substantial hydrophobic environments are provided in order to keep the newly synthesized MPs in a soluble state. The precipitate, that resembles the formation of inclusion bodies in a standard *in vivo* expression, has some substantial differences. The P-CF precipitate can be easily solubilized in detergent, leading in some cases in functional folded MPs, as in the case of the multi drug transporter EmrE (Elbaz et al. 2004) or the human-histamine-1 receptor (Sansuk et al. 2008). In contrast, MPs expressed in inclusion bodies has to be solubilized with high concentration of strong denaturants, like urea or guanidinium chloride, and subsequent time consuming refolding procedure has to be performed in order to obtain functionally folded MPs. Suitable detergents for the solubilization of the P-CF generated precipitates are: SDS, the lyso-phosphoglycerols 1-myristoyl-2-hydroxy-sn-glycero-3-[phospho-rac-(1-glycerol)] (LMPG) and 1-palmitoyl-2-hydroxy-sn-glycero-3-[phospho-rac-(1-glycerol)] (LPPG), as well as milder detergents like the n-dodecylphosphocholine (Fos-12) could also be used depending on the MPs target (Klammt et al. 2004, 2005, Ma et al. 2011).

The detergent used for the solubilization can easily be exchanged with a second detergent upon MPs immobilization by metal chelate affinity chromatography, density gradient centrifugation or dialysis approaches. These procedures were successfully used for stabilization and recovery of ligand binding competent GPCRs (Junge et al. 2010, Klammt et al. 2007)

P-CF expression mode is suitable for a fast screening of basic conditions in order to improve protein expression yields of a specific target and it is a valuable expression tool for screening of

MPs libraries (Savage et al. 2007, Schwarz et al. 2010).

Many of the detergents used for the solubilization of the precipitate are compatible with NMR; opening the possibility for the direct structural characterization of the expressed target proteins (Krueger-Koplin et al. 2004).

In D-CF mode, detergents are directly added in the RM, leading to the solubilization of the nascent MP in a co-translational manner. Detergents have to be provided at a concentration above their critical micellar concentration (CMC) in order to induce efficient solubilization. The synthesized MPs can interact with the detergent micelles during, or shortly after, the translation. In this way the precipitation of the polypeptide is avoided and proteomicelles are formed due to non-specific hydrophobic interactions. Not all the detergents are suitable for D-CF expression, detergents with a high CMC like  $\beta$ -OG or CHAPS start to inhibit the translational machinery at very low concentrations. On the other hand, many commonly used detergents are well tolerated in the CF system, even at high concentration. Extensive screenings for detergent tolerance have been performed using the ECE system (Klammt et al. 2005, Lyukmanova et al. 2012, Roos et al. 2012,).

Highly suitable for the D-CF expression are the long-chain polyoxyethylene-alkyl-ethers such as Brij35, Brij58, Brij78 or Brij98 and the steroid-derivative digitonin. These detergents have a very low specific CMC and they can be added in the reaction even at high concentration, without inducing any toxic effect on the translation/transcription machinery. Many GPCRs have been solubilized in a functional state using these detergents, such as the human vasopressin type 2 receptor, the endothelin A and B receptors the 2 adrenergic receptor, the muscarinic acetylcholine receptor M2 and the neurotensin receptor (Junge et al. 2010, Klammt et al. 2005, Ishihara 2005).

Detergents like Triton X-100 or DDM can also be effective in some cases for the direct solubilization of the MPs. Addition of mixture of different detergents could also be beneficial (Genji et al. 2010) and combination of detergent with lipids can also be an option in order to optimize the expression (Arslan et al. 2013, Müller-Lucks et al. 2013, Nozawa et al. 2007).

As an alternative to classical detergents, in the last few years a whole new series of artificial hydrophobic compounds with improved properties have been used for the co-translational solubilization of MPs. Fluorinated surfactants as well as phospholipid-like surfactants were successfully supplemented in D-CF reactions (Blesneac et al. 2012, Park et al. 2011). The polyfructose uncharged polymer NV10 as well as peptide surfactants proved to be effective in the functional solubilization of different GPCRs (Corin et al. 2011, Klammt et al. 2010, Wang et al. 2011).

Extensive screenings are in general necessary to define optimal detergents and concentrations

for each individual protein, as the detergent itself could have a relevant impact on the efficiency of solubilization as well as on the correct folding of the target MP.

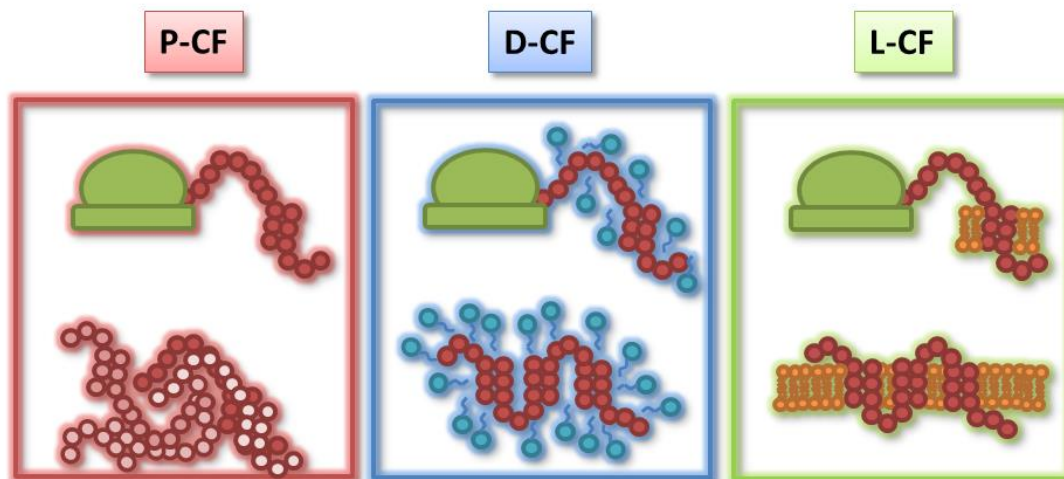


**Fig. 8: Schematic of different CF expression modes.** P-CF: in absence of any detergent the MPs are expressed in form of a precipitate, which can be solubilized in suitable detergents. D-CF: MPs are directly translated into detergent micelles, which may be beneficial for induce correct folding. L-CF: MPs can be directly inserted into membrane mimetic environment, such as liposomes, bicelles or nanodiscs.

Lipids are the most natural environment for MPs and in many cases they are essential for inducing a correct protein folding and functionality.

CF expression offers the possibility to reconstitute the MPs into a defined lipidic environment, both in a post-translational as well as in a co-translational manner. P-CF or D-CF expressed MPs can be *in vitro* reconstituted into a lipidic bilayer. Common protocols are based on the dilution of the detergent used for the solubilization of the protein below the CMC together with addition of pre-formed liposomes (Rigaud and Lévy 2003). The remove of the detergent can be performed in different ways; protocols that involve dialysis or adsorption on hydrophobic resin like Biobeads have been published (Rigaud et al. 1998).

Alternatively, addition of a lipidic environment direct in the RM, using the so called L-CF expression mode, offers the unique option for the co-translational insertion of MPs. Lipid mixtures are well tolerated by CF system even at high concentration (Kalmbach et al. 2007; Roos et al. 2013). Lipids can be provided as preformed liposomes or as planar nano-lipid particles (nanodiscs). L-CF allows analyzing the effect of different lipids on the MPs quality and activity. In addition, thanks to the co-translational insertion, the orientation of the MPs in the lipid bilayer

is more homogenous as compared with the post-translational reconstitution approaches, facilitating functional studies (Moritani et al. 2010).

L-CF expression in the presence of nanodiscs is becoming an attractive option for the functional expression of MPs (Lyukmanova et al. 2012, Proverbio et al. 2013, Roos et al. 2012). Each nanodisc is composed by two amphipathic  $\alpha$ -helical proteins called MSPs (Membrane Scaffold Proteins) surrounding a bilayer of synthetic phospholipids (Schuler et al. 2013). The MSPs, which are derived from the plasma apolipoprotein A-I, can be of different amino acids sequence length. In order to prepare the nanodiscs, MSP and lipids at a specific ratio have to be co-incubated in presence of detergent. The optimal ratio depends by the specific MSP and lipid combination and it is a very critical parameter to take in account in order to obtain a homogenous and monodisperse population of nanodiscs. Upon removal of detergent using dialysis or Biobeads, the discoidal nanoparticles are self assembled (Bayburt and Sligar 2002). Nanodiscs, in comparison with liposomes, lack the internal lumen and don't present the problem of the orientation of the inserted MP, as both side of the bilayer structure are accessible. Furthermore the use of nanodiscs in CF system provides a more stable environment in size and topology, as liposomes tends to fuse and aggregate, resulting in their precipitation during the reaction (Berrier et al. 2011, Proverbio et al. 2013, Roos et al. 2012,).

The events that lead to the insertion of a MP in a lipid bilayer during a L-CF reaction are still largely unknown. Some preliminary experiments have shown that the molecular mechanism could be different from what happens *in vivo*. In the case of the channel protein MscL and the permease MtlA, it is known that *in vivo* these two proteins require the YidC membrane protein insertase and of the SecYEG complex to be correctly transferred into the membrane. Analysis of the L-CF produced proteins revealed that in this system the insertion occurs independently (Cappuccio et al. 2008, Nozawa et al. 2007). Some factors that could facilitate the insertion of MPs could be the high concentration of empty membranes in the CF reactions as well as the specific lipid composition of the supplied bilayer (Roos et al. 2012).

A possible modification of the L-CF system is the addition of lipid/detergent mixtures in the RM. The MPs can associate with the lipomicelles and remain trapped into proteoliposomes as soon as the detergent is dialyzed in the FM. This approach could be an interesting option in order to obtain functional reconstituted MPs (Nozawa et al. 2007, Umakoshi et al. 2009).

### 1.17 Cell-Free expression of the endothelin receptors

The first investigation regarding the CF production of the endothelin receptors started in our group around the year 2000 and spanned three doctoral thesis projects, including this one. Most of the work has been focused on two expression modes: P-CF and D-CF (Junge et al. 2010, Klammt et al. 2007). For the ETA receptor, after CF optimization, an expression of up to 3 mg/ml in the P-CF mode was achieved. The resolubilization of the precipitate was quantitative using the detergent LPPG and resulted in homogenous sample preparation as evaluated in blue-native-PAGE and size exclusion chromatography (SEC). 1 mg/ml of purified receptor was obtained using metal chelate chromatography and high degree of homogeneity was achieved by exchange of LPPG with the detergents Brij35 or Fos-16. Multi angle light scattering experiments suggest a monomeric form of the receptor in Fos-16, whereas monomer and dimer were present in Brij35 micelles. Regarding the D-CF expression mode, best solubilization of the receptor was achieved in presence of Brij35, and a final yield of 0.5 mg/ml was obtained after purification. In this condition the thermal stability of ETA was very high and an observable denaturation started above 50 °C (Junge et al. 2010).

Using both expression modes, up to 50% of ligand binding competent ETA receptor in selected detergent conditions was produced.

Reconstitution of the ETA receptor in artificial liposomes was only successful with P-CF produced samples and a homogenous particle distribution was observed by freeze-fracture analysis. However the majority of proteins precipitated during the reconstitution process and sucrose gradient purification was not effective in the removal of the non-inserted receptors. IC<sub>50</sub> values of the reconstituted ETA in homologous competition experiment using [125I]-ET-1 were 10<sup>3</sup>-10<sup>4</sup> higher if compared with previously reported data (Junge et al. 2010).

Regarding the ETB receptor, optimized CF expression resulted in high preparative yields of 3 mg/ml in P-CF mode; similar yields were also obtained in D-CF mode in presence of Brij78. After immobilized metal affinity chromatography, 1.8 mg of proteins per ml of RM was obtained. Size exclusion chromatography and negative stain electron suggested a higher quality of the D-CF produced sample in Brij78, compared with the P-CF expression mode. The quality of the D-CF sample was further analyzed by ligand binding studies (Klammt et al. 2007).

Surface plasmon resonance and total internal reflection fluorescence spectroscopy revealed dissociation constant for the ligand ET-1 of 6.2 nM and 29 nM, respectively. In further ligand binding studies performed by co-elution of a Cy3-labelled-ET-1, up to 50% of ligand binding competent ETB receptor was obtained (Klammt et al. 2007).

In order to confine binding regions and dimerization interface, different truncated versions of the receptor were prepared and expressed in D-CF mode. Different experiments pointed out the

importance of the first transmembrane segment in ligand binding and homodimerization of ETB (Klammt et al. 2007).

### **1.18 Aim of this project**

Starting from the previously obtained results, the main focus of this project is the biochemical characterization of CF produced ETB and –to some extent- ETA receptors reconstituted in different lipid environments. Lipids are the most natural environment for MPs and the specific composition of the lipid bilayer can have an effect on the protein folding and functionality.

Analysis of the activity of the CF produced receptors has been performed implementing post-translational as well as co-translational reconstitution protocols.

Two different lipidic environments, liposomes and nanodiscs, have been extensively studied and their effect on the quality and quantity of the CF expression of the endothelin receptors evaluated. Furthermore, this project aimed to verify the specificity of the binding properties of a panel of agonist and antagonist to the ETA and ETB receptor. The implementation of different biochemical assays in order to determine the ligand binding competence of the receptor in lipid environment represented a further major aim of this project.

## 2. Materials

### 2.1 General equipment

- Autoclave, Tecnomara AG (Switzerland), Gettinge (Sweden).
- Centrifuge Sorvall Evolution RC, Sorvall Instruments (Germany).
- Centrifuge Sorvall RC 5B, C , Sorvall Instruments (Germany).
- Cooled table top centrifuge Micro 22R, Hettich (Germany).
- Fermenter, 10-liter, B. Braun Biotech (Germany).
- French pressure cell disruptor SLM, Aminco Instruments (USA).
- Incubating shakers, Infors AG (Germany), New Brunswick Scientific (USA).
- MS2 Minishaker, IKA Werke (Germany).
- NanoDrop 1000, Peqlab Biotechnologie (Germany).
- Evaporator Rotavapor RE120, Buechi (Germany).
- Sonifier Labsonic U, B. Braun Biotech (Germany).

### 2.2 DNA template preparation and analysis

- Agarose gel electrophoresis system, Peqlab Biotechnologie Germany).
- Midi DNA preparation kit, NucleoBond AX100, Macherey-Nagel (Germany).
- pET21a(+), pET28a(+), Novagen, MERCK chemicals (Germany).
- QIAquick gel extraction kit, Qiagen (Germany).
- QIAquick PCR purification kit, Qiagen (Germany).
- Thermocycler, Biometra (Germany), Eppendorf (Germany).

### 2.3 Protein expression and analysis

- Dialysis tubes type 27/30, MWCO 12-14 kDa, Spectrum Laboratories (USA).
- Immobilon-P PVDF membrane, Millipore (Germany).
- Lumi Imager F1, Roche Diagnostics (Germany).
- Mini-Protean Electrophoresis system, Bio-Rad (Germany).
- Slide-A-lyzer dialysis cassette, MWCO 10 kDa, Thermo Fisher Scientific (Germany).

## 2.4 Protein processing, quality and functional analysis

- Äkta purifier FPLC system, GE Healthcare (Germany).
- Biobeads SM-2, Bio-Rad (Germany).
- Biacore X100, Biacore (Sweden).
- Biacore X100 chips CM5 and SA, Biacore (Sweden).
- Chemiscreen, ETA or ETB membrane preparation, Millipore (Germany).
- Cobra II Auto gamma, PerkinElmer (Germany).
- Column Superdex 200 3.2/30, GE Healthcare (Germany).
- Column hi-prep IMAC FF16/10, GE Healthcare (Germany).
- Confocal microscope LSM510, Zeiss (Germany).
- Elisa-plate, flat bottom high binding, Microlon, Greiner Bio (Germany).
- Mini-Extruder, Avanti Polar Lipids (USA).
- Microspin G-50 columns, GE Healthcare (Germany).
- Microplate spectrophotometer GeniosPro, Tecan (Germany).
- Microscale thermophoresis (MST), Monolith NT.115, NanoTemper (Germany).
- MultiScreen HTS FB filter, Millipore (Germany).
- MultiScreen HTS HA filter, Millipore (Germany).
- MultiScreen HTS vacuum filtration, Millipore (Germany).
- NUNC Immobilizer nickel-chelate plate, Thermo Fisher Scientific (Germany).
- OCTET system, FortéBio (USA).
- Scintillation counter LS 6500, Beckman Coulter (Germany).
- Spectrofluorometer, FP-6500, Jasco Labortechnik (Germany).
- Spectropolarimeter, J-180, Jasco Labortechnik (Germany).
- Ultracentrifuges (L-70, Optima TLX, Optima LE-80K), Beckman Coulter (Germany).
- Ultra-Clear Centrifuge Tubes, Beckman Coulter (Germany).

## 2.5 Antibodies

- Anti-biotin goat pAb Peroxidase conjugate, Calbiochem, MERCK chemicals (Germany).
- Anti-mouse IgG HRP conjugate from goat, Sigma-Aldrich Chemie (Germany).
- Anti-penta His IgG from mouse, Qiagen (Germany).
- Anti-T7 tag HRP conjugate, Novagen, MERCK chemicals (Germany).



## 2.6 Detergents

- Sigma-Aldrich Chemie (Germany):
  - Brij35, polyoxyethylene-(23)-lauryl-ether.
  - Brij58, polyoxyethylene-(20)-cetyl-ether.
  - Brij78, polyoxyethylene-(20)-stearylether.
  - Brij98, polyoxyethylene-(20)-oleyl-ether.
  - TritonX-100, polyethylene-glycol-P-1,1,3,3-tetramethylbutylphenyl-ether.
  - Cholic acid.
  - Digitonin.
- Carl Roth (Germany):
  - CHAPS, 3-[(3-Cholamidopropyl) dimethylammonio]-1-propansulfonat.
  - SDS, sodium dodecylsulfate.
- Anatrace, Affymetrix (USA):
  - DDM, n-dodecyl- $\beta$ -D-maltoside.
  - DPC, n-dodecylphosphocholine.
  - LMPC, 1-myristoyl-2-hydroxy-sn-glycero-3-[phospho-rac(1-choline)].
  - LMPG, 1-myristoyl-2-hydroxy-sn-glycero-3-[phospho-rac-(1-glycerol)].
  - LPPG, 1-palmitoyl-2-hydroxy-sn-glycero-3-[phospho-rac-(1-glycerol)].

## 2.7 Lipids

- Avanti Polar Lipids (USA):
  - BTE, brain total extract.
  - DMPC, 1,2-dimyristoyl-sn-phosphatidylcholine.
  - DMPG, 1,2-dimyristoyl-sn-glycero-3-phospho-(1'-rac-glycerol).
  - EPL, *E. coli* polar lipid extract.
  - HTE, heart total extract.
  - PE-Lissamine rhodamine B, phosphatidylethanolamine-Lissamine Rhodamine B.
  - POPC, 1-palmitoyl-2-oleoyl-sn-glycero-3-phosphocholine.
- Sigma-Aldrich Chemie GmbH (Germany):
  - L- $\alpha$ -Phosphatidylcholine from soybean, Type IV-S.

## 2.8 General reagents and chemicals

- 1,4-Dithiotreitol (DTT), Carl Roth (Germany).

- 2-Mercaptoethanol, Carl Roth (Germany).
- Acetyl phosphate lithium potassium salt, Sigma-Aldrich Chemie (Germany).
- Adenosine 5'-triphosphate (ATP), Roche Diagnostics (Germany).
- Amino acids (unlabelled), Sigma-Aldrich Chemie (Germany).
- Antifoam Y-30 emulsion, Sigma-Aldrich Chemie (Germany).
- Bactotryptone, Carl Roth (Germany).
- Bovine serum albumin Fraction V, Sigma-Aldrich Chemie (Germany).
- Complete Protease Inhibitor Cocktail, Roche Diagnostics (Germany).
- Cholesteryl hemisuccinate tris salt, Sigma-Aldrich Chemie (Germany).
- Dimethylsulfoxide, Carl Roth (Germany).
- Ethidiumbromide, Carl Roth (Germany).
- Folinic acid calcium salt, Sigma-Aldrich Chemie (Germany).
- Gene ruler 100bp, 1kb DNA ladder, Fermentas (Germany).
- Glucose monohydrate, Carl Roth GmbH+Co.KG (Germany).
- Guanosine 5' diphosphate di-sodium salt , Fluka, Sigma-Aldrich Chemie (Germany).
- Guanosine 5' triphosphate di-sodium salt , Fluka, Sigma-Aldrich Chemie (Germany).
- HEPES, Imidazole, IPTG, K<sub>2</sub>HPO<sub>4</sub>, KCl, KH<sub>2</sub>PO<sub>4</sub>, Carl Roth (Germany).
- Magnesium acetate tetrahydrate, Sigma-Aldrich Chemie (Germany).
- NaCl, Carl Roth (Germany).
- NaN<sub>3</sub>, Fluka, Sigma-Aldrich Chemie (Germany).
- Ni-NTA Agarose, Qiagen (Germany).
- PEG8000, Sigma-Aldrich Chemie (Germany).
- Peptone, Carl Roth (Germany).
- Phenylmethylsulfonyl fluoride (PMSF), Sigma-Aldrich Chemie (Germany).
- Phosphoenol pyruvic acid (PEP), Sigma-Aldrich Chemie (Germany).
- PIERCE Monomeric Avidin Agarose, Thermo Fisher Scientific (Germany).
- Potassium acetate, Sigma-Aldrich Chemie (Germany).
- Pyruvate kinase, Roche Diagnostics (Germany).
- Restriction enzymes, New England Biolabs (Germany).
- RiboLock RNase Inhibitor, Fermentas (Germany).
- T4 DNA-ligase, New England Biolabs (Germany).
- Tris-(hydroxymethyl)-aminomethane, Carl Roth (Germany).
- tRNA *E. coli* MRE 600, Roche Diagnostics (Germany).
- Turbo-Pfu DNA polymerase, Stratagene (Germany).
- Uridine 5' triphosphate tri-sodium salt, Fluka, Sigma-Aldrich Chemie (Germany).

- VentDNA Polymerase, New England Biolabs (Germany).
- Yeast extract, Carl Roth (Germany).

## 2.9 Labelled chemicals and ligands

- ET-1, Biotin [Lys9]-ET-1, Cy3-ET-1, Fluorescein-4-Ala-ET-1 (f-4-Ala-ET1), Dr. Michael Beyermann, FMP Berlin (Germany).
- [35S]- $\gamma$ -GTP, PerkinElmer (Germany).
- BODIPY-GTP- $\gamma$ -S, Life Technologies (Germany).
- [125I]-ET-1; 5, 10, 50  $\mu$ Ci, PerkinElmer (Germany).
- BQ123; IRL-2500; IRL-1620; Tocris Bioscience (United Kingdom).

## 2.10 Microbial strains

- For DNA cloning: *E. coli* DH5 $\alpha$ .
- For Cell-Free extract preparation: *E. coli* K-12 strain A19.
- Form MSPs preparation: *E. coli* BL21 (DE3).

## 2.11 General buffers and media

- Ampicillin stock, 1000-fold: 150 mg/mL Na-ampicillin salt in 50 % EtOH.
- DB salt: 5.22 mM NH<sub>4</sub>H<sub>2</sub>PO<sub>4</sub>, 0.05 mM MgSO<sub>4</sub> x 7H<sub>2</sub>O, 0.2 mM KCl, 44 % glycerol (w/v) in H<sub>2</sub>O. Mix thoroughly on a stirring device for 20 minutes (min) and sterilize by autoclaving. Store at room temperature (RT).
- IPTG stock: 1 M in H<sub>2</sub>O.
- Kanamycin stock, 1000-fold: 75 mg/mL kanamycin sulfate in H<sub>2</sub>O.
- LB medium (1 liter): 10 g bactotryptone, 5 g yeast extract, 10 g NaCl. Sterilize by autoclaving.
- S30 A buffer: 10 mM Tris-acetate, pH 8.2, 14 mM Mg(OAc)<sub>2</sub>, 60 mM KCl, 6 mM  $\beta$ -mercaptoethanol. Sterilize by filtering and store at 4°C.
- S30 B buffer: 10 mM Tris-acetate, pH 8.2, 14 mM Mg(OAc)<sub>2</sub>, 60 mM KCl, 1 mM DTT and 0.1 mM PMSF. It is recommended to prepare a 50-fold stock solution S30 A/B buffer out of Tris acetate, Mg(OAc)<sub>2</sub> and KCl. Sterilize by filtering and store at 4°C. Add  $\beta$ -mercaptoethanol, DTT and PMSF freshly to the 1-fold buffers.
- S30 C buffer: 10 mM Tris-acetate, pH 8.2, 14 mM Mg(OAc)<sub>2</sub>, 60 mM KOAc, 0.5 mM DTT. Store at 4°C. It is recommended to prepare a 50-fold stock without DTT. Add DTT freshly

to the 1-fold buffer.

- 2 x YTPG medium (10 liters of aqueous solution): 22 mM  $\text{KH}_2\text{PO}_4$ , 40 mM  $\text{K}_2\text{HPO}_4$ , 100 mM glucose, 160 g bactotryptone, 100 g yeast extract, 50 g NaCl. Sterilize glucose separately by filtering. Sterilize phosphate buffer components separately by autoclaving. Dissolve remaining media components in distilled water and sterilize by autoclaving. The components should all be freshly prepared. Store at RT.

## 2.12 Reagents and buffers for cell-free expression

- Acetyl phosphate lithium potassium salt, AcP: 1 M stock solution, pH 7.0, adjusted with 10 M KOH.
- Amino acid stock: 20 amino acids containing stock solution at a final concentration of 8 mM each and dissolve in  $\text{H}_2\text{O}$ . Adjust pH to 8.0 with 10 M KOH. Suspensions are pipetted to the Cell-Free reaction set-up.
- Complete<sup>®</sup> protease inhibitors cocktail without EDTA: 50-fold stock solution in  $\text{H}_2\text{O}$ .
- Creatine kinase: 10 mg/ml stock in  $\text{H}_2\text{O}$ .
- DTT: 500 mM stock in  $\text{H}_2\text{O}$ .
- Folinic acid calcium salt: 10 mg/ml stock in  $\text{H}_2\text{O}$ . Completely dissolve by incubation at 37°C.
- HEPES: 2.4 M stock. Adjust to pH 8.0 with 10 M KOH.
- Magnesium acetate tetrahydrate,  $\text{Mg}(\text{OAc})_2$ : 1 M solution in  $\text{H}_2\text{O}$ .
- NTP mix: 75-fold stock containing 90 mM ATP, 60 mM each GTP, CTP and UTP, pH 7.0 adjusted with NaOH.
- Phospho(enol)pyruvic acid monopotassium salt, PEP: 1 M stock. Adjust to pH 7.0 with 10 M KOH.
- Polyethylenglycol 8000, PEG8000: 40 % (w/v) solution dissolved in  $\text{H}_2\text{O}$  by shaking over night (o.n.) at 37°C.
- Potassium acetate, KOAc: 4 M in  $\text{H}_2\text{O}$ .
- Pyruvat kinase (Roche Diagnostics): Stock of 10 mg/ml. Commercial, no separate preparation necessary.
- RiboLock<sup>TM</sup> RNase inhibitor (Fermentas): Stock of 40 U/ $\mu\text{l}$ . Commercial, no separate preparation necessary.
- Sodium acetate, NaOAc: 3 M stock in distilled RNase free water, pH 5.5 adjusted with NaOH. Sterilize by filtering. Store 4°C.
- Sodium azide,  $\text{NaN}_3$ : 3 % and 10 % (w/v) stocks in  $\text{H}_2\text{O}$ .
- tRNA *E. coli* MRE 600: 40 mg/ml stock in  $\text{H}_2\text{O}$ .

### 2.13 Buffers for DNA-Agarose gels, SDS-PAGE and Western Blotting

- Agarose: e.g. 1 % (w/v) agarose boiled in 1-fold TAE buffer. Store at RT.
- Ammoniumperoxid sulfate, APS: 10 % stock solution by dissolving 100 mg/ml.
- Ammoniumperoxid sulfate in H<sub>2</sub>O. Store at 4°C.
- Blotting buffer (Towbin): Dissolve 25 mM Tris, 192 mM Glycin, 3.5 mM (1 %) SDS, 15 % MeOH in H<sub>2</sub>O. pH should adjusted to pH 8.3. Store at 4 °C.
- Coomassie brilliant blue-staining solution for SDS gels: 50 % (v/v) ethanol (96 %), 10 % (v/v) acetic acid (100 %) and 0.1 % (w/v) Coomassie Brilliant Blue G250. Dissolve in H<sub>2</sub>O and store at RT in a dark bottle to avoid exposure to light.
- DNA-loading dye, 6-fold: 40 % (w/v) sucrose, 0.25 % (w/v) bromphenol blue and 0.25 % xylene cyanol FF. Dissolve in H<sub>2</sub>O and store at 4°C.
- EtBr-stock solution: 10 mg/ml stock in H<sub>2</sub>O.
- ECL 1: 100 mM Tris-HCl, pH 7.5, 2.9 mM Luminol, 0.4 % p-coumaric acid in H<sub>2</sub>O. Store at 4°C. Luminol and p-coumaric acid are dissolved in 100 % DMSO.
- ECL 2: 100 mM Tris-HCl, pH 8.0, 0.06 % H<sub>2</sub>O<sub>2</sub> in H<sub>2</sub>O. Store at 4°C.
- Rotiphorese Gel 30: 30 % (v/v) acrylamide, 0.8 % (v/v) bisacrylamide. Store at 4 °C.
- Rotiphorese Gel 40: 40 % (v/v) acrylamide, 1 % (v/v) bisacrylamide. Store at 4 °C.
- SDS-PAGE running buffer: 25 mM Tris-HCl, pH 8.0, 0.1 % (w/v) SDS and 200 mM glycine. Store at RT.
- SDS-PAGE stacking gel buffer: 0.4 % (w/v) SDS, 0.5 M Tris-HCl, pH 6.8. Store at 4°C.
- SDS-PAGE Separating gel buffer: 0.4 % (w/v) SDS, 1.5 M Tris-HCl, pH 8.9. Store at 4°C.
- SDS-PAGE sample buffer, 5-fold: 25 % (w/v) glycerol, 25 % (v/v) β-mercaptoethanol, 7.5 % (w/v) SDS, 0.1 % (w/v) coomassie G250, 300 mM Tris-HCl, pH 6.8. Store at RT.
- TAE buffer, 50-fold: Dissolve 2 M Tris , 5.7 % acetic acid (v/v) and 50 mM EDTA in H<sub>2</sub>O. Store at RT.

### 2.14 Buffers for protein purification and protein analysis

- Filter binding assay proteoliposomes:  
binding and wash buffer: 20 mM potassium phosphate, pH 7.5, 150 mM NaCl, 0.1 % BSA. The pH is adjusted by combination of 1 M K<sub>2</sub>HPO<sub>4</sub> and 1 M KH<sub>2</sub>PO<sub>4</sub>.
- Filter binding assay assay NDs:  
Binding buffer: 50 mM Hepes-NaOH pH 7.5, 5 mM MgCl<sub>2</sub>, 1 mM CaCl<sub>2</sub>, 0.2% BSA.  
Washing buffer: 50 mM Hepes-NaOH pH 7.5, 500 mM NaCl, 0.1% BSA.  
Washing plate buffer: 50 mM Hepes-NaOH pH 7.5, 0.5% BSA.

- Fluorescence anisotropy buffer: 20 mM Tris-HCl, pH 7.5, 150 mM NaCl.
- G protein assay buffers: 10 mM Hepes-NaOH pH 7.5, 10 mM MgCl<sub>2</sub> pH 8, 100 mM NaCl.
- G proteins storage buffer: 20 mM Tris pH 7.5, 150 mM NaCl and 10% glycerol.
- IMAC buffers for ETB:
  - Equilibration buffer: 20 mM Tris-HCl, pH 7.5, 500 mM NaCl, 10 mM imidazole.
  - Wash 1 buffer: 20 mM Tris-HCl, pH 7.5, 500 mM NaCl, 30 mM imidazole.
  - Wash 2 buffer: 20 mM Tris-HCl, pH 7.5, 500 mM NaCl, 80 mM imidazole.
  - Wash 3 buffer: 20 mM Tris-HCl, pH 7.5, 150 mM NaCl.
  - Elution buffer: 20 mM Tris-HCl, pH 7.5, 150 mM NaCl, 350 mM imidazole.
  - (Add the appropriate detergent at a concentration of 5-10 times above CMC).
- Liposome reconstitution buffer: 20 mM potassium phosphate, 150 mM NaCl. The pH 7 was adjusted by a combination of 1M K<sub>2</sub>HPO<sub>4</sub> and 1M KH<sub>2</sub>PO<sub>4</sub>.
- MSPs preparation buffers:
  - MSP-buffer 1: 40 mM Tris-HCl, 300 mM NaCl, 1% (v/v) Triton X-100, pH 8.0.
  - MSP-buffer 2: 40 mM Tris-HCl, 300 mM NaCl, 50 mM cholic acid, pH 8.9.
  - MSP-buffer 3: 40 mM Tris-HCl, 300 mM NaCl, pH 8.0.
  - MSP-buffer 4: 40 mM Tris-HCl, 300 mM NaCl, 50 mM imidazole, pH 8.0.
  - MSP-buffer 5: 40 mM Tris-HCl, 300 mM NaCl, 300 mM imidazole, pH 8.0.
  - MSP-buffer 6: 40 mM Tris-HCl, 300 mM NaCl, 10% (v/v) glycerol, pH 8.0.
  - MSP-resuspension bufferr 3: 40 mM Tris-HCl, 300 mM NaCl, pH 8.0. Supplemented with 1 tablet of protease inhibitor cocktail (Roche, Germany) per 50 ml and 100 mM PMSF.
- MST buffer: 20 mM Tris-HCl, 500 mM NaCl pH 7.5.
- OCTET buffers:
  - Tris buffer: 50 mM Tris pH 7.5, 150 mM NaCl, 1% BSA.
  - Hepes buffer: 20 mM Hepes-NaOH pH 7.5, 500 mM NaCl, 1% BSA.
- PBS, phosphate buffer saline (10-fold): Dissolve 1.37 M NaCl, 0.03 M KCl, 80 mM Na<sub>2</sub>HPO<sub>4</sub> - and 15 mM KH<sub>2</sub>PO<sub>4</sub> in H<sub>2</sub>O. Add 0.05 % Tween 20 to the 1-fold dilution. Store at 4°C.
- Resolubilization buffer for reconstitution, 5-fold: 100 mM potassium phosphate, 0.75 M NaCl. The required pH (pH 7.0, pH 7.5) is adjusted by combination of 1 M K<sub>2</sub>HPO<sub>4</sub> and 1 M KH<sub>2</sub>PO<sub>4</sub>.
- SEC buffer: 20 mM Tris-HCl, pH 7.5, 150 mM NaCl, 0.1 % B35. Sterilize and degase by filtering. Store at 4 or 16 °C.
- sGFP assay-buffer: 20 mM Tris-HCl, 100 mM NaCl, pH 7.4.
- SPR, CM5 chip buffers:
  - Activation buffer: 400 mM EDC- 100 mM NHS.

Coupling buffer: 10 mM acetate buffer pH 5.

De-activation buffer: 1 M ethanolamine.

Regeneration buffer: 10mM Glycine-HCl pH 2.5.

- SPR regeneration buffer: 50 mM NaOH, 1 M NaCl.
- SPR running buffer: Hepes-NaOH pH 7.5, 500 mM NaCl.
- SPR Screening buffers:
  - 20 mM Hepes-NaOH pH 7.5, 150 mM NaCl.
  - 20 mM Hepes-NaOH pH 7.5, 300 mM NaCl.
  - 20 mM Hepes-NaOH pH 7.5, 500 mM NaCl.

The buffers were also tested in combination with 0.2% BSA, 1% Glycerol or 0.05% detergent P-20.

- StrepII-tag affinity purification buffer:
  - Equilibration and wash buffer: 20 mM Tris-HCl, pH 7.5, 150 mM NaCl.
  - Elution buffer: 20 mM Tris-HCl, pH 7.5, 150 mM NaCl, 2.5 mM desthiobiotin as a reversible binding specific competitor.

## 2.15 Softwares

- GraphPad Prism 5, software for analyze, graph and present scientific data.
- Unicorn 5.11, software for control of Äkta system and processing of the results.
- Biaevaluation, software for analysis of SPR data.

### 3. Methods

#### 3.1 DNA techniques

DNA templates were constructed by PCR using the corresponding oligonucleotide primers and Vent-DNA polymerase (Table 3).

Construct (kDa)	Sequence	Modifications	Primer
<b>ETB</b> (47)	E27-S443	N-T7 C-His10	F: CGG GGA TCC GAG GAG AGA GGC TTC CCG CCT GAC R: CGG CTC GAG AGA TGA GCT GTA TTT ATT ACT GGA
<b>ETB-Strep</b> (47)	E27-S443	N-T7 C-Strep	F: CGG GGA TCC GAG GAG AGA GGC TTC CCG CCT GAC R: CTC CGG GTG GCT CCA CGG CCA TGG AGA TGA GCT GTA TTT ATT ACT R2: GGC CTC GAG TTA TTT TTC GAA CTG CGG GTG GCT CCA CCA TGG
<b>ΔETB</b> (43)	S65-S443	N-T7 C-His10	F: CGG GGA TCC TTG GCA CCT GCG GAG GTG CCT AAA R: CGG CTC GAG AGA TGA GCT GTA TTT ATT ACT GGA ACG
<b>ETB-93a</b> (15)	P93-V203	N-T7 C-His10	F: CGG GGA TCC CCC ATC GAGT ATC AAG GAG ACT TTC AAA R: CGG CTC GAG AGC TCG ATA TCT GTC AAT TCT GTC AAT ACT
<b>ETA</b> (48.7)	D20-N427	N-T7 C-His10	F: CGG GGA TCC ATG GAA ACC CTT TGC CTC AGG GCA R: CGG CTC GAG GTT CAT GCT GTC CTT ATG GCT GCT
<b>ETB-sGFP</b> (74)	E27-S443	N-T7 C-His10	F: CGG CTC GAG CTA AAG GTG GAA GAA TTA TTC ACT TGG R: CGG CTC GAG TTA TTT GTA CAA TTC ATC CAT ACC ATG
<b>ETA-sGFP</b> (75.7)	D20-N427	N-T7 C-His10	F: CGG CTC GAG CTA AAG GTG GAA GAA TTA TTC ACT TGG R: CGG CTC GAG TTA TTT GTA CAA TTC ATC CAT ACC ATG
<b>PR</b> (25)	M1-A249	N-T7 C-His10	F: CGG CAT ATG GCA GGT GGT GGT GAC CTT GAT R: CGG CTC GAG AGC ATT AGA AGA TTC TTT AAC
<b>Gas</b> (45)	M1-L394	N-T7 C-His10	F: CGG AAG CTT TC CTT GTA CCA CGT GGT AGT ATG ACT CTG GAG TCC ATC ATG GCG TGC TGC CTG AGC GAG R: CGG CTC GAG GCT GCC GCG CGG CAC CAG GAC CAG ATT GTA CTC CTT CAG GTT CAA CTG GAG GAT
<b>Gaq</b> (42)	M1-V359	N-T7 C-His10	F: CGG AAG CTT TC CTT GTA CCA CGT GGT AGT ATG GGC TGC CTC GGG AAC AGT AAG ACC GAG GAC CAG C R: CGG CTC GAG GCT GCC GCG CGG CAC CAG GAG CAG CTC GTA CTG ACG AAG GTG CAT GCG CTG AAT

**Table 3.** Constructs and oligonucleotides.

Standard PCR reactions were performed using plasmid DNA as template and a reaction volume of 50 or 100  $\mu$ l. Analysis of the amplification reaction was carried out with volumes of 5-10  $\mu$ l on 1 % agarose gels in 1-fold TAE buffer. PCR reaction samples were subsequently purified with Nucleospin PCR purification kits and eluted in water.

Purified DNA fragments were cloned with *Bam*HI and *Xho*I into pET21a(+).

For the ETB-Strep construct, the poly-(His)<sub>10</sub> tag was exchanged into a StrepII-tag by



Quickchange procedure.

For the construction of sGFP fusions, PCR fragments of the sGFP coding region were cloned into the *Xho*I restriction site of pET21a(+) vectors containing the coding sequence for either ETA or ETB.

For the G $\alpha$  subunits G $\alpha_s$  and G $\alpha_q$ , the human coding sequence was cloned into pET21a(+) vectors. Two thrombin cleavage site, one after the T7-tag and one before the poly-(His)<sub>10</sub> tag were also introduced.

PET vectors were chosen as templates for the CF expression as they provide high protein yields under the control of the T7 promoter, furthermore these vectors contain a N-terminal T7-Tag as well as a C-terminal poly-(His)<sub>10</sub> tag. In the ETB-Strep construct, the Strep tag was introduced by quick change mutagenesis of the poly-(His)<sub>10</sub> tag.

Purification of plasmid DNA for sequencing-grade purity was commonly performed with NucleoSpin Plasmid purification kit using a 3 ml o.n. culture. Plasmid DNA used as template for CF expression was isolated with NucleoBond AX100 commercial kits using 150 ml o.n. culture according to manufacturer's recommendations.

### 3.2 Plasmid DNA transformation into competent *E. coli* cells

For transformation of plasmid DNA, chemical competent *E. coli* DH5 $\alpha$  cells (Inoue et al. 1990) were used. 100  $\mu$ l of cells, initially stored at -80 °C, were thawed on ice. 10  $\mu$ l of the ligation reaction was directly added to the cells and incubated on ice for 30 min followed by a heat shock of 42 °C for 45 s. Subsequently, the cells were incubated on ice for additional 5 min. 750  $\mu$ l of pre-warmed LB medium without antibiotics was added and cells were grown at 37 °C for 1 h. The cells were centrifuged at 5,000 x g for 5min at RT and resuspended in 100  $\mu$ l of LB medium. The cell suspension was finally plated on agar plates containing the appropriate antibiotic and incubated at 37 °C o.n.. Single colonies were picked and grown in LB-medium. DNA was isolated, subjected to test restriction and promising clones sequenced by SeqLab Sequence Laboratories (Germany).

### 3.3 Preparation of *E. coli* S30 extract

The extract preparation was principally based on the protocol developed by Zubay (Zubay et al. 1973), with some minor modifications. RNase deficient *E. coli* strain A19 was used for extract preparation (Schneider et al. 2010, Schwarz et al. 2007).

The overall procedure takes generally 3 days and allows the preparation of 70-100 ml of S30

extract for from a 10 L culture.

During the first day all the necessary buffers, media and material were prepared and sterilized. *E. coli* A19 cell, obtained from a freshly prepared plate, were inoculated over night in 100 ml LB medium at 37 °C with vigorous shaking. 5L of 2X YTPG medium was filled in the fermenter and sterilized by autoclaving. 50-fold stock solutions of S30 A/B buffer and S30 C buffer as well as 5 M NaCl, glucose and phosphate buffer were prepared, sterilized by filtering and stored at 4 °C until further use (for the preparation see 2.11).

The second day the YTPG medium was completed by addition of glucose (1 L) and phosphate buffer (2L), as well as 2L of sterilized water. The medium was heated at 37 °C under good aeration condition. The A19 pre-culture was inoculated and cells were then incubated at 37 °C under vigorous stirring at 500 rpm until an OD600 of 4.0 (mid-logarithmic phase) was reached.

Cells were subsequently rapidly chilled below 12 °C in the fermenter by using internal and external cooling sources. The cells were then collected into centrifuge beakers that were kept at 4 °C and harvested by centrifugation at 5,000 x g and 4 °C for 15 min. The pellet was resuspended in 300 ml of pre-cooled 1-fold S30 A buffer supplemented with  $\beta$ -mercaptoethanol and centrifuged for 15 min at 5,000 x g and 4 °C. This washing step was repeated twice with the same buffer and an extended final centrifugation for 30 min was performed. The resulting cell pellet was weighted and resuspended in 110 % (v/w) of pre-cooled 1-fold S30 B buffer supplemented with PMSF and DTT.

Cells were subsequently lysed using a french press cell. The disrupted cells were centrifuged at 30,000 x g for 30 min at 4 °C. The non-turbid upper part of the supernatant was collected and subjected to a second centrifugation step.

Subsequently, a run-off step was performed in order to remove endogenous mRNA. The supernatant was adjusted to a final concentration of 400 mM NaCl and the extract was incubated in a water bath at 42 °C for 45 min. The extract was then transferred into dialysis tubes with a MWCO of 12-14 kDa and was dialyzed once with 5 L of cold S30 C buffer for at least 2 h at 4 °C. Then, the dialysis buffer was exchanged and the dialysis continued o.n. at 4 °C.

During the third day of preparation the dialyzed extract was centrifuged at 30,000 x g for 30 min at 4 °C. The supernatant was immediately aliquoted to appropriate volumes and shock-frozen in liquid nitrogen. The frozen extract was stored at -80 °C for several months.

### 3.4 CECF Configurations

Basic CF expression protocols were previously described (Schneider et al. 2010, Schwarz et al. 2007). Analytical scale reactions were performed in mini-CECF reactors using 24-well

microplates. Appropriate dialysis membranes with a cut-off of 12-14 kDa were used to separate the reaction mixture (RM) from the feeding mixture (FM). The RM volume was 55  $\mu$ l and the ratio RM/FM was 1:15. Preparative scale expression was performed in maxi-CECF reactors (Schneider et al. 2010). The RM volume in this case was in between 1 to 3 ml and the RM to FM ratio of 1:17. A detailed list of all the necessary reaction components is given in Table 4.

Component	Stock concentration	Final concentration	Unit
In RM			
S30-Extract	100%	35%	%
Template DNA	200	0.03	$\mu$ g/ml
RiboLock™	3.8	0.05	U/ $\mu$ l
T7-RNA Polymerase	3.8	0.05	mg/ml
E. coli tRNA	40	0.5	mg/ml
Pyruvate Kinase	10	0.04	mg/ml
In RM and FM			
Amino acids-Mix	8	0.6	mM
RCMWDE-Mix	16.7	1	mM
AcP	1000	20	mM
PEP	1000	20	mM
NTPs Mix	75	1	x
DTT	500	2	mM
Folinic Acid	10	0.1	mg/ml
Complete	50	1	x
Hepes buffer	24	1	x
Mg(OAc) <sub>2</sub>	1000	11.1 <sup>a</sup>	mM
KOAc	4000	110 <sup>a</sup>	mM
PEG8000	40	2	%
NaN <sub>3</sub>	10	0.05	%

**Table 4.** Components required for a P-CF expression of MPs. <sup>a</sup>, Amount necessary for having a final concentration of 16 mM Mg<sup>2+</sup> and 270 mM K<sup>+</sup>. RM: reaction mixture, FM feeding mixture.

CF reactions were incubated for 16 to 20 h with gentle shaking at 30 °C (Schwarz et al. 2007). In order to analyze the effect of the temperature on the quality of the sample produced in L-CF mode in presence of L- $\alpha$ -phosphatidylcholine from soybean, type IV-S (Aso-PC), the reaction was also carried at 27 °C, 25 °C and 20 °C.

Optimal concentrations of Mg<sup>2+</sup> and K<sup>+</sup> ions for each S30 extract batch were analyzed in analytical scale reactions in the P-CF mode.

CF expressed proteins were collected either as a precipitate (P-CF, L-CF + liposomes) or as supernatant (D-CF, L-CF + NDs) by centrifugation at 18,000 x g for 10 min at 4 °C.

P-CF precipitates were washed two times in buffer (20 mM Tris-HCl, pH 7.5 and 150 mM NaCl) and resuspended in buffer supplemented with detergents in a volume equal to the corresponding RM. Protein solubilization was achieved by incubation with gentle shaking for 1 h at 30 °C. Residual precipitate was removed by centrifugation at 18,000 x g for 10 min. Detergents used for resolubilization were 1% LPPG, 1% LMPC, 1% LMPG, 2% or 0.5% DPC.

In the D-CF mode, the detergent Brij78 at a final concentration of 1% was directly added into the RM for the expression of ETB. For the D-CF expression of the G $\alpha$  subunits, the detergents Digitonin 0.4%, Brij78 1%, Brij35 0.5% were used. Stock solutions for the detergents were prepared in distilled water at a concentration of at least 10-fold the working concentration and stored at 20 °C until further use.

The lipids used for L-CF expression were L- $\alpha$ -phosphatidylcholine from soybean, type IV-S (Aso-PC), DMPC, DOPC, heart total lipid extract and *E. coli* polar lipid mixture. To test the effect of cholesterol, Aso-PC liposomes were also supplemented with different concentration of cholesterol hemisuccinate (CHS) (2.5%, 5%, 10%). In order to visualize the liposomes using confocal microscopy, Aso-PC lipids were supplemented with 0.1% phosphatidylethanolamine (PE) labelled with rhodamine. The lipids were solubilized in chloroform, evaporated under vacuum to a thin film and completely dried overnight. The film was resuspended in liposome buffer (20 mM potassium phosphate, pH 7.0, 150 mM NaCl) to a final concentration of 40 mg/ml, briefly sonicated in a sonication bath and extruded to a size of 0.2  $\mu$ m. The formed liposomes were then directly added into the RM to a final concentration of 4 mg/ml. For the L-CF mode in the presence of liposome/detergent mixtures, the detergents Brij35 (0.04%), Brij78 (0.04%), digitonin (0.2%) and Chaps (0.5%) were pre-mixed with pre-formed Aso-PC liposomes and added directly into the RM. For L-CF expression in the presence of NDs, pre-formed NDs were directly added into the RM at different concentrations as indicated.

### 3.5 Nanodiscs preparation

The preparation of nanodiscs was based on previously described protocols (Denisov et al. 2004, Roos et al. 2012). The whole procedure usually requires 3 days.

During the first day all the necessary buffers, media and material were prepared and sterilized. For the complete list of the required buffers, see 2.14. *E. coli* BL21 (DE3) cells, transformed with the plasmid containing the membrane scaffold protein MSP1 or MSP1E3D1, obtained from a freshly prepared plate, were inoculated over night in 100 ml LB medium containing the antibiotic kanamycin diluted 1/1000 at 37 °C with vigorous shaking.

The second day 30 ml of 10% glucose was added to each of two 2L flask containing 600 ml of LB medium and kanamycin (1/1000). 50 ml of the pre-culture was transferred in each flask and incubated at 37 °C with shaking until an optical density of 1 was reached. At this point IPTG, at a final concentration of 1 mmol/L was added and the incubation continued for 1 hour at 37 °C and for additional 4 hours at 28 °C. The cells were then centrifuged at 7000 rpm for 10 minutes at the pellet was stored at -20 °C till the next day.

The third day the pellet was resuspended in 50 ml of resuspension buffer supplemented with Triton X-100 at a final concentration of 1%. In order to disrupt the cells, 3 sonication cycles of 60 seconds followed by 3 sonication cycles of 45 seconds were performed, with a rest period of at least 60 seconds between each cycle and keeping the cells on ice during the procedure. The suspension was then centrifuged 20 min at 16.000 rpm using a SS34 rotor. The supernatant was collected and filtered with 0.45 µm filter tips. In the meantime a 20 ml His-trap column (hi-prep IMAC FF16/10) was equilibrated with 100 ml of buffer 3. The filtered supernatant was loaded on the column and washed with 100ml of buffer 1, 2, 3 and 4. The MSP was then eluted using the buffer 5 and fraction of around 10 ml collected. Presence of MSP was evaluated by Nanodrop and usually around 20-30 ml of MSP at a concentration of around 1.5 mg/ml was obtained. The MSP1 containing fractions were pooled together and transferred into dialysis tubes with a MWCO of 12-14 kDa, dialyzed against buffer 6, first for 3 hours, and subsequently for further 12 hours after buffer exchange at 4°C. The purified protein was then collected and glycerol was added to give a final concentration of 10%. The purified MSP was then stored at -80 °C until use. For the formation of NDs different lipids were used: DMPC, POPC, DMPG, Aso-PC, Aso-PC + 5% cholesterol hemisuccinate and brain total extract (BTE). The lipids were solubilized in chloroform, evaporated under vacuum and dried overnight. The lipid film was resuspended in buffer (20 mM Tris-HCl, 100 mM NaCl, 100 mM Na-cholate) to a final concentration of 50 mM. The lipids were mixed with the purified MSPs in the presence of 0.1% DPC and incubated for 15 min at room temperature. Different ratios of MSP to lipids were used (Table 5). Removal of detergents and formation of NDs were performed by dialysis for 24 h in buffer (20 mM Tris-HCl, 100 mM NaCl).

Prepared NDs were then concentrated using Millipore centrifugal filter units to a final concentration of 8 to 10 mg/ml and stored at 4°C before usage, for maximum a week.

Lipid	MSP1 to lipid ratio	MW (kDa)	MSP1E3D1 to lipid ratio	MW (kDa)
DMPC	1:80	159	1:115	220
POPC	-	-	1:85	193
DMPG	-	-	1:100	215
Aso-PC	-	-	1:50	157
BTE	-	-	1:70	176

**Table 5. Ratio of MSPs to lipid used for the preparation of empty nanodiscs.** The stoichiometries are expressed in molar ratio. The theoretical molecular weight was calculated from the experimental determined values. Table adapted from the PhD Thesis of Christian Roos.

### 3.6 SDS-PAGE and Western-blot

Denaturing SDS-PAGE was used for the analytical separation of proteins, according to their molecular weight (Laemmli et al. 1970). Commonly 2-3  $\mu$ l of resuspended protein pellet or supernatant were supplemented with SDS loading buffer (7.5% SDS (w/v), 50% (v/v) glycerol, 25% (v/v)  $\beta$ -mercaptoethanol, and 0.1% (w/v) bromophenol blue in 0.3 M Tris-HCl pH 6.8). Samples were separated by 12% or 16% (w/v) SDS gels, at 100 V for 15 min, followed by 200 V for 45 min with constant current. The gels were then stained with Coomassie blue or analyzed by immunoblotting.

For the Coomassie staining, the gels were incubated in fresh Coomassie solution for 1 h. The solution was then removed and the gels were extensively washed with water. Distaining solution was added and constantly replaced with fresh solution till clear bands were visible.

For immunodetection, gels were blotted on activated 0.45  $\mu$ m immobilon-P membrane in wet Western blot apparatus for 30-40 min at 340 mA. The membrane was then blocked for 1 h in phosphate buffered saline supplemented with 4% skim milk powder and 0.05% Tween-20 followed by incubation with the first antibody (anti C-terminal His-tag (dilution 1:2000); anti N-terminal T7-tag (dilution 1:2000) or anti-biotin peroxidase conjugate (1:1000)) at 4 °C overnight with gentle shaking in antibody incubation buffer (PBS supplemented with 1% skim milk powder and 0.05% Tween-20). For the anti His-tag and anti T7-tag blots, after three washing steps in wash buffer (PBS and 0.05% Tween-20), the secondary antibody horse radish

peroxidase conjugate was added in antibody incubation buffer at a final concentration of 1:5000 for 1 h at room temperature. After extensive washing in washing buffer, the membranes were analyzed by chemiluminescence in a Lumi-Imager F1 using 5 ml ECL 1 and 2 solutions with incubation time of 1 min, respectively.

### 3.7 Determination of protein concentration

Protein concentrations were routinely estimated by 280 nm absorption using Nanodrop and Lambert-Beer equations. For sGFP tagged proteins, samples were analyzed for fluorescence using a Tecan GeniosPro (excitation: 485 nm, emission: 510 nm). Concentrations of protein samples were determined using a calibration curve obtained from purified sGFP sample. Commonly, 3  $\mu$ l of supernatant containing tagged sGFP protein were used per well, with 297  $\mu$ l of buffer (20 mM Tris-HCl pH 7.5, 100 mM NaCl).

### 3.8 IMAC: Ni-NTA chromatography

After P-CF or D-CF expression, the first detergent could be exchanged to a second detergent upon immobilized metal affinity chromatography (IMAC). Samples were centrifuged at 18,000 x g for 10 min in order to remove precipitate. The supernatant was diluted 1:5 in equilibration buffer (20 mM Tris-HCl, pH 7.5, 500 mM NaCl, 10 mM imidazole and detergent at 5-10x critical micellar concentration (CMC)) and mixed with pre-equilibrated NTA-agarose beads (Qiagen, Germany) loaded with Ni<sup>2+</sup> ions. 300  $\mu$ l of resin for ml of diluted RM were used. The mixture was incubated overnight at 4 °C, or alternatively for 1 h at RT, with gentle shaking and applied on an empty gravity flow column. The beads were washed with 10 column volumes (CVs) of washing buffer 1 (20 mM Tris-HCl, pH 7.5, 500 mM NaCl, 30 mM imidazole and detergent at 5-10 xCMC), 10 CVs of washing buffer 2 (washing buffer 1 with 80 mM imidazole) and 10 CVs of washing buffer 3 (20 mM Tris-HCl, pH 7.5, 150 mM NaCl and detergent at 5-10 xCMC). Proteins were finally eluted with elution buffer (20 mM Tris-HCl, pH 7.5, 150 mM NaCl, 400 mM imidazole and detergent at 5-10x CMC) in 4-5 fractions of 1 CV each. 10  $\mu$ l of each fraction was analyzed by 12% or 16% SDS-PAGE.

For the P-CF expression mode the detergent LMPG 1% (for the ETB sample) or CHAPS 0.1% (in case of the G $\alpha_s$  and G $\alpha_q$  subunit) was used. In D-CF mode, the detergent Brij78 1% was exchanged into LPPG 0.05%, Brij35 0.1%, Chaps 1%, DDM 0.5%, DPC 0.1% as well as Brij78 0.1%. IMAC was further applied to purify co-translationally formed GPCR/NDs complexes. In this case the same buffers described previously were used but in the absence of any detergent.

For the purification of the soluble fraction of  $G\alpha_s$  and  $G\alpha_q$  upon P-CF expression, the samples were diluted 1:5 in equilibration buffer (20 mM Tris-HCl, pH 7.5, 150 mM NaCl, 5 mM imidazole) and mixed with pre-equilibrated NTA-Agarose beads. The beads were then washed with 10 column volumes (CVs) of washing buffer (20 mM Tris-HCl, pH 7.5, 150 mM NaCl, 30 mM imidazole), and eluted with elution buffer (20 mM Tris-HCl, pH 7.5, 150 mM NaCl, 400 mM imidazole).

### 3.9 Low temperature-SDS-PAGE (LT-SDS-PAGE)

SDS resistant receptor/ligand complexes were monitored by LT-SDS-PAGE as previously described (Takasuka et al. 1991). ETB and  $\Delta$ ETB receptors were D-CF expressed in presence of Brij78 1% and affinity purified by IMAC in presence of Brij35 0.1% (see 3.8). Protein aliquots (0.5  $\mu$ g to 2  $\mu$ g) were incubated for 1 h at 4 °C with 10 ng of b-ET-1 in PBS in a total volume of 30  $\mu$ l. Samples were then mixed with SDS-PAGE loading buffer and separated on 16% SDS-PAGE at 10 °C. The gels were blotted on PVDF membranes and analyzed with anti-biotin peroxidase conjugate antibodies (see 3.6).

### 3.10 Streptavidin affinity chromatography

ETB-Strep expressed in presence of NDs in L-CF mode, was purified using the commercially available Strep-tag® Purification kit.

The strepII epitope consists of eight consecutive amino acids (W, S, H, P, Q, F, E and K) and displays intrinsic affinity to streptavidin. The purification was performed using pre-equilibrated streptavidin beads in a plastic gravity flow chromatography column. 500  $\mu$ L of resin was used per 1 mL of RM. Protein supernatant was diluted 1:5 in strepII-equilibration buffer (20 mM Tris-HCl, pH 7.5, 150 mM NaCl) and directly applied on the column. The protein was subsequently washed with 5 CV of strepII- wash buffer (20 mM Tris-HCl, pH 7.5, 150 mM NaCl) . The protein was finally competitively eluted in strepII-elution buffer (20 mM Tris-HCl, pH 7.5, 150 mM NaCl, 2.5 mM desthiobiotin) in three to five fractions of 1 CV each. 10  $\mu$ L aliquots of each fraction were analysed by 12% or 16% SDS-PAGE.

### 3.11 Size exclusion chromatography (SEC)

SEC with pre-packed column was used in order to assess the homogeneity of the produced samples. Protein preparations were centrifuged at 18,000 x g for 10 min prior to loading.



Samples were separated on a pre-equilibrated (20 mM Tris-HCl, pH 7.4, 150 mM NaCl and 0.1 % Brij35 in case of sample resolubilized in detergent) analytical Superdex 200 column (3.2 mm/30 cm) at a flow rate of 50  $\mu$ l/min on an Äkta Purifier station. SEC was conducted at 16 °C and the absorption at 280 was monitored during the run. For the ETB/NDs sample, 50  $\mu$ l fractions were collected.

### 3.12 Reconstitution of proteoliposomes

Reconstitution of proteoliposomes was done with P-CF produced GPCR samples directly after resolubilization with 1% LMPG in liposome buffer at a concentration of approx. 1.5 mg/ml. For D-CF expressed samples, the detergent used for the expression (Brij78 1%) was exchanged against second detergents upon IMAC. *E. coli* polar lipids or Aso-PC lipids were solubilized in 100% chloroform, evaporated under vacuum to a thin film and completely dried under vacuum overnight. After resuspension of the lipidic film in liposome buffer to a final concentration of 20 mg/ml, the liposomes were extruded to a size of 0.2  $\mu$ m. Protein samples and liposomes were then mixed at different molar ratios (from 1:250 to 1:4000). The mixture was incubated 1 h at room temperature and the detergent removed by addition of 500 mg Biobeads SM-2, pre-equilibrated with liposome buffer. After 1 h incubation, a new aliquot of Biobeads was added and the sample incubated for up to 48 h at 18 °C. Proteoliposomes were separated from empty liposomes in a discontinuous sucrose gradient of 10-20-30-40% sucrose in liposome buffer by ultracentrifugation at 83.000 x g (SW28 swing bucket rotor) for 16 h at 4 °C. The liposome layer was collected with a syringe, resuspended in liposome buffer and centrifuged at 195.000 x g (70Ti rotor) two times for 1 h at 4°C. The pelleted proteoliposomes were resuspended in liposome buffer, shock frozen in liquid nitrogen and stored at -80 °C.

### 3.13 Ligand affinity chromatography

Avidin agarose beads were prepared following the manufacturer's recommendations and subsequently incubated with 100  $\mu$ g of b-ET-1 for 100  $\mu$ l of matrix. Peptide loading was continued for 1 h at 4 °C in matrix buffer (20 mM Tris-HCl, pH 7.5, 150 mM NaCl and 0.1% Brij35). Unbound ligand was removed by washing with 3 CVs of matrix buffer. Purified ETB or  $\Delta$ ETB (3  $\mu$ M) in 0.1% Brij35 were diluted 1:3 in matrix buffer and loaded on the matrix. The matrix was then incubated for 2 h at room temperature with gentle shaking. The flow through was collected and the matrix was washed 10 times with 1 CV of matrix buffer in order to remove unbound protein. Elution of the ligand bound receptor was then performed using 2 mM d-

desthiobiotin in matrix buffer. One step of 0.5 CV was followed by 8 elution steps of 1 CV. Aliquots of 32  $\mu$ l (for the flow through and the first elution fraction) and of 55  $\mu$ l (for the washing and elution fractions) were analyzed by 12% SDS-PAGE followed by immunoblotting.

### 3.14 Radioactive ligand binding assays

For radioassays of proteoliposomes, 500 nM protein/well was incubated with 500 pM [ $^{125}$ I]Tyr $^{13}$ ET-1 (specific activity 2200 Ci/mmol) in a final volume of 50  $\mu$ l binding buffer (20 mM potassium phosphate, pH 7.0, 150 mM NaCl, 0.1% (w/v) bovine serum albumin) for 1 h at room temperature in 96-well microplates. In order to determine unspecific binding, the samples were pre-incubated for 1 h at 4  $^{\circ}$ C with 4  $\mu$ M final concentration of unlabeled ET-1 before addition of labeled ligand. Reactions were stopped by addition of cold binding buffer and samples were transferred to GF/B glass fiber filters (Millipore, Eschborn, Germany) pre-treated for 10 min with 0.3% polyethyleneimine and washed with 500  $\mu$ l binding buffer. Unbound ligand was removed by washing filters three times with 150  $\mu$ l of binding buffer. Dry filters were finally collected and the retained radioactivity was determined in a gamma counter (Cobra II Auto gamma). Ligand binding controls were performed using Chem1 mammalian cell membrane preparations containing recombinant human ETA or ETB receptor. Control membrane aliquots of 5  $\mu$ g were incubated with 500 pM of [ $^{125}$ I]Tyr $^{13}$ ET-1 for 1 h at room temperature. Unspecific binding was determined in the presence of 4  $\mu$ M unlabeled ET-1.

For saturation radioassay experiments with NDs, 0.25  $\mu$ l (7 ng) of purified ETB-sGFP/NDs (DMPC) resulting into 5 nM estimated final protein concentration per well was incubated with increasing concentrations of [ $^{125}$ I]Tyr $^{13}$ ET-1 in a final volume of 20  $\mu$ l in binding buffer (50 mM Hepes, pH 7.5, 5 mM MgCl $_2$ , 1 mM CaCl $_2$ , 0.2% BSA) for 1 h at room temperature. In order to determine unspecific binding, the samples were pre-incubated for 1 h at 4  $^{\circ}$ C with 4  $\mu$ M final concentration of unlabeled ET-1 before addition of labeled ligand. After the incubation, the samples were transferred to GF/B glass fiber filters pre-treated for 20 min with 0.3% polyethyleneimine and washed with 300  $\mu$ l of plate washing buffer (50 mM Hepes, pH 7.5, 0.5% BSA). Unbound ligand was removed by washing the filters five times with 150  $\mu$ l washing buffer (50 mM Hepes, pH 7.5, 500 mM NaCl, 0.1% BSA). Radioactivity was finally measured with the dried filters.

For competition experiments, same amounts of NDs or proteoliposome samples were pre-incubated for 1 h at room temperature with increasing concentrations of unlabeled ET-1 before adjusting to 500 pM [ $^{125}$ I]Tyr $^{13}$ ET-1. After 1 h incubation, the samples were transferred to GF/B glass fiber filters pre-treated for 20 min with 0.3% polyethyleneimine and washed with 300  $\mu$ l of plate washing buffer (50 mM Hepes, pH 7.5, 0.5% BSA). Unbound ligand was removed by

washing the filters five times with 150  $\mu$ l washing buffer (50 mM Hepes, pH 7.5, 500 mM NaCl, 0.1% BSA). Unspecific binding was determined in the presence of 2  $\mu$ M unlabeled ET-1.

All the collected data were analyzed by non-linear regression curve fitting using GraphPad Prism 5.

### 3.15 Ligand binding assay using Cy-3-ET-1

For the determination of Cy3-ET-1 binding, 2 nM of IMAC purified ETB-sGFP/ND (DMPC) or PR-sGFP/ND (DMPC) (measured according the sGFP fluorescence), were incubated for 1 h with 10 nM Cy3-ET-1 in a final volume of 25  $\mu$ l in PBS. The mixture was then applied on a Microspin G-50 column and centrifuged at 770 x g for 2 min. The GPCR/ligand complex was collected in the flow-through while the unbound ligand remained in the column. Fluorescence of Cy3 was then measured using Tecan GeniosPro (Excitation: 535 nm, emission: 612 nm). In order to determine the percentage of active receptor in a 1:1 binding model was used the formula: RFU measured in the flow-through/511 RFU X 100, where 511 RFU are the RFU measured for 2 nM Cy3-ET-1. For the ligand binding analysis of the sample after SEC, 2nM of protein from each fraction (according to the sGFP fluorescence) was used.

### 3.16 Ligand binding assay by fluorescence anisotropy

Fluorescence anisotropy experiments of P-CF produced ETB receptor reconstituted into liposomes were performed using a Jasco spectrofluorimeter FP-6500. After expression, the protein was resolubilized in 1% LMPG and purified in the same detergent. Liposomes were prepared using *E. coli* polar lipids and the proteoliposomes, at a ratio protein to lipids of 1:1000, were prepared as described in 3.12. Ligand binding analysis was carried out with the fluorescein-labelled linear derivative 4-Ala-ET-1. Excitation and emission maxima have been determined at 498 nm and 520 nm, respectively. A G-factor for the ligand of 1.50 was measured in assay buffer (20 mM Tris-HCl, pH 7.5, 150 mM NaCl).

For saturation experiment, 30 nM of 4-Ala-ET-1 was incubated with increasing concentrations (0-3  $\mu$ M) of ETB receptor reconstituted into liposomes for 1.5 h at RT in a final volume of 500  $\mu$ L of assay buffer. Anisotropy was determined as mean value of seven repetitions per data point. The observed anisotropy signal was normalized by subtraction of the anisotropy values of 0.038 gained from free 4-Ala-ET-1 in assay buffer. Data were processed by non-linear regression curve fitting using GraphPad Prism 5.

### 3.17 Ligand binding analysis by ELISA assay

In order to detect the binding of the ligand b-ET-1 to immobilized ETB-sGFP/ND (DMPC), experiments were performed using a 96-well NUNC Immobilizer nickel-chelate plate.

The plate was first washed 3 times using 300  $\mu$ l of PBS buffer supplemented with 0.05% Tween (PBS-T). 100 $\mu$ l of IMAC purified and dialyzed (20 mM Tris-HCl pH 7.5, 150 mM NaCl) ETB-sGFP/NDs (DMPC) or Pr-sGFP/NDs (DMPC) at final concentration of 2  $\mu$ M in PBS buffer were incubated in the plate for 2.30 h. The plate was then washed 5 times using 150  $\mu$ l of PBS buffer and 100  $\mu$ l of b-ET-1 at a final concentration of 1  $\mu$ M in PBS buffer was added. The plate was then washed 5 more times and incubated with anti-biotin HRP conjugated antibody (dilution 1:1000) in PBS buffer supplemented with 1% BSA. After 5 further washes with 150  $\mu$ l of PBS, the plate was then incubated with tetramethylbenzidine (TMB) substrate solution in the dark for 30 min. The reaction was stopped by adding 1 M HCl and the absorbance at 450 nm was measured using Nanodrop. In the competition assay, the immobilized ETB-sGFP/NDs were incubated with 100  $\mu$ l of unlabeled ET-1 at a final concentration of 1 $\mu$ M before the addition of the b-ET-1.

In order to detect the binding of ETB-sGFP/ND to other ligands, plain 96-well ELISA plates were used and selected ETB ligands (ET-1; ET-3; ALA-4-ET-1) were directly immobilized via non-specific coupling. 100  $\mu$ l of ligand at 1  $\mu$ M final concentration in coupling buffer (carbonate buffer pH 9.6) were incubated in the plate o.n. at 4 °C. The unbound ligands were removed by a washing step (5 washes with 200  $\mu$ l PBS) and the plate blocked with PBS and 3% BSA for 2 h. The plate was washed again 5 times and 100  $\mu$ l of ETB-sGFP/NDs or PR-sGFP/NDs at the final concentration of 200 nM were then added and incubated for 1h. After 5 more washes, the plate was incubated with 100  $\mu$ l of primary antibody (anti-His tag antibody, dilution 1:2000) in PBS buffer supplemented with 3% BSA for 2 h and, after 5 washing steps using PBS buffer, 100  $\mu$ l of the secondary antibody horse radish peroxidase conjugate was added in PBS buffer plus 3% BSA at a final concentration of 1:5000 for 1 h at RT. After extensive washing, TMB substrate solution was added and incubated for 30 min, after addition of 1M HCl, the absorbance at 450 nm was measured.

### 3.18 Confocal microscopy

Images were acquired using a Zeiss LS 510 confocal microscope with an oil immersion Plan-Apochromat 63x/1.4. Excitation was provided by an argon lamp filtered with standard bandpass excitation/emission filter cubes.

### 3.19 Surface Plasmon Resonance Assay (SPR)

All the SPR measurements were conducted using a Biacore X100 (Biacore, Uppsala, Sweden).

To detect the binding of the receptor reconstituted into NDs to immobilized biotinylated ligands, SA chips were used. 50 resonance units (RUs) of b-ET-1 or b-ET-3 were immobilized on the second flow cell of the chips.

For the preliminary testing of buffer conditions, 50 nM of empty and IMAC purified NDs were used. Different running buffer were tested: 20 mM Hepes-NaOH pH 7.5, 150 mM NaCl; 20 mM Hepes-NaOH pH 7.5, 250 mM NaCl; 20 mM Hepes-NaOH, 500 mM NaCl. Screening was also performed using the same buffers supplemented with 0.2% BSA, 1% Glycerol or 0.05% detergent P-20.

Further experiments were performed using as running buffer 20mM Hepes-NaOH pH 7.5 and 500 mM NaCl. The samples were also diluted in the same buffer before the injection.

ETA, ETB and the sGFP derivatives co-translationally associated with MSP1E3D1-NDs were either IMAC purified or directly injected after CF expression without any previous purification.

In single cycle kinetic experiments, concentration series of the analyte (2.5, 5, 10, 50, 100 nM), with or without preincubation with 2  $\mu$ M ET-1 for 1h, were injected sequentially on the chip without regeneration in between the injections. The samples were injected for 240 sec with a flow rate of 40  $\mu$ l/min, the dissociation time was 600 sec. Signal obtained from the second flow cell was subtracted from the signal of the first flow cell and kinetic parameters were analyzed using a 1:1 interaction model (BIAEvaluation Software). In multi cycle kinetic experiments, the chips were regenerated with regeneration buffer (50 mM NaOH, 1 M NaCl) in between sample injections. Different concentrations of samples (from 0.1 nM to 50 nM) were injected on the chip for 120 or 180 sec at a flow rate of 40  $\mu$ l/min, dissociation curves were recorded for 600 sec. Competition experiments were performed using multi cycle kinetic experiments. Constant concentrations of GPCR/NDs samples (5 nM final protein concentrations according to sGFP fluorescence) were incubated before injection with increasing ligand concentrations from 0.01 nM to 6  $\mu$ M for 1 h at 4 °C. In all sensograms a report point at 10 s after the end of the injection was placed and the RU measured at the report point were plotted against the logarithm of the ligand concentration. Data were analyzed using GraphPad Prism and processed by nonlinear regression curve fitting.

ETB-Strep/NDs (DMPC) were also immobilized on a CM5 chip in order to detect the binding of unlabeled ligands. For the coupling of the anti-Strep antibodies, distilled water was used as running buffer at a flow rate of 10 ml/min. The chip was first activated with a solution of 400 mM EDC- 100 mM NHS for 10 min, after a brief wash with distilled water; three consecutive injections of anti-Strep antibody at a concentration of 10  $\mu$ g/ml in 10 mM acetate buffer pH 5

were performed. The excess of reactive groups was finally removed using 1 M ethanolamine injected on the chip for 10 min. At the end of the coupling procedure, around 8500 RUs of anti-Strep antibody were immobilized. ETB-strep/NDs were directly injected on the chip after CF expression. After 8 consecutive injections of 10 min each, around 1000 RUs were immobilized. Three different ligands (ET-1, IRL-1620, BQ-123) at concentrations from 0.1 nM to 5  $\mu$ M were injected sequentially on the chip. Due to the shape of the obtained curves, affinity analysis (BIAevaluation Software) was used in order to determine the ligand binding constant  $K_D$ . At the end of each cycle the ETB-Strep/NDs were removed using sequential injections of 10mM Glycine-HCl pH 2.5 and new samples were immobilized on the chip.

### 3.20 Microscale Thermophoresis Assay (MST)

MST experiments were performed using a Monolith NT.115 instrument (NanoTemper, Germany). 200 nM of the labeled ligand Cy3-ET-1 were shortly incubated with different concentrations of ETB/NDs (DMPC) (from 0.01 nM to 50 nM) in 20 mM Tris-HCl pH 7.5, 500 mM NaCl. Samples were then loaded on a glass capillary and the thermophoretic pattern of each sample recorded. Non-linear regression curve fitting was used for the determination of the  $IC_{50}$  value.

### 3.21 OCTET Assay

Experiments were performed using an OCTET System (fortéBio, USA). In order to immobilize the biotinylated ligand b-ET-1, SA biosensor tips were used. Experiments were performed in parallel using 96 well microplates. Two different buffer were tested: Tris buffer ( 50 mM Tris pH 7.5, 150 mM NaCl) as well as Hepes buffer ( 20 mM Hepes-NaOH pH 7.5, 500 mM NaCl). Buffers were also supplemented with 1% BSA in order to reduce the unspecific binding. Different concentrations of b-ET-1 were immobilized on the biosensor tips (1.8, 3.75, 15, 30, 60 nM). The biosensors were then incubated with 50 nM of IMAC purified ETB-sGFP/ND or empty ND. To evaluate the unspecific binding of the NDs , in each experiment one empty biosensor, incubated in buffer without b-ET-1, was also used.

### 3.22 Analysis of the activity of the $G\alpha_s$ subunit: fluorescent assay

Experiments were performed using a non-hydrolyzable fluorescent analogue of GTP, the BODIPY-GTP- $\gamma$ -S. For the analysis of the basal activity of the  $G\alpha_s$  subunit, 200 nM of IMAC purified proteins were incubated in buffer (10 mM Hepes-NaOH pH 7.5, 10 mM  $MgCl_2$  pH 8, 100 mM

NaCl) containing 50 nM of BODPY-GTP- $\gamma$ -S, in presence or absence of 1  $\mu$ M GDP. The fluorescent signal was measured in real time or after 40 min incubation using a TECAN GeniosPro. The activity of the sample was also measured after storage for 24h or 48h at 4 °C in 20 mM Tris pH 7.5, 150 mM NaCl and 10% glycerol.

In the activation assay, 200 nM of IMAC purified  $G\alpha_s$  was incubated in buffer (10 mM HEPES-NaOH pH 7.5, 10 mM  $MgCl_2$  pH 8, 100 mM NaCl, 1  $\mu$ M GDP) in presence of 50 nM of IMAC purified ETB/NDs (DMPC) or ETB93a/NDs (DMPC), in presence or absence of the ligand ET-1 (1 $\mu$ M).

### 3.23 Analysis of the activity of the $G\alpha_s$ subunit: radioactive assay

The experiments were performed using a non-hydrolyzable radioactive analogue of GTP, the GTP- $\gamma$ -S<sup>[35]</sup>.

For the analysis of the basal activity, 200 nM of IMAC purified  $G\alpha_s$  were incubated in buffer (10 mM HEPES pH 7.5, 10 mM  $MgCl_2$  pH 8, and 100 mM NaCl) containing 5 nM of GTP- $\gamma$ -S<sup>[35]</sup> in presence or absence of 1 $\mu$ M GDP. Aliquots at different time points were collected and filtered using a MultiScreen HTS HA filter. The collected filters were then incubated o.n. with 2 ml of scintillation cocktail and radioactivity measured using the Scintillation counter LS 6500.

For the activation assay, 50 nM of purified ETB/ND (DMPC) expressed in L-CF mode were incubated in presence of 200 nM  $G\alpha_s$  and 5 nM GTP- $\gamma$ -S<sup>[35]</sup> with or without 1 $\mu$ M of ET-1, IRL-2500 or IRL-1620. Samples were incubated in buffer (10 mM HEPES pH 7.5, 10 mM  $MgCl_2$  pH 8, and 100 mM NaCl) for 40 min, filtered and the radioactivity measured as previously described. As positive control for the activation assay, 5 $\mu$ l of membranes (Chemiscreen, ETB membrane preparation) were incubated with 5 nM GTP- $\gamma$ -S<sup>[35]</sup> with or without 1 $\mu$ M of ET-1, IRL-2500 or IRL-1620. Samples were processed in the same way as for the ETB/NDs samples.

## 4. Results

### 4.1 Cell-Free expression of ETB: P-CF mode

Using the precipitate expression mode (P-CF) is one of the simplest ways to produce a protein in CF. In absence of any provided hydrophobic environment, the synthesized MPs tend to aggregate and precipitate. By centrifugation the MPs can be recovered in the pellet fraction and the expression directly quantified. For this reason this expression mode is very useful for the optimization of the CF reactions protocol, with the aim to maximize the yield of protein expression.

For the P-CF expression mode, as DNA template for the reaction, the expression plasmid pet21a(+) carrying the coding sequence of the human ETB receptor was used. The protein synthesis resulted in the construct T7-ETB-poly(His)<sub>10</sub>, further abbreviated as ETB. The T7 tag at the N-terminus of the receptor was essential for the expression, as no detectable production was achieved in absence of this tag (Klammt et al. 2007). The ETB coding sequence leads to the synthesis of the mature form of the protein, lacking the signal sequence. This signal peptide of 26 amino acids is necessary in vivo for the correct targeting and insertion of the receptor in the ER and is removed by signal peptidases before the export to the cell surface (Köchli et al. 2002). The N-terminal poly(His)<sub>10</sub> tag was added to ensure an efficient IMAC purification.

CECF reactions usually display a defined optimum for Mg<sup>2+</sup> and K<sup>+</sup> ions for every batch of S30 extract. Screening for optimal concentrations were performed each time a new extract was used, and in case of ETB receptor was in general in between 14-18 mM Mg<sup>2+</sup> and 270-300 mM K<sup>+</sup> (Fig. 9). Without any detergent, the ETB receptor precipitated quantitatively. The ETB precipitate obtained from the P-CF expression was recovered by centrifugation at 18,000 x g at 4 °C for 10 min and washed twice with resuspension buffer, in order to remove impurities from the *E. coli* extract as well as to reduce the contaminant proteins that co-precipitate with the target protein. 3µl of supernatant or pellet resuspended in resuspension buffer in the same volume of the RM, were loaded on a 12% SDS-PAGE and analyzed by Coomassie staining. In the SDS-PAGE a band around 45 kDa was detected. Using the optimized basic protocol expression rates in between 1-3 mg of ETB per ml of RM were obtained (Fig. 9).



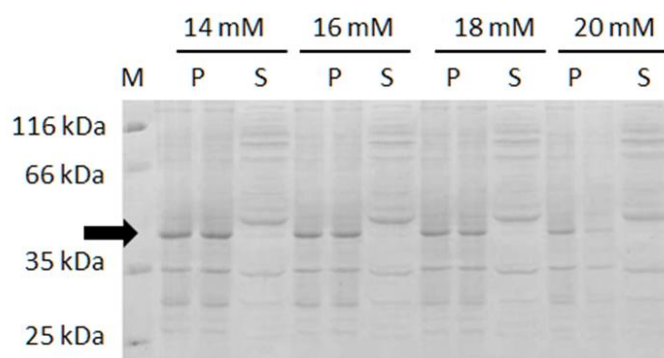


**Fig. 9: Mg<sup>2+</sup> optimization screen.** 3  $\mu$ l of protein samples from the pellet or the supernatant fractions of analytical P-CF reactions were loaded on a 12% SDS-PAGE gel. Different Mg<sup>2+</sup> concentration were tested. The arrow indicates the ETB receptor band.

#### 4.2 Evaluation of detergents for the post-translational solubilization

Specific sets of detergents can be efficiently used for the solubilization of membrane protein. *In vivo*, detergents like DDM, Triton x-100 and digitonin are routinely used for the extraction of MPs directly from the membrane. In the CF system the solubilization of the precipitate obtained from the P-CF expression mode can be achieved by the addition of detergents in the resuspension buffer. ETB could be completely resolubilized in 1% LMPG, LPPG and LMPC as well as in 2% DPC (Fig. 10).

The relatively mild detergent long-chain phosphoglycerol LMPG was chosen for further experiments. This detergent already proved to be efficient in the solubilization of other GPCRs including ETA and V2R (Junge et al. 2010, Klammt et al. 2007).

The solubilized ETB receptor could be efficiently purified via IMAC, taking advantage of the poly(His)<sub>10</sub> tag. Routinely 1-1.5 mg/ml of purified protein were obtained in presence of LMPG 1% (Fig. 10)

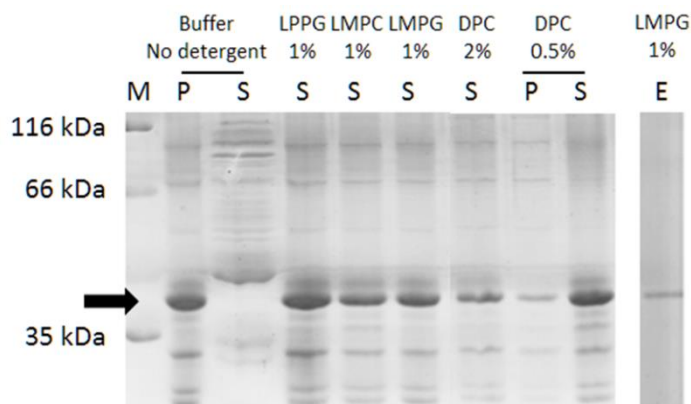


**Fig. 10: Solubilization screen and IMAC purification of P-CF expressed ETB.** ETB precipitates were resuspended in buffer with or without detergent. After resolubilization the samples were centrifuged 18000 x g for 10 min. The supernatant was then collected and the pellet (when present) was resuspended in the same volume used for the resolubilization. 3  $\mu$ l of supernatant or pellet were loaded on a 12% SDS-PAGE. For the IMAC purification 10  $\mu$ l of the elution fraction (E) was separated on 12% SDS-PAGE gel.

#### 4.3 Post-translational reconstitution into liposomes and functional assays

In order to obtain functional information about the ligand binding activity of the ETB receptor in a lipid environment, the solubilized and purified receptor in LMPG 1% obtained from the P-CF expression was reconstituted into pre-formed liposomes composed of *E. coli* polar lipids (EPL) or Aso-PC lipids. The proteoliposomes formation was performed by incubation of the lipid/protein mixture at different ratio for 30 min at RT. Biobeads were then added to the sample in order to remove the detergent and the mixture was incubated over night at 4 °C. Proteoliposomes were then harvested with or without sucrose gradient ultracentrifugation (Fig. 11A) and further analyzed for their binding to the radiolabeled [ $^{125}$ I]Tyr<sup>13</sup>-ET-1 in filter binding assay. Non-specific binding of [ $^{125}$ I]Tyr<sup>13</sup>-ET-1 to the liposome samples was determined after blocking of specific binding sites by preincubation with an excess of 4  $\mu$ M non-labeled ET-1. Separation of the bound from the unbound ligand was achieved upon transfer on GF/B glass fiber filters and extensive washing. The radioactivity retained on the filter was measured in a gamma counter. In order to quantify the quality of the reconstitution, the amount of specific signal over the background was evaluated. Furthermore the analysis of the Bmax value, expressed as pmol/mg, gave important information regarding how many receptors are functionally reconstituted into the liposomes.

The results indicate that the functional reconstitution of P-CF synthesized ETB strongly depends

on the ratio of protein to lipid. The highest specific [ $^{125}\text{I}$ ]Tyr $^{13}$ ET-1 binding of 49% with a Bmax of 2.1 pmol/mg was obtained with EPL in a protein to lipid ratio of 1 to 1000 (Table 6). For the same sample a homologous competition experiment was performed. By using a non-linear regression and a one-site binding model a Ki value of 2.1  $\mu\text{M}$  was measured (Fig. 11B).

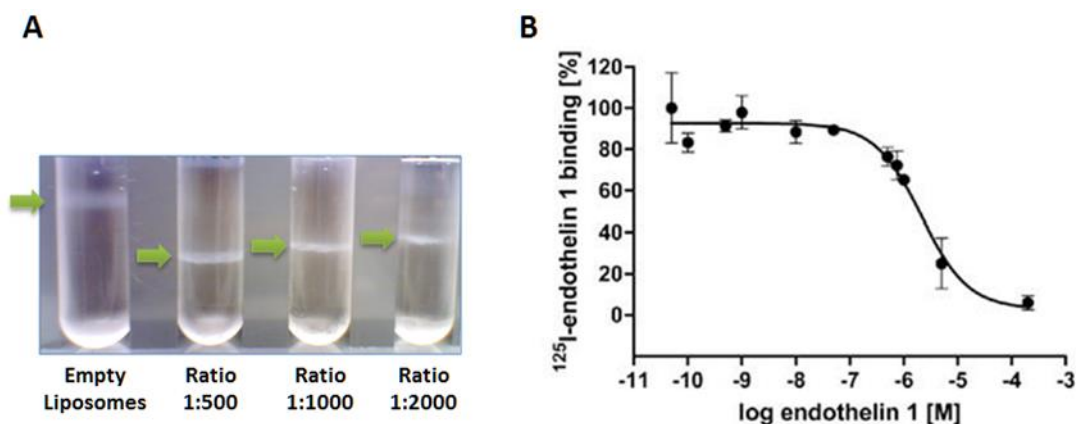


**Fig. 11: A. Sucrose gradient purification of ETB proteoliposomes.** ETB was P-CF expressed, resolubilized and purified in 1% LMPG. The protein was then reconstituted at different protein to lipid ratio (1:500; 1:1000; 1:2000) and subjected to sucrose gradient ultracentrifugation. **B. Radioligand competition assay.** Homologous competition experiments were performed with P-CF expressed ETB reconstituted into *E. coli* polar lipid liposomes (ratio 1:1000). Proteoliposomes were incubated with 500 pM [ $^{125}\text{I}$ ]Tyr $^{13}$ ET-1 and increasing concentrations of unlabeled ET-1 for 1 h at 22°C. Data points obtained from three independent measurements.

The specificity of the radioactive assay was verified using commercially available membrane preparations obtained from Chem1 mammalian cells expressing the human ETB receptor (Chemiscreen GPCR membrane preparation, Millipore, Eschborn, Germany). 5  $\mu\text{g}$  of membrane incubated with [ $^{125}\text{I}$ ]Tyr $^{13}$ ET-1 showed a high specific binding of approximately 85% and a Bmax value in the range of approximately 1 pmol/mg. In a homologous competition experiment a Ki value of 0.06 nM was measured.

detergent <sup>a</sup>	Lipids <sup>b</sup>	P/L-ratio	Specific binding <sup>c</sup> (%)	Specific activity (pmol/mg)	K <sub>i</sub> (nM)
LMPG, 1%	EPL	1:250	32 ± 2	2 ± 0.2	–
	EPL	1:500	26 ± 1	1.2 ± 0.1	–
	EPL	1:1000	49 ± 3.5	2.1 ± 0.3	2100
	EPL	1:2000	26 ± 1	0.8 ± 0.03	–
	EPL	1:4000	15 ± 3.5	0.3 ± 0.1	–
	Aso-PC	1:1000	36 ± 2	1.7 ± 0.1	–
Chemiscreen ETB membranes			85 ± 2	0.5 ± 0.05	0.06

**Table 6: Radioligand binding analysis of P-CF produced ETB reconstituted into liposomes.** a. Detergent used for the solubilization and purification. b. lipid used for the preparation of the liposomes. EPL: *E. coli* polar lipids; c. Percentage of the specific binding over the total binding.

The ligand binding activity of the P-CF produced ETB receptor reconstituted into liposomes was also analyzed by fluorescence anisotropy. In this experiment the binding of the ligand, that is labeled with a fluorophore, to the receptor induces an increase in the anisotropy signal due to a reduction in the rotational time of the fluorophore itself.

In the performed experiment the binding affinity of the linear fluorescein-labelled ligand 4-Ala-ET-1 to the P-CF produced ETB receptor reconstituted into liposomes was analyzed.

4-Ala-ET-1 is a mutated form of ET-1, lacking the two characteristic disulfide bridges due to the substitution of the four cysteines into alanines. This peptide is a specific ETB agonist and it shows a K<sub>D</sub> of 0.3 nM in *in vivo* experiment (Molenaar P. et al. 1992).

Fixed amount of fluorescein-4-Ala-ET-1 was incubated at RT for 1 h with increasing concentrations ETB proteoliposomes. Non specific binding was determined in presence of saturation amount of ET-1. The increase of anisotropy upon titration of ETB proteoliposomes to the ligand allows calculation of an equilibrium dissociation constant K<sub>D</sub> of 700 nM. High unspecific binding of the fluorescent ligand to the proteoliposomes was detected (Fig. 12).

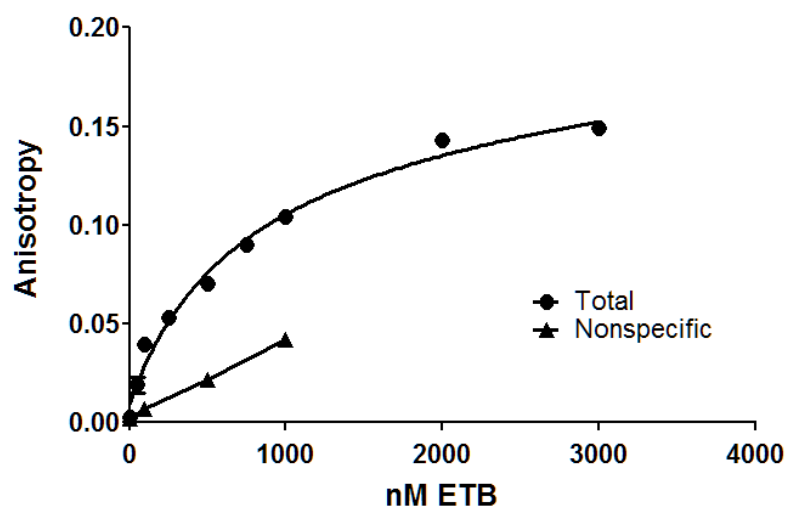


**Fig. 12: Ligand binding of P-CF produced ETB proteomicelles analyzed by fluorescence anisotropy.** 30 nM of fluorescein labelled 4-Ala-ET-1 was incubated with increasing concentration of ETB proteoliposomes (Total). Non-specific binding was determined by pre-incubation of the samples with 4 $\mu$ M ET-1 (Nonspecific). Each data point represents a mean value of 7 measurements. The observed anisotropy signal was normalized by subtraction of the anisotropy value of 0.038 obtained from free f-4-Ala-ET-1 in assay buffer.

#### 4.4 Cell-Free expression of ETB: D-CF mode

D-CF expression mode is an alternative approach for the production of MPs and offers the possibility for the co-translational solubilization of the target protein in a provided micelle environment. Preliminary studies showed that a complete solubilization of the ETB receptor was possible in the presence of the detergents Brij78 and Brij58, at a concentration of 1% and 1.5%, respectively (Klammt et al. 2007). Furthermore, the expression in Brij78 resulted in a ligand binding competent receptor. For this reason we decided to focus on this detergent for subsequent studies.

Effective expression of ETB in Brij78 was confirmed and after IMAC purification in presence of Brij 78 0.1% around 1 mg of receptor per ml of RM were routinely obtained (Fig. 13).

From the analysis by SDS-PAGE, two bands, corresponding to approximately 40 kDa and 35 kDa were observed. This particular event will be discussed in detail in the chapter 4.18.

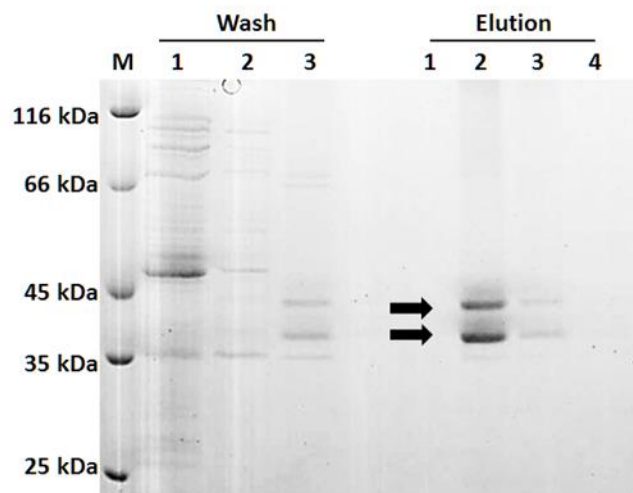


**Fig. 13: IMAC purification of D-CF produced ETB.** The reaction mixture of D-CF expressed ETB in presence of Brij78 1% was incubated over night at 4°C with Ni-Nta Agarose beads. Wash and elution of the protein was performed in buffer supplemented with Brij78 0.1%. 10  $\mu$ l of each fraction was loaded on a 12% SDS-PAGE and stained with Coomassie Blue. The arrows indicate ETB bands.

Immobilization of MPs upon IMAC purification allows exchanging the initial selected detergent for the solubilization of the protein to a second one having better properties. For this reason the possibility to exchange Brij78 into different detergents, usually used for structural and functional studies of GPCRs, were evaluated.

The detergent Brij78 1%, that was used for the D-CF expression, was exchanged into LPPG 0.05%, Brij35 0.1%, Chaps 1%, DDM 0.5%, DPC 0.1% as well as in Brij78 0.1%.

Exchange to the detergent CHAPS considerably reduced the yield of ETB in the elution fractions, since most of the protein was already lost during the washing steps. For the detergents DDM, DPC and LPPG yields around 0.3-0.5 mg/ml were obtained. Highest final yields of purified receptor were achieved in presence of the detergents Brij35 and Brij78 (0.5-1 mg/ml).

In order to address the quality of the purified receptor, the preparations were analyzed by size exclusion chromatography (SEC). The obtained elution profiles can give important information regarding presence of aggregates and protein homogeneity.

The samples purified in the different detergents were injected on an analytical Superdex 200 3.2/30 column. The most homogeneous elution profiles, centered around 1.4 ml (300 kDa) were obtained after exchange to DDM and Brij35 and Brij78, whereas two different peaks were detected upon exchange into the detergent DPC, CHAPS and LPPG (Fig. 14).

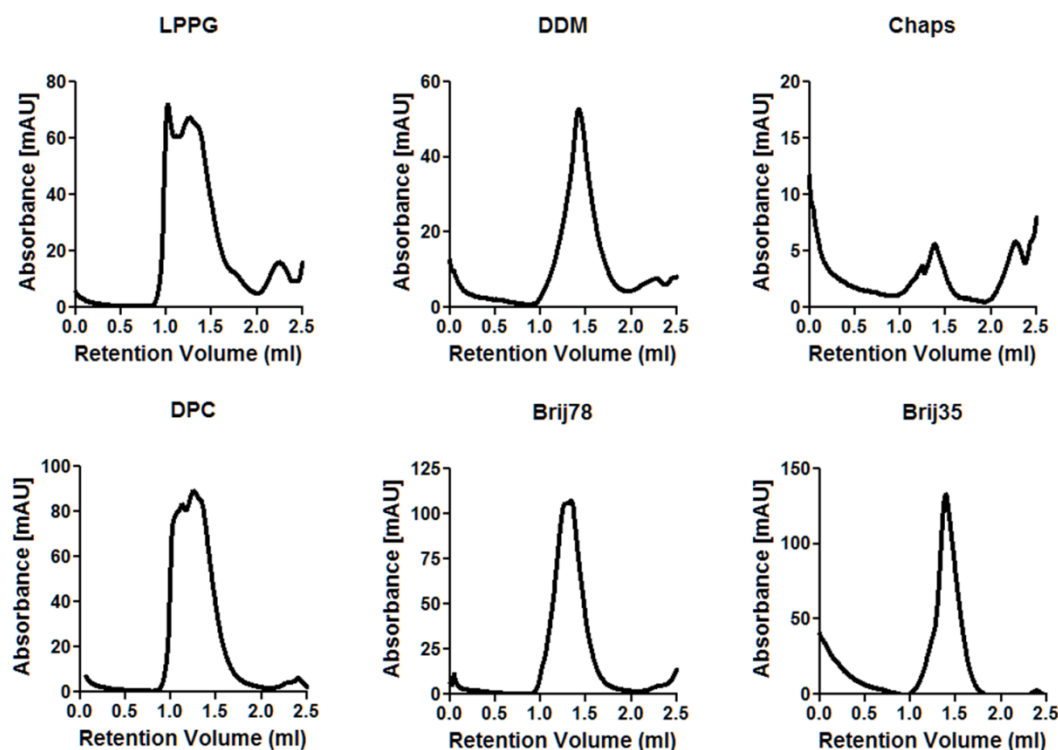


**Fig. 14: SEC analysis of D-CF expressed ETB:** The detergent Brij78 (1%) used for the D-CF expression was exchanged into a secondary detergent upon IMAC purification. 10-30  $\mu$ g of purified proteins were analyzed on a Superdex 200 3.2/30 column. Protein absorbance was recorded at 280 nm. The detergents used were LPPG 0.05%, DDM 0.5%, Chaps 1%, DPC 0.1%, Brij78 0.1%, Brij35 0.1%.

#### 4.5 Post-translational reconstitution into liposomes and functional assays

The ETB receptor produced in D-CF mode in presence of Brij78 1% was purified and reconstituted in liposomes in order to evaluate the ligand binding competence of the receptor in a lipid environment. The first detergent was exchanged to a variety of secondary detergent and the quality of the reconstitution was analyzed by ligand binding experiment with the radiolabeled [ $^{125}$ I]Tyr<sup>13</sup>-ET-1 in filter binding assay. ETB was purified in the detergents LPPG (0.05%), LMPG (0.05%), DPC (0.1%), DDM (0.05%), Chaps (1%), Brij78 (0.1%) and reconstituted into pre-formed liposomes composed of EPL. The proteoliposomes formation was performed by incubation of the lipid/protein mixture at two different ratios, 1:1000 or 1:2000 for 30 min at RT. Biobeads were then added to the sample in order to remove the detergent and the mixture was incubated over night at 4 °C. Proteoliposomes were then harvested and further analyzed.

In all analyzed cases, a background binding of [ $^{125}$ I]Tyr<sup>13</sup>-ET-1 significantly higher than 50% was

detected. Highest specific binding (34%) was obtained with ETB samples in 0.1% DPC as secondary detergent. In the same sample a relatively low Bmax of 0.46 pmol/mg was detected (Table 7).

Due to the low signal to background ratio, competition and saturation binding studies were excluded.

1st detergent <sup>a</sup>	2nd detergent <sup>b</sup>	Lipids <sup>c</sup>	P/L-ratio	Specific binding <sup>d</sup> (%)	Specific activity (pmol/mg)
Brij78 (1%)	LPPG (0.05%)	EPL	1:1000	7 ± 3	0.1 ± 0.01
	LMPG (0.05%)	EPL	1:1000	30 ± 5	0.4 ± 0.02
	DPC (0.1%)	EPL	1:1000	34 ± 6	0.46 ± 0.2
	DPC (0.1%)	EPL	1:2000	26 ± 7	0.37 ± 0.1
	DDM (0.05%)	EPL	1:1000	7 ± 2	0.08 ± 0.02
	Chaps (1%)	EPL	1:2000	14 ± 2.5	0.16 ± 0.03
	Brij78 (0.1%)	EPL	1:1000	6 ± 3	0.05 ± 0.02

**Table 7: Radioligand binding analysis of D-CF produced ETB reconstituted into liposomes.** a. Detergent used for the expression; b. detergent used for the purification and reconstitution; c. Lipid used for the formation of the liposomes: EPL: *E. coli* polar lipids; d. Percentage of the specific binding over the total binding.

#### 4.6 Cell-Free expression of ETB: L-CF mode

The L-CF expression mode offers the unique option for the co-translational insertion of the synthesized MPs into a provided lipid bilayer.

One of the advantages of the L-CF expression mode over the P-CF mode and D-CF mode is that the receptor is synthesized and processed in a detergent free environment. This particular expression mode could therefore be beneficial for the activity of proteins, since contact with detergents could impair their functional folding. Furthermore the orientation of the integrated MPs into the lipid bilayer may be more homogeneous if compared with the random orientation achieved after classical post-translational *in vitro* reconstitution approach.

In this study the effect of two different lipidic environments in the functional folding of the ETB



receptor were extensively analyzed: liposomes and nanodiscs.

In order to monitor and optimize the L-CF expression mode, the ETB receptor was prepared as fusion construct with the red shifted-green fluorescent protein (sGFP).

sGFP has increased fluorescence compared to the wild-type, the major excitation peak is shifted to 490 nm, whereas the emission peak is at 509 nm.

As DNA template for the L-CF reaction, the expression plasmid pet21a(+) was used, which carried the coding sequence of the human ETB receptor fused with sGFP. The protein synthesis resulted in the construct T7-ETB-sGFP-poly(His)<sub>10</sub>, further abbreviated as ETB-sGFP.

After the reaction, pellet and supernatant were routinely collected and analyzed using a Tecan fluorescence plate reader. The detection of folded and fluorescent sGFP served as preliminary indicator for the association of synthesized ETB-sGFP with the provided liposomes or nanodiscs.

#### **4.7 L-CF expression mode in presence of liposomes, functional assays**

Different lipid mixtures were tested in order to verify a possible effect of the liposomes composition on the synthesis and translation of ETB-sGFP.

EPL, Aso-PC lipids, heart total lipid extract (HTE) as well as pure DOPC and DMPC lipids were solubilized in 100% chloroform, evaporated under vacuum to a thin film and completely dried under vacuum overnight. After resuspension of the lipidic film in liposome buffer to a final concentration of 20 mg/ml, the liposomes were extruded to a size of 0.2  $\mu\text{m}$  and directly added in the RM at a final concentration of 4 mg/ml. After 16 h of incubation at 30 °C, the RM was collected and centrifuged at 18,000  $\times g$  at 4 °C for 10 min. Fluorescence of sGFP was only detected in the precipitate, indicating the co-precipitation of the supplied lipids with associated ETB-sGFP. Comparable fluorescence intensities corresponding to a calculated total of approximately 40  $\mu\text{g}$  of ETB-sGFP per ml of RM were detected after addition of liposomes composed out of Aso-PC, EPL or DOPC. The addition of liposomes composed out of HTE or DMPC yielded only approximately 10  $\mu\text{g}/\text{ml}$  of fluorescent ETB-sGFP (Fig. 15).

Analysis of a representative L-CF (Aso-PC) precipitate sample by fluorescence microscopy revealed large heterogeneous liposomes in size ranges in between 5 and 20  $\mu\text{m}$  (Fig. 16). Fluorescent ETB-sGFP particles were only detected in association with the liposomes, indicating a positive effect of the lipids on the folding of at least the sGFP fusion partner.

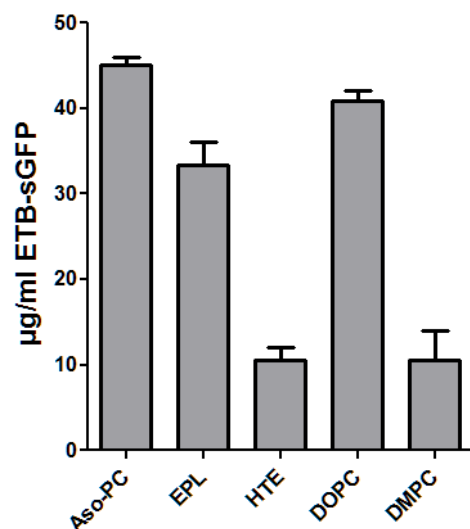


**Fig. 15: L-CF expression screening of ETB-sGFP.** Co-translational association of ETB-sGFP with different liposomes. The RM was centrifuged 18,000 x g at 4 °C for 10 min and 3 µl of pellet were analyzed for fluorescence using a Tecan fluorescence plate reader. The results, expressed in µg/ml, were calculated using a standard curve for sGFP. EPL: *E. coli* polar lipids, HTE: Heart total lipid extract.

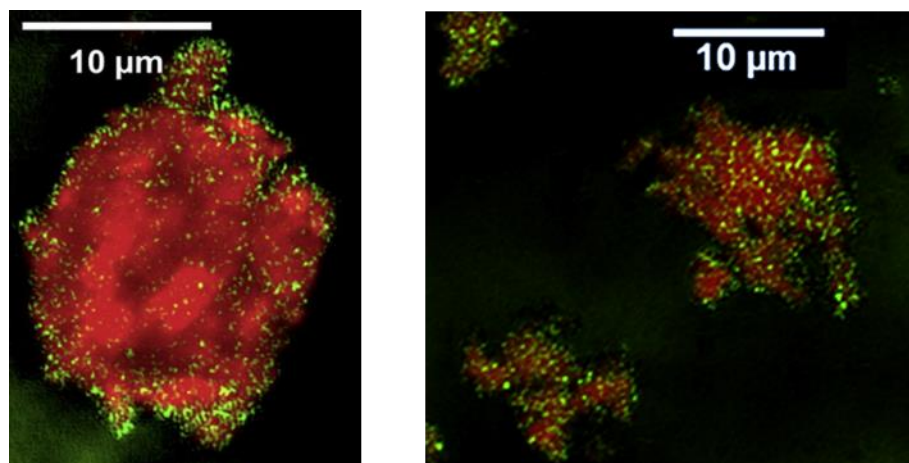


**Fig. 16: Fluorescence microscopy of L-CF expressed ETB-sGFP samples.** Precipitate of L-CF expressed ETB-sGFP with Aso-PC liposomes. Green, ETB-sGFP; red, Aso-PC labeled with rhodamine.

In order to analyze the samples quality, the binding of [<sup>125</sup>I]Tyr<sup>13</sup>ET-1 to selected L-CF produced samples was analyzed by filter binding assays. The non-specific background binding of [<sup>125</sup>I]Tyr<sup>13</sup>ET-1 was again very high and the best specific binding within the range of 31–36% was

obtained with liposomes composed out of Aso-PC or EPL at Bmax values of 3.5 pmol/mg and 2.6 pmol/mg, respectively (Table 8). In homologous competition experiments using proteoliposomes composed out of Asp-PC lipids a  $K_i$  of 1.3  $\mu$ M was measured (Fig. 17). L-CF generated complexes of the control protein PR-sGFP with supplied EPL lipid liposomes showed approximately 27% of [ $^{125}$ I]Tyr $^{13}$ ET-1 signal over the background, but at a low Bmax of only 0.02 pmol/mg.

Lipids <sup>a</sup>	Specific binding <sup>b</sup> (%)	Specific activity (pmol/mg)	$K_i$ (nM)
EPL	31 $\pm$ 3	2.6 $\pm$ 0.3	–
HTE	27 $\pm$ 4	1.1 $\pm$ 0.2	–
DOPC	21 $\pm$ 3	1.2 $\pm$ 0.08	–
DMPC	32 $\pm$ 1	1.6 $\pm$ 0.2	–
Aso-PC	36 $\pm$ 2	3.5 $\pm$ 0.3	1300 ( $K_i$ )

**Table 8: Radioligand binding analysis of L-CF expressed ETB-sGFP in presence of liposomes.** a. Lipids used for the formation of the liposomes: EPL *E. coli* polar lipids; HTE heart total lipid extract; b. Percentage of specific binding over total binding.

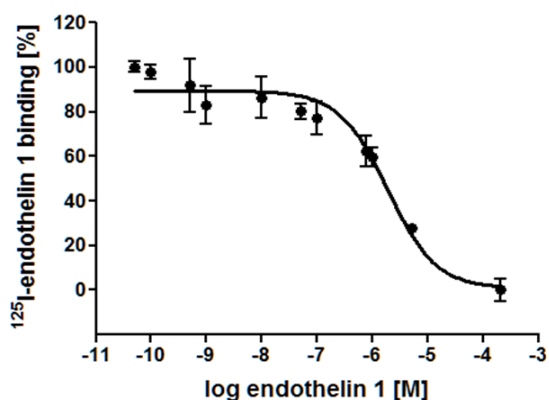


**Fig. 17: Radioligand competition assay.** Homologous competition experiments were performed with L-CF expressed ETB-sGFP co-translationally inserted into *E. coli* polar lipid liposomes. Proteoliposomes were incubated with 500 pM [ $^{125}$ I]Tyr $^{13}$ ET-1 and increasing concentrations of unlabeled ET-1 for 1 h at 22°C. Data points obtained from three independent measurements.

#### 4.8 Effect of the temperature in L-CF mode

In a standard CF expression the reaction is performed at 30 °C for 16 h. As showed by Deniaud and coworkers, reducing the reaction temperature to 20 °C allowed an important decrease of the aggregation of the protein hVDAC1 during the expression (Deniaud et al. 2010).

The effect of the temperature was also tested for the synthesis of the ETB receptor in L-CF mode in presence of liposomes composed out of Aso-PC. At 20 °C no significant expression was detected, whereas at 25 °C or 27 °C, a slight reduction in the expression levels of the ETB-sGFP as compared with the standard expression at 30 °C, was observed. Ligand binding analysis using [<sup>125</sup>I]Tyr<sup>13</sup>ET-1 revealed a still high non-specific binding. A specific binding of 34% for the expression at 25 °C and of 30% for the expression at 27°C were measured (Table 9)

Lipids <sup>a</sup>	Temp. Reaction	Specific binding <sup>b</sup> (%)	Specific activity (pmol/mg)
Aso-PC	30 °C	36 ± 2	3.5 ± 0.3
	27 °C	30 ± 2	2.5 ± 0.2
	25 °C	34 ± 1	2.5 ± 0.2
	20 °C	–	–

**Table 9. Radioligand binding analysis of L-CF expressed ETB-sGFP, effect of the temperature of the reaction.** a. lipid used for the formation of the liposomes. b. Specific binding over total binding.

#### 4.9 Effect of cholesterol in L-CF mode

Cholesterol is an essential compound of mammalian cells membrane; it is involved in membrane fluidity and permeability, as well as in the formation of lipidic structure on the cell surface like the lipids-raft (Burger et al. 2000).

The interaction mechanism of cholesterol with GPCRs in order to modulate their function is individual to each receptor and can hardly be predicted. It might act either via direct specific lipid/protein interaction or by alteration of physical properties of the membrane in which the receptor is localized.

In order to evaluate a possible effect of cholesterol in the liposomes, ETB was expressed in L-CF mode in presence of Aso-PC lipids enriched in cholesterol hemisuccinate (CHS) at different concentration (2.5%, 5%, 10%). Radio ligand binding analysis revealed a slight increase in the specific binding and activity in presence of 2.5% CHS whereas a reduction was observed in the other two tested conditions (Table 10).

CHS (%)	Specific binding <sup>b</sup> (%)	Specific activity (pmol/mg)
0	36 ± 2	3.5 ± 0.3
2.5	39 ± 3	4.8 ± 0.6
5	26 ± 1	2.4 ± 0.2
10	30 ± 1	2.7 ± 0.3

**Table 10. Radioligand binding analysis of L-CF expressed ETB-sGFP, effect of cholesterol.** Aso-PC liposomes were prepared with addition of different concentrations of cholesterol hemisuccinate (CHS) a. lipid used for the formation of the liposomes. b. Specific binding over total binding.

#### 4.10 A mixed approach: L-CF in presence of detergent

An alternative approach to the classical L-CF expression mode is based on the addition of small amount of detergents, together with the preformed liposomes, in the RM. Using this method, Shimono and coworkers were able to functionally express bacteriorhodopsin into proteoliposomes by the addition of cholate-solubilized phosphocolines (Shimono et al. 2009). The addition of detergents to the liposomes prior to the use is thought to relax the tightly packed liposome structure, thereby lowering the energy barrier for a spontaneous incorporation of MPs (Shimono et al. 2009).

In order to evaluate this approach with ETB receptor, lipids were supplied in the RM at final concentrations of 4 mg/ml together with CHAPS at a final concentration of 0.5%.

Due to its high CMC, CHAPS can be easily dialyzed out into the FM during the reaction and thereby pure proteoliposomes are formed. Analysis of the fluorescent pellet revealed a general reduction in the yield of ETB-sGFP when the lipids Aso-PC, EPL and DOPC were pre-mixed with CHAPS. No significant differences were observed in case of HTE and DMPC in presence or absence of the detergent (Fig. 18)

The possibility to use different detergents for the destabilization of the provided proteoliposomes was also evaluated. Aso-PC lipids at a final concentration of 4 mg/ml were pre-mixed with one of the selected detergent: Brij78 0.04%, Brij35 0.04% and digitonin 0.2%.

In the first two detergents a slight increase in the specific activity was measured upon binding with [<sup>125</sup>I]Tyr<sup>13</sup>ET-1, whereas a reduction was detected in presence of digitonin (Table 11).

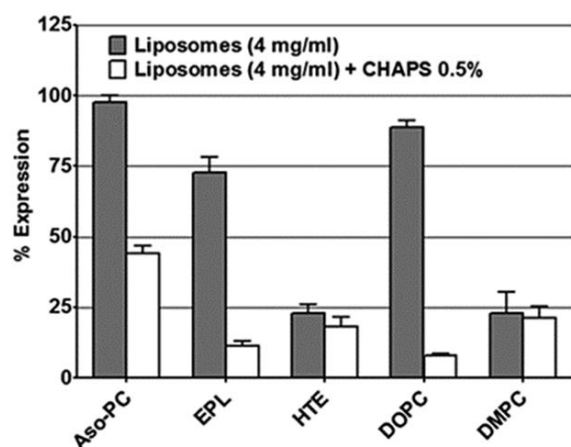


**Fig. 18: L-CF expression screening of ETB-sGFP, Co-translational association with different liposomes.** Fluorescence values were normalized according to the maximum expression (40  $\mu$ g/ml of ETB-sGFP with Aso-PC liposomes).

Lipids <sup>a</sup>	Detergent [%]	Specific binding <sup>b</sup> (%)	Specific activity (pmol/mg)
Aso-PC	-	36 $\pm$ 2	3.5 $\pm$ 0.4
	Chaps, 0.5%	25 $\pm$ 8	1.6 $\pm$ 0.4
	Digitonin, 0.2%	25 $\pm$ 1	1.3 $\pm$ 0.1
	Brij35, 0.04%	38 $\pm$ 1	3.3 $\pm$ 0.1
	Brij78, 0.04%	39 $\pm$ 2	1.5 $\pm$ 0.1

**Table 11: Radioligand binding analysis of L-CF expressed ETB-sGFP, mixed D/L-CF approach.** Different detergents are provided in the RM together with liposomes, specific final concentrations are reported in the table.

a. Lipid used for the preparation of the liposomes. b. percentage specific binding over total binding.

#### 4.11 L-CF expression mode in presence of nanodiscs

Nanodiscs (NDs) are self-assembled discoidal particles composed of a planar phospholipid membrane bilayer surrounded by an apolipoprotein ring, the so called membrane scaffold protein (MSP). Some advantages of NDs include water-solubility, monodispersity, consistency between preparations, flexible lipid composition as well as the possibility to access to both sides of the membrane. Co-translational association of CF expressed MPs with supplied ND resulted into a soluble and ligand binding competent GPCRs (Gao et al. 2012, Katzen et al. 2008, Yang et

al. 2011,). However, the efficient formation of high quality MP/ND complexes depends on multiple parameters. In particular NDs size, concentration and membrane lipids composition play an important role in solubilization efficiency and in the final activity of the synthesized MPs. For the initial screening, NDs of two different sizes were prepared using two variant of MSP: MSP1 and MSP1E3D1. The first construct is the canonical MSP protein derived from APO-AI, the second construct is an elongated version of MSP in which an additional three helices (Helix 4, 5, and 6, indicated as E3) have been inserted in between Helix 3 and Helix 4. NDs generated by MSP1 are around 9 nm in size, whereas bigger nanodiscs of around 12 nm are obtained using the construct MSP1E3D1. Both constructs contain a poly(His)<sub>6</sub> tag at the C-terminal that allows the purification after *in vivo* expression in *E. coli* cells. The purified MSPs were incubated with DMPC lipids at a molar ratio 1:150 in presence of 100mM Na-cholate and 0.1% DPC. After dialysis in buffer the formed NDs were concentrated up to 8-10 mg/ml and supplied directly in the CF reaction.

For the initial optimization of the integration/association efficiency, the ETB-sGFP fusion construct was used and the fluorescence in supernatant and pellet was quantified. The amount of soluble ETB-sGFP increased with increasing concentrations of MSP1E3D1-NDs in the RM and reached a plateau at concentration around 120  $\mu$ M (Fig 19A). According to the sGFP fluorescence, approximately 150  $\mu$ g/ml of ETB-sGFP protein was synthesized having at least a functionally folded sGFP moiety. A MSP1E3D1-ND concentration of approximately 40  $\mu$ M was already sufficient to obtain all detectable fluorescence in the supernatant. With the smaller MSP1-NDs, approximately 25% of the fluorescent ETB-sGFP still remained in the pellet at ND concentrations of 40  $\mu$ M. Analysis by fluorescence microscopy of the produced pellet revealed large clusters of NDs associated ETB-sGFP (Fig. 20). By analysis of the supernatant a higher apparent homogeneity was detected, while the presence of smaller aggregation cluster can still not be excluded (Fig. 20).

As membrane composition could also have an effect on the translation and reconstitution efficiencies, MSP1E3D1-NDs were prepared using different lipids and directly supplied into CF reactions at a final concentration of 40  $\mu$ M. The obtained ETB-sGFP fluorescence was quantified in the supernatants as well as in the pellets. NDs with membranes composed of the anionic lipid DMPG increased the yield of fluorescent ETB-sGFP to a level twice as high if compared with NDs (DMPC) (Fig. 19B). NDs containing membranes composed of other analyzed lipids such as POPC, lipids isolated from brain total extracts or Aso-PC mixtures reduced the yield of fluorescent ETB-sGFP if compared with NDs composed of DMPC lipids. A large fraction of the complexes of fluorescent ETB-sGFP and HTE NDs precipitated in the CF reactions, while complexes with NDs containing any of the other analyzed lipids quantitatively stayed in the supernatant.

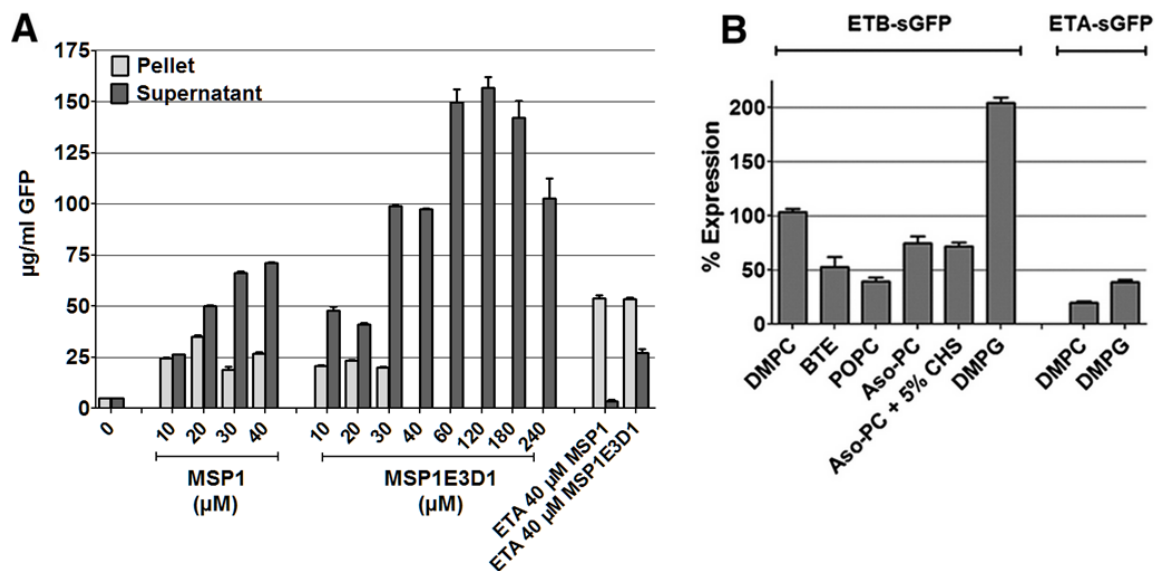


**Fig. 19: L-CF (ND) expression optimization of ETB-sGFP and ETA-sGFP.** **A**, L-CF expression in presence of different concentrations of MSP1-NDs (DMPC) or MSP1E3D1-NDs (DMPC). Aliquots of 3 µl of supernatant or pellet were analyzed for sGFP fluorescence and protein was quantified according to a calibration curve. **B**, Expression levels of ETB-sGFP and ETA-sGFP in presence of NDs (40 µM) of different lipid compositions. Values were normalized according to the expression of ETB-sGFP in presence of 40 µM of MSP1E3D1-NDs (DMPC). BTE: brain total extract, CHS: cholesterol hemisuccinate.

A corresponding screening was performed for the expression optimization of ETA-sGFP (Fig. 19A). At 40 µM of MSP1-NDs composed of DMPC, most of the fluorescent protein fraction was recovered in the pellet. With the larger MSP1E3D1-NDs, approximately 25 µg/ml of fluorescent ETA-sGFP could be obtained in the supernatant. Similar to ETB-sGFP, with NDs composed of DMPG, the fluorescence yield of ETA-sGFP was twice when compared to expression experiments with NDs composed of DMPC (Fig. 19B)

Unfortunately, despite the relatively high fluorescence of the two endothelin receptor co-expressed in presence of NDs composed of DMPG lipids, the ligand binding in this condition could not further be analyzed due to strong interactions of the ligand ET-1 with the anionic lipid DMPG (data not shown).

To reduce the variables to screen in the further ligand binding assay, experiments were performed using the most promising larger NDs formed by the construct MSP1E3D1, and are further referred simply as NDs.



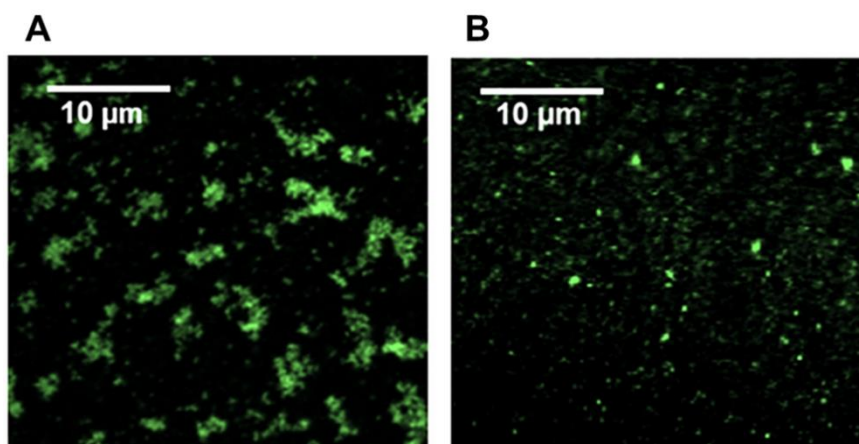


**Fig. 20: Confocal fluorescent microscopy of L-CF expressed ETB-sGFP samples in presence of MSP1E3D1-NDs (DMPC).** Green, ETB-sGFP. **A**, precipitate recovered after the expression at sub-optimal NDs concentration. **B**, supernatant.

#### 4.12 Binding of Cy3-ET-1 to ETB-sGFP/ND complexes

In order to evaluate the ligand binding ability of the produced ETB-sGFP/NDs (DMPC), a binding experiment using the fluorescent ET-1 analog Cy3-ET-1 was performed. Samples were purified by IMAC and 2 nM of protein (according to sGFP fluorescence) was incubated with 10 nM of Cy3-ET-1 for 1 h at room temperature and subsequently applied on a Sephadex G50 Spin column. The Cy3-ET-1 bound to the ETB-sGFP/ND was recovered in the flow-through whereas the free ligand was retained in the column. Amount of active receptor in the ETB-sGFP/ND (DMPC) sample corresponded to  $24 \pm 3\%$  according to the measured Cy3-ET-1 fluorescence. Approximately 75% of the Cy3-ET-1 binding could be blocked by pre-incubation of the receptor sample with 2  $\mu$ M unlabeled ET-1 for 1 h at room temperature. The total Cy3-ET-1 binding of PR-sGFP/NDs (DMPC) or empty NDs (DMPC) was less than 1.5% (Fig. 21).

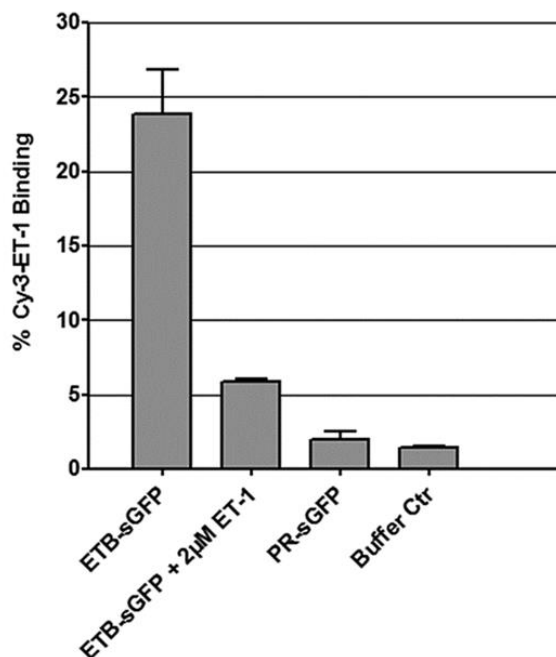


**Fig. 21: Cy3-ET-1 binding to ETB-sGFP/ND (DMPC) complexes.** 2 nM (quantified by sGFP fluorescence) of IMAC purified ETB-sGFP/NDs (DMPC) or PR-sGFP/ND (DMPC), were incubated with 10 nM Cy3-ET-1. Unbound ligand was separated by Sephadex G50 spin column and the amount of fluorescent ligand co-eluted with the protein/ND complex was measured. The percentage of binding was calculated using as 100% the fluorescence measured for 2nM Cy3-ET-1.

In order to evaluate the quality of the IMAC purified ETB-sGFP/NDs (DMPC), the sample was injected on a Superdex 200 3.2/30 column (Fig. 22A). From the elution profile two distinct peaks are visible, a first one with a retention time around 1 ml and a second peak around 1.3 ml. The collected fractions from both peaks were analyzed by western blot or SDS-PAGE (Fig. 22B, Fig. 22C). ETB-sGFP is present in similar concentration in both peaks, whereas MSP1E3D1 is predominantly present in the second peak. From every fraction 2 nM of ETB-sGFP (calculated according to the sGFP fluorescence) were incubated for 1 h with 10 nM of Cy3-ET-1 and applied on a Sephadex G50 Spin column. The fluorescence of Cy3-ET-1 was measured in each fraction and the percentage of active receptor was calculated (Fig. 22D). 50% of active receptor was present in the second peak, whereas in the first peak only a small fraction of receptor was active.

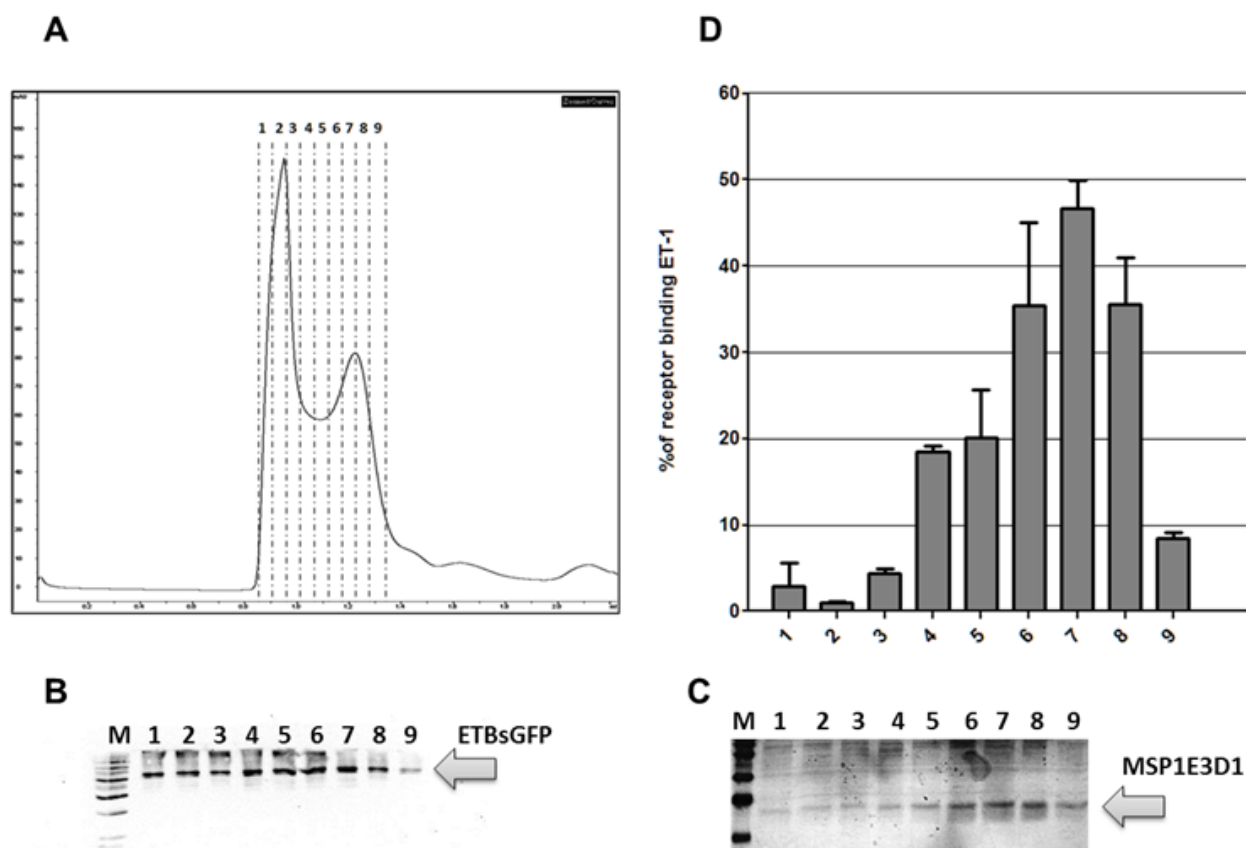
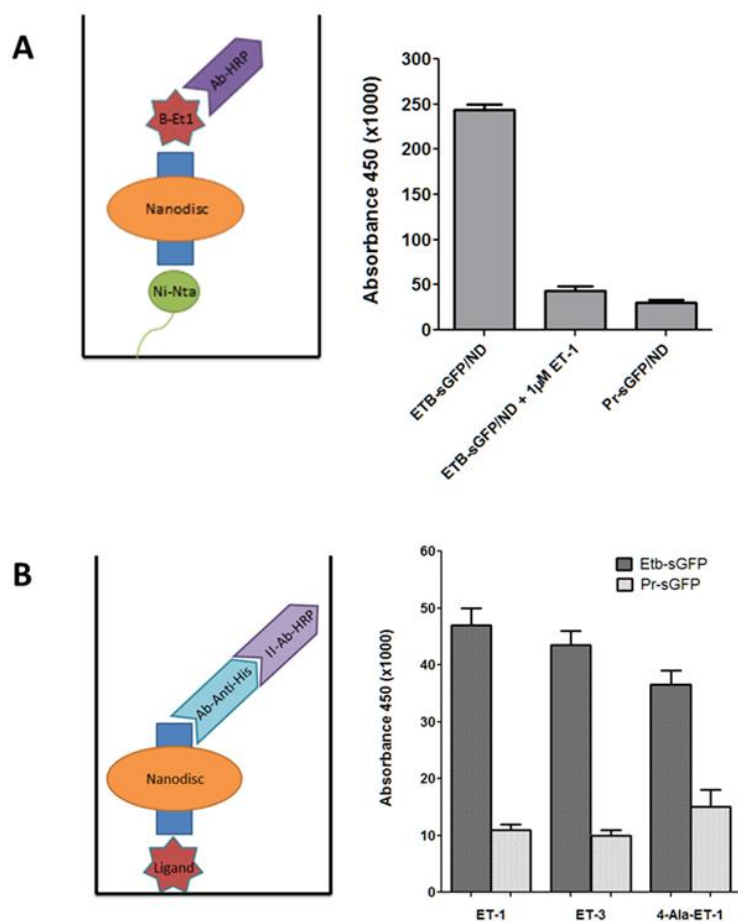


**Fig. 22: L-CF expression of ETBsGFP/ND (DMPC), analysis of sample quality.** **A**, SEC elution profile of purified ETB-sGFP co-expressed in presence of MSP1E3D1 DMPC NDs. Sample was analyzed on a Superdex 200 3.2/30 column; protein absorbance was recorded at 280 nm. 9 fractions of 50  $\mu$ l each were collected. **B**, Western Blot analysis of the 9 collected fractions. The samples were separated by 16% SDS-PAGE gel, blotted and subsequently immunodetected by anti-His antibody. **C**, SDS-PAGE analysis of the 9 collected fractions. The sample were separated on a 16% SDS-PAGE gel and stained with blue Coomassie. **D**, Ligand binding assay of the 9 collected fractions. Fixed amount of ETB-sGFP in NDs (2nM measured by sGFP fluorescence) were incubated with 10 nM Cy3-ET-1. The unbound ligand was separated using a Sephadex G50 spin Column. The percentage of active receptor was calculated using as 100% the fluorescence measured for 2 nM Cy3-ET-1.

#### 4.13 Ligand binding analysis by ELISA

The enzyme-linked immunosorbent assay (ELISA) is a fast and reliable biochemical technique that allows the detection of an antigen upon binding of a specific antibody.

In this study ELISA assays were performed in order to detect ligand binding capability of the ETB receptor co-translationally reconstituted into NDs.



In order to detect the binding of the ligand b-ET-1 to immobilized ETBsGFP/ND (DMPC), experiments were performed using a 96-well Ni-Chelate NUNC Immobilizer plate. This plate is designed for the direct binding of fusion proteins that have been tagged with HisTag.

ETB-sGFP/NDs (DMPC) were IMAC purified and dialyzed against buffer in order to remove the excess of imidazole. 100 $\mu$ l of sample at final concentration of 2  $\mu$ M was incubated in the plate for 2.30 h. Subsequently 100  $\mu$ l of b-ET-1 at a final concentration of 1 $\mu$ M was added and finally the binding was detected via anti-biotin antibody conjugated with HRP. After each step the plate was extensively washed in PBS buffer in order to remove any non-specifically bound proteins or ligands. The plate was then incubated with tetramethylbenzidine substrate solution in the dark for 30 min. The reaction was stopped by adding 1 M HCl and the colorimetric change was measured. Significant signal was detected in presence of ETB-sGFP/ND whereas a much lower signal was measured in presence of PR-sGFP/ND. The signal from ETB-sGFP/ND was greatly reduced if the samples were pre-incubated with 1 $\mu$ M of unlabeled ET-1 (Fig. 23A).

In order to detect binding of ETB-sGFP/ND to other ligands, plain 96-well ELISA plates were used and selected ETB ligands (ET-1; ET-3; ALA-4-ET-1) were directly immobilized via non-specific coupling. Ligands at 1  $\mu\text{M}$  final concentration in coupling buffer were incubated in the plate o.n. at 4  $^{\circ}\text{C}$ . The unbound ligands were removed by a washing step and the plate blocked with PBS and 3% BSA for 2 h. The plate was washed again and ETB-sGFP/NDs or PR-sGFP/NDs were added. Specific binding of the samples to the ligands was detected via anti-His antibodies. With all the tested ligands specific binding was detectable only in presence ETB-sGFP/ND (Fig. 23B).

#### 4.14 Radioligand binding assay

The ligand binding properties of ETB-sGFP/NDs (DMPC) complexes was analyzed by radioactive saturation assays using [ $^{125}\text{I}$ ]Tyr $^{13}$ ET-1. Experiments were performed with IMAC purified complexes at a final concentration of 5 nM as estimated by sGFP fluorescence. A  $K_D$  of 0.45 nM and a  $B_{\text{max}}$  of 58.6 pmol/mg were determined (Fig. 24). Competition experiments with 5 nM of ETB-sGFP/ND complexes pre-incubated for 1 h at RT with increasing concentrations of unlabeled ET-1 and subsequent addition of 500 pM of [ $^{125}\text{I}$ ]Tyr $^{13}$ ET-1 revealed a  $K_i$  of 6.1 nM (Fig. 24).

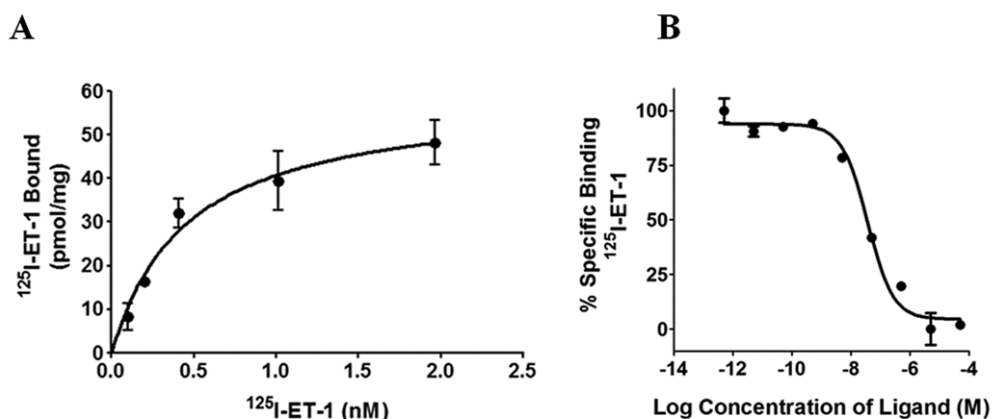


**Fig. 24: Radioligand binding assay of ETB-sGFP/ND (DMPC).** A, saturation binding assay. 5 nM of purified ETB-sGFP/ND (DMPC) was incubated with increasing concentrations of [ $^{125}\text{I}$ ]Tyr $^{13}$ ET-1. Unspecific binding was determined in the presence of 2  $\mu\text{M}$  unlabeled ET-1 and subtracted. B, competition binding assay. 5 nM of purified ETB-sGFP/MSP1E3D1-NDs (DMPC) was incubated with increasing concentrations of unlabeled ET-1 in the presence of 500 pM [ $^{125}\text{I}$ ]Tyr $^{13}$ ET-1. Data are triple measurements of two independent experiments.

#### 4.15 Surface Plasmon Resonance (SPR) Assay

SPR is a powerful technique that allows precise quantification of ligand binding constants. The advantage of this system, compared to a classical approach, is that the biomolecular interactions can be measured in real-time in a label free environment.

This technique is based on a physical process that occurs when a planar polarized light hits a metal film under condition of total internal reflection. When the incident light hits the metal layer at a specific angle, called resonance angle, the hitting photons are converted into plasmons and a “gap” in the reflected light intensity is observed.

In the Biacore system the metal film consists of a gold thin layer covered with dextran matrix. The ligand can be immobilized on the dextran surface while the analyte is injected over the layer through a microfluidic system. The interaction of the two biomolecules induces a change of the refractive index on the sensor surface, which is measured as a change in the resonance angle. In the Biacore system the shift of the resonance angle is expressed as Response Unit (RU). During the injection, as the analyte binds the ligand, an increase in the RU is detected. After a certain amount of time, a solution without the analyte is injected over the surface and the dissociation of the complex is observed as a decrease in RU. By the analysis of the obtained sonogram, association and dissociation rate can be calculated as well as the equilibrium dissociation constant.

ETB-sGFP/NDs (DMPC) complexes are highly soluble and therefore SPR measurements could be performed as a complementary approach in order to study the ligand binding properties of the GPCRs samples.

First experiments were performed in order to optimize the conditions for the ligand binding assay. Optimization of the buffers was an essential step in order to reduce the non-specific binding of the NDs to the dextran matrix surface of the chip.

The effect of salt concentration was screened as well as the presence of BSA and glycerol (Fig. 25). Increasing the concentration of NaCl from 150 mM to 500 mM greatly reduced the non-specific binding. The presence of BSA or glycerol was particularly beneficial at low salt concentration, whereas the effects were less relevant at high salt concentration. Furthermore the effect of the detergent P-20 at a concentration of 0.05% was tested. From the results published by Borch and coworkers (Borch et al. 2011), this detergent should be well tolerated by the NDs. In the presence of 150 mM NaCl and 0.05% P-20 the lowest level of unspecific binding was detected. As previous published ligand binding experiments for the CF expressed ETA and ETB receptors were performed at high salt concentration (Klamm et al. 2007, Junge et al. 2010), a buffer composed of 20 mM HEPES-NaOH pH 7.5 and 500 mM NaCl was used as running buffer in the SPR experiments.

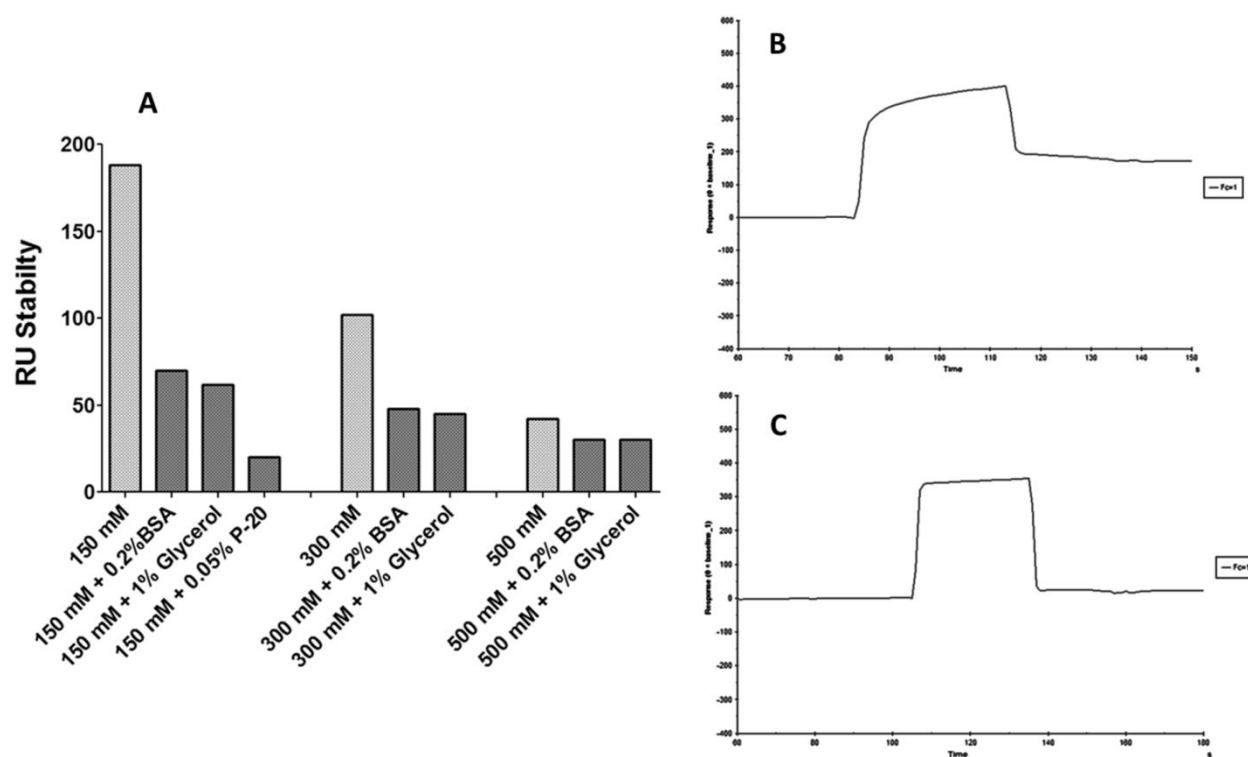


**Fig. 25: SPR buffer optimization.** **A**, 50 nM of empty NDs was injected on a plain surface of an SA chip in presence of different running buffers. After 60 sec, the injection was stopped and the chip washed in running buffer. The RU at the stability point, 30 sec after the end of the injection, was measured. This value indicates the amount of NDs that non-specifically bind to the chip. **B**, Curve obtained using 20 mM HEPES-NaOH pH 7.5, 150 mM NaCl. **C**, Curve obtained using 20 mM HEPES-NaOH pH 7.5, 500 mM NaCl.

Ligand binding properties of the ETB and ETA receptors reconstituted into NDs were analyzed by single-cycle as well by multi-cycles experiments.

In the single cycle experiments, 50 RUs of the ligand b-ET-1 were immobilized on the second flow cell of an SA biosensor chip. Different concentration of ETB-sGFP/NDs, alone or pre-incubated with 2  $\mu$ M of unlabeled ET-1, were sequentially injected without regeneration on the chip. The background signal obtained from the first flow cell was subtracted from the signal obtained from the second flow cell.

ETB-sGFP/NDs show specific binding to the immobilized b-ET-1 and the interaction with the ligand was prevented by pre-incubation of the samples with saturating amounts of ET-1 (Fig. 26).

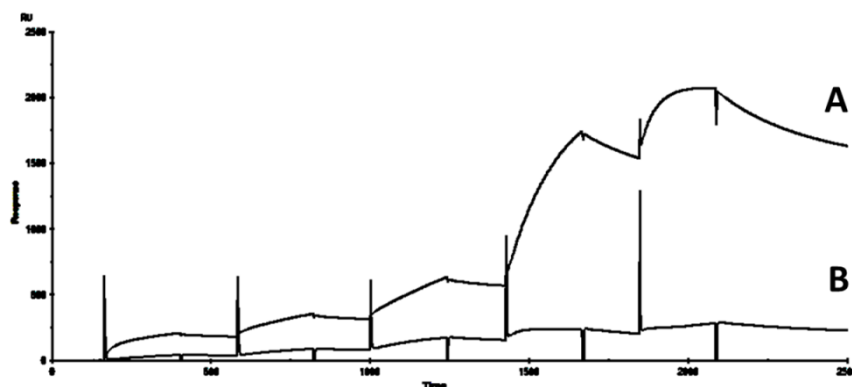


**Fig. 26: SPR of ETB-sGFP/ND, Single-Cycle analysis.** **A**, Different concentrations of ETB-sGFP/NDs (2.5, 5, 10, 50, 100 nM) were injected sequentially on a SA-chip where 50 RU of b-ET-1 were previously immobilized. **B**, curve obtained from same samples pre-incubated with 1  $\mu$ M ET-1 before the injection.

Multi-cycle experiments were performed using ETB-sGFP/NDs (DMPC) as well as ETA-sGFP/NDs (DMPC). In this case the chip was treated with regeneration buffer (1M NaCl, 50 mM NaOH) before each new injection, in order to remove the bound NDs.

50 RU of the non-selective ligand b-ET-1 or of the selective ETB ligand b-ET-3 were immobilized on the second flow cell of on a SA chip. Different concentrations of NDs samples were then injected. The signal obtained from the empty flow cell was subtracted from the signal of the flow cell where the ligand was immobilized. The obtained curves were then analyzed using the BiacoreX100 evaluation software. Results were accepted when the measured affinity constant were within the instrument specification and uniquely determined (U-value below 15) (Table 12).

For non-purified ETB/NDs (DMPC) as well as for the fusion construct ETB-sGFP/NDs (DMPC), an apparent  $K_D$  value for the interaction with b-ET-1 of 0.5 nM was obtained. The apparent  $K_D$  value of IMAC purified ETB-sGFP/NDs (DMPC) complexes were similar and determined at 0.4 nM. For reaction supernatants containing non-purified ETA-sGFP/NDs (DMPC) complexes, an apparent  $K_D$  value for the interaction with ET-1 of approximately 1.7 nM was determined. However, the  $K_D$  values of corresponding GPCR samples were clearly different for their interaction with the peptide b-ET-3. Non-purified ETB-sGFP/NDs (DMPC) still showed high affinity with an apparent  $K_D$  of 0.2 nM, whereas the apparent  $K_D$  value for the non-purified ETA-sGFP/NDs (DMPC) was 3.4  $\mu$ M, significantly higher, indicating low affinities (Fig. 27)



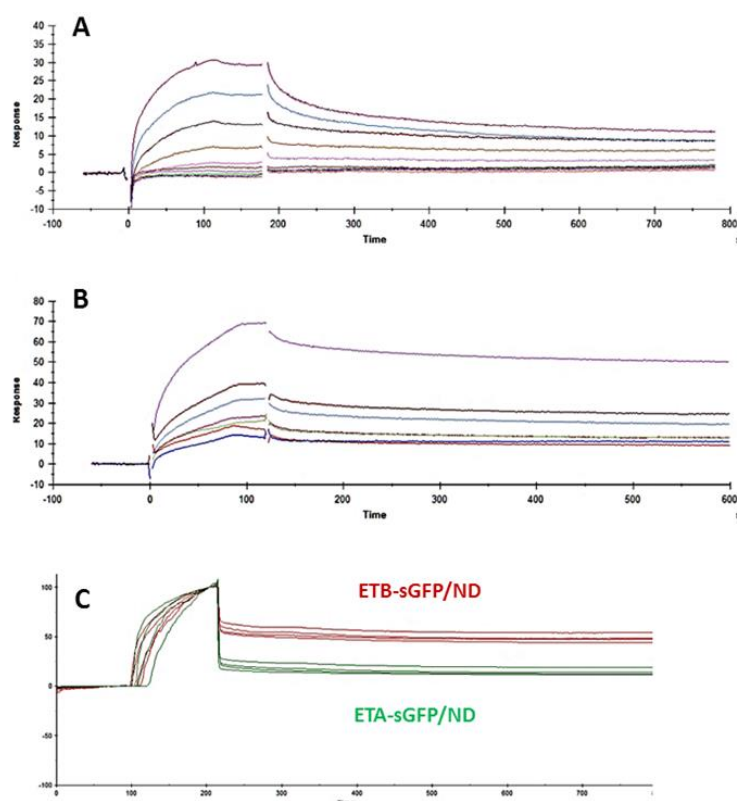


**Fig. 27: SPR analysis of ETB-sGFP/NDs (DMPC) and ETA-sGFP/NDs (DMPC).** Different concentration of ETA-sGFP/NDs (A), or ETB-sGFP/NDs (B), were injected, without previous purification, on a SA chip where 50 RUs of b-ET1 were previously immobilized. The signal from the flow cell 2 was subtracted from the signal obtained from the flow cell 1 and the obtained curves were analyzed using the BiacoreX100 evaluation software. (C), Different interaction of ETB-sGFP/NDs (red curves) and ETA-sGFP/NDs (green curves), to b-ET-3 immobilized on a SA-Chip. The normalized signal has been obtained from the flow cell 2 where the ligand has been immobilized.

Sample	$K_{on}$ ( $M^{-1}s^{-1}$ )	$K_{off}$ ( $s^{-1}$ )	$K_D$ (nM)
<b>b-ET-1</b>			
ETA-sGFP	$1.6 \times 10^5$	$2.7 \times 10^{-4}$	<b>1.69</b>
ETB-sGFP	$1.07 \times 10^6$	$5.9 \times 10^{-4}$	<b>0.55</b>
ETB-sGFP <sup>1</sup>	$1.04 \times 10^6$	$4.12 \times 10^{-4}$	<b>0.4</b>
ETB	$1.1 \times 10^6$	$5.2 \times 10^{-4}$	<b>0.47</b>
<b>b-ET-3</b>			
ETA-sGFP	$6.4 \times 10^3$	$2.19 \times 10^{-2}$	<b>3431</b>
ETB-sGFP	$2.37 \times 10^6$	$4.5 \times 10^{-4}$	<b>0.19</b>

**Table 12.** Binding properties of b-ET-1 and b-ET-3 to ETA-sGFP, ETB-sGFP or ETB associated with DMPC NDs analyzed by SPR. <sup>1</sup>, Purified ETB-sGFP sample.

The effect of the membrane composition on the ligand binding activity of ETB-sGFP/NDs complexes was further analyzed (Fig. 28). ETB-sGFP was expressed in the presence of NDs composed of POPC, Aso-PC, Brain total extract as well as Aso-PC + 5% Cholesterol hemisuccinate (CHS). In general no significant differences, when compared with DMPC NDs, were observed.  $K_D$  values of approximately 0.5-0.7 nM were obtained for the binding to the immobilized b-ET-1. (Table 13).

Lipids	$K_{on}$ ( $M^{-1}s^{-1}$ )	$K_{off}$ ( $s^{-1}$ )	$K_D$ (nM)
Aso-Pc	$1.12 \times 10^6$	$7.77 \times 10^{-4}$	<b>0.69</b>
Aso-Pc + CHS 5%	$1.46 \times 10^6$	$6.93 \times 10^{-4}$	<b>0.47</b>
POPC	$8.62 \times 10^5$	$6.29 \times 10^{-4}$	<b>0.73</b>
BTE	$1.18 \times 10^6$	$6.28 \times 10^{-4}$	<b>0.53</b>

**Table 13.** b-ET-1 binding to ETB-sGFP associated with NDs of different lipid composition.

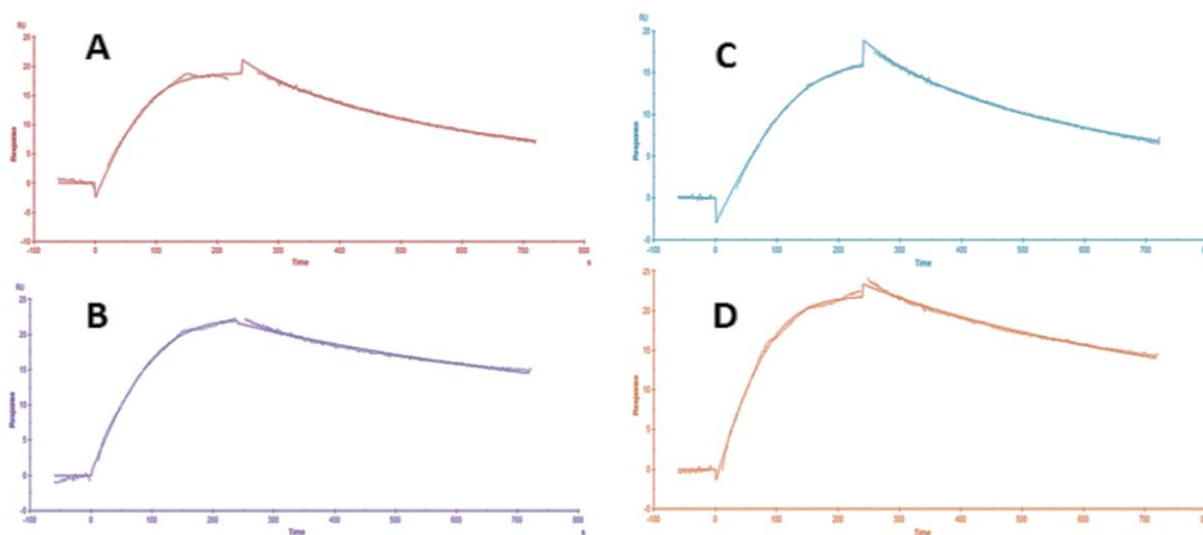


**Fig. 28: SPR analysis, effect of membrane composition.** The activity of ETB-sGFP/NDs of different lipid composition was tested. A: Brain total extract, B: Aso-PC + 5% CHS, C: Aso-PC, D: POPC. The curves represent the binding of the 5 nM sample of ETB-sGFP/ND injected on a SA chip where 50 RU of b-ET-1 were previously immobilize.

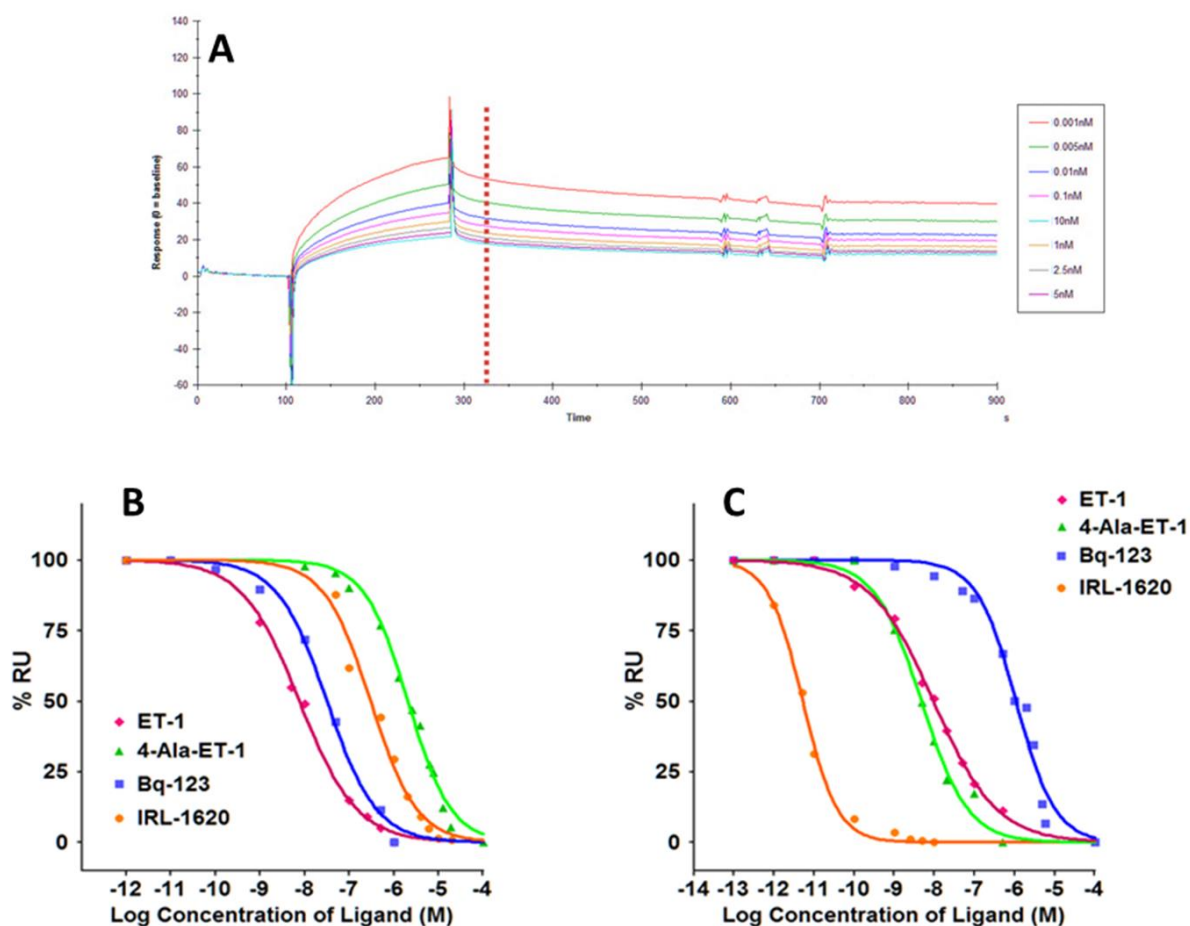
Different peptide ligands, directly obtained via modifications of the natural ET-1, as well as artificially produced non-peptide molecules, are known to show distinct differential binding patterns to ETA and ETB.

While the peptide agonist ET-1 is non-selective for both receptors, the two peptide derivatives ALA-4-ET-1 and IRL-1620 are highly specific agonists for ETB, with more than 1000 fold reduced binding to ETA. *Vice versa*, the antagonist BQ-123 is highly selective for ETA.

The interaction of these ligands with ETA-sGFP/NDs (DMPC) or ETB-sGFP/NDs (DMPC) was analyzed in competition binding assays using SPR (Fig. 29A).

Fixed concentrations (5 nM) of ETA-sGFP/NDs or ETB-sGFP/NDs were preincubated with increasing concentration of ligands in the range from 0.01 nM to 6  $\mu$ M for 1 h and subsequently injected on SA chips where b-ET-1 was previously immobilized.

For ETB-sGFP/NDs complexes, the determined  $IC_{50}$  values were 9.6 nM for ET-1, 4.1 nM for ALA-4-ET-1, 0.005 nM for IRL-1620 and 1.4  $\mu$ M for the ETA specific antagonist BQ-123 (Fig. 29B). For ETA-sGFP/NDs complexes, the  $IC_{50}$  value for the ligand ET-1 was 8 nM and for the specific antagonist BQ-123 38 nM. The  $IC_{50}$  values for the ETB specific agonists ALA-4-ET-1 and IRL-1620 were 2.6  $\mu$ M and 300 nM, respectively (Fig. 29C).



Ligand	IC <sub>50</sub> [nM] ETA	IC <sub>50</sub> [nM] ETB
ET-1	8	9
4-ALA-ET-1	2663	4
BQ-123	38	1395
IRL-1620	300	0.005

**Fig. 29: SPR: competition assay.** **A.** 5 nM of ETB-sGFP/NDs (DMPC) were incubated for 1 hour with increasing concentration of unlabeled ligand (in this case IRL-1620) before the injection on the chip where 50 RUs of b-ET-1 were previously immobilized. A report point was placed 30 sec after the end of the injection and the specific RU were measured. The obtained value was plotted against the logarithmic concentration of the unlabeled ligand. **B.** Competition curves for ETA-sGFP/ND (DMPC). **C.** Competition curves for ETB-sGFP/ND (DMPC). The calculated IC<sub>50</sub> values are summarized in the table.

SPR is a very versatile technique and offers the alternative possibility to analyze the binding affinities by directly immobilization of the receptor, reconstituted into NDs, on the surface of the chip.

ETB-strep tagged receptor cotranslationally expressed into NDs (DMPC) was immobilized to the surface of a CM5 chip precoupled with anti-strep antibodies. Around 8500 RU of anti-strep antibody were conjugated on the surface of a CM5 chip and around 1000 RUs of ETB-strep/NDs (DMPC) were then stably bound (Fig. 30).

This approach, though very useful due to the possibility to measure directly the affinity of label-free ligands, is limited by the very different size of the two interacting partner. The maximum expected RUs can be calculated from the formula:  $(\text{MW ligand}/\text{MW NDs complex}) \times \text{immobilized level of NDs complex}$ . As the ligand are around 2 kDa in size and the NDs complex around 300 kDa, immobilizing 1000 RU of NDs will produce only a maximum signal for the ligands of around 13 RU.

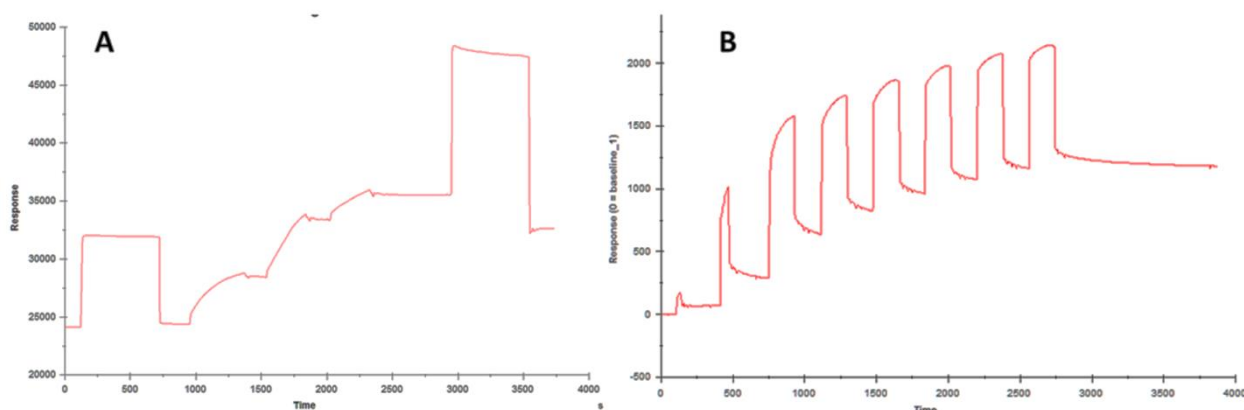


**Fig.30: Preparation of the CM5 chip for the ligand binding analysis.** **A.** At first the CM5 chip has been activated using a EDC/NHS solution. Subsequently three consecutive injections of Anti-Strep antibody at a concentration of 10 $\mu$ g/ml in 10 mM acetate buffer pH 5 have been performed. After the chip quenching using 1M Ethanolamine, around 8500 RUs of antibody were coupled. **B.** Consecutive injections of ETB-Strep/NDs (DMPC). The sample was directly injected after o.n. expression. 1000 RUs were immobilized on the chip.

Three different ligands were analyzed for the interaction to the ETB-Strep/NDs: ET-1, the ETB specific ligand IRL-1620 and the ETA specific ligand BQ-123.

Single cycle experiments were performed; different concentrations of ligands were directly

injected on the chip without any regeneration.

Due to the shape of the curves obtained it was not possible to derive the affinity constant  $K_D$  using a kinetic analysis, and for this reason affinity analysis was used.

A  $K_D$  value of around 1 nM was measured for the ligands ET-1 and 0.2 nM for the ligand IRL-1620, whereas a higher  $K_D$  value of around 2.5  $\mu\text{M}$  was measured for the ETA specific ligand BQ-123 (Fig. 31).

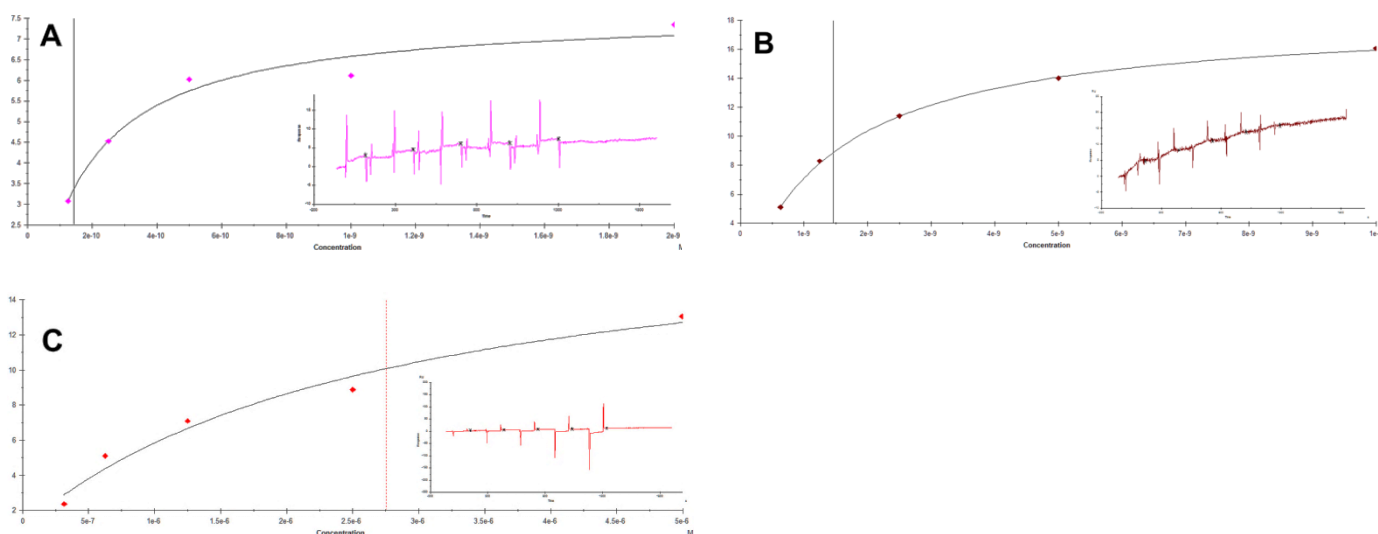


**Fig. 31: Ligand binding analysis using immobilized ETB-Strep/ND (DMPC) on a CM5 chip.** Different concentration of IRL-1620 (A); ET-1 (B) and BQ-123 (C), where injected sequentially on the chip. A report point was placed at the end of the injection and the measured RU plotted against the concentration of ligand used. Results were analyzed using the BiacoreX100 evaluation software.

#### 4.16 Microscale Thermophoresis (MST)

This method, that allows quantification of biomolecular interactions, is based on the analysis of the movement of molecules along a temperature gradient, an effect termed thermophoresis. The thermophoretic pattern of a molecule depends by three main factors: the size, the charge and the solvation entropy of the molecule itself.

In this system a laser is used to create a microscopic temperature gradient into a capillary where the sample is loaded. When the laser is switched on, the molecules start to move away from the locally heated region; their concentration in the spot decreases until they reach a steady-state distribution. Once the laser is switched off, the molecules diffuse back.

If the molecule interacts with another one, a different thermophoretic pattern will be observed. The differences in thermophoresis are then used to quantify the binding in a titration experiment.

This method requires one of the two binding partner fluorescently labeled. The fluorescence can be intrinsic, of an attached dye or fluorescent protein.

The NanoTemper Monolith NT.115 instrument was used for monitoring the fluorescent distribution of the molecules inside the capillary and their thermophoretic movement.

In the performed experiment the fluorescent derivative Cy3-ET-1 was used. The concentration of the fluorescent ligand was kept constant (200 nM), while the concentration of the non-labeled binding partner, ETB/NDs (DMPC), was varied in between 10pM and 50nM.

A relatively high concentration of Cy3-ET-1 was necessary in order to produce sufficient signal.

After a short incubation the samples were loaded into MST standard glass capillaries and analyzed. An  $K_D$  of 4,49 nM was determined. (Fig. 24).

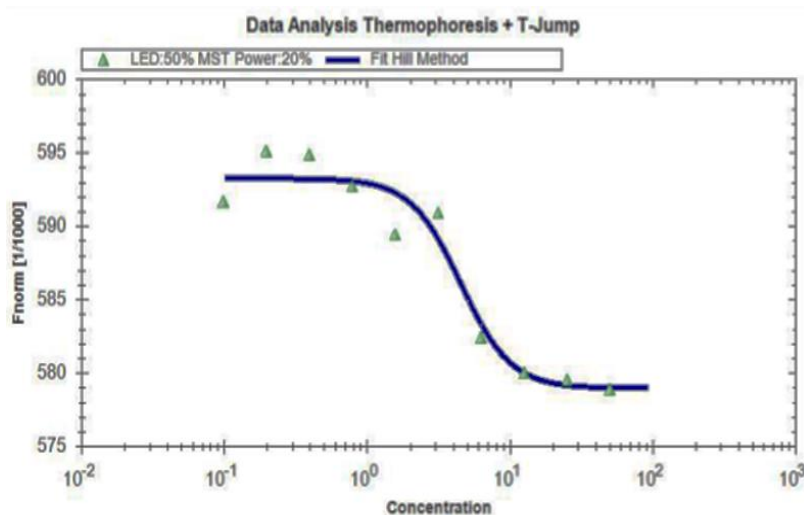


**Fig. 24: MST analysis.** 200 nM of labelled Cy3-ET-1 were shortly incubated with different concentration of ETB/NDs (DMPC) (from 10 pM to 50 nM) and directly loaded into standard glass capillary. MST-analysis was performed using the monolith NT.115 instrument.

#### 4.17 OCTET SYTEM

The OCTET system allows quantification of proteins concentrations as well as analysis of biomolecular interaction.

Advantages of this system are the possibility to obtain real-time data and to perform the experiment in 8 or 16 different conditions in parallel using 96-wells or 384-wells microplates, enabling a fast optimization of the ligand binding assay.

The system is composed of a biosensor tip coated with a capturing molecule.

At the beginning of the experiment the desired ligand is immobilized on the surface of the biosensor. After a washing step, performed in order to remove the unbound ligand, the tip is incubated under shaking in the well containing the analyte. The instrument emits white light down the biosensor and collects the light that is reflected back.

The produced interference pattern is captured by a spectrometer as a unique spectral signature, reported in relative intensity units (nm). Any change in the number of molecules bound to the biosensor tip causes a shift in the interference pattern that can be measured in real time. The wavelength shift is a direct measure of the change in optical thickness (nm) of the biological layer.

When the ligand and the analyte interact, an increase in signal is observed in the sensogram. After the association phase the biosensor is transferred into a well containing only buffer and the dissociation of the analyte is observed.

From the shape of the curves obtained in the sensogram the association and dissociation constant  $k_a$  and  $k_d$  can be measured, as well as the affinity constant  $K_D$ .

The first experiment was performed in order to evaluate the possibility using NDs in combination with the OCTET system.

Different concentrations of b-ET-1 (ranging from 1.8 nM to 60 nM) were immobilized on the surfaces of Streptavidin biosensors. As a control for the unspecific binding of the ETBsGFP/NDs, one biosensor was also incubated in buffer without ligand. The prepared biosensors were then washed in buffer in order to remove the unbound ligand and incubated in presence of 50 nM ETBsGFP/NDs. A higher response was obtained in the biosensors where the ligand was immobilized, whereas a lower response was measured in the empty biosensor, indicating a weak interaction of the ETB-sGFP/ND with the biosensor surface itself. The measured response was directly correlated on the amount of immobilized ligand, giving a first hint of a specific interaction between the ETB-sGFP/ND and b-ET-1 (Fig. 25).

In order to optimize the condition, two different buffers were tested, HEPES-NaOH pH 7.5 and Tris-HCl pH 7.5; BSA was also added in the buffer to minimize unspecific interactions.

Best results were obtained in 50 mM Tris pH 7.5, 150 mM NaCl and 1% BSA (Fig. 26). In this condition, a preliminary  $K_D$  of around 3 nM was measured;  $K_a$  and  $K_d$  were in the same range as already measured in the SPR experiment ( $10^4/10^5$ ). Two different negative controls were also implemented in order to detect unspecific interactions. ETB-sGFP/NDs were incubated with empty biosensor as well as empty NDs were incubated in biosensor where b-ET-1 was immobilized. In both cases similar curve were obtained, indicating a weak interaction of the NDs to the biosensor surface itself.



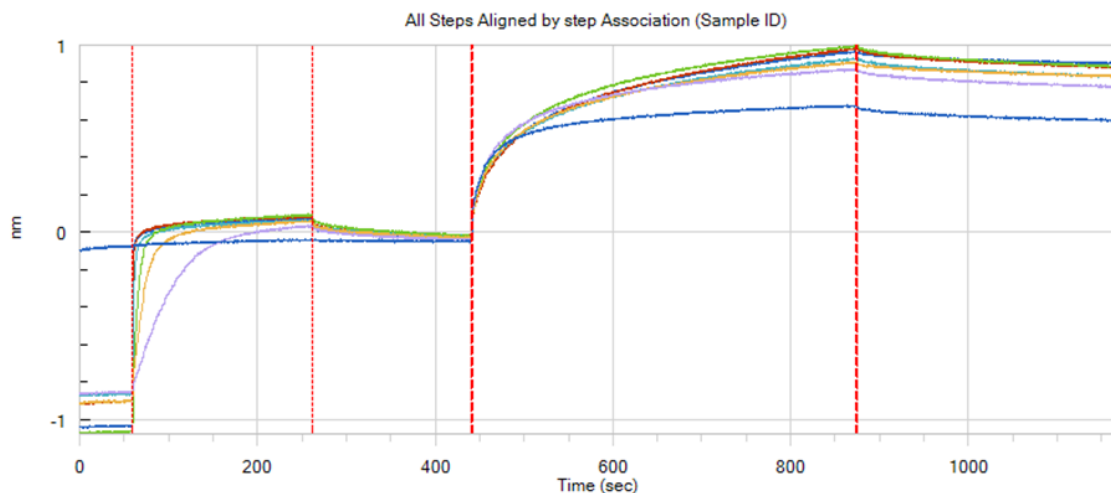


**Fig. 25: Ligand binding analysis using OCTET system.** Different concentrations of b-ET-1 (1.8, 3.75, 8.5, 15, 30, 60 nM) were immobilized on different SA-Chips. One chip was incubated only in buffer without ligand (lower blue line). The chips were then incubated in presence of 50 nM ETB-sGFP/ND. Stronger interaction was detected in the chips where the ligand was immobilized.

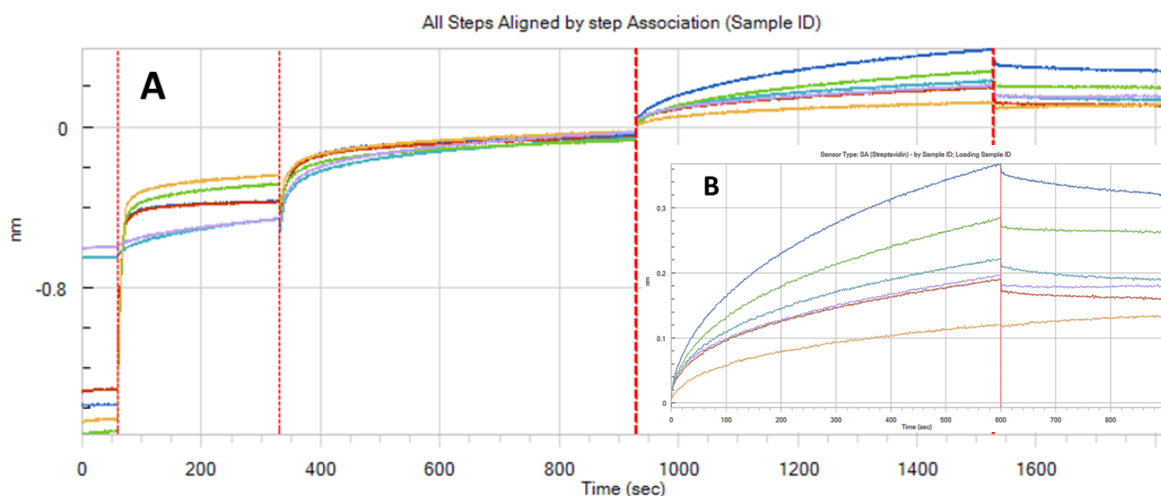


**Fig. 26: Ligand binding analysis using OCTET system.** **A.** Different conditions were tested in order to detect a specific interaction of ETB-sGFP/NDs to the immobilized b-ET-1. In Tris-HCl buffer were obtained the curves: Blue (b-ET-1 and ETB-sGFP/NDs (DMPC)); Red (negative control: b-ET-1 and empty NDs); Light Blue (negative control: no ligand and ETB-sGFP/NDs (DMPC)). In Hepes buffer: Green (b-ET-1 and ETB-sGFP/NDs (DMPC)); Yellow (negative control: b-ET-1 and empty NDs); Violet (negative control: no ligand and ETB-sGFP/NDs (DMPC)). **B.** Association and dissociation phases of the different conditions tested.

#### 4.18 N-terminal processing of the CF synthesized ETB

As already pointed out in chapter 4.4, analysis by SDS-PAGE of the P-CF produced and purified ETB receptor revealed a single band corresponding to a MW of approximately 40 kDa, whereas, after D-CF expression as well as after L-CF expression in presence of NDs, two bands corresponding to approximately 40 kDa and 35 kDa were observed (Fig. 27A)

In contrast, only one band of approximately 41 kDa was detected after D-CF as well as after P-CF expression of ETA (Fig. 27A). The formation of the ETB double band was found to be independent from the selection of supplied detergents during the D-CF expression as well as during the purification (data not shown).

In order to verify the presence of possible truncations or premature termination of translation, the samples were analyzed by Western-blotting.

By immunodetection with an anti-His antibody both bands for the D-CF samples were still visible, indicating the presence of intact C-terminal ends in the two ETB derivatives. ETB further contains an N-terminal T7-tag and anti-T7-tag antibodies reacted after Western blotting only with the larger 40 kDa band, indicating an N-terminal deletion of the 35 kDa ETB derivative (Fig. 27B).

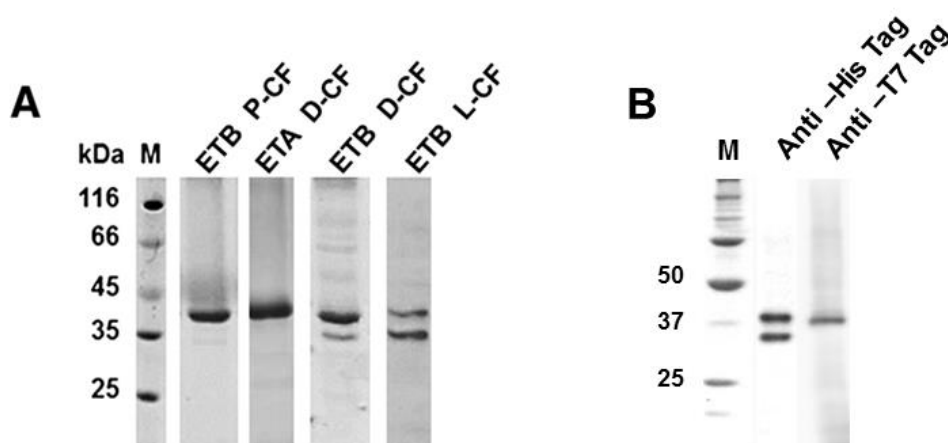


**Fig. 27: Analysis of CF produced ETA and ETB. A.** IMAC purified ETA and ETB after P-CF, D-CF (1% Brij78) and L-CF (MSP1E3D1-ND, DMPC) expression modes. The samples were separated on a 12% SDS-PAGE and stained with Coomassie Blue. **B.** Immunoblot of D-CF (1% Brij78) produced ETB. 1 $\mu$ l of sample was separated on a 12% SDS-PAGE and immunoblotted with anti-His tag or anti-T7 tag antibodies.

A specific cleavage of the first 64 amino acids of ETB produced in HEK293 cells by putative metalloproteases has been reported (Grantcharova et al. 2006).

Increasing the concentration of EDTA in the D-CF reaction led to a decrease in the intensity of

the 35 kDa band in the SDS-PAGE, suggesting an involvement of metalloproteases (Fig. 28A). In order to further analyze whether the origin of the second band is based on a similar N-terminal cleavage has observed in cells, the mutant  $\Delta$ ETB carrying a deletion of the first 64 amino acids was prepared. The D-CF expression of  $\Delta$ ETB resulted in a single band after SDS-PAGE analysis, apparently co-migrating with the lower 35 kDa band of full-length ETB expressed in D-CF mode (Fig. 28B). Edman sequencing of the 35 kDa band indicated the residues alanine, proline and glutamic acid in positions 3, 4 and 6, supporting the hypothesis of the specific cleavage of ETB at amino acid position 64.

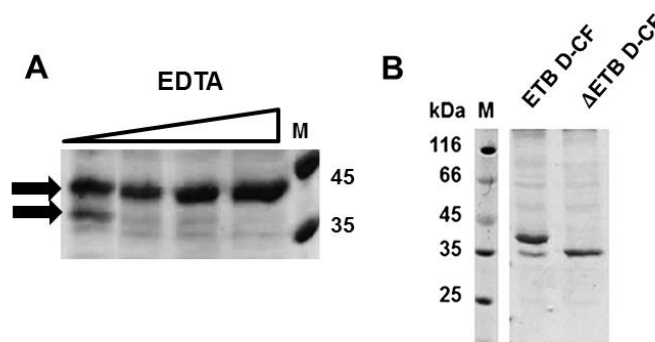


**Fig. 28: Analysis of CF expressed ETB.** **A.** Increasing concentrations of EDTA were supplied in the CF reaction (0; 0.1; 0.2; 0.4 mM). At high concentration of EDTA the second band of ETB disappear. **B.** D-CF expression (Brij78 1%) of ETB and  $\Delta$ ETB. Samples were separated on a 12% SDS-PGE gel and stained with Blue Coomassie.

In order to verify the ligand binding activity of the truncated version  $\Delta$ ETB, a ligand affinity chromatography experiment was performed. Aliquots of 13 nmol of the agonist b-ET-1 were immobilized on monomeric avidin agarose columns and 0.67 nmol of D-CF expressed  $\Delta$ ETB (1% Brij78) purified into 0.1% Brij35 was loaded (Fig. 29). After washing, the bound  $\Delta$ ETB/b-ET-1 complexes were eluted with d-desthiobiotin and quantified by immunoblotting with anti-His antibodies. A binding competence of approximately 25% was measured for  $\Delta$ ETB which is comparable to the previously determined efficiency of full-length ETB at similar conditions (Junge et al. 2010).

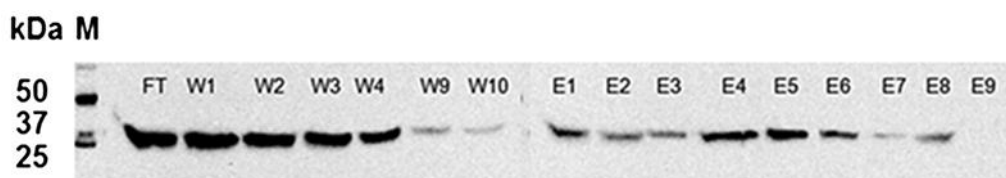


**Fig. 29: Ligand affinity chromatography of D-CF produced  $\Delta$ ETB.** 1  $\mu$ M purified receptor in 0.1% Brij35 was incubated with 100  $\mu$ g of b-ET-1 immobilized on monomeric avidin agarose matrix, washed and eluted with 2 mM D-desthiobiotin. Samples of all fractions were separated by 16% SDS-PAGE and immunoblotted with anti-His-tag antibodies. M, marker; FT, flow-through fraction; W, wash fractions; E, elution fractions.

#### 4.19 SDS resistant complex formation of CF synthesized ETB with the ligand ET-1

A special feature of the ETB receptor, not shared with ETA, is the formation of a very stable and even SDS resistant complex with the ligand ET-1 (Takasuka et al. 1991).

In order to verify if this ability was retained in the CF produced samples, D-CF preparations of ETB,  $\Delta$ ETB and ETA were incubated with the biotin labeled peptide agonist b-ET-1 for 1 h. After separation by low temperature SDS-PAGE, the samples were immunoblotted with anti-biotin antibodies. A clear signal of b-ET-1 was detectable with both bands of full-length ETB. The signal with the truncation  $\Delta$ ETB was weaker but still detectable, while no bound ligand was observed with ETA (Fig. 30A and B). The results gave evidence of SDS-resistant ETB/b-ET-1 complexes, while putatively formed ETA/b-ET-1 complexes were SDS sensitive.

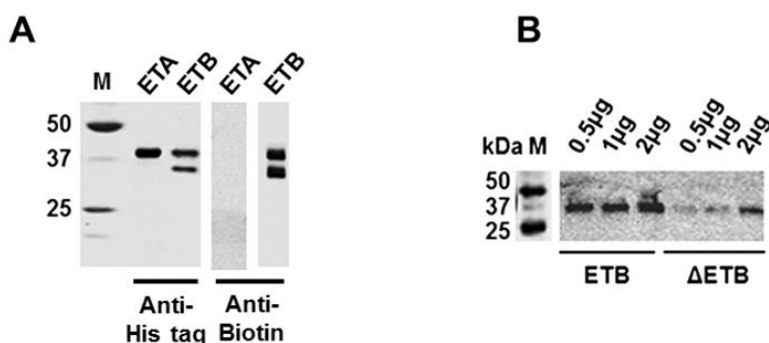


**Fig. 30. Analysis of formation of SDS resistant complex.** **A.** 1  $\mu$ l of D-CF (1% Brij78) produced ETB and ETA was first incubated for 1 h at 4  $^{\circ}$ C with 100 nM of b-ET-1 in PBS. The samples were then separated by 12% SDS-PAGE at 10  $^{\circ}$ C and blotted using anti-His or anti-Biotin antibodies. **B.** 1  $\mu$ l of D-CF (1% Brij78) produced ETB and  $\Delta$ ETB was first incubated for 1 h at 4  $^{\circ}$ C with 100 nM of b-ET-1 PBS. The samples were then separated by 16% SDS-PAGE at 10  $^{\circ}$ C and blotted using anti-Biotin antibodies.

#### 4.20 CF expression of Galpha subunits

ETA and ETB are members of the GPCRs family, the interaction with an agonist ligand causes a re-arrangement of the cytoplasmic domains of the receptors that leads to heterotrimeric G proteins activation.

Heterotrimeric G proteins are composed of an  $\alpha$  subunit that is tightly associated with a  $\beta$  and a  $\gamma$  subunit. Upon activation by a GPCR, the GDP bound to the  $\alpha$  subunit is exchanged into GTP, this event inducing the dissociation of the heterotrimeric complex and activation the typical signaling cascade.

In order to clarify if the ETB receptor co-translationally expressed in NDs is still able to induce activation of the G proteins, two  $\alpha$  subunit,  $G\alpha_s$  and  $G\alpha_q$ , were expressed in CF system.

Both P-CF and D-CF mode were tested for the ability to produce soluble  $G\alpha$  subunits.

As DNA template for the reaction the expression plasmid pet21a(+) carrying the coding sequence of the human  $G\alpha_s$  or  $G\alpha_q$  subunit was used. The protein synthesis resulted in the construct T7- $G\alpha$ (s or q)-poly(His)<sub>10</sub>. Between the  $G\alpha$  subunit and the His-tag a thrombin cleavage site was also inserted.

In the P-CF expression mode, the  $G\alpha_q$  subunit was expressed prevalently as a precipitate, whereas for  $G\alpha_s$  a relatively bigger fraction was detected in the supernatant (Fig. 31A and B). The pellet obtained from both subunits was efficiently resolubilized in LMPG 1% and after IMAC purification and exchange to 0.1% CHAPS, around 0.1-0.5 mg/ml of purified proteins were obtained (Fig. 31C)

For the D-CF expression mode different detergents were screened: digitonin 0.4%, Brij78 1%, Brij35 0.5%. Best soluble expression was achieved in Brij78 1% for the  $G\alpha_s$  subunit and Brij35 0.5% for the  $G\alpha_q$  subunit (Fig. 31D).

We decided to use only the soluble fraction obtained by P-CF expression mode of the  $G\alpha_s$  subunit for the further described functional assays, as the presence of detergents could have a negative effect on the NDs stability.

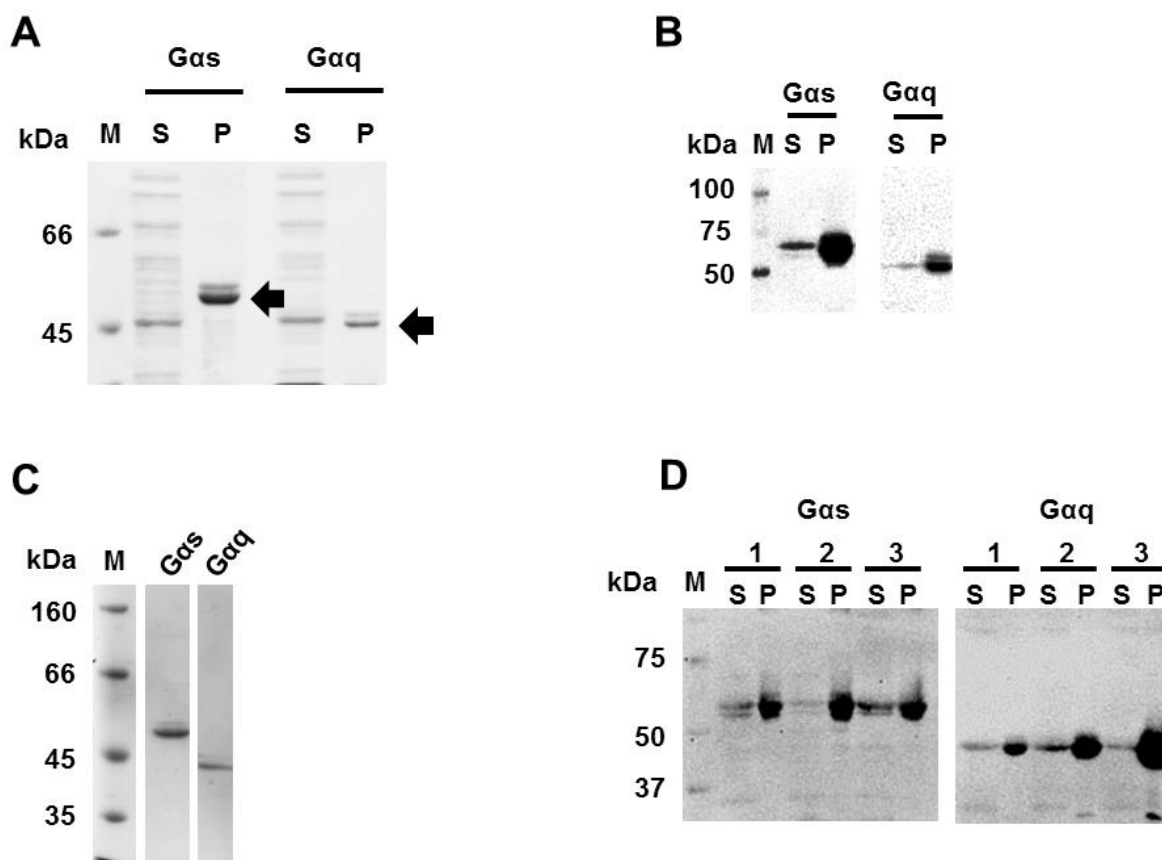


**Fig. 31: P-CF and D-CF expression of G $\alpha$  subunits.** **A.** P-CF expression of G $\alpha_s$  and G $\alpha_q$ . 3  $\mu$ l of pellet or supernatant were separated on a 12% SDS-PAGE gel and stained with blue Coomassie. **B.** Analysis of P-CF expressed proteins by immunoblot. 1  $\mu$ l of pellet or supernatant were separated by 12% SDS-PAGE and immunoblotted with anti-His antibody. **C.** Elution fraction from IMAC purified samples. 10  $\mu$ l of protein was separated on a 12% SDS-PAGE and stained with blue Coomassie. **D.** D-CF screening. G $\alpha_s$  and G $\alpha_q$  were expressed in presence of different detergent. 1  $\mu$ l of sample from the supernatant or the pellet fractions were separated on a 12% SDS-PAGE gel and immunoblotted with anti-His antibody. 1: Digitonin 0.4%. 2: Brij35 0.5%. 3: Brij78 1%. S: Supernatant, P: Pellet.

#### 4.21 Functional analysis of the P-CF produced G $\alpha_s$

The functional activity of the G $\alpha_s$  subunit expressed in CF system was verified before performing interactions studies with ETB/NDs samples.

The experiments were performed using two different analogues of GTP.

A fluorescent assay was performed using BODIPY-GTP- $\gamma$ -S. This molecule is a non-hydrolyzable analogue of GTP, due to the replacement of an oxygen atom with a sulfur one in the  $\delta$ -

phosphate, it remains stably associated with the G proteins and it cannot be converted into GDP. When this molecule is free in solution, the fluorescence of the BODIPY dye is quenched by photoinduced electron transfer from the proximal guanosine base. The fluorescence of the BODIPY GTP- $\gamma$ -S is quenched by ~90% relative to that of the free dye but is recovered upon binding to G proteins.

IMAC purified  $G\alpha_s$  were incubated in buffer containing BODIPY GTP- $\gamma$ -S in presence or absence of GDP and the fluorescence signal was then measured after 40 min using TECAN Genios fluorescence plate reader (Fig. 32A).

In absence of GDP,  $G\alpha_s$  shows high constitutive activity and an increase in fluorescence signal after 40 min incubation is observed. This event is expected due to the lack of the  $\beta$  and  $\gamma$  subunits that have a regulatory effect in the heterotrimeric G protein complex, preventing the exchange of GDP to GTP in the  $G\alpha$  subunit that is not activated by the agonist-receptor complex.

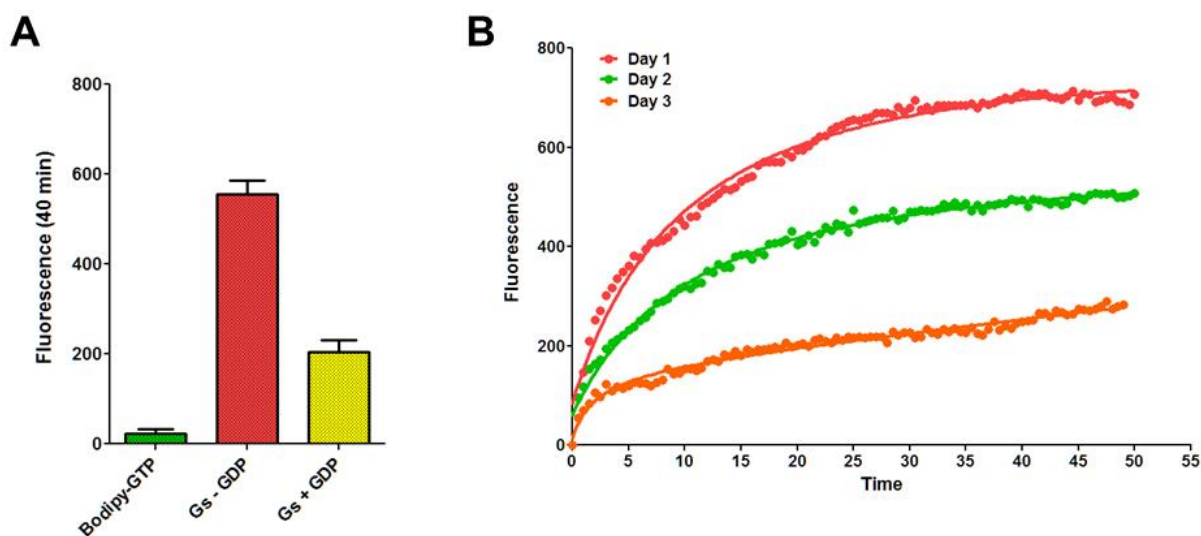


**Fig. 32: Analysis of the basal activity of the  $G\alpha_s$  subunit by fluorescent assay.** **A.** 200 nM of IMAC purified  $G\alpha_s$  were incubated in buffer (10 mM HEPES pH 7.5, 10 mM  $MgCl_2$  pH 8, and 100 mM NaCl) containing 50 nM of BODIPY GTP- $\gamma$ -S in presence or absence of 1  $\mu$ M GDP. The fluorescence signal was measured after 40 min incubation. **B.** Fluorescence real time measurement. 200 nM of IMAC freshly purified  $G\alpha_s$  expressed in CF, or after storage at 4°C for 24h and 48h were incubated in buffer in presence of 50 nM BODIPY GTP- $\gamma$ -S and 1  $\mu$ M GDP. Fluorescent signal was recorded using a TECAN Genios fluorescence plate reader every 30 sec for 50 min.

For the association of BODIPY GTP- $\gamma$ -S a  $t_{1/2}$ sec of  $486 \pm 30$  and a rate constant  $K_{ob}$ :  $0.08 \pm 0.005$   $\text{min}^{-1}$  were measured.

In presence of high concentration of GDP, the activity of the  $G\alpha_s$  subunit is reduced and lower fluorescence signal is detected. When BODIPY GTP- $\gamma$ -S was incubated in buffer without  $G\alpha_s$ , no significant increase in fluorescence was detected.

The activity of the same purified sample was also measured after 24h and 48h. The sample was stored at  $4^\circ\text{C}$  in 20 mM Tris pH 7.5, 150 mM NaCl and 10% glycerol. The increase in fluorescence was measured in real-time using TECAN Genios fluorescence plate reader.

Almost 50% of reduction in activity was detected every 24h (Fig. 32B).

Complementary experiment were performed using a radioactive non-hydrolysable analogue of GTP, the GTP- $\gamma$ -S<sup>[35]</sup>. Experiments were performed in the same condition as for the fluorescent assay and the radioactive incorporation of the GTP- $\gamma$ -S<sup>[35]</sup> was measured at different time point by filtration of the sample using a Millipore HTS plate. The filters were collected and incubated over night in 2 ml of scintillation cocktail and the radioactivity was measured using a scintillation counter. As observed in the fluorescent assay, an increase of incorporation over time of the GTP- $\gamma$ -S<sup>[35]</sup> was detected in absence of GDP ( $t_{1/2}$ sec:  $198 \pm 18$ , rate constant  $K_{ob}$ :  $0.20 \pm 0.01$   $\text{min}^{-1}$ ), whereas the activity of the  $G\alpha_s$  protein was reduced in presence of  $1\mu\text{M}$  GDP (Fig. 33).

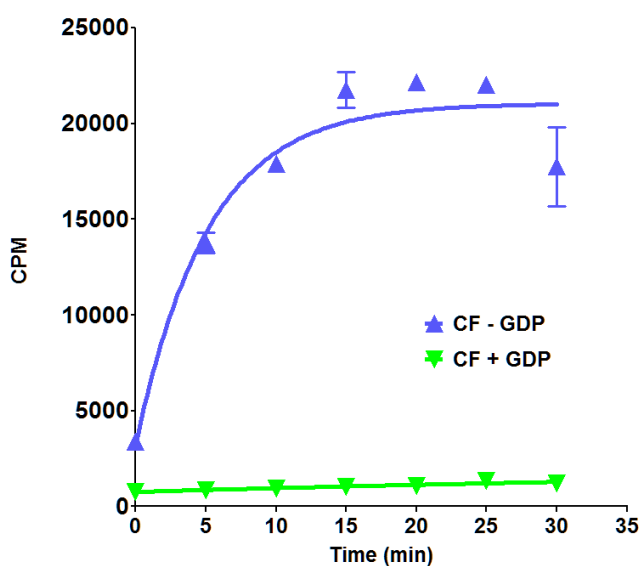


**Fig. 33: Analysis of the basal activity of the  $G\alpha_s$  subunit by radio assay.** 200 nM of IMAC purified  $G\alpha_s$  was incubated in buffer (10 mM HEPES pH 7.5, 10 mM  $\text{MgCl}_2$  pH 8, and 100 mM NaCl) containing 5 nM of GTP- $\gamma$ -S<sup>[35]</sup> in presence or absence of  $1\mu\text{M}$  GDP. Aliquots at different time points were collected and filtered using a Millipore HTS plate. The collected filters were incubated o.n. with 2 ml of scintillation cocktail and the retained radioactivity measured.



#### 4.22 Ligand induced activation of $G\alpha_s$

The possibility to induce an activation of the  $G\alpha_s$  subunit in presence of an agonist and of the receptor ETB, co-translationally expressed into NDs, was evaluated.

50 nM of purified ETB/NDs (DMPC) expressed in L-CF mode were incubated in presence of 200 nM  $G\alpha_s$  and 50 nM BODIPY GTP- $\gamma$ -S with or without the agonist ET-1. The experiments were performed in buffer containing 1  $\mu$ M GDP in order to reduce the constitutive activity of  $G\alpha_s$ . The samples were incubated for 40 min and the fluorescence was then measured (Fig. 34).

Strong increase in fluorescence signal was detected only in presence of ETB/NDs (DMPC) and the ligand ET-1. In negative control where ETB/NDs (DMPC) or ET-1 were incubated with BODIPY GTP- $\gamma$ -S, no significant increase of signal was detected. Incubation of the G protein with the receptor, without addition of ligand, didn't induce an increase in the basal activity of the  $G\alpha_s$  subunit.

As a further negative control, a truncated version of ETB, the ETB93a was prepared in L-CF mode in presence of NDs (DMPC). This truncated version, expressed in D-CF mode, has been shown to bind the ligand with affinity similar to the full length receptor (Klammt et al. 2007). The insertion into NDs was verified by western-blot. This version, lacking most of the cytoplasmatic loops should not be able to interact with the  $G\alpha_s$ . Incubation of purified ETB93a/NDs (DMPC) in presence of the G proteins didn't show any increase in signal in presence of BODIPY-GTP- $\gamma$ -S after 40 min, nor was any effect observed by addition of ET-1.

In the radioactive assay two different ETB agonists (ET-1, IRL-1620) as well as one antagonist (IRL-2500) were tested. Incubation of the  $G\alpha_s$  subunit with the ETB/NDs (DMPC) was sufficient to induce an increase in the basal activity of the G protein, even in absence of any ligand. None of the agonists induced a further increase in the activity of the  $G\alpha_s$  subunit but a strong reduction (50%), was detected in presence of the antagonist IRL-2500 (Fig. 35A).

Positive control experiments were also performed using commercially available mammalian cell membrane preparation containing the ETB receptor. In this case the membranes, that contain the associated heterotrimeric G proteins, were directly incubated in buffer in presence of GTP- $\gamma$ -S [<sup>35</sup>] with or without the different ligands.

An increase in radioactivity was measured in presence of the agonist ET-1 and IRL-1620 whereas a reduction was detected in presence of IRL-2500 (Fig. 35B).

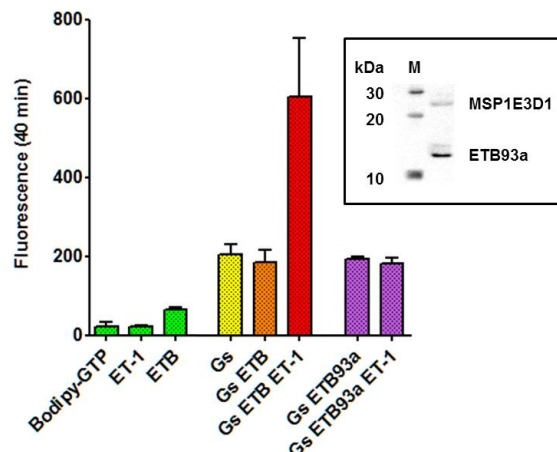


**Fig. 34:  $G\alpha_s$  activation upon agonist binding to the receptor, fluorescent assay.** 50 nM of purified ETB/NDs (DMPC) or ETB93a/NDs (DMPC) expressed in L-CF mode were incubated in presence of 200 nM  $G\alpha_s$  and 50 nM BODIPY GTP- $\gamma$ -S, with or without 1  $\mu$ M of ET-1. Sample were incubated in buffer (10 mM HEPES pH 7.5, 10 mM  $MgCl_2$  pH 8, and 100 mM NaCl) for 40 min and the fluorescent signal measured using TECAN Genios fluorescence plate reader. For the negative control, 50 nM of ETB/NDs (DMPC) or 1  $\mu$ M of ET-1 were incubated with 50 nM BODIPY GTP- $\gamma$ -S. Insert: immunoblot analysis of L-CF expressed ETB93a in presence of DMPC NDs. 10  $\mu$ l of IMAC purified sample was separated on a 12% SDS-PAGE and immunoblotted with anti-His antibody.

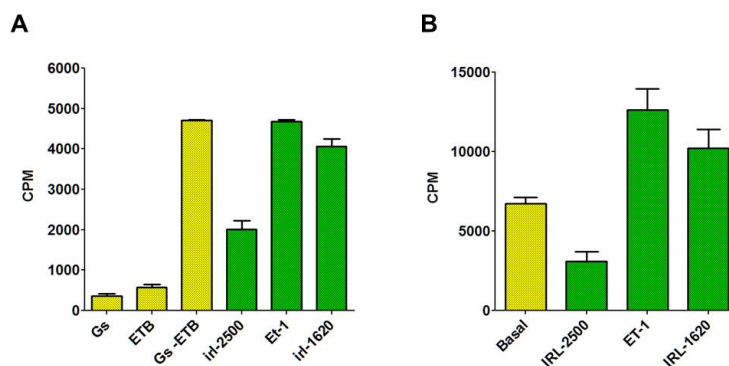


**Fig. 35:  $G\alpha_s$  activation upon agonist binding to the receptor, radioactive assay.** **A.** 50 nM of purified ETB/NDs (DMPC) expressed in L-CF mode were incubated with 200 nM  $G\alpha_s$  and 5 nM GTP- $\gamma$ -S<sup>[35]</sup>, with or without 1  $\mu$ M of ET-1, IRL-2500 or IRL-1620. Samples were incubated in buffer (10 mM HEPES pH 7.5, 10 mM  $MgCl_2$  pH 8, and 100 mM NaCl) for 40 min and subsequently filtered using using a Millipore HTS plate. The collected filters were incubated o.n. with 2 ml of scintillation cocktail and radioactivity measured **B.** 5  $\mu$ l of membranes were incubated with 5 nM GTP- $\gamma$ -S<sup>[35]</sup> with or without 1  $\mu$ M of ET-1, IRL-2500 or IRL-1620. Samples were then filtered and processed in the same way as for the ETB/NDs samples.

## 5. Discussion

### 5.1 Cell-Free expression of GPCRs

Cell-free (CF) expression has emerged in the last decade as an efficient and fast approach for the production of MPs.

This particular expression system eliminates several central bottlenecks that arise from the conventional expression in a cell-based system and allows a fast production of proteins in small scale volumes. On the other hand, in order to achieve good sample quality, the fine tuning of the reaction conditions is a necessary step.

Two major configurations exist for the CF production of proteins, the single compartment batch configuration and the two compartment continuous exchange configuration (CECF) (see 3.4) (Kigawa et al. 2004, Spirin et al. 1988).

The batch configuration is the method of choice for high throughput applications using microplate devices and analytical scale reactions (Kai et al. 2013, Savage et al. 2007, Schwarz et al. 2010). In this configuration, the expression time is limited to few hours with consequently low protein yields.

Using the CECF system higher amount of various GPCRs have been produced (see Table 14).

### 5.2 Optimization of the expression, general considerations

Complexity of MPs production in CF systems reduced by the basic transcription/translation process. The protein expression is usually controlled by the phage T7-RNA polymerase, for this reason the corresponding regulatory promoter and terminator elements, in addition with specific enhancers, have to be present in the template.

ETA and ETB constructs have been expressed using pET vectors as templates for the CF reaction. These vectors are characterized by the presence of specific T7 promoters sequence as well as N-terminal T7 tag and C-terminal poly(His)<sub>10</sub>-tag or Strep-tag (see 3.1).

Of particular importance for obtaining high expression yields of the two receptors was the presence of the N-terminal tag.

Initial problems with low expression efficiency are mainly associated with the translation

process. Low protein yields are frequently caused by the formation of unfavorable secondary structures of the mRNA in the 5-prime end, in proximity of the translational initiation site.

Modulating the nucleotide sequence in this region can therefore be very effective in order to improve protein expression (Ahn et al. 2007, Kralicek et al. 2011).

Addition of the T7-tag was sufficient to increase the expression of the two endothelin receptors, as already previously reported (Klammt et al. 2005). This tag is also advantageous due to its small size (1.5kDa) and due to the possibility to detect it in immunoblot using specific antibody.

Protein <sup>1</sup>	Size [kDa]	Assay <sup>2</sup>	System <sup>3</sup> Yield <sup>4</sup>	Solubilization <sup>5</sup>	Ref.
<b>P-CF</b>					
hETB, hNPY2/5 hMTNR1A/B hSS1/2, hV1BR hHRH1, hV2R rCRF	39 - 51	-	iE [3]	LMPG	Schneider et al. 2010
hCRFR1 mCRFR2 $\beta$	47 49	+	iE [3]	LMPG / Nvoy	Klammt et al. 2011
hETA/B	49/50	+	iE [3]	LPPG, LMPC, SDS, Fos16, Fos12	Junge et al. 2010
hH1R	5	+	cE [1]	DDM	Sansuk et al. 2008
<b>D-CF</b>					
Dopamine D2	50	+	iE, WG		Basu et al. 2013
hTAAR-T4L	45	+	iE [2]	Brij35	Wang et al. 2013
hETA, hETB	49/50	+	iE [3]	Brij35/78	Junge et al. 2010
Olfactory Receptors, hFPR3, hVN1R1, hVN1R5	~30	+	cE [2]	Brij35, peptide surfactants	Corin et al. 2011
OR17-4	36	+	WG, cE [2]	Digitonin	Kaiser et al. 2008
hMTNR1B, hNPY4R, rCRF, hV2R	~40	-	iE [2]	Brij58/78	Klammt et al. 2007
hCHRM2, h $\beta$ 2AR, hNTR	~60	+	iE [2]	Brij35, digitonin	Isihara et al. 2005
hOR17-210, mOR103- 15, hFPR3, hTAAR5	~40	+	iE [2]	Peptide surfactants	Wang et al. 2011
hCRF1, CRF2 $\beta$ ,	~40	+	iE	Nvoy	Klammt et al. 2011
<b>L-CF</b>					
h $\beta$ 2-AR-T4L	63	+	cE	apoA1 (DMPC)	Yang et al. 2011
ADRB2, DRD1, NK1R	~50	+	cE	$\Delta$ 49A1 (DMPC)	Gao et al. 2012

**Table 14. CF expression of GPCRs.** <sup>1</sup>, if documented, the origin of the protein is given; h: human; m: murine. <sup>2</sup>, +: quality analyzed by structural or functional assays. <sup>3</sup>, iE: Individual *E. coli* extracts; cE: Commercial *E. coli* extracts; WG: Wheat germ extracts. <sup>4</sup>, approximate yields for ml of RM, if documented. 1:  $\leq$  0.1 mg/ml; 2: 0.1-1 mg/ml; 3:  $>$  1 mg/ml. <sup>5</sup>, main detergent or lipid used for the solubilization.

The presence of the C-terminal poly(His)<sub>10</sub>-tag or Strep-tag facilitated the purification of the two endothelins receptors and enabled verification of their full-length synthesis.

Adjusting the proper Mg<sup>2+</sup> concentration for each new batch of CF extract was also a mandatory step for optimal expression. As already reported, suboptimal concentrations can have severe impacts on protein production (Rath et al. 2011, Schwarz et al. 2007). In general, Mg<sup>2+</sup> concentration in between 14-18 mM enabled high yield of expression for ETA and ETB (Fig. 9).

In this work, C-terminally attached derivatives of shifted green fluorescent protein (sGFP) were also used as a tool to assist CF expression protocol development and for fast protein quantification. sGFP derivatives were used especially in combination with L-CF expression mode, as the folding of sGFP is hampered in presence of many detergents (Roos et al. 2012).

### 5.3 P-CF and D-CF mode: solubilization of the receptor in detergents

Based on the choice of supplemented additives, several basic expression modes are possible for the CF production of MPs. The selection of an expression mode, which may be dictated by a specific purpose, can have drastic consequences on the resulting MP quality (Junge et al. 2010, Lyukmanova et al. 2011).

In absence of any provided hydrophobic environment, the freshly translated MPs instantly precipitate in the RM. The P-CF precipitate, that resembles the formation of inclusion body in *E. coli*, can be solubilized in mild detergents without any denaturation step (Klammt et al. 2004, Schwartz et al. 2007).

Best results for the solubilization of CF produced GPCRs are usually obtained with the lysophosphatidylglycerols LMPG and the related LPPG (Junge et al. 2010, Klammt et al. 2004). These two detergents were also effective in the solubilization of the ETB receptor, 1-1.5 mg/ml of IMAC purified protein were routinely obtained upon solubilization in LMPG 1% (Fig. 10).

CF expression systems can tolerate a considerable number of supplied hydrophobic compounds. The CF expression in the presence of detergents (D-CF), supplied at a concentration above their critical micellar concentration, can result in the co-translational solubilization of the expressed MPs and in the instant formation of proteomicelles (Fig. 13).

Extensive evaluation of detergent tolerance has been performed with *E. coli* extracts (Gourdon et al. 2008, Klammt et al. 2005, Lyukmanova et al. 2012).

Positive results for the expression of MPs, as well as GPCRs, have been obtained using the long-chain polyoxyethylene-alkyl-ethers such as Brij35, Brij58, Brij78 or Brij98 (Klamm et al. 2005). In case of digitonin, too high concentrations could impair production levels (Kaiser et al. 2008,

Klammt et al. 2005). Commonly employed detergents for the extraction of MPs from native membranes such as DPC, the alkyl-glucoside n-dodecyl- $\beta$ -D-maltoside (DDM) or n-octyl- $\beta$ -D-glucopyranoside ( $\beta$ -OG) are too harsh for the CF system and only tolerated at very low concentrations (Klammt et al. 2005).

Regarding the endothelin receptors, analysis by SDS-PAGE or immunoblot of ETB expressed in P-CF or D-CF mode revealed a different quality of the produced receptor (see 4.18).

After P-CF expression and resolubilization of the receptor in LMPG 1%, a single band corresponding to a molecular weight of approximately 40 kDa was detected upon separation on a 12% SDS-PAGE (Fig. 27A). In D-CF mode, two different bands corresponding to a molecular weight of approximately 35 and 40 kDa were detected (Fig. 27A). The formation of the double band, that was not dependent on the detergent used for the expression, was affected by the concentration of EDTA (Fig. 28).

Formation of the double band in D-CF mode was specific only for the ETB receptor, in case of ETA, a single band of approximately 41 kDa was detected in both expression modes (Fig. 27A).

*In vivo*, the N-terminal domain of ETB is subject to proteolytic cleavage. Protein analysis of purified ETB receptor from human placenta revealed two different isoforms, a full length receptor (416 amino acids), and a N-terminal truncated version, starting with the amino acids serine 65 and comprising 378 amino acids in total (Akiyama et al. 1992). The existence of these two isoforms has been demonstrated in different tissues also in dog, pig and calf, indicating an evolutionary conserved process (Hagiwara et al. 1991, Saito et al. 1991, Takasuka et al. 1991).

The cleavage, in between the amino acids arginine 64 and serine 65, is catalyzed by a yet unidentified metalloprotease, as demonstrated by the sensitivity of the proteolysis to EDTA and different metalloprotease inhibitors (Grantcharova et al. 2002). Furthermore, point mutations of the ETB receptors at the cleavage site or in a surrounding stretch of 9 amino acids, didn't prevent the proteolytic cleavage of the receptor expressed in HEK293T cells (Grantcharova et al. 2002).

The cleavage seems therefore independent from the primary sequence but rather based on specific receptor conformation. This hypothesis is supported by the observation of proteolytic cleavage in different MPs by metalloproteases. For example, the cleavage of the amyloid precursor protein (APP) by the  $\alpha$ -secretase, as well as the cleavage of the protein L-selectin, depends by the  $\alpha$ -helical conformation of these proteins and on the distance of the cleavage site from the plasma membrane (Esch et al. 1990, Sisodia 1992).

The physiological role of the N-terminal proteolysis of the ETB receptor in vascular smooth muscular cells seems related with an increase in the expression of differentiation markers. The full length ETB receptor, but not the truncated  $\Delta$ ETB form, missing the first 64 amino acids,

induces a biphasic activation of ERK1/2 involving the EGF receptor transactivation (Grantcharova et al. 2006). Regarding the ligand binding affinities of the full length and of the truncated form, no differences were detected towards the physiological ligand ET-1 as well as towards other ETB specific agonists and antagonists (Grantcharanova et al. 2002).

The same specific cleavage observed upon D-CF expression of the ETB receptor was confirmed by Edmann sequencing analysis of the 35 kDa band and by immunoblot experiments (Fig. 27B, Fig. 28). Ligand affinity chromatography confirmed that the D-CF expressed truncated version  $\Delta$ ETB was still able to bind the ligand (Fig. 29). About 25% of the produced receptor was correctly folded and the production efficiency was comparable with that one previously determined for the full length ETB receptor in similar conditions (Junge et al. 2010).

The N-terminal cleavage of ETB was only detectable upon soluble expression using the D-CF or L-CF expression modes (Fig. 27A). It seems therefore that the precipitation of ETB in the P-CF mode either restricts the access to the proteolytic site or alters the receptor conformation, thus preventing the recognition by the protease.

Addition in the CF system of the protease inhibitor cocktail, that is effective only on serine and cysteine proteases, did not affect the functionality of the metalloproteases.

A specific property of the ETB receptor, not shared with the ETA receptor, is the formation of a very stable and even SDS resistant complex with ET-1 (Elshuorbagy et al. 1993, Saravanan et al. 2004, Takasuka et al. 1991). ETB receptor does not dissociate from the bound ligand even in presence of 2% SDS and the complex co-migrates in low-temperature SDS-PAGE gel. Comparison of several chimeric receptors of ETA and ETB, ruled out the importance of the N-terminal domain of the ETB receptor for the formation of this super-stable complex. Of particular importance seems to be the amino acids aspartate 75 and proline 93, as point mutations abolished the SDS resistant binding (Takasuka et al. 1991). The specific role of this amino acids is still unclear, they could be directly involved in the binding of the ligand or they can interact with other part of the endothelin receptor, stabilizing the structure of the complex (Takasuka et al. 1991).

The physiological meaning of this special feature of the ETB receptor is still not fully understood but could be related to the role of ETB in the rapid clearance of ET-1 from the vascular system.

Upon D-CF expression, ETB, as well as  $\Delta$ ETB, showed formation of persistent complexes with b-ET-1 after low-temperature-SDS-PAGE, while in contrast ETA/b-ET-1 complexes were SDS sensitive (Fig. 30).

The formation of this super-stable complex observed in D-CF expressed samples suggests a ligand binding capable conformation of the receptor is this condition, confirming the high affinity binding previously reported (Klammt et al. 2007).

#### 5.4 Following the classical track: post-translational reconstitution of ETB into liposomes

The functionality of MPs, as well as GPCRs, is usually analyzed in native membranes or in reconstituted lipid bilayer.

For the ETA receptor, analysis of ligand binding properties after P-CF expression and post-translational reconstitution into liposomes have been previously reported (Junge et al. 2010), for the ETB receptor, no detailed ligand binding analysis in lipid environment have been performed so far.

In the classical post-translational reconstitution approach, the MPs solubilized in detergent after P-CF expression mode, or directly expressed as proteomicelles in D-CF expression mode, are inserted into a lipid bilayer upon removal of the detergent. Dialysis can be used for detergents with high CMC, alternatively, adsorption to hydrophobic resins like Biobeads can be performed (Rigaud et al. 2003).

For the ETB receptor, preliminary studies have investigated the possibility to reconstitute the P-CF expressed receptor, resolubilized in LMPG 1%, into liposomes composed of *E. coli* polar lipids (Klammt et al. 2007). By freeze fracture analysis, a homogenous distribution of the ETB particles was observed. Similar result was obtained for the ETA receptor, despite the very low integration efficiency and the precipitation of the protein during the reconstitution (Junge et al. 2010).

In this study, both P-CF and D-CF expression modes have been used for the post-translational reconstitution of the ETB receptor into liposomes in order to evaluate the binding activity of the receptor in a lipid bilayer (see 4.3, 4.4).

For the reconstitution of the produced samples, the protein-to-lipid ratio used during the proteoliposomes formation was a crucial parameter to take in account in order to increase the quality of the final preparation. For instance, best results were always obtained at a molar protein-to-lipid ratio of 1:1000 during the reconstitution process (Table 6, 7).

The importance of a correct ratio between protein and lipids has also been previously observed for the ETA receptor (Junge et al. 2010), and the drug transporter Oct1 (Keller et al. 2008). Too high protein concentration during the reconstitution process induces a higher aggregation of the MPs, whereas a low concentration reduces the final response obtained in functional assays.

In D-CF mode, the ETB receptor was expressed in presence of Brij78 1% and the detergent was then exchanged into a second one upon IMAC purification (see 4.4).

It is well known that the type, and the specific properties of a detergent, could play an important role in the recovery of an active MP. As a matter of fact, homogeneity of the sample preparation as well as formation of secondary structure elements can be greatly influenced by the selected detergent (Le Maire et al. 2000).

In this study, the effect of different detergents on the sample quality has been analyzed by size



exclusion chromatography (SEC) before the reconstitution of the receptor into liposomes.

SEC analysis is a well established and common tool for the preliminary estimation of protein aggregation and heterogeneity.

A single homogenous peak for the ETB receptor was detected in presence of the detergents DDM (0.05%), Brij78 (0.1%) and Brij35 (0.1%), formation of protein aggregates was detected in presence of LPPG (0.05%), DPC (0.1%) and CHAPS (1%) (Fig. 14).

The receptor was then reconstituted into liposomes and the activity analyzed by radioactive ligand binding assay. No direct correlation was found between the homogeneity of the sample preparation analyzed by SEC and the final activity of the receptor (Table 7). Lack of correlation between homogeneity and activity has also been previously observed for the protein *MraY* (Yi et al. 2011). SEC analysis seems therefore not to be a suitable tool for the preliminary screening of detergents, with the aim to obtain a final functional active MP. Detergents that induce a mono-disperse distribution of the sample could actually impair the functional folding of the protein. In presence of detergent solubilized MPs, CD spectroscopy analysis seems to be a better option for the preliminary screening of conditions (Klammt et al. 2005). In the case of the GPCR V2R, considerable variations in the  $\alpha$ -helical content have been detected in correlation with the specific CF expression mode and detergent used during the IMAC purification (Klammt et al. 2005). For the channel *Tsx*, the  $\beta$ -sheet content, that was dependent from the detergent used for the solubilization, correlated with the final activity of the protein (Kalmmt et al. 2005). Preliminary screening of suitable detergents for MPs solubilization before proteoliposome reconstitution is also complicated due to the fact that in some cases the detergents, that have been reported to be deleterious for the activity of solubilized MPs, could actually result beneficial during the reconstitution process (Levy et al. 1992).

Comparing the results obtained using the proteoliposomes samples with the one obtained using the commercial membrane preparation, a clear difference was the generally higher unspecific background for the radioactive labelled ligand ET-1. Specific binding for the proteoliposomes preparation was in between 25-40%, whereas for the control membranes, up to 85% of specific binding was detected (Table 6).

The observed results could be due to a tight association or integration in the liposomes of partially folded receptor, which still retain some residual binding competence. This effect, that was also previously reported for the ETA receptor reconstituted into liposomes (Junge et al. 2010), could also explain the relatively high  $K_D$  and  $K_i$  obtained in functional assays (Fig. 11, 12).

### 5.5 L-CF expression mode: Co-translational association of ETB to liposomes

A unique option offered by the CF system is the possibility to co-translationally insert MPs into a provided lipid bilayer. Lipids can be directly supplied in the reaction mixture (RM) in different formulations, like bicelles, liposomes or nanodiscs (NDs). This particular expression mode has the advantage, over the more traditional P-CF and D-CF modes, to allow the co-translational insertion of MPs without the need of any detergent. Furthermore, the insertion into liposomes of MPs may be more homogenous, in comparison to the post-translational reconstitution approach, simplifying functional assays and increasing their sensitivity.

Pure lipids and lipids mixtures are tolerated in the CF system even at high concentration (Klammt et al. 2004), but their specific nature can have an effect on MPs synthesis and incorporation.

In this study two different lipid environments have been extensively analyzed in combination with L-CF expression mode: liposomes and NDs.

In order to speed up the screening process, the expression was monitored taking advantage of the fusion construct ETB-sGFP. By the analysis of the liposomes preparation using confocal microscopy, fluorescent ETB-sGFP was detected exclusively in association with the liposomes, supporting the evidence of a functional reconstitution, at least of the sGFP moiety, and indicating sGFP as a useful partner for the first screening of condition in L-CF expression mode (Fig. 16).

The lipid composition determines the thickness, the fluidity and the surface charge of the membrane and can therefore strongly modulate the association of MPs as well as their activity (Roos et al. 2012). For this reason, different lipids were tested for the formation of liposomes and their effect on the synthesis and translation of ETB as well as on its functionality was evaluated.

Best results were obtained in presence of liposomes formed of Aso-PC lipids. In these liposomes the highest expression levels as well as the highest activity was detected (Table 8). Different results were obtained in case of DMPC and DOPC lipids. In the first case a relatively low integration was observed but a high activity, in the second case a low activity, despite a high reconstitution rate (Fig. 15).

The high activity of the ETB receptor reconstituted into liposomes composed of PC lipids well correlate with the fact that in mammalian cells plasma membrane, PC represents the most abundant lipid class. For instance, in endothelial cells that constitutively expressed high levels of the ETB receptor, PC represent up to 60% of the total lipid population (Cansell et al. 1997). On the other hand, the negative effect of pure DOPC lipid on the functional activity of the ETB receptor could be explained by the presence of completely unsaturated hydrocarbon chains that

create a thinner and more fluid lipid bilayer in comparison to the one created by saturated hydrocarbon chain lipids as DMPC, not allowing the receptor to assume a correct folding in this lipid environment (Ulrich 2002).

In order to optimize the functional association of the receptor, liposomes composed of Aso-PC lipids supplemented with different concentrations of cholesterol hemisuccinate (CHS) were also tested (see 4.9). Eukaryotic plasma membranes contain especially large amount of cholesterol, up to 10%- 20%. The presence of cholesterol in the membrane is necessary for the proper function of many GPCRs. Cholesterol is necessary for the activity of the neurotensin receptor (Tucker and Grisshammer 1996), the oxytocin and brain cholecystokinin receptor (Gimpl et al. 1997) the human adenosine A(2a) receptor (Weiss and Grisshammer 2002) and the human  $\beta$ 2-adrenergic receptor (Yao and Kobilka 2005).

Regarding the ETB receptor, no specific requirement of cholesterol for the proper function has been described so far. However, an enrichment of this receptor in caveolae-rich domains, which are characterized by a high content of cholesterol and sphingolipids, may suggest a specific interaction (Burger et al. 2000, Oh et al. 2012).

A slight improvement in specific binding and activity was detected upon L-CF expression of the receptor in presence of Aso-Pc liposomes supplemented with 2.5% CHS (Table 10). Further increase of CHS reduced the functionality of the protein. A possible explanation of this effect could be related to the increase rigidity of the liposome's bilayer in presence of high amounts of CHS (Nakano et al. 2008).

Analysis by radioactive ligand binding assay of the L-CF produced samples revealed a slight increase in the number of functionally inserted ETB receptor, up to around 3.5 pmol/mg, in comparison with the proteoliposomes produced after P-CF and D-CF mode, where only 2 pmol/mg and 0.5 pmol/mg were detected. Nevertheless, also in this case, high unspecific binding of ET-1 was detected.

ETB-sGFP proteoliposomes produced in L-CF expression mode quantitatively precipitated during the reaction, presumably due to rearrangements and fusions of the supplied liposomes upon association with the newly synthesized proteins (Fig. 16). The same event has been previously reported also for other MPs co-translationally reconstituted into liposomes (Roos et al. 2013, Guilvout et al. 2008, Berrier et al. 2011).

In order to improve the efficiency of the insertion and the functionality of the receptor, two different modifications of the standard L-CF expression protocol were tested.

As reported by Deniaud and coworkers, a reduction of the temperature to 20°C during the CF reaction was crucial in order to reduce the aggregation of the protein hVDAC1 expressed in D-CF mode (Deniaud et al. 2010). In this study the effect of temperature was also evaluated in L-CF

expression mode in presence of Aso-PC liposomes. In general no significant differences were detected upon expression at 27 °C or 25 °C in ETB reconstitution or functionality, as compared with the standard expression at 30 °C. At 20 °C no significant expression was detected (Table 9). A second possible modification of the standard L-CF expression protocol is based on the addition of small amount of detergents together with the liposomes in the RM (see 4.10). During the reaction the detergents are slowly diluted into the feeding mixture, allowing the formation of proteoliposomes. The addition of detergent could have the beneficial effect of increasing the fluidity of the bilayer, enhancing the MPs integration. Using this method, bacteriorhodopsin was functionally expressed in L-CF mode by addition of cholate-solubilized phosphocholine lipid (Shimono et al. 2009).

In this study, the detergent CHAPS was tested in association with liposomes of different lipids composition (Fig. 18), as well as the effect of the detergents Brij35, Brij78 and digitonin were tested in presence of Aso-PC lipids (Table 11). In general, addition of detergent together with preformed liposomes seems to be not particular beneficial for the insertion or the functionality of the ETB receptor. Radioligand binding assay revealed the same, or reduced, specific binding and activity in comparison to the sample prepared without the addition of detergent. Furthermore, in presence of CHAPS, a reduction of the expression was also detected.

### **5.6 L-CF expression mode: Co-translational association of ETB to nanodiscs**

NDs are a powerful tool in MPs research and biophysical and biochemical application of this technology are becoming more and more popular (Bayburt and Sligar 2010, Borch et al. 2011). Together with the classical approach, based on post-translational reconstitution of detergent solubilized MPs into NDs (Alami et al. 2007, Bayburt 2011, Inagaki et al. 2012, Leitz et al. 2006, Shenkarev et al. 2013, Whorton et al. 2007), the co-translational reconstitution approach, by means of CF expression, is becoming an emerging technique (Cappuccio et al. 2008, Katzen et al. 2009, Lyukmanova et al. 2012, Roos et al. 2012, Yang et al. 2011).

Detergent sensitive membrane proteins, such as the *E. coli* MraY translocase could be synthesized in presence of NDs in stable and functionally folded conformation (Roos et al. 2012). In the case of GPCRs, the co-translational association with NDs has already been applied with the Neurokinin 1 Receptor, the Dopamine D1 Receptor and the  $\beta$ 2-adrenergic receptor (Gao et al. 2012, Yang et al. 2011).

In this work, two different membrane scaffold protein were used for generating NDs, MSP1 and MSP1E3D1 (see 4.11). The larger MSP13D1 was clearly more efficient for the insertion of the

ETA and ETB receptor (Fig. 19). The obtained result was in accordance with previous published data (Roos et al. 2012).

NDs were tolerated at very high concentration and decrease of the expression yield started only at a concentration above 120  $\mu\text{M}$  (Fig. 19). Final concentration of 100  $\mu\text{M}$  of NDs in the RM would correspond to the relatively high lipid concentration of approximately 10–16 mg/ml (Roos et al. 2012).

At suboptimal concentrations, analysis by confocal fluorescence microscope revealed that a fraction of the supplied NDs aggregate and precipitate together with potentially folded receptors (Fig. 20). NDs aggregation might be caused by an incomplete insertion of ETB due to NDs limitation. Partial insertion into multiple NDs or intermolecular aggregation after unfolding could also be responsible for the observed clustering.

At a NDs concentration of 40  $\mu\text{M}$ , all the fluorescence signal was recovered in the supernatant and no precipitate was detected (Fig. 19). This effect of the NDs to induce a soluble expression of CF produced MPs was previously reported for the protein ErbB3, the voltage-sensing domain of the  $\text{K}^+$  channel KvAP and bacteriorhodopsin (Lyukmanova et al. 2012).

Regarding the lipid composition of the NDs, the fluorescence yields of ETB-sGFP doubled in presence of NDs composed of DMPG, in comparison with NDs composed of DMPC (Fig. 19). The anionic lipid DMPG was also shown to be most effective in the co-translational formation of NDs complexes with the protein MraY (Roos et al. 2012) as well as in the post-translational insertion of bacteriorhodopsin (Inagaki et al. 2012). Unfortunately, high interaction of the ligand ET-1 with the DMPG membranes prevented a more detailed analysis of the ETB binding properties in this environment. In the case of NDs composed of POPC lipids, the low insertion rate could be a result of a partial disintegration of the bilayer structure composed of purely unsaturated lipids (Lyukamanova et al. 2012).

If lipids seem to have a specific role in the final yield of co-translationally associated receptor, the binding of ET-1 to the ETB/NDs complexes appeared to be relatively independent from the selected lipid environments (Fig. 28). Accordingly, the ligand binding properties of the neurotensin-1 receptor in NDs were found to be unaffected by the specific lipid composition of the bilayer, whereas the presence of the lipid POPG was necessary for the efficient coupling with the protein  $\text{G}\alpha_q$  (Inagaki et al. 2012). In case of rhodopsin/ND complexes, the presence of acidic lipid head groups was necessary for modulate the interaction with arrestin (Tsukamoto et al. 2010). Regarding ETB receptor, possible effects of the lipid composition on signal transduction pathways can therefore currently not be excluded and will be subject to further investigation.

Compared to the L-CF expression in the presence of liposomes, three to four times more

insertion of ETB-sGFP could be obtained using NDs (Fig. 19). In the best condition, around 150 µg/ml of the ETB-sGFP were associated with the NDs, according to the sGFP fluorescence. The improved association could be related to the more stable nature and more homogenous dispersion of the NDs, in comparison with liposomes.

However, the molecular mechanism that leads to the insertion of a CF produced MP into a lipid bilayer is still largely unknown. MPs insertion into membranes lacking a translocon system has been previously reported for a number of proteins (Kalmbach et al. 2007, Liguori et al. 2008, Noireaux et al. 2005), but despite the progress in demonstrating a correct MPs insertion into the membranes, the mechanism has been poorly studied at the molecular level.

Regarding the ETA and ETB receptors, different association levels to the NDs have been observed (see 4.11). Despite similar expression yields of ETA-sGFP and ETB-sGFP upon P-CF and D-CF expression, the formation of fluorescent ETB-sGFP was approximately twice as high as compared with the one observed with ETA-sGFP in the presence of equal concentrations of NDs composed of DMPC lipids (Fig. 19). The two receptors show roughly 59% amino acid identity. The transmembrane domains are highly conserved, whereas a higher degree of variation is observed in the extracellular regions (Lättig et al. 2008). One striking difference between these two receptors is the presence of a mainly hydrophilic region in the N-terminal domain of ETA (from the histidine 66 to the serine 77), compared to a hydrophobic region in ETB (from the proline 87 to the glutamate 98). A further hydrophilic stretch is also present in the first extracellular loop of ETA (from the aspartate 149 to the phenylalanyl 153). These structural differences, which are suspected to play a role in the differential ligand binding properties (Orry and Wallace 2000, Sakamoto et al. 1993), may also have an effect in modulating their differential insertion into NDs.

### **5.7 Functional characterization of the ET receptors in NDs**

Different complementary assays were implemented for the functional characterization of the endothelin receptors reconstituted into NDs.

ELISA based ligand binding assay (see 4.13) revealed a specific interaction of the ETB-sGFP NDs with the biotinylated ligand b-ET-1, as well as with the ligands ET-3 and 4-Ala-ET-1. In negative control, a low unspecific binding to b-ET-1 was detected for the seven transmembrane domains protein proteorhodopsin fused with sGFP and co-translationally inserted into DMPC NDs (Fig. 4.13). ELISA proved to be a fast and reliable technique for the preliminary screening of ligand binding activity of the expressed receptor, but still not sufficient for a detailed characterization.

The fluorescent analogue Cy3-ET-1 was then used in order to quantify the amount of functionally folded receptor (see 4.12).

Ligand binding assays of IMAC purified ETB-sGFP/NDs (DMPC) complexes revealed that around 25% of the receptor was in an active ligand binding conformation (Fig. 21). It was possible to increase the fraction of the active receptor up to 50% upon a second purification step using size exclusion chromatography (Fig. 22).

The percentage of active receptor was similar to the one previously obtained for ETA and ETB expressed in detergent micelles (Junge et al. 2010).

Similar result was obtained for another GPCR CF expressed into NDs, the Neurokinin 1 receptor (Gao et al. 2012). Also in this case, around 25% of ligand competent receptor was recovered. In contrast, for the  $\beta$ 2-adrenergic receptor expressed in ND, very little amounts of active receptor were observed (less than 1%) (Yang et al. 2011).

Determination of the affinity constant  $K_D$  was not possible using the ligand Cy3-ET-1 due to the low fluorescence emission at low nM concentrations and for this reason, and for better determine the percentage of active receptor, radioligand binding assays were performed (see 4.14).

In saturation experiments with the radioactive ligand [ $^{125}$ I]Tyr<sup>13</sup>ET-1, a  $B_{max}$  value of approximately 1200 CPM/ $\mu$ g of protein was obtained for the IMAC purified NDs sample (Fig. 24). Comparing this result with the one obtained using control membranes expressing the ETB receptor (4200 CPM/ $\mu$ g), approximately 28% of active ETB-sGFP receptor can be estimated.

The calculated amount of produced functional receptor (58.6 pmol/mg) is higher if compared with membrane fractions of ETB overexpressed in CHO cells (0.5 pmol/mg), while it is similar to the amount obtained upon overexpression in COS cells (60 pmol/mg) as well as in *P. pastoris* (20-60 pmol/mg) (Elshourbagy et al. 1993, Schiller et al. 2000). Insect cells Sf9 appear to be more productive with 100 pmol/mg (15-20 nmol/L) for the ETB receptor, whereas for other GPCR, such as the  $\beta$ 2-adrenergic or the muscarinic receptor, lower expression levels in the range in between 5 and 30 pmol/mg are obtained (Doi et al. 1997). Using the radioactive assay, a  $K_D$  of 0.45 nM was determined in saturation experiments, whereas a  $K_i$  of 6.1 nM was obtained in homologues competition experiments with the ligand ET-1 (Fig. 24). The obtained  $K_D$  value is close to the one obtained for ETB expressed in CHO cells (0.3 nM) (Takagi et al. 1995), but higher if compared with the one measured using the commercially available ETB membrane preparations (0.06 nM) (Table 6). Different  $K_D$  value, in the range in between 20 pM and 0.7 nM have been previously published for the ETB receptor, depending on the chosen expression system (Buchan et al. 1994, Desmarets et al. 1996, Haendler et al. 1993, Schiller et al. 2000, Takagi et al. 1995). Discrepancy in the measured  $K_D$  and  $K_i$  value for the ligand ET-1 has been

previously observed for membrane preparation of the ETA receptor (Desmartes et al. 1996). The authors proposed that the artifactual shift of the  $K_i$  to a higher value that was observed in the competition experiment is a result of the picomolar affinity of the ligand to the receptor and the slow dissociation rate of the formed complex.

Due to the soluble nature of the NDs, ligand binding analysis can be performed using different techniques that have been initially established for soluble proteins, like for example surface plasmon resonance (SPR), OCTET system and Microscale Thermophoresis (MST). Advantages and drawbacks of these different techniques have been summarized in Table 15.

Regarding SPR, the use of integral MPs reconstituted into NDs as analyte for binding studies have been previously reported (Borch et al. 2008, Glück et al. 2011).

In all the tested assays, a  $K_D$  in the low nM range was obtained for the binding of ET-1 to ETB-sGFP/NDs (DMPC). Compared to the value obtained in radioligand binding experiment (0.45 nM), closer result was obtained by SPR (0.5nM) (Table 12), followed by OCTET system (3nM) (Fig. 26) and MST (4.5 nM) (Fig. 24). Regarding the association and dissociation rate constant, similar value were obtained using the OCTET system and SPR ( $K_{on}$ :  $10^5$ ,  $K_{off}$ :  $10^{-4}$ ).

In MST experiment a  $K_D$  ten times higher was determined, in comparison to the one obtained by SPR or by radioligand binding assays. In this specific assay, the necessity to use the fluorescent analogue Cy3-ET-1 could explain the higher  $K_d$  value obtained. Previous experiments have already reported a reduction of about 5- to 10- fold in the affinity of this fluorescent derivative, in comparison with the radioactive labeled ligand, in the binding of ETB receptor overexpressed in mammalian cells (Ocksche et al. 2000). Nevertheless, further experiments will be necessary to confirm this preliminary result.

Regarding the OCTET system, the lower measured affinity of the b-ET-1 to ETB-sGFP/NDs (DMPC) could be explained by a non sufficient optimization of the conditions, which was not possible to perform due to the unavailability of the instrument. Also in this case, further experiments are necessary to confirm the obtained data.

Buffer optimization was indeed an essential step to perform in order to obtain reproducible and consistent data in SPR experiments (Fig. 25). Particularly beneficial for the reduction of the unspecific binding of the NDs to the dextran-matrix surface of the SA chip was a high salt concentration in the running buffer. Positive results were also obtained by incubation of the samples with BSA (0.2%) or Glycerol (1%). In the case of ETA and ETB, previous studies have already shown the possibility to obtain high affinity binding to the ligand ET-1 in presence of high salt concentration (500 mM NaCl) (Klammet et al. 2007, Junge et al. 2010).

Analyses of ligand binding by SPR was performed in two different configurations (see 4.15), in one case the biotinylated analogues b-ET-1 or b-ET-3 were immobilized on the surface of a SA



chip and the NDs, containing one of the two endothelin receptors, were injected at different concentrations (Fig. 26, 27). In the second case, ETB-Strep cotranslationally inserted into NDs was immobilized on a CM5 chip that was previously pre-coupled with anti-Strep antibodies (Fig. 30, 31). Even though similar results were obtained in both configurations, most of the experiments were performed immobilizing the biotinylated ligands on the chip. In fact, using the second configuration, low response units were obtained due to the very different molecular weight of the two interacting partner (Fig. 31).

Using the first described configuration, ligand binding analysis of the sGFP fusion construct ETA and ETB co-translationally inserted in DMPC NDs gave similar results to the one obtained with the non-fused receptors and comparable to the expected values from literature (Table 12) (Okshe et al. 2000). Furthermore, no significative differences were detected in the ligand binding capability between the IMAC purified sample and the crude sample, directly injected on the chip without any previous purification step (Table. 12).

The necessity to have a biotinylated ligand that can be immobilized on the chip could be a problem in developing this specific assay. For instance, in the case of the endothelin receptors, many ligands were not available as biotinylated conjugates. In order to overcome this limitation a competition assay was developed. ETB-sGFP/NDs or ETA-sGFP/NDs at fix concentrations were incubated with increasing concentrations of unlabeled ligands and the binding affinity, represented as  $IC_{50}$  value in competition with the immobilized b-ET-1, was measured (Fig. 29).

Selective binding of ETA and ETB to a panel of ligands was confirmed (Fig. 29) and the obtained  $IC_{50}$  values closely match with previously published results (Karet et al. 1993, Ishikawa et al. 1994, Nambi et al. 1994). Quite interesting was the result obtained for the ligand IRL-1620. For this peptide enhanced binding affinity was detected toward isolated membranes fractions in comparison to intact cells (Hara et al. 1998). We could observe this effect also with the CF produced ETB-sGFP/NDs (DMPC) complexes, where an  $IC_{50}$  value of 5 pM was obtained.

Assay Format	Principle	Advantages	Disadvantages
Filtration assay	Radioactive	-robust -labeling doesn't affect affinity of the ligand	-radioactive -low-medium throughput
SPR	Refractive index	-real time binding (KD, Kon, Koff) -automation -sensitive -no labeling necessary -medium-high throughput	-receptor or ligand immobilization -unspecific binding to the dextran matrix -Sensitivity depends on the molecular weight of ligand and analyte
MST	Thermophoresis	-no immobilization steps -low sample consumption -low non-specific binding to the capillary -medium throughput	-fix em-ex filters -need proper fluorescent molecule -no Kon or Koff
OCTET	Interferometry	-real time kinetics (KD, Kon, Koff) -no labeling necessary -possibility to collect the sample after the experiment -single use biotips (no need for regeneration) -high throughput	-receptor or ligand immobilization -optimized for soluble protein -pure literature -unspecific binding to the biotips

**Table 15.** Comparison between different techniques used for the determination of the ligand binding affinity.

### 5.8 CF expression of G $\alpha$ subunits

Heterotrimeric G proteins are responsible for the transmission of the signal from the plasma membrane, where the GPCRs are localized, to the interior of the cells. The activated signaling cascade, upon binding of an agonist to the receptor, controls a wide range of cellular processes. Regarding the endothelin receptors, little is known about the selective coupling to the different  $\alpha$  subunits. ETA and ETB seem to couple to different sub-families of  $\alpha$  subunit and the specificity seems related to the cell type in which the receptors are expressed (Table 16).

Of the twenty different sub-types of  $\alpha$  subunit, only four have been successfully expressed in *E. coli*: G $\alpha_s$ , G $\alpha_{i2}$ , G $\alpha_{i3}$  and G $\alpha_o$ . Nevertheless, the over expression of these proteins is very challenging, long growth time of the cells is required as well as multiple purification steps; in most of the cases, only 10% of the protein is active, while the rest accumulates in inclusion bodies from which their solubilization and refolding have not been yet successful (McCusker and Robinson 2008).

Cell line	ETA	ETB
<b>Fibroblast</b> (Shranga-Levine and Sokolovsky 2000)	Gα <sub>q</sub>	Gα <sub>i</sub> Gα <sub>o</sub>
<b>CHO</b> (Takagi et al. 1995) (Aramori and Nakanishi 1995)	Gα <sub>i</sub> Gα <sub>s</sub>	Gα <sub>i</sub>
<b>COS7</b> (Takigawa et al. 1995)	Gα <sub>q</sub> Gα <sub>i</sub> Gα <sub>s</sub>	Gα <sub>q</sub> Gα <sub>i</sub> Gα <sub>s</sub>
<b>HEK293T</b> (Kitamura et al. 1999)	-	Gα <sub>12/13</sub>
<b>Hepatic cells</b> (female rat 20% ETA, 80% ETB) (Jouneaux et al. 1994)	-	Gα <sub>q</sub> Gα <sub>s</sub>
<b>Hepatic cells</b> (male rat 50% ETA, 50% ETB) (Gandhi et al. 1992)	-	Gα <sub>i</sub>

**Table 16.** Cell-dependent coupling of the endothelin receptors to different Gα subunit.

In this work the possibility to express two α subunits, Gα<sub>s</sub> and Gα<sub>q</sub>, by CF expression system have been evaluated (see 4.20).

Even though these proteins are expressed in a soluble form *in vivo*, after expression in P-CF mode the proteins tend to aggregate and precipitate (Fig. 31).

Gα<sub>s</sub> and Gα<sub>q</sub> are post-translationally modified with the addition of the fatty acid palmitate at the N-terminal (Chen and Manning 2001, Linder et al. 1993). This modification, that is required for the correct localization of the G protein to the plasma membrane, could also have a role in the stabilization of the protein (Graziano et al. 1989). Furthermore, the lacking of the βγ subunit could be responsible for the reduced soluble expression observed (McCusker and Robinson 2008). In order to improve the soluble yields, modification of the standard expression protocol, by means of a reduction of the temperature during the reaction, as well as by the addition of chaperone proteins or other components of the G protein signaling, may be tested.

A slightly better soluble expression of Gα<sub>s</sub> was detected in comparison with Gα<sub>q</sub>. IMAC purification of the soluble fractions leads to 0.5-1 mg of protein per ml of RM. Different expression levels of soluble Gα proteins have been reported in literature using a bacterial expression system, for Gα<sub>s</sub>, typically yields in between 0.1 and 1 mg for L of culture are obtained,

$G\alpha_i$  can be expressed up to 40mg/L (Lee et al. 1994). In contrast,  $G\alpha_q$  have not been yet successfully expressed in *E. Coli* (McCusker and Robinson 2008), the production of this subunit in Sf9 cells requires an extensive purification procedure, in order to remove contaminating endogenous  $G\alpha$  subunits, leading to final yields of few  $\mu\text{g/L}$  (Hepler et al. 1993).

For further characterization of the activity, we decide to focus on the soluble fraction of the  $G\alpha_s$  subunit expressed in P-CF mode, as detergents could have a negative effect in functional assays in presence of the ETB/NDs complexes.

$G\alpha$  subunits *in vivo* are normally coupled with GDP and only upon binding at the cell surface to a GPCR that is activated by an agonist, GDP is exchanged with GTP.  $G\alpha$  subunit *in vitro*, incubated in buffer without GDP but only GTP, can incorporate GTP over time even in absence of their signaling partners (Ferguson et al. 1986, Graziano et al. 1989, Higashijima et al. 1987, McEwen et al. 2001). Two complementary assays were therefore performed in order to detect the basal activity of the  $G\alpha_s$  subunit, a fluorescent assay using BODIPY-GTP- $\gamma$ -S and a radioactive assay using GTP- $\gamma$ -S<sup>[35]</sup>. These two analogues of GTP are both characterized by the substitution of oxygen with sulfur atom in the  $\gamma$ -phosphate, for this reason they cannot be hydrolyzed to GDP and released upon binding to the  $G\alpha$  subunit (see 4.21).

In both assays, upon incubation of the protein with the GTP analogues and in absence of GDP, an increase of signal over time was detected (Fig. 32, 33). Nevertheless the two molecules seem to interact differently with  $G\alpha_s$ .

In the case of the radioactive analogue GTP- $\gamma$ -S<sup>[35]</sup>, a faster association was detected ( $t_{1/2\text{sec}}$ :  $198 \pm 18$ , rate constant  $K_{\text{ob}}$ :  $0.20 \pm 0.01 \text{ min}^{-1}$ ), whereas for the fluorescent analogue BODIPY-GTP- $\gamma$ -S a slower association was observed ( $t_{1/2\text{sec}}$ :  $486 \pm 30$  rate constant  $K_{\text{ob}}$ :  $0.08 \pm 0.005 \text{ min}^{-1}$ ). Furthermore, no increase of signal was detected upon pre-incubation of the  $G\alpha_s$  subunit in an excess of GDP in the radioactive assay, whereas, in the same condition, 30% of binding of the fluorescent analogue was still detected (Fig. 32, 33).

The association rate observed using the radioactive analogue GTP- $\gamma$ -S<sup>[35]</sup> is similar to the one previously published for the *E. coli* expression of soluble  $G\alpha_s$  ( $0.16 \pm 0.01 \text{ min}^{-1}$ ) (Graziano et al. 1989). The obtained result that is equivalent to one obtained in mammalian cells (Grazano et al. 1989), confirmed the use of the CF expression system for the production of guanine nucleotides functional binding  $G\alpha_s$  protein.

IMAC purified  $G\alpha_s$  stored at 4°C in presence of 1% glycerol seems to be relatively unstable. A 50% reduction in the incorporation of BODIPY-GTP- $\gamma$ -S was detected every 24h (Fig. 32). Instability of the  $G\alpha$  subunit at 4°C, independently from the employed expression system, has been previously reported (McCusker and Robinson 2008).

To verify the possibility to induce a change in the activity of  $G\alpha_s$  in presence of ETB/NDs

complex and a ligand (agonist or antagonist), further experiments were performed. In these sets of experiments an excess of GDP was added to the incubation buffer in order to reduce the basal activity of the  $G\alpha_s$  subunit.

Also in this case, using the two different analogues of GTP, two different results have been obtained.

In the fluorescent assay, addition of agonist ET-1 with the ETB/NDs complex induced an activation of the G protein (300%) (Fig. 34). In negative controls, in which one of the component was missing (either ET-1 or ETB/NDs), no increase was detected. A further negative control was performed using the truncated version ETB93a co-translationally inserted into NDs. This version of ETB was shown to be able to interact with the ligand ET-1 (Klammt et al. 2007), with affinity similar to the full-length receptor. The ETB93a, in which only the first three transmembrane domains are present and that is lacking most of the cytoplasmatic loops, should not be able to interact with the G protein.

In the fluorescent assay, no increase in signal was detected upon incubation of ETB93a/NDs complexes with  $G\alpha_s$  even in presence of the ligand ET-1 (Fig. 34), confirming a specific activation of the G protein by the full-length receptor.

In the radioactive assay, the addition of ETB/NDs without any agonist was already sufficient for induce an activation of the G protein (Fig. 35). Two different agonists were tested, ET-1 and IRL-1620, but both failed in inducing an increase in activity. In control experiment, using mammalian cell membranes expressing the ETB receptor as well as the endogenous full set of heterotrimeric G proteins, an increase in signal was detected upon incubation with the same agonists. Similar effect in the ETB/ND samples and in the control sample was detected upon incubation with the antagonist IRL-2500. In this case, a reduction of the activity of around 50% was detected (Fig. 35).

The interpretation of the obtained results is particularly difficult due to the lack of published data, especially regarding the analogue BODIPY-GTP- $\gamma$ -S. Analysis of the affinity of the radioactive and fluorescent GTP analogues to  $G\alpha_s$  in Sf9 cells over expressing the  $\beta$ 2-adrenergic receptor, revealed a 5600-fold lower affinity of BODIPY-GTP- $\gamma$ -S in comparison with GTP- $\gamma$ -S<sup>[35]</sup> (Gille et al. 2003). This result is probably related to the presence of the bulkier BODIPY (Gille et al 2003). The reduced affinity could explain the slower binding rate observed in the time-course experiment, as the BODIPY-GTP- $\gamma$ -S has to compete for the binding with the pre-coupled GDP. On the other hand, the increase of signal observed even at saturating concentrations of GDP, could be related to unspecific interaction of the BODIPY-GTP- $\gamma$ -S with the purified  $G\alpha_s$  (Fig. 32). A different behavior of the two analogues has also been reported with regards to the binding to  $G\alpha_t$  (Ramachandran and Cerione 2004). Slower dissociation of the heterotrimer has been

reported upon incubation with BODIPY-GTP- $\gamma$ -S, in comparison with GTP- $\gamma$ -S<sup>[35]</sup>. The authors of the paper speculate that the fluorescent analogue could interact with the  $G\alpha_t$  subunit that is in a conformational state that might represent an intermediate between the GDP-bound state and the fully activated state.

In case of the radioactive analogue GTP- $\gamma$ -S<sup>[35]</sup>, a very similar experiment has been previously published in order to detect the activation of purified  $G\alpha_s$  induced by agonist binding to  $\beta$ 2-adrenergic receptor reconstituted into NDs (Leitz et al. 2006). In this case, a 10 fold increase in signal was detected upon incubation with isoproterenol. In the described experiment, the G protein was provided in the heterotrimeric form, together with the  $\beta$  and  $\gamma$  subunits. These two proteins are known to regulate the basal activity of the  $G\alpha_s$  subunit (Graziano et al. 1989). The absence of them could explain the high activation rate observed upon incubation of  $G\alpha_s$  with the ETB/NDs complex in absence of agonist (Fig. 35).

Further problems in the activation assay could be related to the CF expression of the ETB receptor. Previous studies on the endothelins receptors expressed in Sf9 cells and reconstituted into liposomes, revealed an important role of the palmitoylation in the C-terminal domain of the receptors. Palmitoyl-deficient mutants of ETA and ETB were less effective in activating  $G\alpha_i$  and  $G\alpha_q$ , whereas no difference between were detected in the activation of  $G\alpha_o$ , in comparison with the wild type receptors (Doi et al. 1999). In our case, we cannot exclude that the absence of this post-translational modification could play a role in the interaction with  $G\alpha_s$ .

In order to clarify the interaction between the ETB receptor and  $G\alpha_s$ , further experiments are therefore necessary. The possibility to have a positive control for the receptor, G protein, as well as the full heterotrimer, would be very valuable in order to understand the activation mechanism.

## 5.9 Conclusions and perspectives

The analysis of the results obtained in this dissertation document a new process to produce the two endothelin receptors, ETA and ETB, in a ligand-binding competent form. In particular, the combination of the CF expression system with the NDs technology appear to be a promising option for the characterization of binding properties of GPCRs.

The co-translational association of MPs with pre-formed empty NDs overcomes the need to use a solubilizing detergent, which could have a negative effect on the stability and functionality of the MPs. Furthermore, NDs, in comparison with liposomes, appear to be a more homogenous and stable lipid environment.

GPCR-sGFP fusion constructs have been shown to be a useful tool, not only for the initial screening of expression conditions, but also for developing of functional assays.

Among the different methods tested for ligand binding analysis, SPR proved to be one of the best options. The CF produced GPCR/NDs complexes can be directly injected on a biochip without the need of any previous purification step, considerably speeding up the research process. The CF expression of the two endothelins receptors and the ligand binding study can be performed within two to three days, opening new possibilities for GPCR high throughput screening approaches in a lipid environment.

Furthermore, NDs allows characterizing the specific signaling pathway activated upon the binding of a ligand to a GPCR. In contrast to liposomes, both side of the lipid membrane are directly accessible, facilitating the development of activation assays upon co-incubation with signaling partners and ligands. Experiments performed using the coupled  $G\alpha$  subunit proved to be feasible, however further experiments will be necessary to better understand the activation mechanism.

In regards to the expression of the  $G\alpha$  subunits, CF expression system proved, once more, to be an efficient tool for the production of proteins that are notoriously difficult to be expressed in a conventional *in vivo* system. Furthermore, the measured guanine nucleotide binding activity of the  $G\alpha$ s subunit has proved to be equal to the mammalian expressed one.

In conclusion, the application of the CF technology for studying other GPCRs co-translationally expressed into a lipid environment seems to be, in light of the obtained results, a reasonable approach for the future characterization of these receptors.

## 6. References

- Abassi ZA, Klein H, Golomb E, Keiser HR. 1993. Urinary endothelin: a possible biological marker of renal damage. *Am. J. Hypertens.* 6(12):1046–54
- Adachi M, Furuichi Y, Miyamoto C. 1994. Identification of specific regions of the human endothelin-b receptor required for high affinity binding with endothelin-3. *Biochim. Biophys. Acta.* 1223(2):202–8
- Ahn J-H, Hwang M-Y, Lee K-H, Choi C-Y, Kim D-M. 2007. Use of signal sequences as an in situ removable sequence element to stimulate protein synthesis in cell-free extracts. *Nucleic Acids Res.* 35(4):e21
- Akiyama N, Hiraoka O, Fujii Y, Terashima H, Satoh M, et al. 1992. Biotin derivatives of endothelin: utilization for affinity purification of endothelin receptor. *Protein Expr. Purif.* 3(5):427–33
- Alami M, Dalal K, Lelj-Garolla B, Sligar SG, Duong F. 2007. Nanodiscs unravel the interaction between the secyeg channel and its cytosolic partner seca. *EMBO J.* 26(8):1995–2004
- André N, Cherouati N, Prual C, Steffan T, Zeder-Lutz G, et al. 2006. Enhancing functional production of g protein-coupled receptors in pichia pastoris to levels required for structural studies via a single expression screen. *Protein Sci.* 15(5):1115–26
- Angers S, Salahpour A, Joly E, Hilairat S, Chelsky D, et al. 2000. Detection of beta 2-adrenergic receptor dimerization in living cells using bioluminescence resonance energy transfer (bret). *Proc. Natl. Acad. Sci. U.S.A.* 97(7):3684–89
- Arai H, Hori S, Aramori I, Ohkubo H, Nakanishi S. 1990. Cloning and expression of a cDNA encoding an endothelin receptor. *Nature.* 348(6303):730–32
- Aramori I, Nakanishi S. 1992. Coupling of two endothelin receptor subtypes to differing signal transduction in transfected chinese hamster ovary cells. *J. Biol. Chem.* 267(18):12468–74
- Arslan Yildiz A, Kang C, Sinner E-K. 2013. Biomimetic membrane platform containing hERG potassium channel and its application to drug screening. *Analyst.* 138(7):2007–12
- Auricchio A, Casari G, Staiano A, Ballabio A. 1996. Endothelin-b receptor mutations in patients with isolated hirschsprung disease from a non-inbred population. *Hum. Mol. Genet.* 5(3):351–54
- Banères J-L, Popot J-L, Mouillac B. 2011. New advances in production and functional folding of g-protein-coupled receptors. *Trends Biotechnol.* 29(7):314–22
- Barlowe C. 2003. Molecular recognition of cargo by the copII complex: a most accommodating coat. *Cell.* 114(4):395–97
- Basu D, Castellano JM, Thomas N, Mishra RK. 2013. Cell-free protein synthesis and purification of human dopamine d2 receptor long isoform. *Biotechnol. Prog.* 29(3):601–8
- Battistini B, D'Orléans-Juste P, Sirois P. 1993. Endothelins: circulating plasma levels and presence in other biologic fluids. *Lab. Invest.* 68(6):600–628
- Bayburt TH, Sligar SG. 2002. Single-molecule height measurements on microsomal cytochrome p450 in nanometer-scale phospholipid bilayer disks. *Proc. Natl. Acad. Sci. U.S.A.* 99(10):6725–30
- Bayburt TH, Sligar SG. 2010. Membrane protein assembly into nanodiscs. *FEBS Lett.* 584(9):1721–27



- Bayburt TH, Vishnivetskiy SA, McLean MA, Morizumi T, Huang C-C, et al. 2011. Monomeric rhodopsin is sufficient for normal rhodopsin kinase (grk1) phosphorylation and arrestin-1 binding. *J. Biol. Chem.* 286(2):1420–28
- Berrier C, Guilvout I, Bayan N, Park K-H, Mesneau A, et al. 2011. Coupled cell-free synthesis and lipid vesicle insertion of a functional oligomeric channel mscl mscl does not need the insertase yidc for insertion in vitro. *Biochim. Biophys. Acta.* 1808(1):41–46
- Bjarnadóttir TK, Fredriksson R, Höglund PJ, Gloriam DE, Lagerström MC, Schiöth HB. 2004. The human and mouse repertoire of the adhesion family of g-protein-coupled receptors. *Genomics.* 84(1):23–33
- Blesneac I, Ravaud S, Juillan-Binard C, Barret L-A, Zoonens M, et al. 2012. Production of ucp1 a membrane protein from the inner mitochondrial membrane using the cell free expression system in the presence of a fluorinated surfactant. *Biochim. Biophys. Acta.* 1818(3):798–805
- Borch J, Roepstorff P, Møller-Jensen J. 2011. Nanodisc-based co-immunoprecipitation for mass spectrometric identification of membrane-interacting proteins. *Mol. Cell. Proteomics.* 10(7):O110.006775
- Bouallegue A, Daou GB, Srivastava AK. 2007. Endothelin-1-induced signaling pathways in vascular smooth muscle cells. *Curr. Vasc. Pharmacol.* 5(1):45–52
- Bridges TM, Lindsley CW. 2008. G-protein-coupled receptors: from classical modes of modulation to allosteric mechanisms. *ACS Chem. Biol.* 3(9):530–41
- Buchan KW, Alldus C, Christodoulou C, Clark KL, Dykes CW, et al. 1994. Characterization of three non-peptide endothelin receptor ligands using human cloned eta and etb receptors. *Br. J. Pharmacol.* 112(4):1251–57
- Burger K, Gimpl G, Fahrenholz F. 2000. Regulation of receptor function by cholesterol. *Cell. Mol. Life Sci.* 57(11):1577–92
- Butcher AJ, Kong KC, Prihandoko R, Tobin AB. 2012. Physiological role of g-protein coupled receptor phosphorylation. *Handb. Exp. Pharmacol.*, pp. 79–94
- Cansell M, Gouygou JP, Jozefonvicz J, Letourneur D. 1997. Lipid composition of cultured endothelial cells in relation to their growth. *Lipids.* 32(1):39–44
- Cappuccio JA, Blanchette CD, Sulchek TA, Arroyo ES, Kralj JM, et al. 2008. Cell-free co-expression of functional membrane proteins and apolipoprotein, forming soluble nanolipoprotein particles. *Mol. Cell. Proteomics.* 7(11):2246–53
- Chandrashekar J, Mueller KL, Hoon MA, Adler E, Feng L, et al. 2000. T2rs function as bitter taste receptors. *Cell.* 100(6):703–11
- Chelikani P, Reeves PJ, Rajbhandary UL, Khorana HG. 2006. The synthesis and high-level expression of a beta2-adrenergic receptor gene in a tetracycline-inducible stable mammalian cell line. *Protein Sci.* 15(6):1433–40
- Chen CA, Manning DR. 2001. Regulation of g proteins by covalent modification. *Oncogene.* 20(13):1643–52
- Chini B, Parenti M. 2009. G-protein-coupled receptors, cholesterol and palmitoylation: facts about fats. *J. Mol. Endocrinol.* 42(5):371–79

- Corin K, Baaske P, Ravel DB, Song J, Brown E, et al. 2011. Designer lipid-like peptides: a class of detergents for studying functional olfactory receptors using commercial cell-free systems. *PLoS One*. 6(11):e25067
- Craig D, Howell MT, Gibbs CL, Hunt T, Jackson RJ. 1992. Plasmid cdna-directed protein synthesis in a coupled eukaryotic in vitro transcription-translation system. *Nucleic Acids Res*. 20(19):4987–95
- D'Alto M, Romeo E, Argiento P, Correr A, Sarubbi B, et al. 2012. Ambrisentan for pulmonary arterial hypertension: long term effects on clinical status, exercise capacity and haemodynamics. *Int. J. Cardiol*. 156(2):244–45
- Dann CE, Hsieh JC, Rattner A, Sharma D, Nathans J, Leahy DJ. 2001. Insights into wnt binding and signalling from the structures of two frizzled cysteine-rich domains. *Nature*. 412(6842):86–90
- Davenport AP, Maguire JJ. 2002. Of mice and men: advances in endothelin research and first antagonist gains fda approval. *Trends Pharmacol. Sci*. 23(4):155–57
- Davenport AP, Maguire JJ. 2006. Endothelin. *Handb. Exp. Pharmacol.*, pp. 295–329
- Deniaud A, Liguori L, Blesneac I, Lenormand JL, Pebay-Peyroula E. 2010. Crystallization of the membrane protein hvdac1 produced in cell-free system. *Biochim. Biophys. Acta*. 1798(8):1540–46
- Denisov IG, Grinkova Y V, Lazarides AA, Sligar SG. 2004. Directed self-assembly of monodisperse phospholipid bilayer nanodiscs with controlled size. *J. Am. Chem. Soc*. 126(11):3477–87
- Desmarests J, Gresser O, Guedin D, Frelin C. 1996. Interaction of endothelin-1 with cloned bovine eta receptors: biochemical parameters and functional consequences. *Biochemistry*. 35(47):14868–75
- DeWire SM, Ahn S, Lefkowitz RJ, Shenoy SK. 2007. Beta-arrestins and cell signaling. *Annu. Rev. Physiol*. 69:483–510
- Digby GJ, Lober RM, Sethi PR, Lambert NA. 2006. Some g protein heterotrimers physically dissociate in living cells. *Proc. Natl. Acad. Sci. U.S.A*. 103(47):17789–94
- Dohlman HG, Caron MG, DeBlasi A, Frielle T, Lefkowitz RJ. 1990. Role of extracellular disulfide-bonded cysteines in the ligand binding function of the beta 2-adrenergic receptor. *Biochemistry*. 29(9):2335–42
- Doi T, Hiroaki Y, Arimoto I, Fujiyoshi Y, Okamoto T, et al. 1997. Characterization of human endothelin b receptor and mutant receptors expressed in insect cells. *Eur. J. Biochem*. 248(1):139–48
- Doi T, Sugimoto H, Arimoto I, Hiroaki Y, Fujiyoshi Y. 1999. Interactions of endothelin receptor subtypes a and b with gi, go, and gq in reconstituted phospholipid vesicles. *Biochemistry*. 38(10):3090–99
- Elbaz Y, Steiner-Mordoch S, Danieli T, Schuldiner S. 2004. In vitro synthesis of fully functional emre, a multidrug transporter, and study of its oligomeric state. *Proc. Natl. Acad. Sci. U.S.A*. 101(6):1519–24
- Ellgaard L, Helenius A. 2003. Quality control in the endoplasmic reticulum. *Nat. Rev. Mol. Cell Biol*. 4(3):181–91
- Elshourbagy NA, Korman DR, Wu HL, Sylvester DR, Lee JA, et al. 1993. Molecular characterization and regulation of the human endothelin receptors. *J. Biol. Chem*. 268(6):3873–79
- Endo Y, Sawasaki T. 2005. Advances in genome-wide protein expression using the wheat germ cell-free system. *Methods Mol. Biol*. 310:145–67
- Endoh T, Kanai T, Imanaka T. 2008. Effective approaches for the production of heterologous proteins using the thermococcus kodakaraensis-based translation system. *J. Biotechnol*. 133(2):177–82

- Esch FS, Keim PS, Beattie EC, Blacher RW, Culwell AR, et al. 1990. Cleavage of amyloid beta peptide during constitutive processing of its precursor. *Science*. 248(4959):1122–24
- Evans NJ, Walker JW. 2008. Endothelin receptor dimers evaluated by fret, ligand binding, and calcium mobilization. *Biophys. J.* 95(1):483–92
- Ezure T, Suzuki T, Shikata M, Ito M, Ando E, et al. 2007. Expression of proteins containing disulfide bonds in an insect cell-free system and confirmation of their arrangements by maldi-tof ms. *Proteomics*. 7(24):4424–34
- Ezure T, Suzuki T, Shikata M, Ito M, Ando E. 2010. A cell-free protein synthesis system from insect cells. *Methods Mol. Biol.* 607:31–42
- Ferguson KM, Higashijima T, Smigel MD, Gilman AG. 1986. The influence of bound gdp on the kinetics of guanine nucleotide binding to g proteins. *J. Biol. Chem.* 261(16):7393–99
- Fraser MJ. 1992. The baculovirus-infected insect cell as a eukaryotic gene expression system. *Curr. Top. Microbiol. Immunol.* 158:131–72
- Fraser NJ. 2006. Expression and functional purification of a glycosylation deficient version of the human adenosine 2a receptor for structural studies. *Protein Expr. Purif.* 49(1):129–37
- Fredriksson R, Lagerström MC, Lundin L-G, Schiöth HB. 2003. The g-protein-coupled receptors in the human genome form five main families. phylogenetic analysis, paralogon groups, and fingerprints. *Mol. Pharmacol.* 63(6):1256–72
- Fritze O, Filipek S, Kuksa V, Palczewski K, Hofmann KP, Ernst OP. 2003. Role of the conserved npxxy(x)<sub>5</sub>6f motif in the rhodopsin ground state and during activation. *Proc. Natl. Acad. Sci. U.S.A.* 100(5):2290–95
- Galantino M, de Castiglione R, Cristiani C, Vaghi F, Liu W, et al. D-amino acid scan of endothelin: importance of amino acids adjacent to cysteinyl residues in isomeric selectivity. *Pept. Res.* 8(3):154–59
- Galés C, Rebois RV, Hogue M, Trieu P, Breit A, et al. 2005. Real-time monitoring of receptor and g-protein interactions in living cells. *Nat. Methods.* 2(3):177–84
- Galés C, Van Durm JJJ, Schaak S, Pontier S, Percherancier Y, et al. 2006. Probing the activation-promoted structural rearrangements in preassembled receptor-g protein complexes. *Nat. Struct. Mol. Biol.* 13(9):778–86
- Gallie DR. 2002. The 5'-leader of tobacco mosaic virus promotes translation through enhanced recruitment of eif4f. *Nucleic Acids Res.* 30(15):3401–11
- Gandhi CR, Behal RH, Harvey SA, Nouchi TA, Olson MS. 1992. Hepatic effects of endothelin. receptor characterization and endothelin-induced signal transduction in hepatocytes. *Biochem. J.* 287 ( Pt 3:897–904
- Gao T, Petrlova J, He W, Huser T, Kudlick W, et al. 2012. Characterization of de novo synthesized gpcrs supported in nanolipoprotein discs. *PLoS One.* 7(9):e44911
- Genji T, Nozawa A, Tozawa Y. 2010. Efficient production and purification of functional bacteriorhodopsin with a wheat-germ cell-free system and a combination of fos-choline and chaps detergents. *Biochem. Biophys. Res. Commun.* 400(4):638–42
- Gille A, Seifert R. 2003. Low-affinity interactions of bodipy-fl-gtppgammas and bodipy-fl-gppnhp with g(i)- and g(s)-proteins. *Naunyn. Schmiedeberg's. Arch. Pharmacol.* 368(3):210–15

- Gimpl G, Burger K, Fahrenholz F. 1997. Cholesterol as modulator of receptor function. *Biochemistry*. 36(36):10959–74
- Goerke AR, Swartz JR. 2008. Development of cell-free protein synthesis platforms for disulfide bonded proteins. *Biotechnol. Bioeng.* 99(2):351–67
- Golfman LS, Hata T, Beamish RE, Dhalla NS. 1993. Role of endothelin in heart function in health and disease. *Can. J. Cardiol.* 9(7):635–53
- Gouldson PR, Higgs C, Smith RE, Dean MK, Gkoutos G V, Reynolds CA. 2000. Dimerization and domain swapping in g-protein-coupled receptors: a computational study. *Neuropsychopharmacology*. 23(4 Suppl):S60–77
- Gourdon P, Alfredsson A, Pedersen A, Malmerberg E, Nyblom M, et al. 2008. Optimized in vitro and in vivo expression of proteorhodopsin: a seven-transmembrane proton pump. *Protein Expr. Purif.* 58(1):103–13
- Grace CRR, Perrin MH, DiGruccio MR, Miller CL, Rivier JE, et al. 2004. Nmr structure and peptide hormone binding site of the first extracellular domain of a type b1 g protein-coupled receptor. *Proc. Natl. Acad. Sci. U.S.A.* 101(35):12836–41
- Graf R, Mattera R, Codina J, Evans T, Ho YK, et al. 1992. Studies on the interaction of alpha subunits of gtp-binding proteins with beta gamma dimers. *Eur. J. Biochem.* 210(2):609–19
- Grant K, Loizidou M, Taylor I. 2003. Endothelin-1: a multifunctional molecule in cancer. *Br. J. Cancer.* 88(2):163–66
- Grantcharova E, Furkert J, Reusch HP, Krell H-W, Papsdorf G, et al. 2002. The extracellular n terminus of the endothelin b (etb) receptor is cleaved by a metalloprotease in an agonist-dependent process. *J. Biol. Chem.* 277(46):43933–41
- Grantcharova E, Reusch HP, Grossmann S, Eichhorst J, Krell H-W, et al. 2006. N-terminal proteolysis of the endothelin b receptor abolishes its ability to induce egf receptor transactivation and contractile protein expression in vascular smooth muscle cells. *Arterioscler. Thromb. Vasc. Biol.* 26(6):1288–96
- Graziano M, Freissmuth M, Gilman A. 1989. Expression of gs alpha in escherichia coli. purification and properties of two forms of the protein. *J. Biol. Chem.* 264(1):409–18
- Griffith TM, Lewis MJ, Newby AC, Henderson AH. 1988. Endothelium-derived relaxing factor. *J. Am. Coll. Cardiol.* 12(3):797–806
- Grudnik P, Bange G, Sinning I. 2009. Protein targeting by the signal recognition particle. *Biol. Chem.* 390(8):775–82
- Guilvout I, Chami M, Berrier C, Ghazi A, Engel A, et al. 2008. In vitro multimerization and membrane insertion of bacterial outer membrane secretin puld. *J. Mol. Biol.* 382(1):13–23
- Haberstock S, Roos C, Hoevels Y, Dötsch V, Schnapp G, et al. 2012. A systematic approach to increase the efficiency of membrane protein production in cell-free expression systems. *Protein Expr. Purif.* 82(2):308–16
- Haendler B, Hechler U, Becker A, Schleuning WD. 1993. Extracellular cysteine residues 174 and 255 are essential for active expression of human endothelin receptor etb in escherichia coli. *J. Cardiovasc. Pharmacol.* 22 Suppl 8:S4–6

- Hagiwara H, Kozuka M, Sakaguchi H, Eguchi S, Ito T, Hirose S. 1991. Separation and purification of 34- and 52-kda species of bovine lung endothelin receptors and identification of the 34-kda species as a degradation product. *J. Cardiovasc. Pharmacol.* 17 Suppl 7:S117–8
- Hara M, Tozawa F, Itazaki K, Mihara S, Fujimoto M. 1998. Endothelin et(b) receptors show different binding profiles in intact cells and cell membrane preparations. *Eur. J. Pharmacol.* 345(3):339–42
- Harada N, Himeno A, Shigematsu K, Sumikawa K, Niwa M. 2002. Endothelin-1 binding to endothelin receptors in the rat anterior pituitary gland: possible formation of an eta-etb receptor heterodimer. *Cell. Mol. Neurobiol.* 22(2):207–26
- Harrison C, Traynor JR. 2003. The [35s]gtpgammas binding assay: approaches and applications in pharmacology. *Life Sci.* 74(4):489–508
- Hashido K, Gamou T, Adachi M, Tabuchi H, Watanabe T, et al. 1992. Truncation of n-terminal extracellular or c-terminal intracellular domains of human eta receptor abrogated the binding activity to et-1. *Biochem. Biophys. Res. Commun.* 187(3):1241–48
- Hassaine G, Wagner R, Kempf J, Cherouati N, Hassaine N, et al. 2006. Semliki forest virus vectors for overexpression of 101 g protein-coupled receptors in mammalian host cells. *Protein Expr. Purif.* 45(2):343–51
- Higashijima T, Ferguson KM, Sternweis PC, Smigel MD, Gilman AG. 1987. Effects of mg2+ and the beta gamma-subunit complex on the interactions of guanine nucleotides with g proteins. *J. Biol. Chem.* 262(2):762–66
- Horstmeyer A, Cramer H, Sauer T, Müller-Esterl W, Schroeder C. 1996. Palmitoylation of endothelin receptor a. differential modulation of signal transduction activity by post-translational modification. *J. Biol. Chem.* 271(34):20811–19
- Howard AD, McAllister G, Feighner SD, Liu Q, Nargund RP, et al. 2001. Orphan g-protein-coupled receptors and natural ligand discovery. *Trends Pharmacol. Sci.* 22(3):132–40
- Hurowitz EH, Melnyk JM, Chen YJ, Kouros-Mehr H, Simon MI, Shizuya H. 2000. Genomic characterization of the human heterotrimeric g protein alpha, beta, and gamma subunit genes. *DNA Res.* 7(2):111–20
- Inagaki S, Ghirlando R, Grisshammer R. 2012a. Biophysical characterization of membrane proteins in nanodiscs. *Methods*
- Inagaki S, Ghirlando R, White JF, Gvozdenovic-Jeremic J, Northup JK, Grisshammer R. 2012. Modulation of the interaction between neurotensin receptor nts1 and gq protein by lipid. *J. Mol. Biol.* 417(1-2):95–111
- Inoue A, Yanagisawa M, Kimura S, Kasuya Y, Miyauchi T, et al. 1989. The human endothelin family: three structurally and pharmacologically distinct isopeptides predicted by three separate genes. *Proc. Natl. Acad. Sci. U.S.A.* 86(8):2863–67
- Inoue H, Nojima H, Okayama H. 1990. High efficiency transformation of escherichia coli with plasmids. *Gene.* 96(1):23–28
- Ishihara G, Goto M, Saeki M, Ito K, Hori T, et al. 2005. Expression of g protein coupled receptors in a cell-free translational system using detergents and thioredoxin-fusion vectors. *Protein Expr. Purif.* 41(1):27–37

- Ishikawa K, Ihara M, Noguchi K, Mase T, Mino N, et al. 1994. Biochemical and pharmacological profile of a potent and selective endothelin b-receptor antagonist, bq-788. *Proc. Natl. Acad. Sci. U.S.A.* 91(11):4892–96
- Janaki N, Krishna VM, Ramaiah K V. 1995. Phosphorylation of wheat germ initiation factor 2 (eif-2) by n-ethylmaleimide-treated wheat germ lysates and by purified casein kinase ii does not affect the guanine nucleotide exchange on eif-2. *Arch. Biochem. Biophys.* 324(1):1–8
- Janda CY, Li J, Oubridge C, Hernández H, Robinson C V, Nagai K. 2010. Recognition of a signal peptide by the signal recognition particle. *Nature.* 465(7297):507–10
- Janes RW, Peapus DH, Wallace BA. 1994. The crystal structure of human endothelin. *Nat. Struct. Biol.* 1(5):311–19
- Jensen N, Hasselblatt M, Sirén AL, Schilling L, Schmidt M, Ehrenreich H. 1998. Et(a) and et(b) specific ligands synergistically antagonize endothelin-1 binding to an atypical endothelin receptor in primary rat astrocytes. *J. Neurochem.* 70(2):473–82
- Jerabek-Willemsen M, Wienken CJ, Braun D, Baaske P, Duhr S. 2011. Molecular interaction studies using microscale thermophoresis. *Assay Drug Dev. Technol.* 9(4):342–53
- Ji TH, Grossmann M, Ji I. 1998. G protein-coupled receptors. i. diversity of receptor-ligand interactions. *J. Biol. Chem.* 273(28):17299–302
- Jordan BA, Devi LA. 1999. G-protein-coupled receptor heterodimerization modulates receptor function. *Nature.* 399(6737):697–700
- Jordan BA, Trapaidze N, Gomes I, Nivarthi R, Devi LA. 2001. Oligomerization of opioid receptors with beta 2-adrenergic receptors: a role in trafficking and mitogen-activated protein kinase activation. *Proc. Natl. Acad. Sci. U.S.A.* 98(1):343–48
- Jouneaux C, Mallat A, Serradeil-Le Gal C, Goldsmith P, Hanoune J, Lotersztajn S. 1994. Coupling of endothelin b receptors to the calcium pump and phospholipase c via gs and gq in rat liver. *J. Biol. Chem.* 269(3):1845–51
- Junge F, Luh LM, Proverbio D, Schäfer B, Abele R, et al. 2010. Modulation of g-protein coupled receptor sample quality by modified cell-free expression protocols: a case study of the human endothelin a receptor. *J. Struct. Biol.* 172(1):94–106
- Kai L, Dötsch V, Kaldenhoff R, Bernhard F. 2013. Artificial environments for the co-translational stabilization of cell-free expressed proteins. *PLoS One.* 8(2):e56637
- Kaiser L, Graveland-Bikker J, Steuerwald D, Vanberghem M, Herlihy K, Zhang S. 2008. Efficient cell-free production of olfactory receptors: detergent optimization, structure, and ligand binding analyses. *Proc. Natl. Acad. Sci. U.S.A.* 105(41):15726–31
- Kalmbach R, Chizhov I, Schumacher MC, Friedrich T, Bamberg E, Engelhard M. 2007. Functional cell-free synthesis of a seven helix membrane protein: in situ insertion of bacteriorhodopsin into liposomes. *J. Mol. Biol.* 371(3):639–48
- Karet FE, Kuc RE, Davenport AP. 1993. Novel ligands bq123 and bq3020 characterize endothelin receptor subtypes eta and etb in human kidney. *Kidney Int.* 44(1):36–42
- Katzen F, Chang G, Kudlicki W. 2005. The past, present and future of cell-free protein synthesis. *Trends Biotechnol.* 23(3):150–56

- Katzen F, Fletcher JE, Yang J-P, Kang D, Peterson TC, et al. 2008. Insertion of membrane proteins into discoidal membranes using a cell-free protein expression approach. *J. Proteome Res.* 7(8):3535–42
- Katzen F, Kudlicki W. 2006. Efficient generation of insect-based cell-free translation extracts active in glycosylation and signal sequence processing. *J. Biotechnol.* 125(2):194–97
- Katzen F, Peterson TC, Kudlicki W. 2009. Membrane protein expression: no cells required. *Trends Biotechnol.* 27(8):455–60
- Kedzierski RM, Yanagisawa M. 2001. Endothelin system: the double-edged sword in health and disease. *Annu. Rev. Pharmacol. Toxicol.* 41:851–76
- Keenan RJ, Freymann DM, Stroud RM, Walter P. 2001. The signal recognition particle. *Annu. Rev. Biochem.* 70:755–75
- Kigawa T, Yabuki T, Matsuda N, Matsuda T, Nakajima R, et al. 2004. Preparation of escherichia coli cell extract for highly productive cell-free protein expression. *J. Struct. Funct. Genomics.* 5(1-2):63–68
- Kirkby NS, Hadoke PWF, Bagnall AJ, Webb DJ. 2008. The endothelin system as a therapeutic target in cardiovascular disease: great expectations or bleak house? *Br. J. Pharmacol.* 153(6):1105–19
- Klabunde T, Hessler G. 2002. Drug design strategies for targeting g-protein-coupled receptors. *Chembiochem.* 3(10):928–44
- Klammt C, Löhr F, Schäfer B, Haase W, Dötsch V, et al. 2004. High level cell-free expression and specific labeling of integral membrane proteins. *Eur. J. Biochem.* 271(3):568–80
- Klammt C, Perrin MH, Maslennikov I, Renault L, Krupa M, et al. 2011. Polymer-based cell-free expression of ligand-binding family b g-protein coupled receptors without detergents. *Protein Sci.* 20(6):1030–41
- Klammt C, Schwarz D, Fendler K, Haase W, Dötsch V, Bernhard F. 2005. Evaluation of detergents for the soluble expression of alpha-helical and beta-barrel-type integral membrane proteins by a preparative scale individual cell-free expression system. *FEBS J.* 272(23):6024–38
- Klammt C, Schwarz D, Löhr F, Schneider B, Dötsch V, Bernhard F. 2006. Cell-free expression as an emerging technique for the large scale production of integral membrane protein. *FEBS J.* 273(18):4141–53
- Klammt C, Srivastava A, Eifler N, Junge F, Beyermann M, et al. 2007. Functional analysis of cell-free-produced human endothelin b receptor reveals transmembrane segment 1 as an essential area for et-1 binding and homodimer formation. *FEBS J.* 274(13):3257–69
- Kleymann G, Boege F, Hahn M, Hampe W, Vasudevan S, Reiländer H. 1993. Human beta 2-adrenergic receptor produced in stably transformed insect cells is functionally coupled via endogenous gtp-binding protein to adenylyl cyclase. *Eur. J. Biochem.* 213(2):797–804
- Köchl R, Alken M, Rutz C, Krause G, Oksche A, et al. 2002. The signal peptide of the g protein-coupled human endothelin b receptor is necessary for translocation of the n-terminal tail across the endoplasmic reticulum membrane. *J. Biol. Chem.* 277(18):16131–38
- Kohan DE. 2009. Biology of endothelin receptors in the collecting duct. *Kidney Int.* 76(5):481–86
- Kohout TA. 2003. Regulation of g protein-coupled receptor kinases and arrestins during receptor desensitization. *Mol. Pharmacol.* 63(1):9–18
- Kovtun O, Mureev S, Jung W, Kubala MH, Johnston W, Alexandrov K. 2011. Leishmania cell-free protein expression system. *Methods.* 55(1):58–64

- Kralicek A V, Radjainia M, Mohamad Ali NAB, Carraher C, Newcomb RD, Mitra AK. 2011. A pcr-directed cell-free approach to optimize protein expression using diverse fusion tags. *Protein Expr. Purif.* 80(1):117–24
- Krueger-Koplin RD, Sorgen PL, Krueger-Koplin ST, Rivera-Torres IO, Cahill SM, et al. 2004. An evaluation of detergents for nmr structural studies of membrane proteins. *J. Biomol. NMR.* 28(1):43–57
- Kudla G, Murray AW, Tollervey D, Plotkin JB. 2009. Coding-sequence determinants of gene expression in escherichia coli. *Science.* 324(5924):255–58
- Kunishima N, Shimada Y, Tsuji Y, Sato T, Yamamoto M, et al. 2000. Structural basis of glutamate recognition by a dimeric metabotropic glutamate receptor. *Nature.* 407(6807):971–77
- Kusserow H, Unger T. 2004. Vasoactive peptides, their receptors and drug development. *Basic Clin. Pharmacol. Toxicol.* 94(1):5–12
- Laemmli UK, Beguin F, Gujer-Kellenberger G. 1970. A factor preventing the major head protein of bacteriophage t4 from random aggregation. *J. Mol. Biol.* 47(1):69–85
- Lättig J, Oksche A, Beyermann M, Rosenthal W, Krause G. 2009. Structural determinants for selective recognition of peptide ligands for endothelin receptor subtypes eta and etb. *J. Pept. Sci.* 15(7):479–91
- Laursen BS, Sørensen HP, Mortensen KK, Sperling-Petersen HU. 2005. Initiation of protein synthesis in bacteria. *Microbiol. Mol. Biol. Rev.* 69(1):101–23
- Le Maire M, Champeil P, Moller J V. 2000. Interaction of membrane proteins and lipids with solubilizing detergents. *Biochim. Biophys. Acta.* 1508(1-2):86–111
- Lee E, Linder ME, Gilman AG. 1994. Expression of g-protein alpha subunits in escherichia coli. *Methods Enzymol.* 237:146–64
- Lee W-TN, Kirkham N, Johnson MK, Lordan JL, Fisher AJ, Peacock AJ. 2011. Sitaxentan-related acute liver failure in a patient with pulmonary arterial hypertension. *Eur. Respir. J.* 37(2):472–74
- Leitz AJ, Bayburt TH, Barnakov AN, Springer BA, Sligar SG. 2006. Functional reconstitution of beta2-adrenergic receptors utilizing self-assembling nanodisc technology. *Biotechniques.* 40(5):601–2, 604, 606, passim
- Lerman A, Edwards BS, Hallett JW, Heublein DM, Sandberg SM, Burnett JC. 1991. Circulating and tissue endothelin immunoreactivity in advanced atherosclerosis. *N. Engl. J. Med.* 325(14):997–1001
- Lévy D, Gulik A, Bluzat A, Rigaud JL. 1992. Reconstitution of the sarcoplasmic reticulum ca(2+)-atpase: mechanisms of membrane protein insertion into liposomes during reconstitution procedures involving the use of detergents. *Biochim. Biophys. Acta.* 1107(2):283–98
- Liguori L, Marques B, Lenormand J-L. 2008. A bacterial cell-free expression system to produce membrane proteins and proteoliposomes: from cdna to functional assay. *Curr. Protoc. protein Sci. Editor. board John E Coligan al.* Chapter 5(November):Unit 5.22
- Linder ME, Middleton P, Hepler JR, Taussig R, Gilman AG, Mumby SM. 1993. Lipid modifications of g proteins: alpha subunits are palmitoylated. *Proc. Natl. Acad. Sci.* 90(8):3675–79
- Lyukmanova EN, Shenkarev ZO, Khabibullina NF, Kopeina GS, Shulepko MA, et al. 2012a. Lipid-protein nanodiscs for cell-free production of integral membrane proteins in a soluble and folded state: comparison with detergent micelles, bicelles and liposomes. *Biochim. Biophys. Acta.* 1818(3):349–58



- Lyukmanova EN, Shenkarev ZO, Khabibullina NF, Kulbatskiy DS, Shulepko MA, et al. 2012b. N-terminal fusion tags for effective production of g-protein-coupled receptors in bacterial cell-free systems. *Acta Naturae*. 4(4):58–64
- Ma Y, Münch D, Schneider T, Sahl H-G, Bouhss A, et al. 2011. Preparative scale cell-free production and quality optimization of mray homologues in different expression modes. *J. Biol. Chem*. 286(45):38844–53
- Marheineke K, Grünewald S, Christie W, Reiländer H. 1998. Lipid composition of *spodoptera frugiperda* (sf9) and *trichoplusia ni* (tn) insect cells used for baculovirus infection. *FEBS Lett*. 441(1):49–52
- Marinissen MJ, Gutkind JS. 2001. G-protein-coupled receptors and signaling networks: emerging paradigms. *Trends Pharmacol. Sci*. 22(7):368–76
- Marques B, Liguori L, Pacllet M-H, Villegas-Mendéz A, Rothe R, et al. 2007. Liposome-mediated cellular delivery of active gp91(phox). *PLoS One*. 2(9):e856
- Martin KH, Grosenbach DW, Franke CA, Hruby DE. 1997. Identification and analysis of three myristylated vaccinia virus late proteins. *J. Virol*. 71(7):5218–26
- Masaki T, Ninomiya H, Sakamoto A, Okamoto Y. 1999. Structural basis of the function of endothelin receptor. *Mol. Cell. Biochem*. 190(1-2):153–56
- McCusker E, Robinson AS. 2008. Refolding of g protein alpha subunits from inclusion bodies expressed in *escherichia coli*. *Protein Expr. Purif*. 58(2):342–55
- McEwen DP, Gee KR, Kang HC, Neubig RR. 2001. Fluorescent bodipy-gtp analogs: real-time measurement of nucleotide binding to g proteins. *Anal. Biochem*. 291(1):109–17
- Mikami S, Kobayashi T, Masutani M, Yokoyama S, Imataka H. 2008. A human cell-derived in vitro coupled transcription/translation system optimized for production of recombinant proteins. *Protein Expr. Purif*. 62(2):190–98
- Mikami S, Masutani M, Sonenberg N, Yokoyama S, Imataka H. 2006. An efficient mammalian cell-free translation system supplemented with translation factors. *Protein Expr. Purif*. 46(2):348–57
- Miyauchi T, Goto K. 1999. Heart failure and endothelin receptor antagonists. *Trends Pharmacol. Sci*. 20(5):210–17
- Molenaar P, Kuc RE, Davenport AP. 1992. Characterization of two new etb selective radioligands, [125i]-bq3020 and [125i]-[ala1,3,11,15]et-1 in human heart. *Br. J. Pharmacol*. 107(3):637–39
- Mollaaghababa R, Davidson FF, Kaiser C, Khorana HG. 1996. Structure and function in rhodopsin: expression of functional mammalian opsin in *saccharomyces cerevisiae*. *Proc. Natl. Acad. Sci. U.S.A*. 93(21):11482–86
- Moore CAC, Milano SK, Benovic JL. 2007. Regulation of receptor trafficking by grks and arrestins. *Annu. Rev. Physiol*. 69:451–82
- Moritani Y, Nomura SM, Morita I, Akiyoshi K. 2010. Direct integration of cell-free-synthesized connexin-43 into liposomes and hemichannel formation. *FEBS J*. 277(16):3343–52
- Müller-Lucks A, Gena P, Frascaria D, Altamura N, Svelto M, et al. 2013. Preparative scale production and functional reconstitution of a human aquaglyceroporin (aqp3) using a cell free expression system. *N. Biotechnol*.
- Mumford RA, Pickett CB, Zimmerman M, Strauss AW. 1981. Protease activities present in wheat germ and rabbit reticulocyte lysates. *Biochem. Biophys. Res. Commun*. 103(2):565–72

- Nagase T, Aoki T, Oka T, Fukuchi Y, Ouchi Y. 1997. Et-1-induced bronchoconstriction is mediated via etb receptor in mice. *J. Appl. Physiol.* 83(1):46–51
- Nakajima K, Kubo S, Kumagaye S, Nishio H, Tsunemi M, et al. 1989. Structure-activity relationship of endothelin: importance of charged groups. *Biochem. Biophys. Res. Commun.* 163(1):424–29
- Nakano K, Tozuka Y, Yamamoto H, Kawashima Y, Takeuchi H. 2008. A novel method for measuring rigidity of submicron-size liposomes with atomic force microscopy. *Int. J. Pharm.* 355(1-2):203–9
- Nakashima N, Tamura T. 2004. Cell-free protein synthesis using cell extract of pseudomonas fluorescens and cspa promoter. *Biochem. Biophys. Res. Commun.* 319(2):671–76
- Nambi P, Pullen M, Spielman W. 1994. Species differences in the binding characteristics of [125i]ir1-1620, a potent agonist specific for endothelin-b receptors. *J. Pharmacol. Exp. Ther.* 268(1):202–7
- Nelson J, Bagnato A, Battistini B, Nisen P. 2003. The endothelin axis: emerging role in cancer. *Nat. Rev. Cancer.* 3(2):110–16
- Nett PC, Teixeira MM, Candinas D, Barton M. 2006. Recent developments on endothelin antagonists as immunomodulatory drugs--from infection to transplantation medicine. *Recent Pat. Cardiovasc. Drug Discov.* 1(3):265–76
- Noireaux V, Bar-Ziv R, Godefroy J, Salman H, Libchaber A. 2005. Toward an artificial cell based on gene expression in vesicles. *Phys. Biol.* 2(3):P1–8
- Nozawa A, Nanamiya H, Miyata T, Linka N, Endo Y, et al. 2007. A cell-free translation and proteoliposome reconstitution system for functional analysis of plant solute transporters. *Plant Cell Physiol.* 48(12):1815–20
- Oh P, Horner T, Witkiewicz H, Schnitzer JE. 2012. Endothelin induces rapid, dynamin-mediated budding of endothelial caveolae rich in et-b. *J. Biol. Chem.* 287(21):17353–62
- Okamoto Y, Ninomiya H, Tanioka M, Sakamoto A, Miwa S, Masaki T. 1997. Palmitoylation of human endothelinb. its critical role in g protein coupling and a differential requirement for the cytoplasmic tail by g protein subtypes. *J. Biol. Chem.* 272(34):21589–96
- Oksche A, Boese G, Horstmeyer A, Furkert J, Beyermann M, et al. 2000. Late endosomal/lysosomal targeting and lack of recycling of the ligand-occupied endothelin b receptor. *Mol. Pharmacol.* 57(6):1104–13
- Oldham WM, Hamm HE. 2008. Heterotrimeric g protein activation by g-protein-coupled receptors. *Nat. Rev. Mol. Cell Biol.* 9(1):60–71
- Opekarová M, Tanner W. 2003. Specific lipid requirements of membrane proteins--a putative bottleneck in heterologous expression. *Biochim. Biophys. Acta.* 1610(1):11–22
- Orry AJ, Wallace BA. 2000. Modeling and docking the endothelin g-protein-coupled receptor. *Biophys. J.* 79(6):3083–94
- Ozaki S, Ohwaki K, Ihara M, Ishikawa K, Yano M. 1997. Coexpression studies with endothelin receptor subtypes indicate the existence of intracellular cross-talk between et(a) and et(b) receptors. *J. Biochem.* 121(3):440–47
- Paolillo M, Russo MA, Curti D, Lanni C, Schinelli S. 2010. Endothelin b receptor antagonists block proliferation and induce apoptosis in glioma cells. *Pharmacol. Res.* 61(4):306–15

- Papachristou E, Papadimitropoulos A, Kotsantis P, Goumenos DS, Katsoris PG, Vlachojannis JG. 2010. Interaction of endothelin-1 and nitric oxide pathways in human tubular epithelial cells under the influence of cyclosporine-a. *Ren. Fail.* 32(6):727–32
- Park K-H, Billon-Denis E, Dahmane T, Lebaupain F, Pucci B, et al. 2011. In the cauldron of cell-free synthesis of membrane proteins: playing with new surfactants. *N. Biotechnol.* 28(3):255–61
- Proverbio D, Roos C, Beyermann M, Orban E, Dötsch V, Bernhard F. 2013. Functional properties of cell-free expressed human endothelin a and endothelin b receptors in artificial membrane environments. *Biochim. Biophys. Acta*
- Ramachandran S, Cerione RA. 2004. Stabilization of an intermediate activation state for transducin by a fluorescent gtp analogue. *Biochemistry.* 43(27):8778–86
- Rath P, Demange P, Saurel O, Tropis M, Daffé M, et al. 2011. Functional expression of the porah channel from corynebacterium glutamicum in cell-free expression systems: implications for the role of the naturally occurring mycolic acid modification. *J. Biol. Chem.* 286(37):32525–32
- Rigaud J-L, Lévy D. 2003. Reconstitution of membrane proteins into liposomes. *Methods Enzymol.* 372:65–86
- Rigaud J-L, Levy D, Mosser G, Lambert O. 1998. Detergent removal by non-polar polystyrene beads. *Eur. Biophys. J.* 27(4):305–19
- Roos C, Kai L, Proverbio D, Ghoshdastider U, Filipek S, et al. 2013. Co-translational association of cell-free expressed membrane proteins with supplied lipid bilayers. *Mol. Membr. Biol.* 30(1):75–89
- Roos C, Zocher M, Müller D, Münch D, Schneider T, et al. 2012. Characterization of co-translationally formed nanodisc complexes with small multidrug transporters, proteorhodopsin and with the e. coli mray translocase. *Biochim. Biophys. Acta.* 1818(12):3098–3106
- Roos M, Soskic V, Poznanovic S, Godovac-Zimmermann J. 1998. Post-translational modifications of endothelin receptor b from bovine lungs analyzed by mass spectrometry. *J. Biol. Chem.* 273(2):924–31
- Roosild TP, Greenwald J, Vega M, Castronovo S, Riek R, Choe S. 2005. Nmr structure of mistic, a membrane-integrating protein for membrane protein expression. *Science.* 307(5713):1317–21
- Rovati GE, Capra V, Neubig RR. 2007. The highly conserved dry motif of class a g protein-coupled receptors: beyond the ground state. *Mol. Pharmacol.* 71(4):959–64
- Russell FD, Molenaar P. 2000. The human heart endothelin system: et-1 synthesis, storage, release and effect. *Trends Pharmacol. Sci.* 21(9):353–59
- Ryabova LA, Vinokurov LM, Shekhovtsova EA, Alakhov YB, Spirin AS. 1995. Acetyl phosphate as an energy source for bacterial cell-free translation systems. *Anal. Biochem.* 226(1):184–86
- Saeki T, Ihara M, Fukuroda T, Yamagiwa M, Yano M. 1991. [ala1,3,11,15]endothelin-1 analogs with etb agonistic activity. *Biochem. Biophys. Res. Commun.* 179(1):286–92
- Saito Y, Mizuno T, Itakura M, Suzuki Y, Ito T, et al. 1991. Primary structure of bovine endothelin etb receptor and identification of signal peptidase and metal proteinase cleavage sites. *J. Biol. Chem.* 266(34):23433–37
- Sakamoto A, Yanagisawa M, Sawamura T, Enoki T, Ohtani T, et al. 1993. Distinct subdomains of human endothelin receptors determine their selectivity to endothelina-selective antagonist and endothelinb-selective agonists. *J. Biol. Chem.* 268(12):8547–53

- Sakurai T, Yanagisawa M, Takawa Y, Miyazaki H, Kimura S. 1990. Cloning of a cDNA encoding a non-iso peptide-selective subtype of the endothelin receptor. *Nature*. 348(6303):732–35
- Sampaio ALF, Rae GA, Henriques M das GMO. 2004. Effects of endothelin eta receptor antagonism on granulocyte and lymphocyte accumulation in LPS-induced inflammation. *J. Leukoc. Biol.* 76(1):210–16
- Sansuk K, Balog CIA, van der Does AM, Booth R, de Grip WJ, et al. 2008. GPCR proteomics: mass spectrometric and functional analysis of histamine h1 receptor after baculovirus-driven and in vitro cell free expression. *J. Proteome Res.* 7(2):621–29
- Saravanan K, Paramasivam M, Dey S, Singh TP, Srinivasan A. 2004. Biotinyl endothelin-1 binding to endothelin receptor and its applications. *J. Cardiovasc. Pharmacol.* 44(3):287–93
- Sato K, Oka M, Hasunuma K, Ohnishi M, Kira S. 1995. Effects of separate and combined eta and etb blockade on et-1-induced constriction in perfused rat lungs. *Am. J. Physiol.* 269(5 Pt 1):L668–72
- Savage DF, Anderson CL, Robles-Colmenares Y, Newby ZE, Stroud RM. 2007. Cell-free complements in vivo expression of the *e. coli* membrane proteome. *Protein Sci.* 16(5):966–76
- Sawasaki T, Morishita R, Gouda MD, Endo Y. 2007. Methods for high-throughput materialization of genetic information based on wheat germ cell-free expression system. *Methods Mol. Biol.* 375:95–106
- Schiller H, Haase W, Molsberger E, Janssen P, Michel H, Reiländer H. 2000. The human et(b) endothelin receptor heterologously produced in the methylotrophic yeast *Pichia pastoris* shows high-affinity binding and induction of stacked membranes. *Receptors Channels.* 7(2):93–107
- Schmidt CJ, Thomas TC, Levine MA, Neer EJ. 1992. Specificity of G protein beta and gamma subunit interactions. *J. Biol. Chem.* 267(20):13807–10
- Schneider B, Junge F, Shirokov VA, Durst F, Schwarz D, et al. 2010. Membrane protein expression in cell-free systems. *Methods Mol. Biol.* 601:165–86
- Schneider MP, Boesen EI, Pollock DM. 2007. Contrasting actions of endothelin et(a) and et(b) receptors in cardiovascular disease. *Annu. Rev. Pharmacol. Toxicol.* 47:731–59
- Schuler MA, Denisov IG, Sligar SG. 2013. Nanodiscs as a new tool to examine lipid-protein interactions. *Methods Mol. Biol.* 974:415–33
- Schulz GE. 2000. Beta-barrel membrane proteins. *Curr. Opin. Struct. Biol.* 10(4):443–47
- Schwarz D, Daley D, Beckhaus T, Dötsch V, Bernhard F. 2010. Cell-free expression profiling of *e. coli* inner membrane proteins. *Proteomics.* 10(9):1762–79
- Schwarz D, Dötsch V, Bernhard F. 2008. Production of membrane proteins using cell-free expression systems. *Proteomics.* 8(19):3933–46
- Schwarz D, Junge F, Durst F, Frölich N, Schneider B, et al. 2007. Preparative scale expression of membrane proteins in *Escherichia coli*-based continuous exchange cell-free systems. *Nat. Protoc.* 2(11):2945–57
- Shenkarev ZO, Lyukmanova EN, Butenko IO, Petrovskaya LE, Paramonov AS, et al. 2013. Lipid-protein nanodiscs promote in vitro folding of transmembrane domains of multi-helical and multimeric membrane proteins. *Biochim. Biophys. Acta.* 1828(2):776–84
- Shimizu Y, Inoue A, Tomari Y, Suzuki T, Yokogawa T, et al. 2001. Cell-free translation reconstituted with purified components. *Nat. Biotechnol.* 19(8):751–55

- Shimono K, Goto M, Kikukawa T, Miyauchi S, Shirouzu M, et al. 2009. Production of functional bacteriorhodopsin by an escherichia coli cell-free protein synthesis system supplemented with steroid detergent and lipid. *Protein Sci.* 18(10):2160–71
- Shraga-Levine Z, Sokolovsky M. 1998. Functional role for glycosylated subtypes of rat endothelin receptors. *Biochem. Biophys. Res. Commun.* 246(2):495–500
- Shraga-Levine Z, Sokolovsky M. 2000. Functional coupling of g proteins to endothelin receptors is ligand and receptor subtype specific. *Cell. Mol. Neurobiol.* 20(3):305–17
- Siderovski DP, Willard FS. 2005. The gaps, gefs, and gdis of heterotrimeric g-protein alpha subunits. *Int. J. Biol. Sci.* 1(2):51–66
- Sisodia SS. 1992. Secretion of the beta-amyloid precursor protein. *Ann. N. Y. Acad. Sci.* 674:53–57
- Soma S, Takahashi H, Muramatsu M, Oka M, Fukuchi Y. 1999. Localization and distribution of endothelin receptor subtypes in pulmonary vasculature of normal and hypoxia-exposed rats. *Am. J. Respir. Cell Mol. Biol.* 20(4):620–30
- Spirin AS, Baranov VI, Ryabova LA, Ovodov SY, Alakhov YB. 1988. A continuous cell-free translation system capable of producing polypeptides in high yield. *Science.* 242(4882):1162–64
- Stech M, Merk H, Schenk JA, Stöcklein WFM, Wüstenhagen DA, et al. 2012. Production of functional antibody fragments in a vesicle-based eukaryotic cell-free translation system. *J. Biotechnol.* 164(2):220–31
- Stow LR, Jacobs ME, Wingo CS, Cain BD. 2011. Endothelin-1 gene regulation. *FASEB J.* 25(1):16–28
- Strader CD, Sigal IS, Dixon RA. 1989. Structural basis of beta-adrenergic receptor function. *FASEB J.* 3(7):1825–32
- Takagi Y, Ninomiya H, Sakamoto A, Miwa S, Masaki T. 1995. Structural basis of g protein specificity of human endothelin receptors. a study with endothelina/b chimeras. *J. Biol. Chem.* 270(17):10072–78
- Takai K, Sawasaki T, Endo Y. 2010. The wheat-germ cell-free expression system. *Curr. Pharm. Biotechnol.* 11(3):272–78
- Takasuka T, Horii I, Furuichi Y, Watanabe T. 1991a. Detection of an endothelin-1-binding protein complex by low temperature sds-page. *Biochem. Biophys. Res. Commun.* 176(1):392–400
- Takasuka T, Satoh N, Horii I, Furuichi Y, Watanabe T. 1991b. Heterogeneity of endothelin receptor. *J. Cardiovasc. Pharmacol.* 17 Suppl 7:S109–12
- Takigawa M, Sakurai T, Kasuya Y, Abe Y, Masaki T, Goto K. 1995. Molecular identification of guanine-nucleotide-binding regulatory proteins which couple to endothelin receptors. *Eur. J. Biochem.* 228(1):102–8
- Terrillon S, Durroux T, Mouillac B, Breit A, Ayoub MA, et al. 2003. Oxytocin and vasopressin v1a and v2 receptors form constitutive homo- and heterodimers during biosynthesis. *Mol. Endocrinol.* 17(4):677–91
- Tilley DG. 2011. G protein-dependent and g protein-independent signaling pathways and their impact on cardiac function. *Circ. Res.* 109(2):217–30
- Tolkovsky AM, Levitzki A. 1978. Mode of coupling between the beta-adrenergic receptor and adenylate cyclase in turkey erythrocytes. *Biochemistry.* 17(18):3795
- Tsukamoto H, Sinha A, DeWitt M, Farrens DL. 2010. Monomeric rhodopsin is the minimal functional unit required for arrestin binding. *J. Mol. Biol.* 399(3):501–11

- Tucker J, Grisshammer R. 1996. Purification of a rat neurotensin receptor expressed in escherichia coli. *Biochem. J.* 317 ( Pt 3):891–99
- Ulmschneider MB, Sansom MSP, Di Nola A. 2006. Evaluating tilt angles of membrane-associated helices: comparison of computational and nmr techniques. *Biophys. J.* 90(5):1650–60
- Ulrich AS. 2002. Biophysical aspects of using liposomes as delivery vehicles. *Biosci. Rep.* 22(2):129–50
- Umakoshi H, Suga K, Bui HT, Nishida M, Shimanouchi T, Kuboi R. 2009. Charged liposome affects the translation and folding steps of in vitro expression of green fluorescent protein. *J. Biosci. Bioeng.* 108(5):450–54
- Uzawa T, Yamagishi A, Oshima T. 2002. Polypeptide synthesis directed by dna as a messenger in cell-free polypeptide synthesis by extreme thermophiles, thermus thermophilus hb27 and sulfolobus tokodaii strain 7. *J. Biochem.* 131(6):849–53
- Wall MA, Coleman DE, Lee E, Iñiguez-Lluhi JA, Posner BA, et al. 1995. The structure of the g protein heterotrimer gi alpha 1 beta 1 gamma 2. *Cell.* 83(6):1047–58
- Wallin E, von Heijne G. 1998. Genome-wide analysis of integral membrane proteins from eubacterial, archaean, and eukaryotic organisms. *Protein Sci.* 7(4):1029–38
- Wang X, Corin K, Baaske P, Wienken CJ, Jerabek-Willemsen M, et al. 2011. Peptide surfactants for cell-free production of functional g protein-coupled receptors. *Proc. Natl. Acad. Sci. U.S.A.* 108(22):9049–54
- Wang X, Cui Y, Wang J. 2013. Efficient expression and immunoaffinity purification of human trace amine-associated receptor 5 from *e. coli* cell-free system. *Protein Pept. Lett.* 20(4):473–80
- Wang X, Liu J, Zheng Y, Li J, Wang H, et al. 2008. An optimized yeast cell-free system: sufficient for translation of human papillomavirus 58 l1 mrna and assembly of virus-like particles. *J. Biosci. Bioeng.* 106(1):8–15
- Wang Z. 2006. Controlled expression of recombinant genes and preparation of cell-free extracts in yeast. *Methods Mol. Biol.* 313:317–31
- Weiss HM, Grisshammer R. 2002. Purification and characterization of the human adenosine a(2a) receptor functionally expressed in escherichia coli. *Eur. J. Biochem.* 269(1):82–92
- Wheatley M, Hawtin SR. Glycosylation of g-protein-coupled receptors for hormones central to normal reproductive functioning: its occurrence and role. *Hum. Reprod. Update.* 5(4):356–64
- Whorton MR, Bokoch MP, Rasmussen SGF, Huang B, Zare RN, et al. 2007. A monomeric g protein-coupled receptor isolated in a high-density lipoprotein particle efficiently activates its g protein. *Proc. Natl. Acad. Sci. U.S.A.* 104(18):7682–87
- Wild K, Halic M, Sinning I, Beckmann R. 2004. Srp meets the ribosome. *Nat. Struct. Mol. Biol.* 11(11):1049–53
- Yanagisawa M, Kurihara H, Kimura S, Goto K, Masaki T. 1988. A novel peptide vasoconstrictor, endothelin, is produced by vascular endothelium and modulates smooth muscle ca<sup>2+</sup> channels. *J. Hypertens. Suppl.* 6(4):S188–91
- Yang J-P, Cirico T, Katzen F, Peterson TC, Kudlicki W. 2011. Cell-free synthesis of a functional g protein-coupled receptor complexed with nanometer scale bilayer discs. *BMC Biotechnol.* 11:57
- Yao Z, Kobilka B. 2005. Using synthetic lipids to stabilize purified beta2 adrenoceptor in detergent micelles. *Anal. Biochem.* 343(2):344–46

- Yoshiyoshi M, Nishioka K, Nakao K, Saito Y, Matsumura M, et al. 1991. Plasma endothelin concentrations in patients with pulmonary hypertension associated with congenital heart defects. evidence for increased production of endothelin in pulmonary circulation. *Circulation*. 84(6):2280–85
- Zhang JT, Ling V. 1995. Involvement of cytoplasmic factors regulating the membrane orientation of p-glycoprotein sequences. *Biochemistry*. 34(28):9159–65
- Zhou Y, Asahara H, Gaucher EA, Chong S. 2012. Reconstitution of translation from thermus thermophilus reveals a minimal set of components sufficient for protein synthesis at high temperatures and functional conservation of modern and ancient translation components. *Nucleic Acids Res*. 40(16):7932–45
- Zubay G. 1973. In vitro synthesis of protein in microbial systems. *Annu. Rev. Genet*. 7:267–87

## Acknowledgements

First of all, I would like to thank Prof. Dr. Volker Dötsch and Dr. Frank Bernhard for giving me the opportunity to perform my PhD study in their laboratories and for providing me a great working environment.

A special thank to Dr. Frank Bernhard for his continuous supervision and support through all of these years, for the stimulating discussions and new ideas for my project.

I would like to deeply thank all the current and former members of the Dötsch group, without their support, not only scientific, this thesis would have hardly been possible.

In particular, I would like to thank the whole “cell-free group” for the stimulating environment, which allowed me to grow both professionally and personally. Dr. Sina Reckel, Dr. Friederike Junge, Dr. Sebastian Richers, Dr. Christian Roos, Dr. Stefan Haberstock, Yi Ma, Dr. Edith Buchinger, Erik Henrich, Dr. Lei Kai, Dr. Erika Orban and Beate Hoffmann for the fruitful discussions, good ideas and help with the various experiments. A special thank to Christopher Hein and Sebastian Kehrlößer for proof-reading the German summary.

Very big thanks go to three special friends that made my life here in the lab and in Frankfurt much “lighter”. Dr. Solmaz Sobhanifar, for the endless drinking, smoking and dancing nights, but also for introducing me to the lab practices. Mikhail Karbyshev, for all the great times we spend together, for being every time present when I needed an helping hand and for spicing up my life with pure Russian humor. Dr. Aisha Laguerre, for all the lunches at the delicious mensa, when she had to listen me mumbling about my experiments, for the parties and the “horror nights”, for the help in the lab as well as for her patience and time in reading my thesis.

A big thank to Birgit Schäfer, for all the support in the lab and for being every time kind and gentle in answering all of my questions.

Thanks to Sigrid Oğuzer-Fachinger for finding me an accommodation when I moved to Frankfurt and for the great ability in taking care of all the administrative matters.

Lastly, I would like to thank my family.

Thomas, for all your support and your love, thanks to be next to me.

Ai miei genitori e a mio fratello, perché mi avete sostenuto fin dall’inizio in questa avventura, sapendomi ascoltare e consigliare anche nei momenti di difficoltà e non facendomi mai mancare il vostro affetto nonostante la lontananza. Grazie.



## Curriculum vitae

### Daide Proverbio

Date of Birth: 3.3.1984

Gender: Male

Nationality: Italian

Address: Institute of Biophysical Chemistry  
Biocenter, Campus Riedberg  
Goethe University Frankfurt  
Max-von-Laue Str. 9  
60438 Frankfurt am Main

Telephone: +49 17662342115

E-mail: [davide.proverbio@hotmail.it](mailto:davide.proverbio@hotmail.it)

Website: [http://www.bpc.uni-frankfurt.de/doetsch/wiki/index.php/Davide\\_Proverbio](http://www.bpc.uni-frankfurt.de/doetsch/wiki/index.php/Davide_Proverbio)

My research interest lies primarily in the field of biochemistry and especially in the functional and structural characterization of G-protein coupled receptors (GPCRs). My current focus is the optimization of the expression and the functional analysis of the human endothelin receptors in combination with Cell-free protein synthesis.

#### Content:

- Education & Professional Experience
- Personal Skills and Competence
- Publications
- Conferences and Workshops

---

## EDUCATION & PROFESSIONAL EXPERIENCE

- 2009-2013 **PhD in Biochemistry:** *Functional and structural analysis of cell-free produced G-protein coupled receptors*  
Supervisors: Dr. Frank Bernhard and Prof. Dr. Volker Dötsch,  
Department of Biophysical Chemistry, Goethe University Frankfurt/Main.  
Funded by Marie-Curie ITN<sup>1</sup> (SBMP<sup>2</sup>) and the European Project FP7<sup>3</sup>.
- 2006-2009 **Master Degree in Experimental Medicine.**  
Diploma: March 2009 (Score: 110/110)
- 2009 **Master Practical Stage I** (6 months): *Cellular localization and functionality of the V2 vasopressin receptor mutant R137H*  
Supervisor: Prof. Dr. Marco Parenti,  
Department of Experimental Medicine, School of Medicine,  
University of Milano-Bicocca. Italy.
- Master Practical Stage II - International Fellowship** (6 months): *Comparison of trimeric G-protein levels in Percoll-purified plasma membrane isolated from brain cortex of morphine-treated rats*  
Supervisor: Prof. Dr. Petr Svoboda,  
Institute of Physiology, Academy of Science of the Czech Republic, Prague.  
Funded by the Erasmus Programme.
- 2003-2006 **Bachelor Degree in Medical Biotechnology.**  
Diploma: October 2006 (Score: 102/110)
- 2006 **Bachelor Practical Stage** (6 months): *Expression analysis of genes involved in iron metabolism*  
Supervisor: Prof. Dr. Raffaella Meneveri,  
Department of Experimental Medicine,  
University of Milano-Bicocca, Monza, Italy.
- 2003 **High School.**  
Liceo Scientifico G.B. Grassi, Saronno, Italy

---

<sup>1</sup> Marie Curie Initial Training Networks: [http://ec.europa.eu/research/mariecurieactions/about-mca/actions/itn/index\\_en.htm](http://ec.europa.eu/research/mariecurieactions/about-mca/actions/itn/index_en.htm).

<sup>2</sup> Structural biology of Membrane Proteins: <http://www.sbmp-itn.eu/sbmpps/home/>.

<sup>3</sup> European Commission – Seventh Framework Programme: [http://cordis.europa.eu/fp7/home\\_en.html](http://cordis.europa.eu/fp7/home_en.html).

## PERSONAL SKILLS AND COMPETENCE

### SCIENTIFIC

#### Cell culture:

- mammalian and bacterial cell culture
- *in vitro* cell manipulation

#### Biochemistry:

##### *expression and purification of protein*

- cell-free and *E.coli* expression
- gel electrophoresis (SDS-PAGE)
- Western-Blot
- column chromatography (Äkta System)
- liposomes and nanodiscs preparation

##### *functional assays*

- surface plasmon resonance (Biacore X100)
- radioactive and fluorescent ligand binding assays and G proteins activation
- Microscale Thermophoresis (MST)
- Octet
- ELISA assay
- Confocal Laser Scanning microscopy (Carl Zeiss LSM 510 Meta/Axiocam)

#### Molecular Biology:

- PCR
- plasmid preparation and purification
- restriction/digest gel electrophoresis

**INFORMATIC OS:** Windows, Linux (Ubuntu)

**Office pack:** Word, Power Point, Excel

**Graphic:** Adobe Photoshop and Illustrator

**Scientific:** Protein data-bank (EXPASY, NCBI), ClustalW, 3d structures (PDB Viewer), Unicorn, GraphPad, Origin, ImageJ, LSM (Carl Zeiss), BiaEvaluation (Biacore).

**TEACHING EXPERIENCE** Practical course Biophysical Chemistry

**LANGUAGES English:** fluent

**Italian:** mother tongue

**German:** basic

## PUBLICATIONS

### **Functional properties of cell-free expressed human endothelin A and endothelin B receptors in artificial membrane environments.**

**Proverbio D**, Roos C, Beyermann M, Orbán E, Dötsch V, Bernhard F.

Biochim Biophys Acta. 2013 Sep;1828(9):2182-92. doi: 10.1016/j.bbamem.2013.05.031. Epub 2013 Jun 6.

### **Characterization of co-translationally formed nanodisc complexes with small multidrug transporters, proteorhodopsin and with the *E. coli* MraY translocase.**

Roos C, Zocher M, Müller D, Münch D, Schneider T, Sahl HG, Scholz F, Wachtveitl J, Ma Y,

**Proverbio D**, Henrich E, Dötsch V, Bernhard F.

Biochim Biophys Acta 2012;1818(12):3098-106.

### **Co-translational association of cell-free expressed membrane proteins with supplied lipid bilayers.**

Roos C, Kai L, **Proverbio D**, Ghoshdastider U, Filipek S, Dötsch V, Bernhard F

Mol Membr Biol. 2012 Jun 20. [Epub ahead of print]

### **Systems for the cell-free synthesis of proteins.**

Kai L, Roos C, Haberstock S, **Proverbio D**, Ma Y, Junge F, Karbyshev M, Dötsch V, Bernhard F.

Methods Mol Biol. 2012;800:201-25.

### **Advances in cell-free protein synthesis for the functional and structural analysis of membrane proteins.**

Junge F, Haberstock S, Roos C, Stefer S, **Proverbio D**, Dötsch V, Bernhard F.

N Biotechnol. 2011 Apr 30;28(3):262-71. Epub 2010 Jul 15.

### **Modulation of G-protein coupled receptor sample quality by modified cell-free expression protocols: a case study of the human endothelin A receptor.**

Junge F, Luh LM, **Proverbio D**, Schäfer B, Abele R, Beyermann M, Dötsch V, Bernhard F.

Struct Biol. 2010 Oct;172(1):94-106. Epub 2010 May 9.

## CONFERENCES AND WORKSHOPS

### CONFERENCES:

- SFB 807/TRAM Retreat – Naurod, March 22nd-24th, 2010
- Invited talk 'Alternative applications in Proteomics and Biotechnology' at the Symposium on Crystallization and Cell-Free Protein Production of Membrane Proteins, Ringberg, May 25th-28th, 2010
- The 2<sup>nd</sup> Annual Meeting of SBMPs, Basel, June 8-11, 2010
- The 3<sup>rd</sup> Annual Meeting of SBMPs, Utrecht, May 23-35, 2011
- EuroMar Conference, Frankfurt am Main, August 21-25, 2011
- GBM Molecular Life Science, Frankfurt am Main, September 25-28, 2011
- The 4<sup>th</sup> annual meeting of SBMPs, Maratea, May 30 – June 2, 2012

### WORKSHOPS:

- SBMP workshop of Protein crystallization, Grenoble, March 15-18, 2010
- SBMP workshop of cell-free expression of membrane proteins, Frankfurt/Main, February 21-27, 2010 (organizing team member)
- SBMP workshop of career development and management, Basel, June 9 2010

## **Eidesstattliche Versicherung**

Ich erkläre hiermit an Eides statt, dass ich die vorgelegte Dissertation über „Cell-Free expression of GPCRs: the endothelin system“ selbständig angefertigt und mich anderer Hilfsmittel als der in ihr angegebenen nicht bedient habe. Des Weiteren versichere ich, dass Entlehnungen aus anderen Schriften, soweit sie in der Dissertation nicht ausdrücklich als solche mit Angabe der betreffenden Schrift bezeichnet sind, nicht stattgefunden haben.

Ich habe an keiner anderen Universität ein Gesuch um Zulassung zur Promotion eingereicht oder die vorliegende oder eine andere Arbeit als Dissertation vorgelegt. Ich versichere außerdem, nicht die Hilfe einer kommerziellen Promotionsvermittlung in Anspruch genommen zu haben.

Frankfurt am Main, den 12. Dezember 2013

Davide Proverbio